



Faculteit Wetenschappen

Departement Biologie

Per- and polyfluoroalkyl substances (PFAS) in private gardens: factors affecting accumulation in homegrown food and characterization of human exposure risk

Per- en polyfluoralkylstoffen (PFAS) in private tuinen: onderzoek naar factoren die opstapeling in zelf geteelde voeding beïnvloeden en beschrijving van het humane blootstellingsrisico

Proefschrift voorgelegd tot het behalen van de graad van doctor in de wetenschappen

Te verdedigen door Robin Lasters

Promotoren:

Prof. Dr. Marcel Eens

Prof. Dr. Lieven Bervoets

Antwerpen, 2024

© Robin Lasters

Disclaimer

The author allows to consult and copy parts of this work for personal use. Further reproduction or transmission in any form or by any means, without the prior permission of the author is strictly forbidden.

This work has been financially supported by the Research Foundation – Flanders (FWO) and the IMPULS project (University of Antwerp)

Table of contents

Voorwoord	6
List of Abbreviations	9
Summary	12
Samenvatting	15
Chapter 1: General introduction	18
1.1 Welcome to the Anthropocene	19
1.2 The rise of organic pollutants	19
1.3 The PFAS universe	20
1.4 Classification and terminology	21
1.4.1 Polymer substances	21
1.4.2 Non-polymer substances	22
1.5 Properties and usage	25
1.6 Environmental fate and behaviour	27
1.6.1 Soil pollution	28
1.6.2 Transport and partitioning in the soil	29
1.7 Human exposure	29
1.7.1 Entrance in the human food-chain	29
1.7.2 Exposure pathways	30
1.7.3 Exposure assessment	31
1.7.4 Health effects	33
1.8 Food contamination	34
1.8.1 Commercial food	34
1.8.2 Homegrown food: a major knowledge gap	35
1.9 Thesis outline: main research hypotheses and objectives	37
1.10 Study area	39
Chapter 2: Home-produced eggs: an important human exposure pathway of perfluoroalkylated substances (PFAAs)	44

2.1 Abstract	45
2.2 Introduction	46
2.3 Materials and methods	49
2.3.1 Study area and sample collection	49
2.3.2 Volunteer selection and survey data	50
2.3.3 Chemical analysis	50
2.3.4 Chemical extraction	51
2.3.5 UPLC-TQD analysis	52
2.3.6 Quality control and assurance	52
2.3.7 Health risk indications	53
2.3.8 Statistical analysis	54
2.4 Results	55
2.4.1 PFAS profile and concentrations in the buffer zones	55
2.4.2 PFAS relationships with survey data	58
2.4.3 Human health risk	59
2.5 Discussion	61
2.5.1 PFAS profile and concentrations in the distance buffer zones	61
2.5.2 PFAS relationships with survey data	64
2.5.3 Human health risk indications	66
2.5.4 Future research perspectives	67
2.6 Conclusion	67
Chapter 3: Prediction of perfluoroalkyl acids (PFAAs) in homegrown eggs: insights into abiotic and biotic factors affecting bioavailability and derivation of potential remediation measures	70
3.1 Abstract	71
3.2 Introduction	72
3.3 Materials and methods	75
3.3.1 Volunteer recruitment	75
3.3.2 Sample collection	75
3.3.3 Sample processing	76
3.3.4 Soil physicochemical characteristics	77
3.3.5 PFAA chemical extraction	77

3.3.6 Quality control and quality assurance	77
3.3.7 Chemical analysis	78
3.3.8 Data processing	79
3.3.9 Data analyses	80
3.3.9.1 Predictive modeling	80
3.3.9.2 Explanatory analysis	81
3.4 Results	83
3.4.1 Matrix profile and concentrations	83
3.4.2 Predictive modeling	84
3.4.3 Explanatory analysis	89
3.5 Discussion	91
3.5.1 Matrix profile and concentrations	91
3.5.2 Predictive modeling	93
3.5.3 Explanatory analysis	96
3.5.4 Potential remediation implications	99
3.6 Conclusions	100
Chapter 4: Per- and perfluoroalkyl substances in homegrown crops: accumulation and human exposure risk	103
4.1 Abstract	104
4.2 Introduction	105
4.3 Materials and methods	107
4.3.1 Study area	107
4.3.2 Volunteer recruitment	107
4.3.3 Sample collection	108
4.3.4 Sample processing	108
4.3.5 PFAS analysis	109
4.3.6 Soil physicochemical characteristics	109
4.3.7 Data processing	110
4.3.8 Human exposure risk	110
4.3.9 Statistical analysis	111
4.4 Results and Discussion	113
4.4.1 General PFAS soil depth profile	113

4.4.2 Soil PFAS depth profile and concentrations along the distance gradient	117
4.4.3 General PFAS profile and concentrations in crops	119
4.4.4 Crop- and compound-specific PFAS accumulation	121
4.4.5 Modeling of PFAS soil-crop relationships	124
4.4.6 Human exposure risk estimation	131
4.5 Conclusion	133

Chapter 5: Dynamic spatiotemporal changes of per- and polyfluoroalkyl substances (PFAS) in private gardens at different distances from a fluorochemical plant **137**

5.1 Abstract	138
5.2 Introduction	139
5.3 Materials and Methods	141
5.3.1 Data collection	141
5.3.2 Sample pre-treatment	142
5.3.3 PFAS chemical extraction	142
5.3.4 PFAS chemical analysis	143
5.3.5 Quality control and quality assurance	143
5.3.6 Data processing	144
5.3.7 Statistical analysis	145
5.4 Results and discussion	146
5.4.1 PFAS profile and concentration patterns within private gardens	146
5.4.2 Short-term spatiotemporal trends (2018/2019-2021)	153
5.4.2.1 Large-scale changes in PFAS concentrations	153
5.4.2.2 Influence wind orientation towards point source	156
5.4.2.3 Small-scale changes in PFAS concentrations (2019-2021)	158
5.4.3 Long-term spatiotemporal trends: soil and homegrown eggs (2010-2022)	160
5.5 Conclusion	163

Chapter 6: General discussion and future research perspectives **166**

6.1 Homegrown food: general accumulation patterns	166
6.2 Influence of local abiotic and biotic factors on food concentrations	170
6.3 Potential human exposure risks	173
6.4 Potential remediation and mitigation measures	177

6.5 Risk communication and perception	180
6.6 General conclusions	181
Bibliography	183
Supplementary information	219
Chapter 2	220
Chapter 3	227
Chapter 4	241
Chapter 5	261
Curriculum Vitae	279

Voorwoord

Het is zo nodig nog moeilijker dan een doctoraat om met woorden te beschrijven wat voor een onwaarschijnlijke reis ik de afgelopen jaren heb beleefd. Aanvankelijk koos ik voor de studierichting biologie omwille van mijn intrinsieke interesse van kleins af aan in levende organismen, waarom en hoe ze zich als dusdanig laten verschijnen en zich gedragen. Mijn keuze om een ecotoxicologisch onderwerp te kiezen als master-thesis was dan ook een grote sprong in het onbekende. Het was vooral een strategische keuze met het beoogde doel om mijn latere loopbaankansen- en keuzemogelijkheden te verbreden, zo dacht ik toen. Gaandeweg ik ervaring opdeed tijdens mijn master-thesis met per- en polyfluoralkylstoffen (PFAS) in mezen, ontdekte ik een onweerstaanbare interesse in wetenschappelijk onderzoek. Het veldwerk dat ik toen verrichtte, inclusief de avondcontroles van de nestkasten in barslechte weersomstandigheden, handelingen met vogels en ze van zo dichtbij kunnen bewonderen, lieten een diepe indruk op mij na. Naast het veldwerk werd mijn enthousiasme voor het onderzoek alleen maar groter door de aangename atmosfeer waarin ik samen met mijn biologievrienden ijverig schreef aan mijn thesis, altijd met een glimlach en een intens gevoel van saamenhorigheid waarbij we mekaar door dik en dun steunden. Wat ben ik dankbaar voor die periode waarin ik zoveel over mezelf kon ontdekken en, nog belangrijker, kon voelen wat mijn drijfveer in het leven was, namelijk onderzoek doen met een maatschappelijk relevante betekenis.

Toen ik niet veel later erin was geslaagd om drie artikels te publiceren op basis van mijn master-thesis, kreeg ik een bevestiging dat mijn gevoel toen juist was. Geladen met een karrenvracht aan enthousiasme en gedrevenheid kreeg ik in 2018 het vertrouwen en de kans van mijn promotoren Lieven Bervoets en Marcel Eens om een doctoraatsproject te schrijven rond PFAS. Met de dankbare hulp van hen en Thimo, mijn toenmalige begeleider van mijn master-thesis, kon ik een boeiend project uitschrijven, waarna ik een doctoraatsbeurs ontving van het Fonds Wetenschappelijk Onderzoek (FWO) in 2019 om écht van start te gaan met mijn wondermooie reis, met vele ups en downs.

Tijdens de eerste twee jaren van mijn doctoraat ging er een hele nieuwe wereld voor mij open en leerde ik mezelf wederom op een geheel andere manier kennen. Van nature ben ik een persoon

die graag in een levendige, bruisende omgeving werkt waarin beleving en samenwerking centraal staan, zoals ik het tijdens mijn master thesis jaren altijd had ervaren. Dit was voor mij altijd een belangrijke energiebron geweest van waaruit ik bergen werk kon verzetten. Deze energiebron werd echter genadeloos weggenomen toen in maart 2020 de corona maatregelen van kracht gingen. Plots kon ik niet meer mijn enthousiasme kwijt over onderzoek op mijn gebruikelijke manier, interageren met collega's, studenten helpen en ontspanning hebben met mijn vrienden. Tesamen met een reeks parallel lopende tegenslagen in mijn privé leven leek het alsof alle krachten mij tegenwerkten en werd ik opeens voor een noodgedwongen keuze gesteld: opgeven of doorzetten en mijzelf heruitvinden om het avontuur verder te zetten en in schoonheid af te werken.

Op dat moment had ik het ongelooflijke geluk om te kunnen rekenen op enkele mensen die me onvoorwaardelijk steunden en er op elk moment voor me waren wanneer ik daar behoefte aan had. In de eerste plaats wil ik mijn moeder ontzettend bedanken voor alle momenten waarop ze geduldig naar mijn bekommernissen luisterde en voor de zorgen waarmee ze mijn lasten een stuk lichter maakte: je bent een goede moeder en vrouw! Daarnaast wil ik ook Caroline, mijn vriendin, bedanken om er altijd aan mijn zijde te staan: jouw onafgebroken vreugde, positiviteit en warme lach straalden als een fel licht op mij dat aanstekelijk werkte. Tenslotte wil ik ook Johan en Marilou bedanken: jullie levenswijsheid heeft mij op weg gezet om belangrijke inzichten te verwerven om energie en kracht te puren vanuit mezelf, het omgaan en accepteren van tegenslagen in het leven. Aan mijn broer Jens en zus Eline wil ik ook mijn oprechte dank toeschrijven: we lopen niet de deur plat bij mekaar, maar ik kon en kan altijd bij jullie terecht met mijn bekommernissen en we begrijpen mekaar beter en beter. Ik kan niet genoeg benadrukken hoeveel ieder van jullie betekent voor mij, jullie liggen me nauw aan het hart.

Met deze hernieuwde energie besloot ik het avontuur van mijn doctoraat voort te zetten. Een volgende interessante wending was de verhoogde publieke aandacht in Vlaanderen naar PFAS in 2021. Dit bleek zowel een vloek als een zegen te zijn, maar achteraf gezien toch vooral een zegen. Het combineren van de werkzaamheden binnen mijn doctoraat met bijdrages voor publieke wetenschapscommunicatie en medewerking voor overheids- en onderzoeksprojecten waren een heuse uitdaging voor mij. Ik wil mijn promotoren Lieven en Marcel, maar ook Thimo erg bedanken om mij hierin te steunen en bij te staan wanneer dat nodig was. Ik heb tijdens deze periode enorm veel mogen bijleren over wetenschapscommunicatie en ben zeer dankbaar voor alle onvergetelijke

opportunities en kansen die op mijn pad kwamen. De manier waarop mijn onderzoek een maatschappelijke bijdrage kon leveren tijdens de PFAS crisis en het gevoel dat ik mensen kon helpen, zorgden mede voor een onafgebroken gedrevenheid en doorzettingsvermogen om mijn doctoraat te kunnen afwerken. Ik ben dan ook heel dankbaar aan alle vrijwilligers die hebben deelgenomen aan mijn onderzoek, zonder hen had dit ganse doctoraatsproject nooit tot stand kunnen komen.

Tot slot wil ik ook benadrukken dat dit doctoraat niet tot stand had gekomen zonder de hulp van een aantal mensen. Tim en Anne, jullie hebben me ontzettend goed bijgestaan in het labo en veel van jullie kennis gedeeld omtrent de analytische aspecten van PFAS- en bodemanalyses. Wanneer er iets misliep, stonden jullie steeds klaar om mij te helpen en mee tot een oplossing te komen: bedankt daarvoor! Te veel namen om op te noemen, maar ik wil ook mijn collega's bedanken die bereid waren voor een fijn gesprek en een interessante uitwisseling van ideeën. Ik wil graag alle betrokken mensen van het VITO, PIH en VUB bedanken voor de aangename samenwerking tijdens het HBM project. Bovenal ben ik mijn vrienden van het middelbaar (Gregory, Gilles, Lennart en Dieter), vrienden van de biologie opleiding (Kevin, Wim, Gilles, Yorick en Fred) en mijn ploeg van de voetbal dankbaar om te waken over mijn mentale gezondheid. Een speciale dank gaat ook nogmaals uit naar mijn promotoren Lieven en Marcel, maar ook naar Thimo waarmee ik vele mooie onderzoekservaringen heb mogen beleven en op belangrijke momenten mij steeds bijstond als schaduwpromotor. Ondanks de soms tegengestelde verwachtingen die ik ervoer tijdens mijn doctoraat door de enorme tijds- en werkdruk die jullie hadden, heb ik voor ieder van jullie zeer veel respect als onderzoeker en als mens. Jullie hebben steeds in mij geloofd en me de vrijheid gegeven om mij te ontwikkelen als persoon en onderzoeker: daar zal ik jullie altijd dankbaar voor zijn.

List of Abbreviations

Abbreviation	Meaning
3,6-OPFHpA	Perfluoro-3,6-dioxaheptanoic acid
4:2 FTS	4:2 fluorotelomer sulfonic acid
6:2 FTS	6:2 fluorotelomer sulfonic acid
8:2 FTS	8:2 fluorotelomer sulfonic acid
9Cl-PF3ONS	9-chlorohexadecafluoro-3-oxanonane-1-sulfonate
11Cl-PF3OUdS	11-chloroeicosafluoro-3-oxaundecane-1-sulfonate
ACN	Acetonitril
AFFF	Aqueous film-forming foam
AIC	Akaike information criterion
ADONA	4,8-dioxa-3H-perfluorononanoic acid
ANCOVA	Analysis of covariance
ANOVA	Analysis of variance
ATSDR	Agency for toxic substances and disease registry
bw	Bodyweight
CEC	Cation-exchange capacity
CF	Commercial feed
CFCs	Chlorofluorocarbons
CH ₃ COOH	Glacial acetic acid
CI	95% confidence interval
DDT	Dichlorodiphenyltrichloroethane
dw	Dry weight
EC	European Commission
ECHA	European chemicals agency
EDTA	Ethylenediaminetetraacetic acid
EFSA	European food safety authority
ESI	Electrospray ionization
EWI	Edible weekly intake
FASA	Perfluoroalkane sulfonamide
FBSA	Perfluorobutane sulfonamide
FLEHS	Flemish environment and health studies
FTOH	Fluorotelomer alcohol
FTS	Fluorotelomer sulfonate
FWO	Research foundation - Flanders
GDPR	General data protection regulation
HBM4EU	European human biomonitoring initiative
HFPO-DA	Hexafluorpropylene oxide-dimer acid
HPE	Home-produced eggs
HPLC	High performance liquid chromatography
ICP-OES	Inductively coupled plasma atomic emission spectroscopy
ITRC	Interstate technology & regulatory council

ISTD	Isotopically mass-labelled internal standards
LDA	Linear discriminant analysis
LF	Kitchen leftovers
LMM	Linear mixed effect model
LOI	Loss on ignition
LOQ	Limit of quantification
MAE	Mean absolute error
MLR	Multiple linear regression
MRM	Multiple reaction monitoring
MS	Mass spectrometer
MTR	Maximum tolerable risk
NaDONA	Sodium dodecafluoro-3H-4,8-dioxanonanoate
NH ₄ Ac	Ammonium acetate
NH ₄ ⁺	Ammonium
NH ₄ OH	Ammonium hydroxide
NO ₃ ⁻	Nitrate
OW	Oosterweel link
PCB	Polychlorinated biphenyl
PES	Polyether sulfone
PF4OPeA	Perfluoro-4-oxapentanoic acid
PF5OHxA	Perfluoro-5-oxahexanoic acid
PFAAs	Perfluoroalkyl acids
PFAS	Per- and polyfluoroalkyl substances
PFBA	Perfluorobutanoic acid
PFBS	Perfluorobutane sulfonic acid
PFCA	perfluoroalkyl carboxylic acid
PFDA	Perfluorodecanoic acid
PFDoDA	Perfluorododecanoic acid
PFDS	Perfluorodecane sulfonic acid
PFEA	Perfluoroalkyl ether acid
PFEESA	Perfluoro(2-ethoxyethane) sulfonate
PFHpA	Perfluoroheptanoic acid
PFHpS	Perfluoroheptane sulfonic acid
PFHxA	Perfluorohexanoic acid
PFHxS	Perfluorohexane sulfonic acid
PFNA	Perfluorononanoic acid
PFOA	Perfluorooctanoic acid
PFOS	Perfluorooctane sulfonic acid
PFOSA	Perfluorooctane sulfonamide
PFOSAA	Perfluorooctanesulfonamido acetic acid
PFPEA	Perfluoropentanoic acid
PFPeS	Perfluoropentane sulfonic acid
PFSA	Perfluoroalkyl sulfonic acid
PFTeDA	Perfluorotetradecanoic acid
PFTrDA	Perfluorotridecanoic acid
PFUnDA	Perfluoroundecanoic acid

pH	Acidity
PI	95% Prediction interval
pKa	Acid dissociation constant
PO ₄ ³⁻	Phosphate
POP	Persistent organic pollutant
PP	Polypropylene
PTFE	Polytetrafluorethylene
RIVM	National institute for public health and the environment
RMSE	Root mean squared error
S/N	Signal-to-noise
SD	Standard deviation
SE	Standard error
SiO ₂	Quartz
SOM	Soil organic matter
SPE	Solid-phase extraction
STD	Isotopically unlabelled standards
TDCA	Taurodeoxycholic acid
TOC	Total organic carbon
TON	Total organic nitrogen
TOP	Total organic phosphorus
TOPA	Total oxidizable precursor assay
TQD	Tandem quadrupole
TWI	Tolerable weekly intake
UNEP	United nations environment programme
UPLC	Ultrahigh performance liquid chromatography
VIF	Variance inflation factor
VITO	Flemish institute for technological research
VLAM	Flanders' agricultural marketing board
VMM	Flemish environment agency
ww	Wet weight
WAX	Weak anion exchange

Summary

Since the early 20th century, human impact on the environment has increased dramatically, which has led to the "Anthropocene" era. In particular, it refers to the increased release of chemicals into the environment by humans. Many of these chemicals, especially the Persistent Organic Pollutants (POPs), have received increasing public attention worldwide over the years. Indeed, it became increasingly clear that this group of substances is being found everywhere in our environment and could have large-scale, adverse effects on living organisms, including humans. Therefore, known POPs, such as some pesticides and dioxins, have been extensively studied for their mode of distribution in the environment, accumulation in organisms and toxic effects. However, much less is known about this about the more recently discovered per- and polyfluoroalkyl substances (PFAS).

Despite the broad consensus among scientists that food is the main source of PFAS exposure for humans, relatively little is known about the distribution of PFAS in food and this is particularly true for homegrown food. However, over the past decades, consumption of homegrown food has become a notable trend in private gardens located in rural and urban areas, as well as near industry. In particular, keeping free-ranging chickens for egg production and growing vegetables in private gardens have gained popularity worldwide.

The main objective of this thesis was to investigate the accumulation of PFAS in a wide variety of homegrown food categories and the related exposure risk to humans. This involved the identification of local factors in private gardens that may affect PFAS levels in food and a better mapping of the geographical distribution of PFAS in private gardens. An extensive network of 135 volunteers was set up across the province of Antwerp to collect and analyze the necessary data.

The results of chapter 2 and 4 showed that PFAS accumulated most strongly in eggs, followed by vegetables, walnuts and fruits. The Σ PFAS concentrations were significantly higher in annual plants, compared to perennial plants, which could be explained by differences in life-history traits and species-specific characteristics. Free-ranging laying hens fed a diet consisting almost exclusively of kitchen scraps showed higher perfluorooctane sulfonic acid (PFOS) and perfluorooctanoic acid (PFOA) levels in their eggs than hens fed exclusively commercial food. The age of laying hens

seemed to affect levels of some PFAS in eggs, with younger hens showing significantly higher PFOA levels in their eggs. The consumption of two eggs per week could be associated with an exceedance of existing health guidelines at the majority of locations, so health risks due to exposure via homegrown eggs cannot be ruled out. Human intake estimations of plant-based food, based on an average weekly consumption of 1015 g of vegetables and 945 g of fruits, showed that the exposure risk was similar both near and far from the factory site, although the overall contribution to dietary exposure may be relatively large.

In chapter 3, statistical models were developed which showed that egg PFAS concentrations for major compounds (e.g. PFOA, perfluorononanoic acid (PFNA) and PFOS) could be accurately predicted by means of the PFAS soil concentrations, soil pH, clay content and their synergistic interaction effect. These models show application potential for time- and cost-effective risk assessment of PFAS in eggs for gardens. Strong evidence was also found that the bioavailability of PFAS in the eggs is governed by complex interactions of PFAS with diverse soil physicochemical characteristics. Based on this result, directly applicable measures could be formulated that could potentially reduce human exposure to PFAS through egg consumption. In contrast to the models for eggs, the relationships between soil levels and characteristics and vegetable concentrations were weak (chapter 4), indicating that other factors (such as porewater) are likely better measures to explain the accumulation of PFAS in vegetables.

Chapter 5 showed that private gardens closer to a large PFAS point source in Zwijndrecht (Flanders) showed higher concentrations for some compounds in soil, rainwater and eggs which could be associated with historical and recent industrial emissions. Ratios of homologue compound pairs suggested that PFAS concentrations in gardens further away from this point source may be related to long-range airborne transport of precursors and subsequent atmospheric degradation from diffuse sources. PFAS profiles and concentrations within gardens differed greatly between the soil from the vegetable garden segment and the chicken enclosure, which may be due to differences in soil management practices and soil composition. Short-term (2018-2022) changes in PFAS levels were most evident in soil from the chicken enclosure and eggs, while PFAS concentrations in soil from the vegetable garden hardly changed over time. A long-term analysis from 2010-2022 suggests that phase-out and regulatory measures were effective in reducing PFOS and PFOA concentrations

in soil and chicken eggs from gardens near the plant site, but had limited effect at farther distances from the plant site, necessitating further action and monitoring of PFAS diffusion.

Samenvatting

Sinds het begin van de 20^{ste} eeuw is de invloed van de mens op het milieu drastisch toegenomen, hetgeen heeft geleid tot het "Anthropoceen" tijdperk. Het verwijst met name naar de toegenomen uitstoot van chemische stoffen in het milieu door de mens. Veel van deze chemische stoffen, vooral de zeer moeilijk afbreekbare organische pollutanten (POP's), hebben wereldwijd steeds meer publieke aandacht gekregen in de loop der jaren. Het werd namelijk duidelijk dat deze groep stoffen overal in ons milieu werden aangetroffen en grootschalige, nadelige effecten konden hebben op levende organismen, inclusief de mens. Daarom zijn bekende POP's zoals sommige pesticiden en dioxines, uitgebreid bestudeerd op de wijze van verspreiding in het milieu, opstapeling in organismen en toxische effecten. Er is echter veel minder hierover bekend van de recenter ontdekte per- en polyfluoralkylstoffen (PFAS).

Ondanks de brede consensus onder wetenschappers dat voeding de belangrijkste blootstellingsbron is van PFAS voor de mens, is er relatief weinig bekend over de verspreiding van PFAS in voeding en dit geldt in het bijzonder voor zelf geteelde voeding. Nochtans is het consumeren van dergelijke voeding overheen de afgelopen decennia een opmerkelijke trend geworden in private tuinen die landelijk en stedelijk zijn gelegen, zelfs nabij industrie. Vooral het houden van loslopende kippen voor de eiproduktie en het kweken van groenten in private tuinen hebben wereldwijd aan populariteit gewonnen.

Het hoofddoel van deze thesis bestond er in om de opstapeling van PFAS in een grote verscheidenheid aan zelf gekweekte voeding te onderzoeken en het daaraan gerelateerde blootstellingsrisico voor de mens. Er werd hierbij onderzocht welke lokale factoren in de private tuinen een invloed kunnen hebben op de PFAS gehalten in de voeding en de geografische verspreiding van PFAS in private tuinen werd beter in kaart gebracht. Hiervoor werd een uitgebreid netwerk van 135 vrijwilligers opgezet overheen de provincie Antwerpen om de nodige gegevens te kunnen verzamelen en analyseren.

De resultaten toonden aan dat PFAS het sterkst opstapelen in eieren, gevolgd door groenten, walnoten en fruit. De som PFAS gehalten waren beduidend hoger in eenjarige planten vergeleken met meerjarige planten, wat kon worden verklaard door verschillen in levensstrategieën en soort-specifieke verschillen. Vrijlopende legkippen, die een dieet kregen dat bijna uitsluitend bestond uit

keukenresten, hadden hogere perfluorooctaansulfonzuur (PFOS)- en perfluorooctaanzuur (PFOA) gehalten in hun eieren dan kippen die uitsluitend commerciële voeding kregen. De leeftijd van de legkippen beïnvloedde de PFAS gehalten in eieren, waarbij jongere kippen beduidend hogere PFOA-gehalten in eieren vertoonden. Het consumeren van twee eieren per week werd op het merendeel van de locaties geassocieerd met een overschrijding van bestaande gezondheidsrichtlijnen, waardoor gezondheidsrisico's t.g.v. blootstelling via eigen gekweekte eieren niet kunnen worden uitgesloten. Menselijke inname schattingen toonden verder aan dat het blootstellingsrisico via consumptie van plantaardig voedsel, gebaseerd op een gemiddelde wekelijkse consumptie van 1015 g groenten en 945 g fruit, vergelijkbaar was zowel dichtbij als veraf van het bedrijf, hoewel de absolute bijdrage tot de totale blootstelling via de voeding relatief groot kon zijn.

Statistische modellen werden ontwikkeld die aantoonde dat de PFAS gehalten voor belangrijke verbindingen (PFOA, perfluornonaanzuur (PFNA) en PFOS) in de eieren nauwkeurig konden worden voorspeld a.d.h.v. PFAS bodemgehalten en bodemkarakteristieken, zoals het kleigehalte, de pH en hun onderlinge, synergistische interactie effect. De PFAS gehalten in eieren konden accuraat worden voorspeld voor een aantal belangrijke PFAS stoffen, waaronder PFOS. Deze predictiemodellen vertonen sterk toepassingspotentieel voor een tijd- en kosteneffectieve risicobeoordeling van PFAS in eieren voor tuinen. Er werden ook sterke aanwijzingen gevonden dat de biobeschikbaarheid van PFAS in de eieren wordt bepaald door complexe interacties van PFAS met verscheidene fysicochemische bodemkarakteristieken. Op basis hiervan konden direct inzetbare maatregelen worden geformuleerd die toepasbaar zijn om de PFAS gehalten in de eieren blootstelling aan PFAS via consumptie van eieren te verlagen. In tegenstelling tot de modellen voor de eieren, waren de relaties tussen de bodemgehalten en -karakteristieken en de groentengehalten zwak, wat erop wijst dat andere factoren (zoals het poriewater) wellicht betere maatstaven zijn om de opstapeling van PFAS in groenten te verklaren.

Private tuinen dicht bij een grote PFAS puntbron in Zwijndrecht (Vlaanderen) vertoonden hogere gehalten in bodem, regenwater en eieren die in verband kunnen worden gebracht met historische en recente industriële emissies. Verhoudingen van homologe PFAS-verbindingen suggereerden dat PFAS gehalten in verder afgelegen tuinen van deze puntbron konden worden gerelateerd met langeafstand transport via de lucht en atmosferische afbraak van precursoren, afkomstig van diffuse bronnen. Het PFAS profiel en de gehalten binnen tuinen verschilden in sterke mate tussen de bodem afkomstig van de moestuin en de kippenren, wat mogelijks te wijten is aan verschillen in

bodembeheer praktijken. Korte termijn (2018-2022) veranderingen in PFAS gehalten waren het duidelijkst merkbaar in bodem van kippenrennen en eieren, terwijl PFAS gehalten in de bodem van de moestuin nauwelijks veranderden overheen de tijd. Een lange termijn tijdsanalyse van 2010-2022 duidt erop dat uitfaserings- en regelgevende maatregelen effectief zijn geweest bij het terugdringen van de PFOS- en PFOA-concentraties in bodem en kippeneieren van tuinen in de buurt van de fabriekslocatie, maar dat ze op ruimere afstand van de fabriekslocatie een beperkt effect hadden, waardoor verdere maatregelen en opvolging van de PFAS verspreiding nodig is.

Chapter 1: General introduction

1.1 Welcome to the Anthropocene

The human impact on the environmental conditions of planet Earth have undergone profound changes over the last $\pm 10\,000$ years, which represents the geological timeframe often referred to as the Holocene (Rockström et al., 2009). Initially, fire-making and deforestation for agricultural purposes were the earliest manifestations of environmental pollution (Rockström et al., 2009; Steffen et al., 2007). Subsequently, during the Roman reign and medieval period, exploitation of metals (e.g. lead and copper) and coal for supply of military weapons, cookware and fuel were other instances of human-induced environmental pollution (Steffen et al., 2007). Indeed, preindustrial societies already affected the environment on various levels, although their impact was restricted to regional scales (Steffen et al., 2007). Moreover, global biogeochemical processes and climatological conditions remained stable and within the natural variation of the planet's resilience (Borzenkova et al., 2015; Hopcroft et al., 2023).

However, the industrial revolution in the 18th century dramatically increased and accelerated the human-induced impact on our environment (Steffen et al., 2007). This pivotal event abruptly marked both the relatively stable period of the Holocene and the onset of a period with unprecedented environmental changes (Rockström et al., 2009). Termed the Anthropocene or Age of Humans, this period has been characterized by an exponential population growth and extensive global exploitation of natural resources, particularly fossil fuels (Rockström et al., 2009; Steffen et al., 2007). Over the last century, the expansion of industrial (agro)chemistry has led to an enormous increase in the production of chemical substances (Shatalov et al., 2003). Nowadays, the culmination of all these human activities in the Anthropocene has already led to the alarming exceedance of six out of nine defined planetary boundaries (Richardson et al., 2023), with a substantial contribution from global chemical pollution (Persson et al., 2022).

1.2 The rise of organic pollutants

Since the 1950s, the production and usage of new chemical substances has strongly increased (Scheringer et al., 2022; Shatalov et al., 2003). In the last decades, research and public attention has been directed towards a specific group of mainly organic compounds, often categorized as "Persistent Organic Pollutants" (POPs) (Scheringer et al., 2022). Although POPs are diverse in terms

of functional properties and toxicity, they share common characteristics to exhibit relatively large resistance to environmental degradation and bioaccumulation potential in organisms (Shatalov et al., 2003). Bioaccumulation is the phenomenon that a chemical is taken up in an organism at a faster rate than it is egested (Miller et al., 2020). Therefore, the concentrations of a chemical can build up within an organism over time.

The first large-scale occasions of the harmful effects of organic pollutants included the population crash in predatory birds due to egg-shell thinning effects after exposure to pesticides, such as dichlorodiphenyltrichloroethane (DDT), as well as depletion of the ozone layer by chlorofluorocarbons (CFCs) (Richardson et al., 2023). These events demonstrated the widespread environmental distribution and potentially catastrophic impacts that organic pollutants can exert, which led to increased public concern and awareness towards these substances (Newman, 2001). Moreover, regulatory measures quickly emerged to restrict the use of DDT and CFCs (Scheringer et al., 2022). Despite these clear warning-signals and well-documented cases of pollution due to organic pollutants, the importance of their environmental persistence and bioaccumulative properties remained insufficiently acknowledged (Scheringer et al., 2022). Unfortunately, in the beginning of the 21st century, this inattention became evident as perfluorooctane sulfonic acid (PFOS), a major compound within the family of per- and polyfluoroalkyl substances (PFAS), was globally detected in polar bears (*Ursus maritimus*) of Alaska by Giesy and Kannan (2001). Since this influential publication, an exponential increase in articles has been observed describing pollution of numerous PFAS in the global environment and virtually all organisms.

1.3 The PFAS universe

PFAS have been industrially produced and extensively applied on a large scale since the 1940s (Gaines, 2022). Despite their global presence and relatively long production history, our understanding of the impacts of PFAS on the environment and organisms lags behind in comparison to most of the other POPs (Ng et al., 2021). This discrepancy can be partly attributed to the very large diversity of PFAS, containing millions of compounds, which complicates comprehensive risk assessment (Schymanski et al., 2023). Therefore, the next section will introduce the main classification system of PFAS to navigate through this complex PFAS universe. To reduce the risk of

getting lost along the way, a specific focus will be devoted to those PFAS that are of relevance for this thesis.

1.4 Classification and terminology

1.4.1 Polymer substances

PFAS can be broadly divided into two overarching classes as illustrated in Fig. 1.1: the polymer and the non-polymer substances.

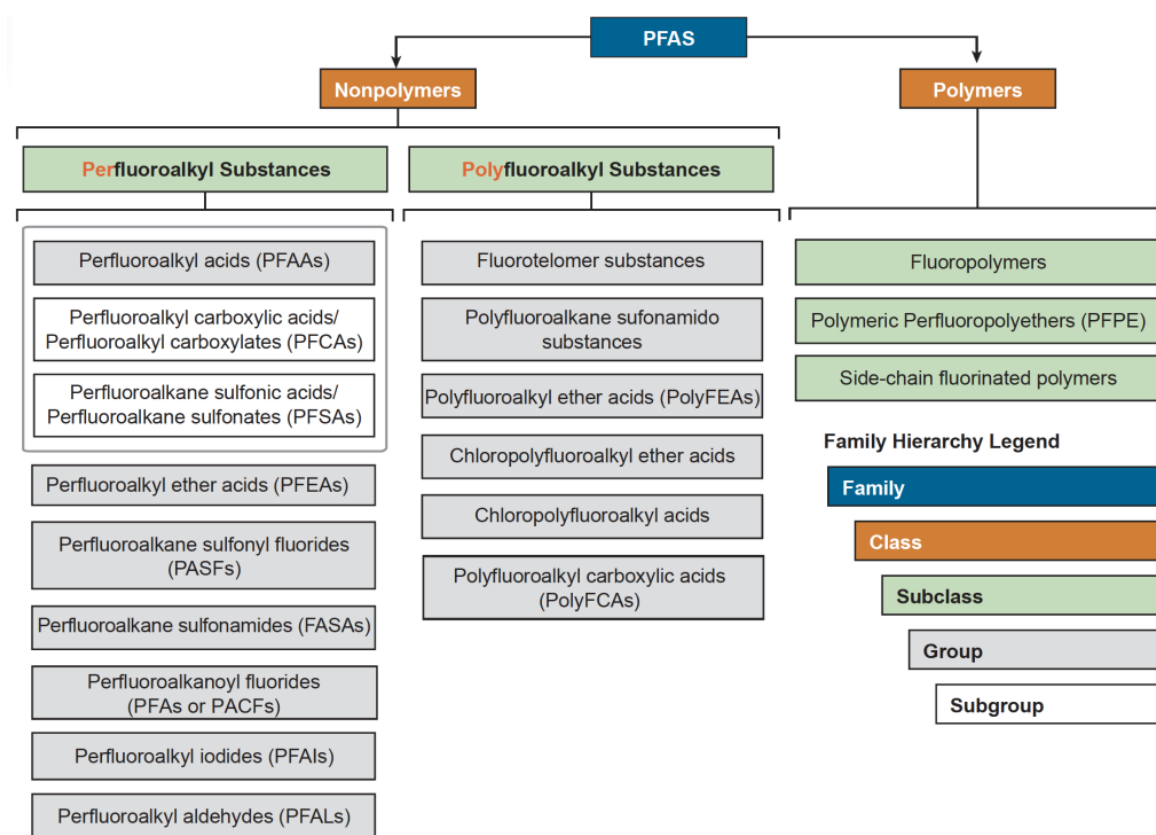


Fig. 1.1: Family tree showing the broad classification of the main groups of per- and polyfluoroalkyl substances (PFAS) that are most commonly reported in the environment. Adapted from ITRC (2023).

The polymer substances are stable, of high-molecular weight that are typically formed via specific polymerization reactions (Buck et al., 2011). Polymerization is the merging of smaller molecules, called monomers, into a larger molecule (i.e. the polymer). One prominent example is polytetrafluorethylene (PTFE), better known under the brand name Teflon, which has been used in numerous commercial applications (e.g. anti-stick layer in Tefal pans) (Henry et al., 2018). Polymer

substances are very stable to a variety of extreme conditions and due to their high-molecular weight, they are considered non-bioaccumulative in organisms and thus of low concern (Henry et al., 2018). However, it should be noted that non-polymer substances, which are used as processing aids for the production of polymers and are of high concern (see 1.4.2), can be released into the environment during the production process (Cousins et al., 2020). Moreover, waste treatment (e.g. incineration and landfill disposal) at the end of the polymer product's life cycle can also result in degradation into non-polymer substances and release to the environment (Cousins et al., 2020).

1.4.2 Non-polymer substances

The second major class of PFAS are non-polymeric substances which commonly contain an alkyl chain with at least one C_nF_{n2+1} moiety as basic chemical structure, in combination with at least one functional group (Wang et al., 2021). Their alkyl chain can be partly (*poly*) or completely (*per*) fluorinated and each of these two subclasses can be further divided into separate groups, according to specific modifications of the functional group(s) and/or alkyl chain (Henry et al., 2018). This class contains nearly 78% of the commercially relevant PFAS that have been globally produced in large quantities (Buck et al., 2021). Moreover, numerous compounds within this class have been associated with widespread environmental contamination, accumulation in organisms and adverse health effects (De Silva et al., 2021; Fenton et al., 2021). For these reasons, the 29 targeted PFAS considered in the present thesis belong to this class (Table 1.1), which will be further explained in more detail.

To date, most research and public attention has been devoted to the group of perfluoroalkyl acids (PFAAs), which have a completely fluorinated alkyl chain combined with a functional acid head group (Fig. 1.2) (Buck et al., 2011).

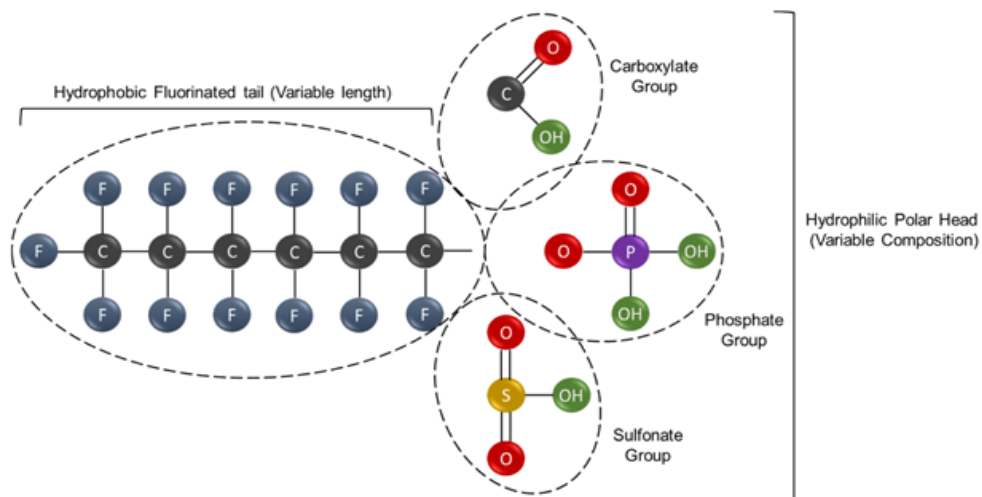


Fig. 1.2: The generic chemical structure of perfluoroalkyl acids (PFAAs) with the typical fully fluorinated alkyl chain and the functional head group, which are variable among the individual PFAAs. Adapted from Panieri et al. (2022).

The subgroup of perfluoroalkyl carboxylic acids (PFCAs) contains a carboxylic head group and the perfluoroalkyl sulfonic acids (PFSAs) a sulfonic head group (Buck et al., 2011). Some of the representatives in these subgroups belong to the best studied PFAS in terms of environmental distribution and toxicity (Henry et al., 2018). Well-known examples include perfluorooctanoic acid (PFOA) and perfluorooctane sulfonic acid (PFOS). Moreover, PFCAs and PFSAs with respectively ≥ 7 and ≥ 6 perfluorinated carbons are often defined as “long-chain PFCAs” and “long-chain PFSAs”, while lower respective number of perfluorinated carbons are often referred to as “short-chain PFCAs” or “short-chain PFSAs” (Cousins et al., 2020).

Over the last two decades, increasing scientific evidence revealed the bioaccumulation potential and toxicity of PFAAs, which resulted in the industrial phase-out of PFOS, PFOA and related long-chain PFAAs from 2002 onwards (Ng et al., 2021). As a result, the fluorochemical industry has redirected its production focus in recent years towards short-chain PFAAs and the development of new substitute compounds (Buck et al., 2021). These new substitutes have been assumed to be less bioaccumulative than the long-chain PFAAs, but much less monitoring data are available for these compounds (Munoz et al., 2019). The majority of the other groups shown in Fig. 1.1, that have not been discussed yet, belong to these substitute compounds.

Globally, the most commonly reported substitute compounds include the perfluoroalkyl ether acids (PFEAs), which have a chemical structure homologous to the PFAAs, but have at least one ether functional group in their alkyl chain (Cousins et al., 2020; Munoz et al., 2019). Moreover, fluorotelomer substances also represent a large group of replacement compounds (Buck et al., 2021; Lu et al., 2017). These compounds are named using an “n:x” prefix in which the “n” indicates the number of fully fluorinated carbon atoms and the “x” the number of non-fluorinated carbon atoms (Washington et al., 2014). Notably, these fluorotelomer substances are precursor compounds that can (bio)degrade into short-chain PFCAs (Harding-Marjanovic et al., 2015). Finally, perfluorobutane sulfonamide (FBSA) is a member of the perfluoroalkane sulfonamides (FASAs) and has a fully fluorinated alkyl chain with a sulfonamide functional head group (Chu et al., 2016).

For the present thesis project, 17 PFAAs (both short-chain and long-chain compounds), eight perfluoroalkyl ether acids, three fluorotelomer substances and one perfluoroalkane sulfonamide were selected as targeted analytes (Table 1.1).

Table 1.1: List of all the targeted per- and polyfluoroalkyl substances (PFAS) in this thesis project and the PFAS group to which each of them belongs, according to the conventional classification system of PFAS (ITRC, 2023).

Compound name	Abbreviation	PFAS group
Perfluorobutanoic acid	PFBA	Perfluoroalkyl carboxylic acids
Perfluoropentanoic acid	PFPeA	
Perfluorohexanoic acid	PFHxA	
Perfluoroheptanoic acid	PFHpA	
Perfluorooctanoic acid	PFOA	
Perfluorononanoic acid	PFNA	
Perfluorodecanoic acid	PFDA	
Perfluoroundecanoic acid	PFUnDA	
Perfluorododecanoic acid	PFDoDA	
Perfluorotridecanoic acid	PFTrDA	
Perfluorotetradecanoic acid	PFTeDA	
Perfluorobutane sulfonic acid	PFBS	Perfluoroalkyl sulfonic acids
Perfluoropentane sulfonic acid	PFPeS	
Perfluorohexane sulfonic acid	PFHxS	
Perfluoroheptane sulfonic acid	PFHpS	
Perfluorooctane sulfonic acid	PFOS	
Perfluorodecane sulfonic acid	PFDS	Fluorotelomer substances
4:2 fluorotelomer sulfonic acid	4:2 FTS	
6:2 fluorotelomer sulfonic acid	6:2 FTS	
8:2 fluorotelomer sulfonic acid	8:2 FTS	

Perfluorobutane sulfonamide	FBSA	Perfluoroalkane sulfonamides
Hexafluoropropylene oxide-dimer acid	HFPO-DA	
4,8-dioxa-3H-perfluorononanoic acid	ADONA	
Perfluoro-4-oxapentanoic acid	PF4OPeA (PFMPA)	
Perfluoro-5-oxahexanoic acid	PF5OHxA (PFMBA)	Perfluoroalkyl ether acids
Perfluoro-3,6-dioxaheptanoic acid	3,6-OPFHpA (NFDHA)	
Perfluoro(2-ethoxyethane) sulfonate	PFEESA	
9-chlorohexadecafluoro-3-oxanonane-1-sulfonate	9Cl-PF3ONS	
11-chloroeicosafluoro-3-oxaundecane-1-sulfonate	11Cl-PF3OUdS	

Despite the phase-out of some long-chain PFAAs, they are still widespread in the environment and concentrations remain high (Cousins et al., 2020; Miller et al., 2015). On the other hand, short-chain PFAAs have been increasingly produced over the last decades, as previously discussed. The selected substitute compounds (i.e. fluorotelomer substances and perfluoroalkane sulfonamides) are understudied compared to the PFAAs, but have also been increasingly reported over the last decades (Dhore and Murthy, 2021). Finally, the motivation to select compounds was sometimes also based on site-specific expectations. For instance, FBSA is the main precursor of post-2002 fluorinated surfactant products (e.g. Scotchgard fabric protector) of the 3M Company, which was the main point source within the study area of the present thesis (see section 1.10).

1.5 Properties and usage

When looking into more detail at the chemical structure of PFAS (e.g. Fig. 1.2), some rather exceptional physicochemical properties can be observed. The covalent C-F bond is extremely strong and stable, due to the very high electronegativity and small size of the fluorine atom (Buck et al., 2011). These multiple C-F bonds in the alkyl chain provide very high resistance to environmental and biological degradation (Grgas et al., 2023). Moreover, the fluorinated alkyl chain of PFAS has both lipophobic and hydrophobic characteristics, which provides them stain-, oil- and water repellent properties and making them effective surfactants (Buck et al., 2011; Glüge et al., 2020).

Additionally, their functional (head) groups enable binding with polar molecules and result in water soluble (i.e. hydrophilic) properties to various degrees, depending on the alkyl chain length, structure and type of functional groups (Buck et al., 2011). For instance, shorter-chained PFAS generally exhibit a larger degree of hydrophilicity than their longer-chained counterparts. PFAS are

strong acids and their pKa values are generally much lower than the majority of prevailing pH values in the environment (Ding and Peijnenburg, 2013). Consequently, they are predominantly present in their charged ionic form under common environmental conditions. Unlike most other POPs, PFAS show relatively large affinity towards protein structures due to hydrophobic and hydrogen-bonding interactions of the alkyl chain and functional groups, respectively, with amino-acids (Zhang et al., 2013).

Due to the combination of their surfactant-, water-, stain-, oil- repellent properties and very high resistance to degradation, PFAS have been very useful in an enormous range of industrial and commercial applications (Buck et al., 2011; Glüge et al., 2020). Large-scale examples in the industry are the usage of PFAS as processing-aids for the production of fluoropolymers (e.g. Teflon), as mist suppressants during chrome metal plating and as additives in semi-conductors and hydraulic fluids in the electro, automotive and aviation industry (Gaines, 2022; Glüge et al., 2020). For commercial products, PFAS have been widely used as surfactants in firefighting foams, as water- and oil repellent agents in food-packaging and paper products (Glüge et al., 2020), as well as in many daily household products (Gaines, 2022). Clearly, the versatile physicochemical properties and usage of PFAS have given them an important economic role and large degree of dependency in our society (Cousins et al., 2019; De Silva et al., 2021). Unfortunately, the major downside of this success has also led to complex and global contamination of our environment, which will be further elucidated in the following section.

1.6 Environmental fate and behaviour

The environmental fate and behaviour of chemicals is defined as their transport, partitioning and potential transformation reactions in environmental compartments (e.g. soil and atmosphere), after release into the environment (Ahrens and Bundschuh, 2014). These main processes are summarized for PFAS in Fig. 1.3 and will be explained with a specific focus on the soil and the terrestrial ecosystem, within the scope of the present thesis project.

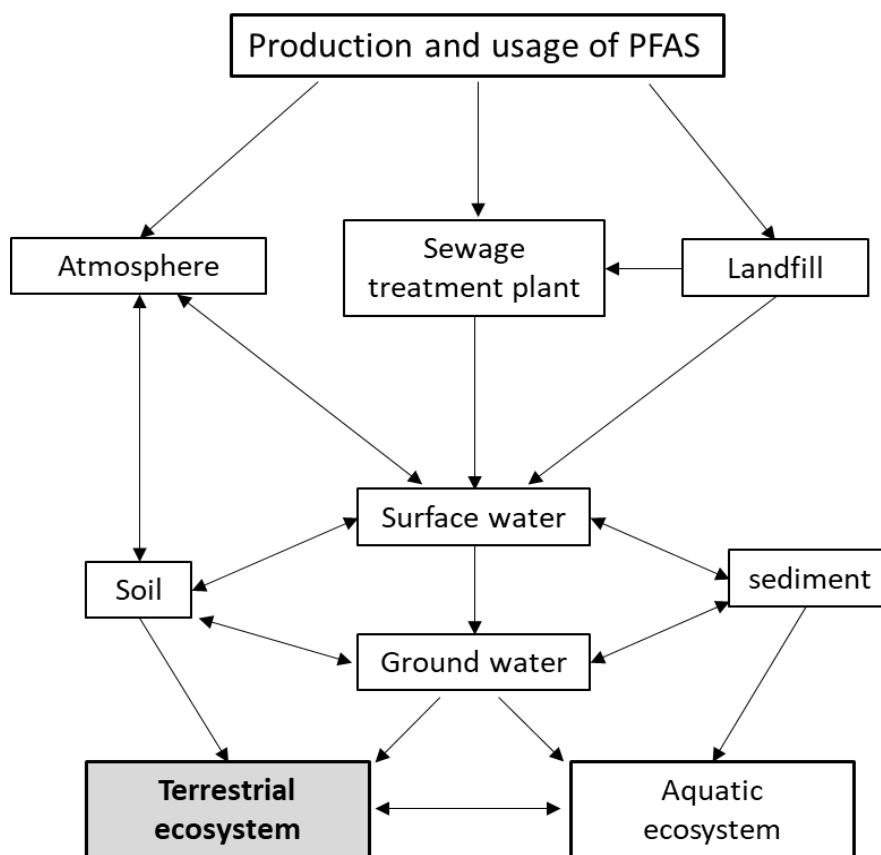


Fig. 1.3: Conceptual framework showing the pathways of PFAS into various environmental compartments and their fate. The present thesis project took place within the terrestrial ecosystem, highlighted in gray. Adapted from Ahrens and Bundschuh (2014) with minor modifications.

PFAS are introduced into the environment via direct release from primary point sources (e.g. fluorochemical production plants, landfills and sewage treatment plants) and through diffuse sources via the usage of consumer products (De Silva et al., 2021). Additionally, gas-phase and dust particle-bound PFAS can undergo (long-range) atmospheric transport. This is especially relevant for

precursor compounds (e.g. fluorotelomer substances and FBSA), as they are more volatile than PFAAs (Ahrens and Bundschuh, 2014). Precursors can be further subject to degradation into PFAS in the atmosphere or in other environmental compartments under (an)aerobic conditions (Prevedouros et al., 2006). As previously discussed, PFAS are water-soluble to various degrees and they are dominantly present in their anionic form under common environmental conditions, due to their low pKa values. Therefore, water represents the main transfer medium throughout the environment (Fig. 1.3) (Ghisi et al., 2019). The subsequent pollution of the soil and the water in the terrestrial ecosystem depends on the partitioning between these two compartments (Fig. 1.3). On its turn, this partitioning process will be largely affected by both the site-specific soil characteristics and the physicochemical properties of the PFAS (Ahrens and Bundschuh, 2014).

1.6.1 Soil pollution

Soils are important reservoirs of many POPs, including PFAS, and can be contaminated via multiple pathways (Rankin et al., 2016). In aquatic ecosystems, the natural water flow can dilute and disperse pollutants, which is limited in soils (Xiao et al., 2015). The strong C-F bond makes PFAS extremely persistent in the environment, posing exposure risks for generations. For instance, the environmental half-life of PFOS in soil under common environmental conditions has been estimated to be at least 41 years (Hekster et al., 2002).

Besides contamination through atmospheric deposition from point and diffuse PFAS sources (Ahrens and Bundschuh, 2014), the disposal of PFAS waste through burial in landfills and industrial wastewater can also contribute to soil pollution (Lang et al., 2017; Panieri et al., 2022). Digested sewage sludge (i.e. biosolids) represents a major source of soil contamination when applied to agricultural fields (Johnson, 2022). Moreover, field irrigation with contaminated surface or ground water can be an important source of soil pollution (Ghisi et al., 2019; Scher et al., 2018). Soils can also be directly polluted during training activities at military-, airport- and firefighting sites through the release from firefighting foams (Glüge et al., 2020). Clearly, the source and degree of contamination can largely vary according to the site-specific usage. Numerous studies observed that concentrations of individual PFAS in soil vary across multiple orders of magnitude, from as low as <1 ng/g dry weight (dw) in remote non-suspect areas up to concentrations exceeding 1000 ng/g dw near hotspots (Ranking et al., 2016; Brusseau et al., 2020). However, it should be noted that monitoring studies at sites without nearby known sources are still limited (Brusseau et al., 2020).

As mentioned earlier, PFAS pollution of the soil does not only depend on site-specific usage, but also on the site-specific soil characteristics and the physicochemical properties of PFAS.

1.6.2 Transport and partitioning in the soil

PFAS can migrate with water percolating through the soil and be adsorbed to soil particles, which can affect their transport. They can bind to naturally occurring soil organic matter (e.g. organic carbon) and clay minerals via hydrophobic and electrostatic interactions of the fluorinated alkyl chain and the functional groups, respectively (Li et al., 2018a). The adsorption strength of PFAS generally increases with longer chain lengths, while the functional group also affects the partitioning behavior in the soil. For instance, PFAS with a carboxylic (e.g. PFCAs) group will show lower sorption strength than those with a sulfonic acid group (e.g. PFSAAs) (Li et al., 2018a). Moreover, the ether linkage and hydrogen substitution inserted in perfluoroalkyl ether and fluorotelomer substances (Table 1.1) will also lower the sorption strength to the soil (Nguyen et al., 2020). Furthermore, adsorption increases with lower soil pH levels and higher concentrations of divalent cations (Cai et al., 2022).

1.7 Human exposure

1.7.1 Entrance in the human food-chain

Based on the previous section, it is clear that PFAS are omnipresent in the terrestrial environment through various pathways and that they can reside for years in the soil. Evidently, the soil not only represents a major reservoir for PFAS, but also forms the foundation of the terrestrial food-chain. Therefore, soils represent an important exposure medium to terrestrial organisms, of which some can serve as important food sources to humans, i.e. crops and livestock. These organisms can bioaccumulate PFAS and these substances can further biomagnify in humans (Death et al., 2021; Ghisi et al., 2019). Biomagnification is defined as the increase of the chemical's concentration in an organism, compared to its prey (Miller et al., 2020).

Crops grown on contaminated soil largely accumulate PFAS via uptake by the roots and can subsequently translocate them to other plant organs via passive (e.g. diffusion) and active transport pathways (e.g. transport proteins, aquaporin and anion channels) (Adu et al., 2023). Moreover,

PFAS can also be taken up via leaf absorption of deposited contaminated dust onto the leaf surface, although the contribution of this pathway is generally considered to be low (Adu et al., 2023). Studies have demonstrated that the amount of PFAS in plants is directly proportional to the soil concentrations (Ghisi et al., 2019), but uptake is largely controlled by a complex combination of factors: the chain lengths, functional group, plant species and soil characteristics (Xu et al., 2022). Livestock can take up PFAS via multiple pathways, through the consumption of contaminated soil, dust, drinking water and feed when foraging (Death et al., 2021; Xing et al., 2023). Generally, PFAS with short-chain lengths tend to accumulate more in plants, while long-chain PFAS are accumulated more in animal-derived foods (Vorst et al., 2021). The uptake mechanisms and the role of various affecting (a)biotic factors on this process in both plants and animals under different exposure scenarios (e.g. close versus remotely from point sources) remain poorly understood.

Humans can have a relatively high trophic position in the terrestrial food-chain and hence have a high biomagnification potential of chemicals (Darimont et al., 2015; Roopnarine, 2014). Furthermore, PFAS show large affinity towards proteins (cf., section 1.5), which are the building blocks of all living organisms on earth and therefore they tend to bioaccumulate relatively easy (De Silva et al., 2021).

1.7.2 Exposure pathways

Humans can take up PFAS via intake of food, water and dust through the digestion system, but also via inhalation of dust through the respiratory system and via dermal uptake through the skin (Roth et al., 2020). Generally, intake of PFAS via food followed by water are the most important exposure pathways (Panieri et al., 2022). However, factors such as lifestyle habits, professional occupation and behavioural differences among age groups can greatly affect the relative contribution of these various pathways (De Silva et al., 2021; Schultes et al., 2018). For instance, frequent usage of personal care products may increase the relative contribution via dermal uptake (Ragnarsdóttir et al., 2022) and hand-to-mouth contact in toddlers may increase the relative contribution of dust ingestion (De Silva et al., 2021).

Once PFAS are taken up in the human body via ingestion, the blood circulation will transfer these compounds to various targeted organs. Due to their protein affinity, PFAS will be mainly distributed in the blood serum, bound to carrier-proteins (e.g. albumin) and also to other protein-rich organs

including the liver and the kidney (Roth et al., 2020). The biological serum half-lives of PFAS in humans greatly vary among individual compounds and may range from several days for the short-chain compounds to >5 years for the long-chain compounds in the case of PFAAs (Goodrum et al., 2020). Moreover, the type, number and position of functional groups in the chemical structure can also affect the biological half-lives of PFAS (Goodrum et al., 2020). The effective absorption of PFAS into the human body can be influenced by their bioavailability (i.e. the fraction of the chemical that reaches the systemic circulation). The bioavailability of PFAS is determined by the structural properties (e.g. chain length and functional groups) and the nutrient composition of the food (Zhu et al., 2023). After inhalation of contaminated dust, PFAS may be accumulating primarily in the lungs (Pan et al., 2023; Pérez et al., 2013).

Human exposure to PFAS is generally higher in the northern hemisphere than in the southern hemisphere, which is probably due to industrialization and dietary differences (Schiavone et al., 2023). Multiple PFAS have been detected in more than 98% of the population in the United States (Roth et al., 2020). However, the actual accumulation can also be highly site-specific as demonstrated by Sonne et al. (2023). The authors examined blood serum concentrations of an Inuit cohort, which lived in a hunter-gatherer community in East Greenland. Despite their remoteness from industrial activities, some of the highest blood serum concentrations were measured out of non-occupational exposure populations. This result could be attributed to the diet rich in muscle of large marine mammals, which also demonstrates the importance of biomagnification and bioaccumulation in exposure scenarios.

1.7.3 Exposure assessment

Basically, human exposure to substances can be assessed by means of two methods: monitoring to know the external, indirect exposure and biomonitoring to know the internal, direct exposure (Papadopoulou et al., 2016). The external exposure can be evaluated by measuring the chemicals in various relevant, environmental compartments (e.g. air, water, dust and food) than can potentially be linked with the human exposure (De Silva et al., 2021; Papadopoulou et al., 2016). On the other hand, internal exposure is examined by measuring the chemical concentrations in human tissues (e.g. blood, urine or hair) (De Silva et al., 2021; Papadopoulou et al., 2016). Eventually, both methods can be supplemented with questionnaire data and, in the case of external exposure, through the assessment of exposure factors such as the inhalation rate of dust or the

intake amount and frequency of food (De Silva et al., 2021). Both methods have strengths and limitations in their own right.

External exposure is useful to assess the importance of different exposure pathways and is very helpful to elucidate each of the underlying factors that ultimately drive the internal exposure (Papadopoulou et al., 2016). In this way, a broad range of fundamental information can be obtained that may be translated into applicable mitigation and remediation measures to lower internal exposure. However, monitoring can be costly, laborious and time-consuming when multiple sources are considered, while sometimes no *a priori* probable factors can be identified that may be important to include in the monitoring. The present thesis is an example of external exposure assessment, as will be clear from section 1.9.

Conversely, internal exposure can provide a direct proxy of the body contamination burden and takes implicitly into account the uptake via digestion, inhalation or dermal uptake (Jeddi et al., 2022). In addition, potentially relevant health biomarkers (i.e. a biological response that indicates a potential health effect) can be measured in the tissue. The disadvantages of biomonitoring are the difficulties in disentangling potential exposure sources which hamper the interpretation of the tissue measurement. Moreover, ethical considerations that should be weighed when targeting certain study cohorts (e.g. children) can be challenging for the feasibility to obtain the necessary research criteria. The recently launched projects of the Flemish government from 2021 onwards to measure PFAS in blood are all examples of internal exposure (see Textbox 1.1). Fortunately, the external and internal exposure method complement each other, and combining them offers a more comprehensive view of both the indirect and direct human exposure, aiding in identifying dominant exposure routes and implementing appropriate mitigation measures.

Textbox 1.1:

The PFAS pollution in Antwerp, nearby a major fluorochemical production site of the 3M Company, received huge public and media attention in the spring of 2021. This gave rise to several research projects launched by the government to measure the blood in participating citizens living within a radius of 5 km from this point source. Noteworthy, the PFAS@Home study (Colles et al., 2022) and the human biomonitoring study in young adolescents (Consortium UAntwerpen et al., 2023) were partially concurrent with the present thesis.

1.7.4 Health effects

Over the last years, increasing scientific evidence from both experimental studies (both *in vitro* using human cell assays and *in vivo* exposure studies on laboratory animals) and epidemiological research has indicated that PFAS can be associated with concerning health effects (Fenton et al., 2021; Panieri et al., 2022; Zeng et al., 2019). Based on the integration of these study outcomes, PFAS have been related with increased cholesterol levels, reduced immune response, disturbance of the sex- and thyroid endocrine system, developmental effects and fatty liver disease (Fenton et al., 2021; Panieri et al., 2022). Elevated, long-term exposure (e.g. in occupational fluorochemical plant workers) has also associated PFAS with increased risk of certain cancer types, such as breast- and testicular cancer (Fenton et al., 2021; Roth et al., 2020; Sunderland et al., 2019).

It should be stressed that there are still a lot of uncertainties and knowledge gaps regarding the potential health outcomes of PFAS. Firstly, the majority of the available data on health effect studies have only been focusing on the group of PFAAs. Within this group, the well-known PFOS and PFOA are the most thoroughly studied compounds (Pelch et al., 2022), as they are probably among the most widespread and abundant PFAS in our environment (Rankin et al., 2016). However, it should be stressed that the environmental distribution of many other PFAS is still poorly characterized. Nevertheless, these compounds may also be ubiquitous in environmental compartments and biota, e.g. ultra-short chain PFAS in rainwater (Pike et al., 2021). Secondly, the chronic and mixed exposure effects taking into account the interaction with other pollutants are still poorly understood (Fenton et al., 2021; Pan et al., 2023) and the mode of action (i.e. the actual mechanism) for the potential health effects is still not fully elucidated. Lastly, it is still unclear to which extent these health outcomes are a result of either chronic, cumulative exposure throughout life or exposure during critical developmental stages (e.g. *in utero*, childhood, puberty, or adulthood) (Ng et al., 2021).

These uncertainties with respect to health risks are also reflected in the established health guidelines (i.e. threshold values, based on health effects, for evaluation of potential health risks) for PFAS, which can considerably vary among continents. For instance, the USA has applied individual intake thresholds for PFOS and PFOA of 14 and 21 ng/kg bodyweight (bw) per week, respectively (ATSDR, 2021). These values were based on the lowest concentration level at which no effects were observed on immune, liver- and developmental health endpoints in laboratory animals. On the other hand, the European Union established a combined intake threshold of 4.4

ng/kg bw per week for the sum of four commonly detected PFAAs in human blood (i.e. PFHxS, PFOS, PFOA and PFNA), derived on the basis of a decreased immune response after vaccination (EFSA, 2020).

Importantly, despite the differences in these guideline values, their evolution over time have all been pointed towards the same direction: they have become much more stringent over the last decades (Cousins et al., 2022). In 2008, the EFSA established a health guideline for PFOS and PFOA of 150 and 1500 ng/kg bw per day, based on the liver toxicity in rats as underlying endpoint (EFSA, 2020). This is a 2-3 orders of magnitude difference compared to the guideline of 4.4 ng/kg bw per week, established in 2020 (EFSA, 2020). Similar time trends can also be observed with respect to drinking water guidelines (Cousins et al., 2022). Clearly, these time trends demonstrate that continuing exposure monitoring and risk assessment of PFAS remains crucial.

1.8 Food contamination

Until now, we have described how PFAS can enter the terrestrial ecosystem, due to their widespread usage, mobility in water, persistence and bioaccumulation potential. Clearly, the soil represents an important environmental sink of PFAS and way to enter the human food-chain. Food is the main exposure source of PFAS in humans and these substances can be associated with an array of health effects, as outlined in the previous section. Therefore, the following sections will examine more closely the distribution of PFAS in food and the major knowledge gaps that still exist, particularly with respect to homegrown food.

1.8.1 Commercial food

As a result of their bioaccumulation potential, PFAS have been detected in a wide range of commercial food items. In addition, contamination can also occur via industrial processing of food and migration from food-contact materials (Gebbinck et al., 2013; Lerch et al., 2023). Early monitoring studies (during the first decade of the 21st century) in commercial food were hampered by low analytical sensitivity, low number of targeted analytes and differences among sampling designs (e.g. pooled food baskets versus individual food items) (D'Hollander et al., 2015). These methodological issues decreased comparability among studies and made it difficult to derive reliable estimates of human exposure.

From 2009 to 2013, the European PERFOOD project was conducted which developed a harmonized sampling design and increased analytical performance to monitor commercial food in four countries (Belgium, Czech Republic, Italy and Norway). The highest concentrations were found in seafood, eggs, (offal) meat and fruits although the measured concentrations were in overall low (i.e. below the limit of quantification (LOQ) to ± 0.50 ng/g wet weight (ww)). In line with the expectations, foods derived from plants, such as fruits and vegetables, played a crucial role in the intake of mainly short-chain PFAAs in our diet. Meanwhile, long-chain PFAAs were dominantly present in animal-based foods, especially fish, seafood and offal food (Cornelis et al., 2012; D'Hollander et al., 2015; Herzke et al., 2013; Klenow et al., 2013). Recently, the general occurrence of PFAS in food was reviewed by Pasecnaja et al. (2022) and mostly confirmed the reported results from the PERFOOD project.

Although these monitoring studies provided valuable data on the general presence of PFAS in a wide variety of food items, important uncertainties could be identified that required further research. Generally, standardized methods of sampling are a great shortcoming of PFAS monitoring in commercial food (Vorst et al., 2021). The origin of the food items was based on the country level and the precise geographic origin of the food was not known. Therefore, the exposure background of the food was not known which may hamper an accurate interpretation of the monitoring outcome. Moreover, the food items were often pooled under variably defined food categories with a different composition of individual food items, which could bias the inter-study comparability. Lastly, the targeted list of compounds only included PFAAs and was mostly focused on four compounds for which health guidelines were established (EFSA, 2020; Pasecnaja et al. 2022)

1.8.2 Homegrown food: a major knowledge gap

In contrast to commercial food, very limited data on PFAS concentrations in homegrown food are currently available in the literature. If the terms “PFAS”, “food”, “garden” and/or “home” are given as input keywords into literature databanks (e.g. Web of Science), resulting hits for only 20 publications become available. From those publications, only three articles report data of PFAS in homegrown food: three on homegrown eggs (D'Hollander et al., 2011; Gazzotti et al., 2021; Zafeiraki et al., 2016) and only one on homegrown crops (Scher et al., 2018). Moreover, only very few of these studies take into account the factors that contribute to PFAS accumulation in the homegrown food, and if so, these are limited to the husbandry type (Gazzotti et al., 2021).

Over the last decade, humans consuming products from self-cultivation have become a remarkable trend in rural, urban and even industrial areas (Church et al., 2015; Van der Jagt et al., 2017). Particularly, the maintenance of free-ranging chickens (*Gallus gallus domesticus*) for egg production and cultivation of vegetables in private gardens have gained worldwide popularity (Capoccia et al., 2018; Padhi, 2016). Despite this increasing popularity of self-cultivated food and the widespread existence of PFAS, there is very little information on the potential human health risks linked to PFAS exposure through homegrown food. Crucial data regarding the geographic distribution of PFAS on local and regional levels, which could significantly aid in risk assessment, are also lacking. Therefore, extensive monitoring of PFAS in homegrown food is urgently needed.

From various perspectives, private gardens also represent an interesting study system to monitor PFAS and assess the human exposure risk. These particular areas are highly prone to human interventions and can be influenced by various degrees of urbanization and industrialization (Tresch et al., 2018). This enables the implicit inclusion of a large range of site-specific variation and thus a broad risk assessment for various exposure scenarios. Furthermore, monitoring in homegrown food can overcome some of the difficulties experienced in monitoring of commercial food (cf., section 1.9.1). As the samples are collected *in situ* at the private gardens, precise knowledge of the geographic origin and exposure background can be obtained, which considerably reduces sampling bias. Moreover, standardized sampling methodologies and procedures can be effectively applied through the set-up of consistent volunteering criteria to the participating gardeners.

Apart from their relevance with respect to human exposure, homegrown eggs and crops represent promising targeted matrices to monitor PFAS. Eggs are high in protein content, to which PFAS show high affinity, and represent an important elimination route in birds (Wang et al., 2019; Groffen et al., 2019a). Chickens are the most prevalent bird species in terms of biomass and live in close proximity to humans, which enhances the generalization potential of the obtained monitoring results (Scaramozzino et al., 2019). Free-ranging laying hens can also be potential bioindicators of organic pollutants as they live in close proximity to humans and share similar exposure pathways as other terrestrial organisms (Kudryavtseva et al., 2020).

Free-ranging laying hens have continuous access to outdoor terrain of private gardens and hence can be exposed to PFAS via multiple sources (e.g. soil, water, dust and feed), which allows us to gain

knowledge on the relative contribution of various exposure sources (Waegeneers et al., 2009). Moreover, free-ranging laying hens are geophagous animals that actively ingest soil particles (Kijlstra, 2004). This makes them an ideal model species to study the influence of soil characteristics on the bioavailability of PFAS to hens, which is still very poorly understood in terrestrial organisms. As opposite to chickens, crops have very different exposure pathways (see section 1.7.1) which allows an interesting comparative approach in terms of accumulation between two contrasting taxa.

1.9 Thesis outline: main research hypotheses and objectives

The overarching hypotheses of this thesis project are formulated as followed:

Hypothesis 1. PFAS concentrations in homegrown eggs and vegetables can be predicted by means of soil PFAS concentrations and characteristics.

Hypothesis 2. The PFAS accumulation in the food and relative exposure risk is dependent on the food type, local abiotic and biotic factors within the private garden and the orientation and distance towards a major fluorochemical plant.

Hypothesis 3. Homegrown food represents an important exposure source of PFAS to humans by exceeding available health risk guidelines.

These hypotheses were tested in four chapters, which are further described below. Hypothesis 1 was investigated in chapters 3 and 4. Hypothesis 2 was examined throughout all the chapters and hypothesis 3 was elaborated in chapters 2 and 4. The connection between the chapters and how they are related to each other is conceptually shown in Fig. 1.5.

Chapter 2: Home-produced eggs: an important human exposure pathway of perfluoroalkylated substances (PFAS)

The PFAS profile and concentrations was assessed in homegrown eggs in relation to the distance from a major point source in Antwerp (Belgium). Additionally, the potential influence of housing

conditions and age of laying hens was examined, based on survey data. Lastly, the human exposure risk was evaluated with available health risk guidelines.

Chapter 3: Prediction of perfluoroalkyl acids (PFAAs) in homegrown eggs: Insights into abiotic and biotic factors affecting bioavailability and derivation of potential remediation measures

Robust generalizable empirical models were developed and validated to predict PFAS concentrations in homegrown eggs, taking into account the potential influence of corresponding soil concentrations, rain water concentrations and a broad set of soil characteristics. These models were based on an extensive dataset of gardens from industrial, urban and rural areas. Moreover, an explanatory analysis was conducted between the soil characteristics and egg concentrations to gain insights into the potential role of soil characteristics on the bioavailability of PFAS in the eggs. Furthermore, potential relationships between egg concentrations and feed sources (e.g. soil, earthworms and homegrown crops) of the free-ranging laying hens were examined to assess their role in the possible transfer of PFAS to the eggs.

Chapter 4: Per- and polyfluoroalkyl substances (PFAS) in homegrown crops: accumulation and human exposure risk

The accumulation of PFAS in the edible parts from a large variety of selected crop categories (both annual and perennial species) was examined in relation to the distance from a major point source in Antwerp (Belgium). Additionally, the PFAS profile and concentrations in the soil of these gardens was assessed along a depth range of 0-45 cm. Moreover, empirical regression models were constructed to identify soil parameters that could potentially affect crop bioavailability and to evaluate the predictability of PFAS concentrations in crops, taking into account the soil concentrations, rainwater concentrations and multiple soil characteristics. Furthermore, the dietary intake and potential health risks to humans from consuming crops were evaluated according to existing health guidelines

Chapter 5: Dynamic spatiotemporal changes of per- and polyfluoroalkyl substances (PFAS) in private gardens at different distances from a fluorochemical plant

Based on all the obtained data of the sampling campaigns, the spatiotemporal distribution of PFAS in private gardens across the Province of Antwerp was examined, taking into account the wind orientation towards a major fluorochemical plant. Moreover, potential differences in terms of PFAS profile and concentrations between functionally different garden segments (i.e. vegetable garden soil versus chicken enclosure soil) were investigated. Potential changes in repeatedly sampled private gardens before and after local, intensive road infrastructure works (i.e. Oosterweel) were assessed. Finally, potential long-term changes in PFOS and PFOA concentrations for soil and eggs were examined by adopting literature data from the same study area.

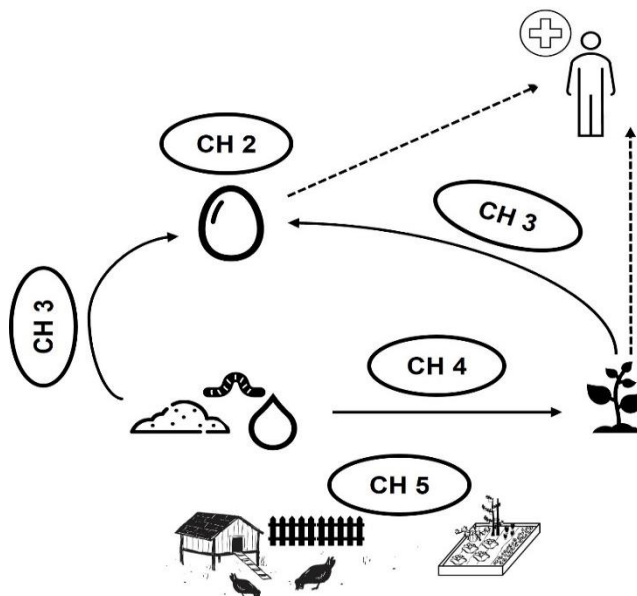


Fig. 1.4: Schematic outline of the present thesis showing the chapters and how they are related to each other.

1.10 Study area

The present thesis was conducted in Flanders (Belgium), which is a densely populated region in Western Europe with a high degree of industrialization (Verbruggen, 1997). The sampling was mainly focused on the Province of Antwerp on private gardens located within a distance buffer zone of ± 10 km from the fluorochemical plant of the 3M Company (Fig. 1.4). This plant is situated in the

Antwerp harbour nearby the Scheldt river and has been an active production site of PFAS since 1971 (3M Company, 2021).

Over the last 20 years, numerous ecotoxicological studies have been performed that monitored PFAS in wildlife nearby the 3M fluorochemical plant (e.g. Buytaert et al., 2023; Hoff et al., 2005; Dauwe et al., 2007; D'Hollander et al., 2014; Groffen et al., 2019a; Lasters et al., 2021).

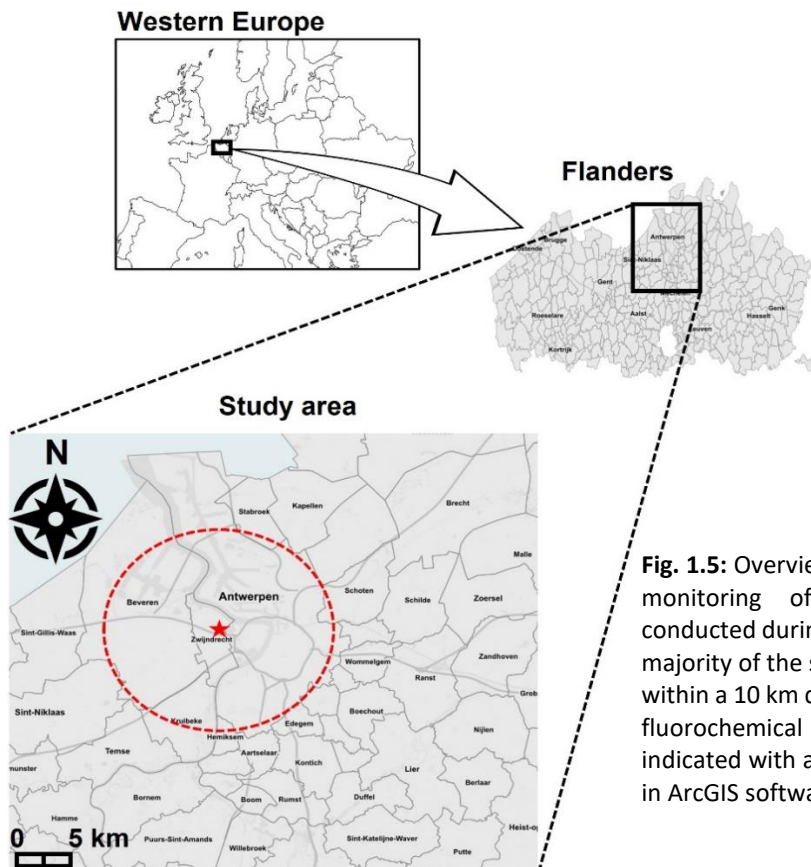
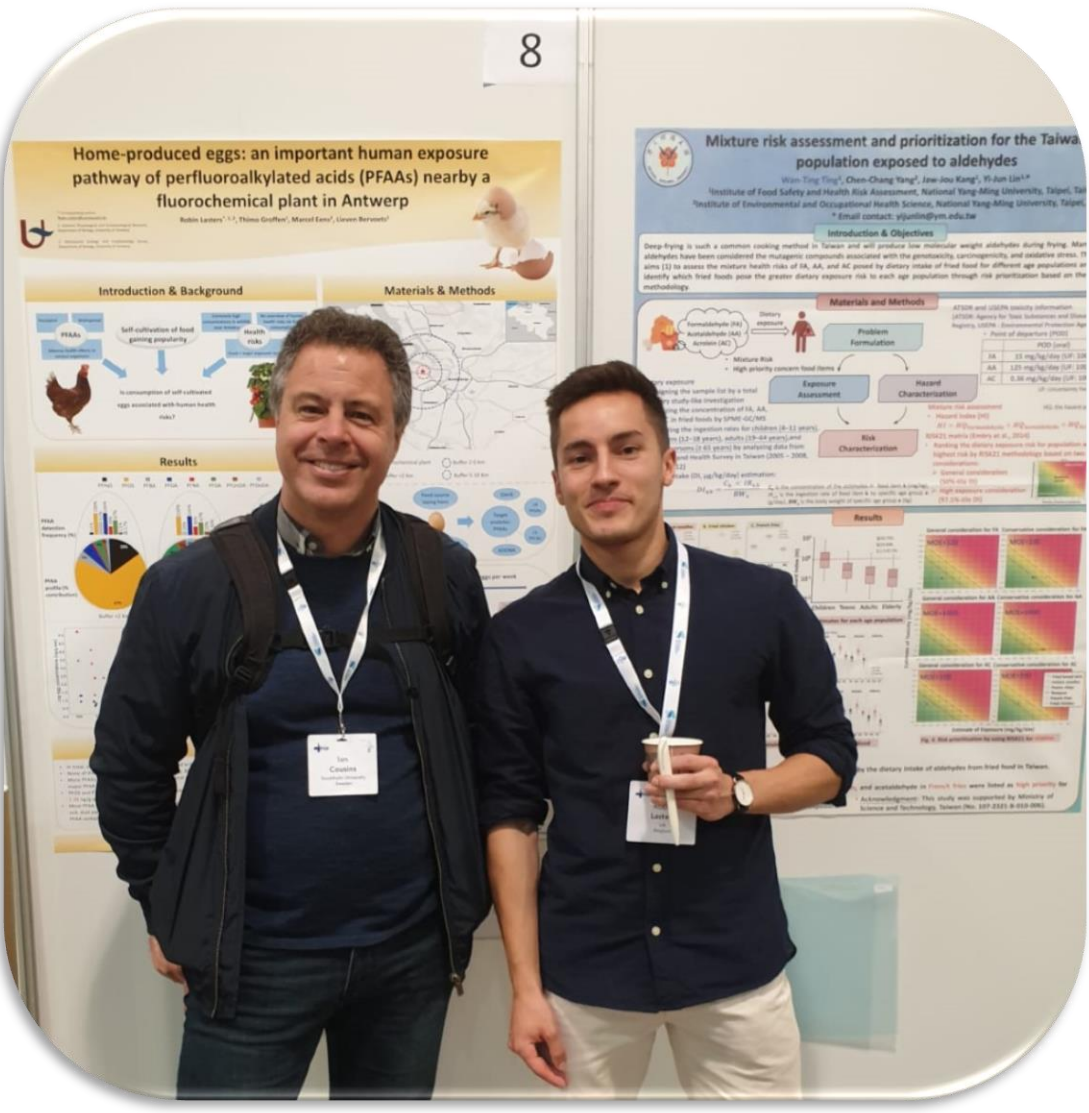


Fig. 1.5: Overview of the study area in which the monitoring of the private gardens was conducted during the present thesis project. The majority of the sampling locations were situated within a 10 km distance buffer zone from the 3M fluorochemical plant in Antwerp (Belgium), indicated with an asterisk. The map was created in ArcGIS software (version 10.7.1).

Together, these studies have reported very high concentrations of PFAS across a broad range of organisms (e.g. invertebrates, small rodents, freshwater fish and wild birds) and showed that the fluorochemical plant in Antwerp is a major PFAS point source. Until the present, research has largely been focused on biomonitoring of PFAS in the great tit (*Parus major*) and Groffen et al. (2019a) reported concentrations up to 187 032 ng/g ww for PFOS (i.e. a phased-out compound since 2002) in eggs of this species. Moreover, PFOS levels were still relatively high in supposed reference sites. For instance, at Fort IV which is \pm 11 km away from the 3M plant, PFOS concentrations up to 55 ng/g ww were measured in eggs of great tit (Lasters et al., 2019; Lasters et al., 2021).

These worrying PFAS concentrations in various tissues of wildlife, especially in eggs, prompted the question to which extent eggs of domestic birds (e.g. chickens), and other homegrown food, would present an exposure risk to humans. Apparently, almost no information in the literature was available on PFAS in homegrown food (cf., section 1.8.2), which was the main incentive of the present thesis project. One preliminary study by D'Hollander et al. (2011) showed that PFOS and PFOA concentrations in home-produced eggs strongly exceeded the current EFSA health guideline values in private gardens close to the plant site. However, this investigation only reported data of these two PFAAs. Moreover, the role of potential exposure sources and soil physicochemical characteristics on the bioavailability in the eggs was not examined. Furthermore, other types of homegrown food were not included in the sample collection and the spatial distribution of the egg concentrations, in relation to potential exposure sources (e.g. the fluorochemical plant in Antwerp), was not examined. These knowledge gaps and the other ones discussed in section 1.8.2 will be addressed in this thesis.

To this end, a total of four sampling campaigns in private gardens were conducted in the respective summer periods of 2018, 2019, 2021 and 2022. The sampling area was mainly focused on private gardens in the Province of Antwerp which were located within a distance buffer zone of ± 10 km from the fluorochemical plant of 3M. However, as the sampling campaigns proceeded, additional locations were selected outside this 10 km buffer zone to have maximal contrast in explanatory variables. For instance, private gardens comparable in orientation (e.g. southwest) from the plant site but differing considerably in distance towards it and vice versa. Moreover, gardens nearby other (local) point sources with potentially other emission characteristics were also selected, including private gardens nearby a former paper mill (i.e. De Naeyer, Willebroek) and the Antwerp airport. For the sampling campaign of 2018, a network of 35 volunteers could be established via informal contacts and social media. As the thesis project proceeded, this network could ultimately be extended to 135 participating volunteers in the other sampling periods.



Chapter 2: Home-produced eggs: an important human exposure pathway of perfluoroalkylated substances (PFAAs)

This chapter was published in *Chemosphere*:

Lasters, R., Groffen, T., Eens, M., Coertjens, D., Gebbink, W. A., Hofman, J. & Bervoets L. (2022). Home-produced eggs: An important human exposure pathway of perfluoroalkylated substances (PFAS). *Chemosphere*. 308: 136283-136293. <https://doi.org/10.1016/j.chemosphere.2022.136283>.

2.1 Abstract

Humans are generally exposed to per- and polyfluoroalkyl substances (PFAS) through their diet. Whilst plenty of data are available on commercial food products, little information exists on the contribution of self-cultivated food, such as home-produced eggs (HPE), to the dietary PFAS intake in humans. The prevalence of 17 legacy and emerging PFAS in HPE ($N = 70$) from free-ranging laying hens was examined at 35 private gardens, situated within a 10 km radius from a fluorochemical plant in Antwerp (Belgium). Potential influences from housing conditions (feed type and number of individuals) and age of the chickens on the egg concentrations was examined, and possible human health risks were evaluated. Perfluorooctane sulfonic acid (PFOS) and perfluorooctanoic acid (PFOA) were detected in all samples. PFOS was the dominant compound and concentrations (range: 0.13 – 241 ng/g wet weight) steeply decreased with distance from the fluorochemical plant, while there was no clear distance trend for other PFAS. Laying hens receiving an obligate diet of kitchen leftovers, exhibited higher PFOS and PFOA concentrations in their eggs than hens feeding only on commercial food, suggesting that garden produce may be a relevant exposure pathway to both chickens and humans. The age of laying hens affected egg PFAS concentrations, with younger hens exhibiting significantly higher egg PFOA concentrations. Based on a modest human consumption scenario of two eggs per week, the European health guideline was exceeded in $\geq 67\%$ of the locations for all age classes, both nearby and further away (till 10 km) from the plant site. These results indicate that PFAS exposure via HPE causes potential human health risks. Extensive analysis in other self-cultivated food items on a larger spatial scale is highly recommended, taking into account potential factors that may affect PFAS bioavailability to garden produce.

2.2 Introduction

The human population will reach over 9 billion people by 2050 and projections estimate that 70% of humans will then live in urban areas (Galhena et al., 2013; Zipperer and Pickett, 2012). In parallel, food production will have to increase by 70% to meet the daily calorie intake demands of this growing population (Galhena et al., 2013). Consequently, novel food cultivation strategies will be required as available resources for food production, most importantly land surface, are limited. Hereby, self-cultivation of food, by means of crop production and farm animals, has been promoted and has become an increasing trend in private gardens from rural, urban and even industrial areas (Church et al., 2015; van der Jagt et al., 2017).

Particularly, the housing of free-ranging chickens (*Gallus gallus domesticus* L.) has gained worldwide popularity over recent years (Capoccia et al., 2018; Padhi, 2016; Sioen et al., 2008). Chickens provide environmental and economic assets by means of kitchen waste disposal, egg production and low-cost maintenance (Waegeneers et al., 2009). Furthermore, home-produced eggs (HPE) are often perceived by the general public to have high nutritional value (Van Overmeire et al., 2006; Waegeneers et al., 2009). For instance, HPE accounted in 2017 for 17% of the egg consumption in Belgium and this number has been steadily increasing (VLAM, 2017). In this regard, free-ranging chickens offer unique opportunities for monitoring human exposure, as they are the most prevalent birds on earth in terms of biomass and usually live in close contact with humans (Bar-On, 2018; Scaramozzino et al., 2019). HPE have also been associated with higher concentrations of organic pollutants (Sioen et al., 2008; Waegeneers et al., 2009), including per- and polyfluoroalkyl substances (PFAS) (D'Hollander et al., 2011; Gazotti et al. 2021; Zafeiraki et al. 2016).

PFAS are synthetic and organic compounds that have been produced for more than 70 years (Post, 2021). The combination of their amphiphilic properties and strong C-F bond makes them useful for a diverse range of commercial applications, such as soil- and water repellent clothing, cleaning products, food-packaging, paper coating and firefighting foams (Buck et al., 2011). On the other hand, these distinctive chemical properties make PFAS highly persistent in the environment and bioaccumulative in biota (Death et al., 2021; Giesy and Kannan, 2002). For instance, the serum half-lives in humans of perfluorooctane sulfonic acid (PFOS) and perfluorooctanoic acid (PFOA), which are the most widely studied PFAS to date, can reach approximately 5 and 3 years, respectively

(Goodrum et al., 2020). Both experimental studies on laboratory animals and human epidemiological studies have identified PFAS with various health effects including liver damage, altered immune functioning, neurotoxicity and cancer (Briels et al., 2018; Fenton et al., 2021; Lilienthal et al., 2017; Sunderland et al., 2019).

Generally, the most important human exposure pathway of PFAS our diet (Cornelis et al., 2012; Roth et al., 2020). Numerous studies have reported PFAS concentrations in commercial food, notably those within the European PERFOOD project (<https://ibed.fnwi.uva.nl/perfood/>), in which fish and offal food were identified as the main dietary sources of PFAS (Cornelis et al., 2012; Klenow et al., 2013). Based on intake modelling, dietary PFAS exposure was estimated to be of no concern with respect to the former health guideline values for PFOS and PFOA set in 2008 (Klenow et al., 2013). However, PFAS intake exposures were mostly compared to outdated health guidelines derived from critical toxic endpoints, such as liver toxicity (Zafeiraki et al., 2016; Su et al., 2017), while recently established health guidelines point out that PFAS effects on more sensitive toxic endpoints, for instance immune toxicity, can occur at much lower intake levels (EFSA, 2020). These sensitive endpoints have rarely been evaluated and the additional contribution of home-produced food to the PFAS intake has only been considered to a limited extent in human health risk assessments (Gazotti et al., 2021).

Therefore, self-cultivated food can be a major source of PFAS exposure to humans, especially in the neighbourhood of PFAS hot-spots, and should be taken into account for PFAS risk assessments (Death et al., 2021; Xu et al., 2021b). Recent human biomonitoring research across Flanders has consistently linked internal serum PFOS concentrations with the consumption of HPE (Buekers et al., 2021; Colles et al., 2020). HPE are often produced in less controlled housing and feeding conditions than commercial eggs, which have been shown to contain much lower PFAS concentrations (Zafeiraki et al., 2016; Su et al., 2017). In contrast to commercial laying hens, free-ranging laying hens in private gardens have continuous access to an outdoor enclosure. As such, they may be exposed to PFAS via ingestion of contaminated soil and dust particles, intake of rain water, soil invertebrates (eg. worms and insects) and kitchen waste products (Waegeneers et al., 2009; Wang et al., 2010). These intake media may be directly contaminated with PFAS through transfer from primary sources, such as direct emissions from fluorochemical industry via air and surface water into ground water and soil (Schroeder et al., 2021; Xu et al., 2021a). Additionally,

secondary sources including precursor degradation and domestic emissions from consumer products and application products may also contribute to local contamination of the private garden (Liu et al., 2019).

Human intake assessments of PFAS are mostly restricted to the level of the general population, while very little is known about the potential exposure routes and scenarios for inhabitants living near PFAS point sources. Zafeiraki et al. (2016) measured relatively low PFAS concentrations in yolk of HPE from the Netherlands and Greece, with median sum PFAS concentrations of 3.1 and 1.1 ng/g wet weight (ww), respectively. However, these data were not reported in relation to any fluorochemical point source, that may explain variation across the samples. Recently, a few studies in China have reported mean sum PFAS concentrations of 122 ng/g egg yolk nearby PFAS industry, but only a limited spatial scale was considered (Wang et al., 2019) and sample sizes were too small (Su et al., 2017) to make any claims about representativity or potential health risks. Moreover, the impact of different feeding regimes (e.g. kitchen waste versus commercial feed) and local housing conditions of the laying hens on egg PFAS concentrations has, to the best of our knowledge, never been addressed.

The main objective of this study was therefore to examine the PFAS profile and concentrations in HPE in relation to the distance towards a known PFAS point source in Antwerp, Belgium. Secondly, we aimed to investigate the potential influence of housing conditions (feed type and number of individuals) and age of the laying hens on the egg PFAS concentrations, based on survey data. Lastly, possible human health risks of PFAS intake through consumption of HPE were assessed with respect to currently available health guidelines, by means of both critical (liver toxicity) and sensitive (immune toxicity) endpoints.

Given that eggs of several free-living bird species breeding near the fluorochemical plant site in Antwerp contained among the highest PFAS concentrations ever reported in bird eggs (Groffen et al., 2017, 2019a, 2019b; Lasters et al., 2021) and that egg PFAS concentrations in wild birds decreased from 3 km onwards of the plant site (Groffen et al., 2017), we hypothesize that the most diverse PFAS profile and highest concentrations in HPE are present within a 3 km radius from the plant site. As a consequence, the potential risk for public health through HPE consumption is expected to be highest within this 3 km radius. Regarding the potential influences of housing and

feeding conditions, the following hypotheses were tested: (i) higher egg PFAS concentrations may be related with a higher number of laying hens as increased scratching behaviour would result in less vegetation coverage and increased exposure with contaminated soil particles and invertebrates; (ii) eggs of younger hens contain higher egg PFAS concentrations due to less elimination time and fewer sequestration possibilities compared to older laying hens; and (iii) higher PFAS concentrations are detected in eggs from hens that are primarily fed with kitchen waste products, which may contain potentially contaminated garden produce that is cultivated in a less-controlled way compared to commercial feed.

2.3 Materials and methods

2.3.1 Study area and sample collection

During the period July - September 2018, HPE ($N = 70$) were collected from 35 volunteers that kept free-ranging laying hens. Two eggs from each location were sampled at the same day to ensure that the eggs originated from different individual hens. These samples were collected within a 10 km radius from a known PFAS point source in Antwerp, Belgium (Groffen et al., 2019a; Lopez-Antia et al., 2019), as displayed in Fig. 2.1. The study area was divided into three concentric buffer zones (A: 0-2 km, $N = 18$; B: 2-4 km, $N = 30$; C: 4-10 km, $N = 22$) with increasing distances from this point

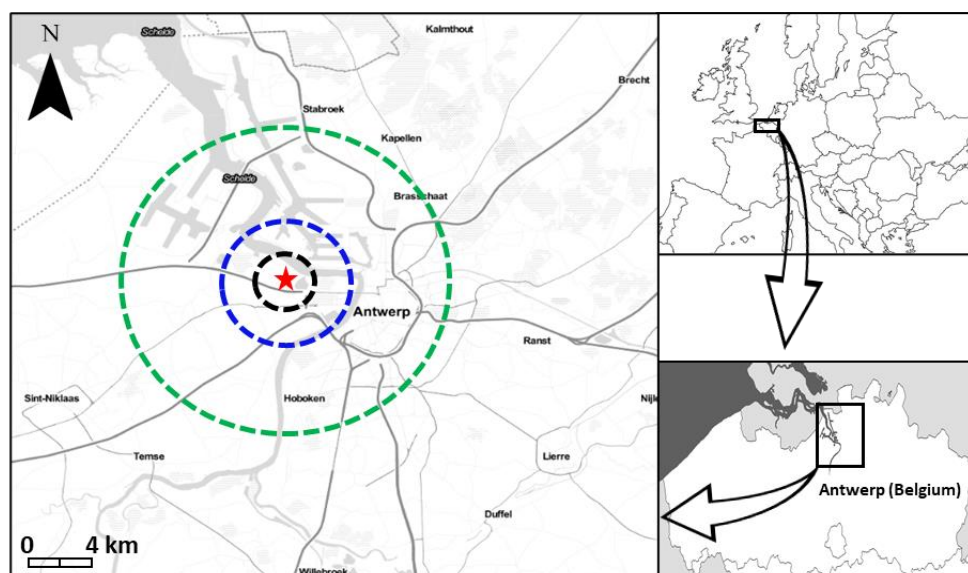


Fig. 2.1: Overview of the study area in which the home-produced eggs were sampled in 2018 in three concentric distance buffers located within a radius of 2 km (buffer A, $N = 18$), 4 km (buffer B, $N = 30$) and 10 km (buffer C, $N = 22$) from the fluorochemical plant site (red asterisk) in Antwerp, Belgium, respectively.

source. The buffer zone categories were based on the typical spatial decrease of PFAS observed in earlier studies on terrestrial bird eggs in the studied area (Groffen et al., 2017, 2019a).

2.3.2 Volunteer selection and survey data

Volunteers that housed at least two free-ranging laying hens in their gardens were recruited via existing social networks and regular call-ups on social media. Moreover, only volunteers were selected that kept free-ranging laying hens of at least six months of age and which had continuous access to an uncovered outdoor enclosure.

After the eggs were collected, each volunteer completed a self-reporting survey in which information on the age and flock size of the laying hens was given (Table S2.1). Additionally, categorical data were obtained on the feed origin of the laying hens, consisting of the following subcategories: kitchen leftovers (LF: mainly vegetable scraps and/or garden produce), commercial feed (CF: commercial layer feed) or a mix of both (M). The age dataset of the laying hens was merged into three age classes, based on the age classification system of Joyner et al. (1987): young layers (< 1 year old), older layers (1-2 years old) and old layers (>2 years old). Moreover, the distance (Euclidean) of each sampling location to the PFAS point source was assessed and each location was assigned to its associated buffer zone (0-2, 2-4, 4-10 km).

The personal data of all volunteers were treated confidentially, according to the current privacy regulations (GDPR). Data management was approved by the privacy policy of the University of Antwerp. Every volunteer gave explicit approval for the processing of their data within the context of the specific research goals of this study via an informed consent. The personal results were communicated to each volunteer via a short report containing background information on PFAS, a consumption advice based on their individual results and general strategies that may lower overall PFAS exposure. The researchers were available for tackling questions of the participating volunteers.

2.3.3 Chemical analysis

All used abbreviations of PFAS are based on Buck et al. (2011). Four target perfluoroalkyl sulfonic acids (PFASs) (PFBS, PFHxS, PFOS and PFDS), 11 target perfluoroalkyl carboxylic acids (PFCAs) (PFBA,

PFPeA, PFHxA, PFHpA, PFOA, PFNA, PFDA, PFUnDA, PFDoDA, PFTTrDA and PFTeDA) and two emerging fluoroether PFAS (sodium dodecafluoro-3H-4,8-dioxanonanoate (NaDONA) and 2,3,3,3-tetrafluoro-2-(1,1,2,2,3,3,3-heptafluoropropoxy)-propanoic acid (HFPO-DA or GenX) were analysed in the samples. The following isotopically mass-labelled internal standards (ISTDs) were used in the analysis: $^{18}\text{O}_2$ -PFHxS, [1,2,3,4- $^{13}\text{C}_4$]PFOS, $^{13}\text{C}_4$ -PFBA, [1,2- $^{13}\text{C}_2$]PFHxA, [1,2,3,4- $^{13}\text{C}_4$]PFOA, [1,2,3,4,5- $^{13}\text{C}_5$]PFNA, [1,2- $^{13}\text{C}_2$]PFDA, [1,2- $^{13}\text{C}_2$]PFUnDA and [1,2- $^{13}\text{C}_2$]PFDoDA (Wellington Laboratories, Guelph, Canada). The stock ISTD solution was diluted in a mixture of 50:50 (v:v) of HPLC grade acetonitrile (ACN) and Milli-Q water (VWR International, Leuven, Belgium) to a concentration of $125 \text{ pg } \mu\text{L}^{-1}$ to spike the samples.

2.3.4 Chemical extraction

Prior to the extraction of the egg samples, three analytical methods were tested on a spiked blank matrix sample (= commercial eggs low in PFAS contamination, Table S2.2) in order to select a relatively robust, accurate and sensitive extraction procedure (see SI section 2.1: optimization extraction method). The clean-up extraction using graphitized Envicarb carbon powder (adopted from Powley et al., 2005) was selected for extraction of the samples, as the extraction recoveries of PFSAAs were low when using the other two procedures (weak anion exchange solid-phase extraction (WAX method), detailed in Groffen et al. (2019c), and a combination of clean-up extraction with Envicarb powder followed by the WAX method) and would imply that PFHxS cannot be quantified (Fig. S2.1).

The egg content was transferred into a polypropylene (PP) tube and homogenized by repeatedly sonicating and vortex-mixing. The homogenized samples were weighed and around 0.3 g of homogenized sample was used ($\pm 0.01 \text{ mg}$, Mettler Toledo, Zaventem, Belgium) for the extraction. Homogenates were spiked with $80 \text{ } \mu\text{L}$ of $125 \text{ pg } \mu\text{L}^{-1}$ ISTD solution. After adding 10 mL of acetonitrile (ACN), the samples were sonicated three times (with vortex-mixing in between periods) and left overnight on a shaking plate (135 rpm, room temperature, 20°C , GFL 3020, VWR International, Leuven, Belgium). Afterwards, the samples were centrifuged (4°C , 10 min, 2400 rpm, 1037 g, Eppendorf centrifuge 5804R, rotor A-4-44) and the supernatant was stored in a 15 mL PP tube. Then, the supernatant was vacuum-dried to approximately 0.5 mL using a rotational vacuum concentrator (30°C , type 5301, Hamburg, Germany). The extract was transferred to a PP Eppendorf tube which was filled with 50 mg of graphitized carbon powder (Supelclean ENVI-Carb, Sigma-

Aldrich, Overijse, Belgium) and 35 μL of glacial acetic acid to remove chemical impurities. The 15 mL tube was rinsed twice with 250 μL of ACN, which was transferred to the Eppendorf tube. After thoroughly vortex-mixing the tube, the extracts were centrifuged (4°C, 10 min, 10000 rpm, 1037 g, Eppendorf centrifuge 5415R, rotor F 45-24-11). Then, the supernatant was transferred to a new Eppendorf tube and vacuum-dried until it was nearly completely dry. The dried extract was reconstituted in 100 μL of a 2% ammonium hydroxide solution diluted in ACN and filtered through a 13 mm Acrodisc Ion Chromatography Syringe Filter with 0.2 μm Supor (PES) membrane (VWR International, Leuven, Belgium) into a PP injector vial prior to instrumental analysis.

2.3.5 UPLC-TQD analysis

The target analytes were analysed using an ACQUITY Ultrahigh Performance Liquid Chromatography (ACQUITY, TQD, Waters, Milford, MA, USA) coupled to a tandem quadrupole (TQD) mass spectrometer (UPLC-MS/MS) with negative electrospray ionisation. To separate the different target analytes, an ACQUITY UPLC BEH C18 VanGuard Pre-column (2.1 x 50 mm; 1.7 μm , Waters, USA) was used. The mobile phase solvents consisted of ACN and HPLC grade water, which were both dissolved in 0.1% HPLC grade formic acid. The solvent gradient started at 65% of water to 0% of water in 3.4 min and back to 65% water at 4.7 min. The flow rate was set to 450 $\mu\text{L}/\text{min}$ and the injection volume was 6 μL . PFAS contamination that might originate from the LC-system was retained by insertion of an ACQUITY BEH C18 pre-column (2.1 x 30 mm; 1.7 μm , Waters, USA) between the solvent mixer and the injector. The target PFAS analytes were identified and quantified based on multiple reaction monitoring (MRM) of the diagnostic transitions that are displayed in Table S2.3.

2.3.6 Quality control and assurance

Per batch of ten samples, one procedural blank (= 10 mL ACN spiked with ISTD) was included to detect any contamination during the extraction. To prevent cross-over contamination among samples during detection in the UPLC-MS/MS, ACN was regularly injected to rinse the columns. Limits of quantification (LOQs) were calculated for each analyte, in matrix, as the concentration corresponding to a signal-to-noise ratio of 10. Calibration curves were prepared by adding a constant amount of the ISTD to varying concentrations of an unlabelled PFAS mixture. The serial dilution of this mixture was performed in ACN. A linear regression function with highly significant

linear fit (all $R^2 > 0.98$; all $P < 0.001$) described the ratio between concentrations of unlabelled and labelled PFAS. Individual PFAS were quantified using their corresponding ISTD with exception of PFPeA, PFHpA, PFTTrDA, PFTeDA, PFBS, PFDS, HFPO-DA and NaDONA for which no ISTD were present. These analytes were all quantified using the ISTD of the compound closest in terms of functional group and size (Table S2.3), which was validated by Groffen et al. (2019c, 2021).

2.3.7 Health risk indications

The potential risk of PFAS intake via HPE consumption was estimated for each of the three buffer zones. The consumption scenario was based on the intake of two HPE per week, which is the general Flemish governmental health guideline for HPE and approximately corresponds to the average weekly egg consumption for a modal Belgian citizen (Lebacqz, 2015; Sioen et al., 2008). The calculation of the PFAS intake values via eggs was conducted per age category, as younger people will have a higher relative PFAS intake per kg bodyweight (bw) compared to adults. To this end, mean body weight values were adopted from the latest food consumption datasets of the Belgian population (De Hoge Gezondheidsraad, 2003; Van der Heyden et al., 2018) for the following age intervals: 3-5, 6-9, 10-13, 14-17, 18-64 years old (Table S2.4). For the two latter age intervals, data were provided for both males and females as considerable weight differences exist between sexes within these age intervals. Finally, the estimated weekly intake (EWI) of PFAS was calculated by the following formula, according to Su et al. (2017):

$$EWI \text{ (ng/kg bw/week)} = \text{egg consumption (g/week)} \times \text{egg PFAS concentration (ng/g ww of whole egg content)} / \text{body weight (kg)} \quad (1)$$

The EWI was compared with two frequently used health guideline criteria with respect to the maximum tolerable intake of PFAS via food: the tolerable weekly intake value (TWI: 4.4 ng/kg bw per week) which considers the sum of PFHxS, PFOS, PFOA and PFNA (EFSA, 2020) and the maximum tolerable risk values (MTR: 43.8 ng/kg bw per week for PFOS and 87.5 ng/kg bw per week for PFOA) which are derived for PFOS and PFOA (Zeilmaker et al., 2016). These two criteria are based on a relatively sensitive toxic endpoint (= reduced antibody response to vaccination in infants) and a more critical endpoint (= liver hypertrophy in rats), respectively, in order to obtain a comprehensive risk estimate.

2.3.8 Statistical analysis

Statistical analyses were performed in the statistical software R (version 3.5.2) and in GraphPad Prism (version 9). The significance level for model testing was set at $P \leq 0.05$. The model assumptions were evaluated with the Shapiro-Wilk test for normality and data were $\log(x+1)$ transformed to comply with normality assumptions. For PFAS concentrations that were <LOQ, replacement concentration values were assigned following a maximum likelihood estimation method (Villanueva, 2005; de Solla et al., 2012).

For each distance buffer zone (A = 0 – 2 km; B = 2 – 4 km and C = 4 – 10 km), the PFAS profile and concentrations in the HPE ($N = 70$) were calculated using descriptive statistical parameters. The composition profile of the PFAS was given as the contribution of the concentrations from single compounds to the sum of PFAS concentrations in the eggs.

Potential relationships among the PFAS concentrations and the variables from the survey data were tested on location level ($N = 35$) for the following reasons: (i) due to practical constraints, some of the survey data (e.g. age) could not be derived for each individual egg and (ii) each egg cannot be considered as an independent replicate due to the hierarchical structure of the dataset (i.e. two eggs originated from different chickens which share one common environment and thus are nested within the same location). Therefore, the individual PFAS concentrations for the two eggs at each location were aggregated, resulting in independent mean values for each location ($N = 35$). Moreover, PFAS with an overall detection frequency <50% were omitted from the analyses to minimize left-skewness of the respective data distribution. A one-way ANOVA was used to test for potential differences in egg PFAS concentrations among the considered buffer zones at varying distance from the fluorochemical plant site in Antwerp. A general linear model, containing the number and average age of the laying hens as explanatory variables, was used to test their potential association with PFAS concentrations. Finally, the potential effect of feed origin on the egg concentrations was examined with a one-way ANOVA. For these two latter analyses, the data were tested independently from the buffer zones to increase the statistical power of the models that were fit.

2.4 Results

2.4.1 PFAS profile and concentrations in the buffer zones

The detection frequencies of all the detected PFAS in the eggs are given in Table 2.1 and displayed in Fig. 2.2. In total, eight out of 17 target PFAS were detected in the eggs of each buffer zone, except for PFHxS. This latter compound was not detected in buffer B, although the detection of PFHxS in buffer C originated from one location that was situated on the edge of buffer B and C. Only PFOA, PFDA and PFOS were detected in >50% of the eggs in each buffer zone. PFOS and PFOA were the most frequently detected compounds and were found in all the eggs from every buffer zone (Fig. 2.2). The highest detection frequency for PFBA and PFHxS was observed in buffer A, respectively in 61% and 11% of the eggs, compared to the other buffer zones. On the other hand, three long-chain

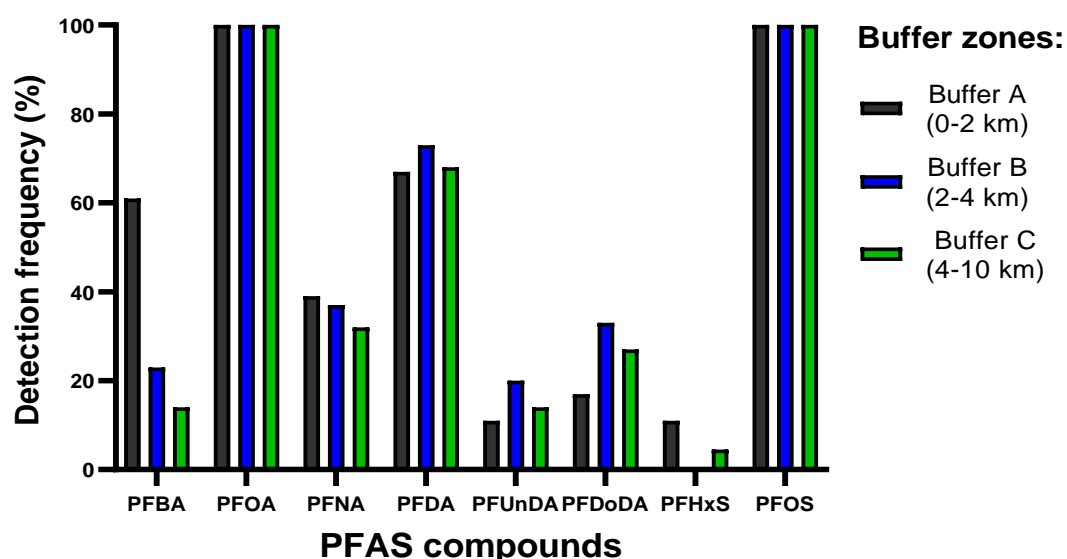


Fig. 2.2: Overview of the detection frequencies (%) of all the target PFAS in home-produced eggs of free-ranging laying hens within a radius of 2 km (buffer A, $N = 18$), 4 km (buffer B, $N = 30$) and 10 km (buffer C, $N = 22$) from the fluorochemical plant site in Antwerp, Belgium. PFHxS values for buffer A and buffer C are based on one datapoint.

PFCAs (PFDA, PFUnDA and PFDoDA) were all most frequently detected in buffer B (Fig. 2.2). None of the target emerging compounds (GenX and NaDONA) were detected in any of the eggs. The descriptive statistics (min. – max., median and mean concentrations) of all the detected PFAS in the eggs are provided in Table 2.1.

Table 2.1: Limits of quantification (LOQs; ng/g ww, determined as 10x the S/N ratio), median and mean concentrations (ng/g ww), ranges (min. - max. in ng/g ww) and detection frequencies (Freq. (%)) of the target PFAS analytes in the individual home-produced eggs of free-ranging laying hens within each buffer zone (range 0 - 10 km) from the fluorochemical plant site in Antwerp, Belgium.

		PFCAs (ng/g ww)					PFSAs (ng/g ww)		
		PFBA	PFOA	PFNA	PFDA	PFUnDA	PFDoDA	PFHxS ¹	PFOS
	LOQ	0.10	0.13	0.16	0.21	0.14	0.080	2.5	0.13
Buffer A: 0-2 km (N = 18)	Median	1.8	0.64	0.29	0.55	0.70	0.52	3.4	11
	Mean	2.8	0.78	0.30	0.53	0.70	0.55	3.4	39
	Range (min. - max.)	0.44 - 9.1	0.26 - 2.4	<LOQ - 0.73	<LOQ - 0.78	0.49 - 0.91	0.48 - 0.65	<LOQ - 3.5	<LOQ - 241
	Freq. (%)³	61	100	39	67	11	17	11	100
	Contribution to ΣPFAS (%)	4.1	1.8	0.3	0.8	0.2	0.2	0.9	91.7
Buffer B: 2-4 km (N = 30)	Median	0.75	0.54	0.21	0.51	0.66	0.40	ND ²	3.5
	Mean	0.75	0.57	0.27	0.66	0.78	0.57	ND	6.5
	Range (min. - max.)	0.54 - 0.96	0.21 - 1.0	<LOQ - 0.68	0.22 - 1.6	0.33 - 1.4	0.21 - 1.6	ND	0.54 - 44
	Freq. (%)	23	100	37	73	20	33	0	100
	Contribution to ΣPFAS (%)	2.2	7.1	1.2	6.0	1.9	2.3	0	79.3
Buffer C: 4-10 km (N = 22)	Median	0.50	0.53	0.28	0.48	0.87	0.47	3.6	3.3
	Mean	0.81	0.57	0.27	0.52	0.77	0.57	3.6	4.4
	Range (min. - max.)	0.40 - 1.5	0.13 - 1.0	<LOQ - 0.44	<LOQ - 0.99	0.54 - 0.90	0.23 - 1.3	3.6	0.78 - 13
	Freq. (%)	14	100	32	68	14	27	4.5	100
	Contribution to ΣPFAS (%)	1.8	9.6	1.4	5.9	1.8	2.6	2.7	74.1

¹ PFHxS values for buffer A and buffer C are based on one datapoint.

² ND = compound not detected.

³ Detection frequency included calculated concentrations above the limit of detection (LOD)

The mean PFOS concentrations in the eggs were significantly higher in buffer A (39 ng/g ww) compared to those from buffer B and C (both $P < 0.05$, $F_{2,32} = 4.0$), for which mean concentrations of, respectively, 6.5 ng/g ww and 4.4 ng/g ww were measured (Table 2.1, Fig. 2.3). The mean PFBA concentrations tended to decrease from buffer A to B ($P = 0.06$, Fig. S2.3), while there were no significant differences among the buffer zones for all the other PFCA (all $P > 0.05$, Fig. S2.3). PFOS and PFOA concentrations in the eggs were positively correlated within buffer zone A (Fig. S2.4; $P < 0.001$; $R^2 = 0.81$), while this was not the case within other buffer zones.

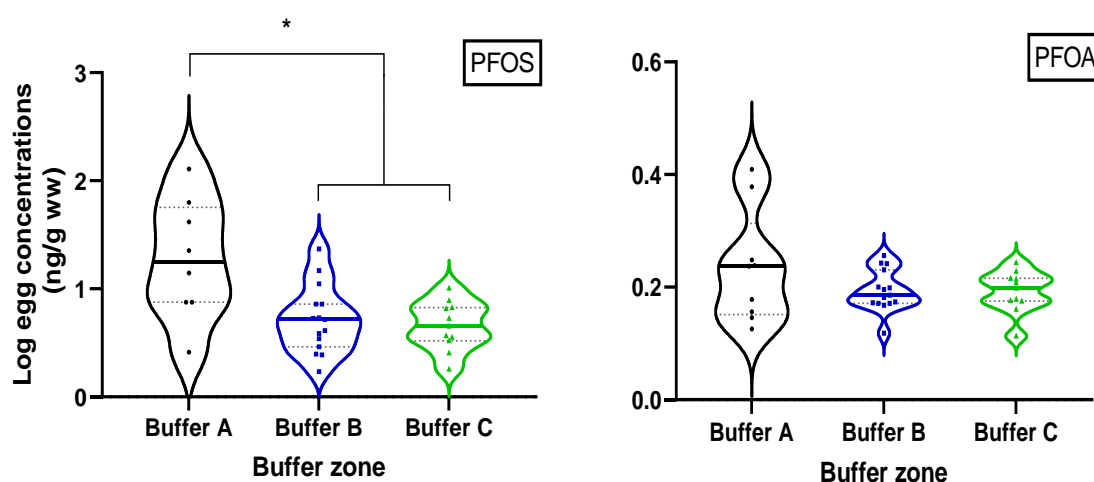


Fig. 2.3: Log PFOS and PFOA concentrations (ng/g ww) in home-produced eggs of free-ranging laying hens within each buffer zone (buffer A = 0 – 2 km, $N = 18$; buffer B = 2 – 4 km, $N = 30$; buffer C = 4 – 10 km, $N = 22$) from the fluorochemical plant site in Antwerp, Belgium. The asterisk indicates significantly higher PFOS concentrations in eggs of buffer zone A compared to those in eggs from both buffer zone B and buffer zone C (left graph; $P < 0.05$), while no significant differences were found among the buffer zones for PFOA (right graph; $P > 0.05$). Thick horizontal line in the violin plot represents the mean.

Overall, PFOS was the dominant compound in all buffer zones, contributing for 91%, 79% and 74% to the Σ PFAS in respectively buffer A, buffer B and C (Fig. 2.4). For the Σ PFCA, PFBA was the major compound in buffer A (55% contribution), whereas PFOA contributed most to the Σ PFCA in buffer B and C (34% and 41% contribution, respectively). The contribution of the short-chain PFBA to the Σ PFCA decreased from buffer A to buffer B, while the reverse was true for all the detected long-chain PFCA (Fig. 2.4).

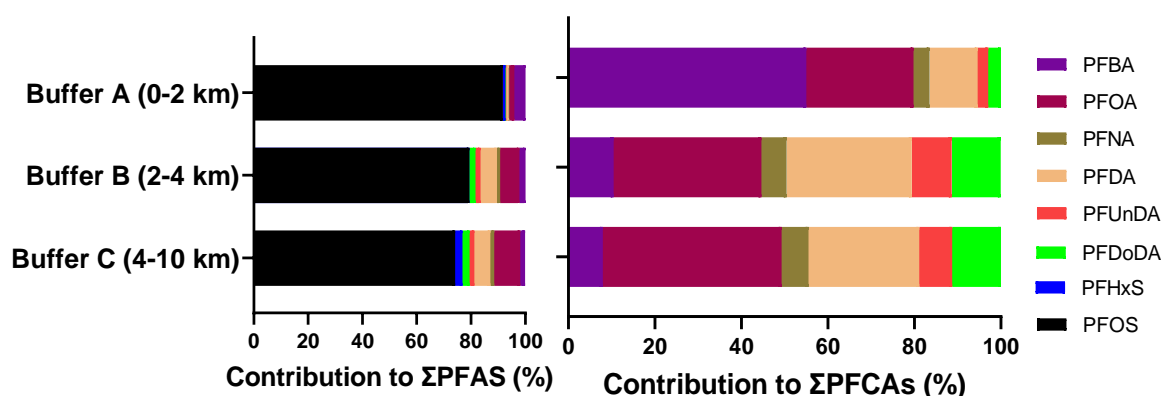


Fig. 2.4: Composition profile of the Σ PFAS (left graph) and Σ PFCAs (right graph) in home-produced eggs of free-ranging laying hens within a radius of 2 km (buffer A, $N = 18$), 4 km (buffer B, $N = 30$) and 10 km (buffer C, $N = 22$) from the fluorochemical plant site in Antwerp, Belgium. PFHxS values for buffer A and buffer C are based on one datapoint.

2.4.2 PFAS relationships with survey data

Eggs that originated from young laying hens were associated with higher PFOA concentrations compared to old laying hens ($P < 0.01$, Fig. 2.5), while there was no clear relationship with age and PFOS concentrations in the eggs ($P = 0.10$, $F_{2,28} = 5.9$). Laying hens that were fed an obligate diet of kitchen leftovers tended to contain higher egg PFOS concentrations ($P = 0.08$, $F_{2,31} = 2.8$) and PFOA concentrations ($P = 0.07$, $F_{2,31} = 2.9$) compared to laying hens that were provided with commercial feed only. The number of chickens in the enclosure was not associated with PFAS concentrations in the eggs (all $P > 0.05$).

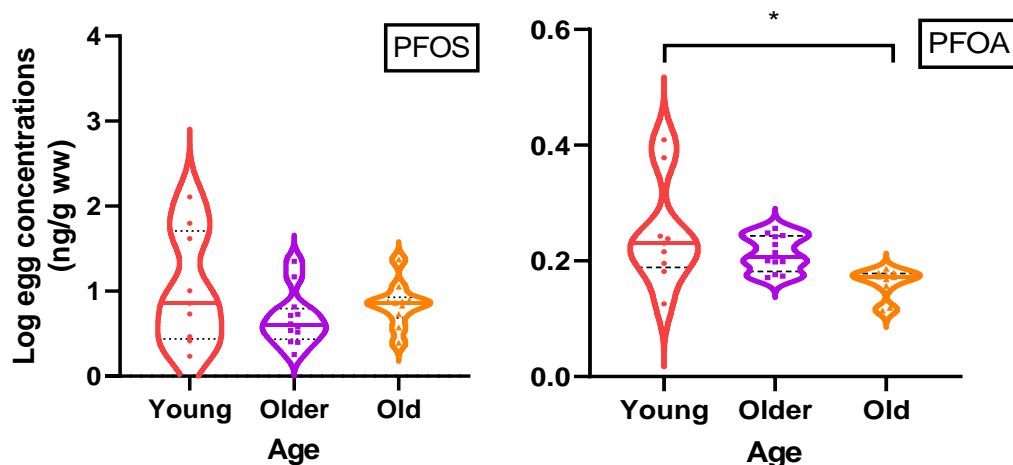


Fig. 2.5: Comparison of the log PFOS and PFOA concentrations (ng/g ww) in home-produced eggs among young, older and old laying hens (young: <1 year old, older: 1-2 years old, old: >2 years old). Young laying hens laid eggs with significantly higher PFOA concentrations ($P < 0.01$) compared to old laying hens, while no significant difference ($P = 0.10$) was found in egg PFOS concentrations among the age groups.

2.4.3 Human health risk

The intake estimations for the sum of four PFAS (PFHxS, PFOS, PFOA and PFNA) in different age intervals are provided in Table 2.2, based on a weekly egg consumption scenario of two HPE. In addition, the percentage exceedance of both the EFSA threshold (TWI; intake sum of four PFAS) and the RIVM threshold (MTR; intake of PFOS and PFOA separately) is given (Table 2.2). Overall, the EFSA health guideline was exceeded in the majority of the locations for all the age intervals ($\geq 67\%$) within 10 km from the fluorochemical plant site. The median intake values for the sum of four PFAS were highest in buffer A, ranging from 75 ng/kg bw per week to 18 ng/kg bw per week in the average infant (3 – 5 years old) and average male adult (18 – 64 years old), respectively (Table 2.2). The intake values for the sum of four PFAS were on average 2.5 times higher in buffer A compared to both buffer B and C, while intake was only slightly higher in buffer B compared to buffer C. The RIVM health guideline for PFOS was exceeded in 22 – 56% of the locations from buffer A (Table 2.2), while only infants (3 – 5 years old) and children (6 – 9 years old) exceeded this health guideline in $\leq 22\%$ of the locations in the other buffer zones (Table 2.2). With respect to PFOA, the RIVM health guideline was never exceeded in any of the buffer zones.

Table 2.2: Overview of the total PFAS intake values (min., median, mean and max. ng/kg bodyweight (bw) per week) for the sum of four PFAS (PFHxS, PFOS, PFOA and PFNA) in different age intervals per distance buffer zone.

BUFFER A (0-2 km, N = 18)	Intake parameters (ng/kg bw per week)				Percentage locations above health guideline (%)³		
	Min.	Median	Mean	Max.	EFSA threshold	<u>RIVM threshold</u> PFOA	PFOS
Age interval (years)							
3-5	2.3	75	208	726	89	0	56
6-9	1.7	56	154	538	89	0	55
10 - 13	1.1	36	100	348	89	0	44
14-17 Male	0.68	23	63	220	78	0	33
Female	0.77	26	71	247	78	0	33
18-64 Male	0.53	18	49	172	78	0	22
Female	0.64	22	59	207	78	0	33

³ The percentage of sampling locations exceeding the EFSA health guideline (4.4 ng/kg bw per week) and the RIVM health guideline (PFOS: 43.8 ng/kg bw per week and PFOA: 87.5 ng/kg bw per week) are provided for each age interval. The consumption scenario was based on the intake of two home-produced eggs per week of free-ranging laying hens.

Table 2.2: (Continued).

BUFFER B (2-4 km, N = 30)	Intake parameters (ng/kg bw per week)			Percentage locations above health guideline (%)			
	Min. Median		Mean	Max.	EFSA threshold	RIVM threshold PFOA	PFOS
Age interval (years)							
3-5	6.8	29	34	90	100	0	22
6-9	5.0	21	25	66	100	0	11
10 - 13	3.3	14	16	43	80	0	0
14-17 Male	2.1	8.7	10	27	73	0	0
Female	2.3	9.7	11	31	80	0	0
18-64 Male	1.6	6.8	8.0	21	67	0	0
Female	1.9	8.2	9.7	26	73	0	0

BUFFER C (4-10 km, N = 22)	Intake parameters (ng/kg bw per week)			Percentage locations above health guideline (%)			
	Min. Median		Mean	Max.	EFSA threshold	RIVM threshold PFOA	PFOS
Age interval (years)							
3-5	7.0	24	25	52	100	0	9
6-9	5.2	18	18	38	100	0	0
10 - 13	3.4	12	12	25	91	0	0
14-17 Male	2.1	7.4	7.4	16	91	0	0
Female	2.4	8.3	8.4	18	91	0	0
18-64 Male	1.7	5.8	5.8	12	73	0	0
Female	2.0	7.0	7.0	15	73	0	0

2.5 Discussion

2.5.1 PFAS profile and concentrations in the distance buffer zones

Table 2.3 shows an overview of available literature data reporting PFAS concentrations (min. – max. range) in HPE from Europe and China. In Belgium, D'Hollander et al. (2011) measured among the highest PFOS concentrations ever reported in HPE within a similar distance from the fluorochemical plant in Antwerp. However, PFAS compounds other than PFOS and PFOA were not examined and it was not clear how spatial variation in PFAS concentrations related to the fluorochemical plant site as 29 samples were collected across Flanders, with only three samples being obtained close to the fluorochemical plant site in Antwerp. Nevertheless, maximum PFOS concentrations (up to 3473 ng/g ww) were more than 14 times higher compared to those reported in the present study (Table 2.3). This apparent decrease may be explained by the phase-out of PFOS, PFOA and related compounds since 2002 at this production facility (3M, 2000). However, subsequent and more extensive monitoring campaigns are necessary to evaluate whether there is indeed a decrease over time.

Furthermore, the PFAS detection profile in HPE largely overlaps with those in eggs of wild great tits that were sampled within similar distance from the plant site in Antwerp (Groffen et al., 2017, 2019a). Nevertheless, much higher concentrations of PFAS were measured in great tit eggs, along with the detection of additional long-chain PFCAs (>C₁₃), which were not present in HPE. This suggests that wild birds are being exposed to PFAS to a larger degree than domestic chickens through frequent consumption of highly exposed prey items. Compared to laying hens, wild birds may consume more highly contaminated animal prey items, as they are not confined to an enclosure and hence have access to a broader foraging area. In addition, domestic chickens are given more non-contaminated vegetable feed and may also be able to deposit PFAS into a larger amount of eggs than wild birds, as their egg laying cycle is longer and not restricted to a breeding season. Fewer target compounds could be detected in wild great tit eggs than in HPE, within similar range (4 – 10 km) from the plant site (Groffen et al., 2019a; Lasters et al., 2019).

Table 2.3: Concentration range (in ng/g ww; min. – max.) of frequently detected PFAS in home-produced eggs from various locations, based on the present study and available literature data. <LOQ: below limit of quantification, NA: data not available, NA: compound not detected.

Reference	Location	Egg matrix	Year	Range from fluorochemical plant (km)	PFAS							
					PFBA	PFOA	PFNA	PFDA	PFUnDA	PFDoDA	PFHxS	PFOS
Present study	Antwerp (Belgium)	Whole egg	2018	0-2 km	0.44 - 9.1	0.26 - 2.4	<LOQ- 0.73	<LOQ - 0.78	0.49 - 0.91	0.48 - 0.65	3.3 - 3.5	<LOQ - 241
	Antwerp (Belgium)	Whole egg	2018	2-4 km	0.54 - 0.96	0.21 - 1.0	<LOQ - 0.68	0.22 - 1.6	0.33 - 1.4	0.21 - 1.6	ND	0.54 - 44
	Antwerp (Belgium)	Whole egg	2018	4-10 km	0.40 - 1.5	0.13 - 1.0	<LOQ - 0.44	<LOQ - 0.99	0.54 - 0.90	0.23 - 1.3	3.6 *	0.78 - 13
D'Hollander et al. (2011)	Antwerp (Belgium)	Whole egg	2010	0-1 km	NA	0.12 - 5.86	NA	NA	NA	NA	NA	53 - 3473
Wang et al. (2010)	Wuhan (central China)	NA	NA	0-2 km	NA	ND - 1.91	NA	NA	NA	NA	ND - 2.24	0.80 - 283
	Wuhan (central China)	NA	NA	>3 km	NA	ND - 0.53	NA	NA	NA	NA	ND - 3.18	2.7 - 18.1
Wang et al. (2019)	Wuhan (central China)	Yolk	NA	0.5-3.65 km	ND - 1698	ND - 69.7	ND - 6.2	ND - 4.0	ND - 4.3	ND - 7.7	ND - 85	ND - 1062
Su et al. (2017)	Shandong (north China)	Whole egg	2015	0-20 km	0.54- 22.5	2.5 - 125	0.14 - 0.33	0.17 - 0.40	<0.04 - 0.13	<0.02 - 0.12	<0.02	0.32 - 0.86
Zafeiraki et al. (2016)	Netherlands	Yolk	2013-2014	NA	NA	<0.5 - 2.7	<0.5 - 2.0	<0.5 - 3.0	<0.5 - 2.3	ND	<0.5 - 5.2	<0.5 - 24.8
	Greece	Yolk	2013-2014	NA	NA	<0.5 - 1.0	<0.5 - 8.0	<0.5 - 4.5	ND	<0.5	<0.5	<0.5 - 8.9
Gazotti et al. (2021)	Italy	Yok	2018-	NA	NA	ND - 0.62	0.25 - 1.2	NA	NA	NA	0.25 - 0.50	0.25 - 3.47
			2019			NA	0.62	1.2	NA	NA	NA	0.50

For PFOS, a significantly exponential decrease was observed in egg concentrations with increasing distance from the fluorochemical plant site (Fig. S2.2), while there was a declining trend for PFBA (Fig. S2.3). Until 2002, PFOS was the main product of 3M at their production sites (3M, 2000). The spatial variability of PFOS suggests that most of its accumulation in HPE within vicinity of the plant site is originating from historical industrial emissions. Previous studies on wildlife around this area also described this rapidly declining trend for PFOS (Dauwe et al., 2007; D'Hollander et al., 2014; Groffen et al., 2019a). Interestingly, the concentrations in HPE from buffer B and C were similar to those in other European studies, in which HPE were randomly collected without considering a distance gradient from a PFAS point source (Gazzotti et al., 2021; Zafeiraki et al., 2016). Although PFOA and PFOS concentrations in HPE from buffer A were correlated, this was not the case for eggs in buffer B and C (Fig. S2.4). Together, these findings indicate that PFOS and PFOA contamination in HPE within ± 2 km from a fluorochemical point site (0 – 2 km) is largely influenced by this primary source, whereas exposure in laying hens at more remote locations is more diffuse and complex.

In agreement with other European studies on HPE, PFOS was the dominant compound and contributed for at least 75% to the total PFAS profile in the eggs, followed by long-chain PFCAs ($\geq C_8$). Furthermore, this finding was in accordance with previous monitoring studies of HPE in Europe (the Netherlands and Greece: Zafeiraki et al. (2016) and Italy: Gazzotti et al. (2021)). Moreover, PFOS is an extremely persistent compound and can be firmly retained in the subsurface soil layer for years, due to its very strong adsorption capacity with soil particles (Groffen et al., 2019d; Liu et al., 2020). The total organic carbon (TOC) content in the soil plays a central role in the adsorption capacity of PFAS to soil particles (Lu et al., 2018). Soil in chicken enclosures usually contains enriched amounts of TOC, due to the build-up of feed waste and manure (Ravindran et al., 2017). Consequently, it is hypothesized that subsurface soil in chicken enclosures from private gardens may be an important sink of PFAS, especially for those PFAS that have large soil adsorption capacity, such as PFOS and long-chain PFCAs (Lu et al., 2018). Hence, free-ranging laying hens may be directly exposed to these PFAS via digestion of contaminated soil particles and indirectly through intake of invertebrates, such as earthworms, which live in close contact with the soil. Furthermore, these long-chain PFAS show strong binding affinity towards egg (lipo)proteins, which may also explain the relatively large accumulation in eggs (Fedorenko et al., 2021).

Table 2.3 shows that, in contrast to studies in Europe, monitoring studies on HPE in north (Su et al., 2017) and central (Wang et al., 2019) China reported that PFBA and PFOA were the largest contributors to the total PFAS profile, instead of PFOS. Furthermore, the egg concentrations of these two formerly mentioned compounds were several orders of magnitude higher in China compared to those in Europe, both nearby and remotely from a PFAS point source. This discrepancy between both regions is most likely due to different historical and ongoing PFAS emission quantities and product output. In Europe, PFOS and PFOA have been gradually phased out from 2002 by its main manufacturers (Lau et al., 2007). Since then, China has become one of the largest global producers of PFOA (Land et al., 2018; Liu et al., 2021a). In parallel with the phase out of long-chain PFAS, such as PFOA and PFOS, the short-chain PFBA has become one of the major substitute compounds in fluorochemical industry, resulting in frequent detection and increased concentrations in the environment and biota over recent years (Liu et al., 2021a). This is also reflected in the present study, as the detection frequency and concentrations of PFBA in HPE tend to increase at locations closer to the plant site.

2.5.2 PFAS relationships with survey data

To the best of our knowledge, our study is the first to investigate whether housing conditions (feed type and flock size) and age of the laying hens affect PFAS concentrations in HPE. The survey results indicated that young laying hens contained on average higher egg PFOA concentrations compared to relatively old laying hens. This age difference has also been observed in other studies on both terrestrial birds (Park et al., 2021) and waterfowl (*Uria aalge*; Holmström and Berger, 2008), and can be explained by both maternal transfer and fewer elimination possibilities of young birds compared to older individuals (Holmström and Berger, 2008).

Eggs are an important elimination route for pollutants in birds and laying order effects of PFAS have been demonstrated in laying hens, with the first laid eggs containing higher PFAS concentrations (Kowalczyk et al., 2020; Wilson et al., 2020). On average, laying hens start their first egg laying cycle around the age of 18 – 24 weeks (Colin et al., 2020). Therefore, young laying hens (<1 year old) might depurate larger amounts of PFAS in their eggs than older individuals (>2 years old), as they have only had their first egg laying cycle and relatively high PFAS body burdens due to the maternal transfer. Furthermore, older individuals have experienced multiple moulting periods by which they can sequester more PFAS into feathers, which is an important sequestration tissue of pollutants,

including PFAS, in birds (Jaspers et al., 2009; Groffen et al., 2020). The relationship between age and egg PFOS concentrations was less clear, which may indicate that the intake of PFOS throughout the lifespan of the laying hen remains higher than the elimination rate.

Notably, backyard chickens in private gardens can become old and often keep laying eggs until the age of 8 years, whereas commercial laying hens are usually restrained for egg laying until 1.5 years of age (Ali et al., 2020). Moreover, the egg production of the average laying hen starts decreasing around the age of 16 months (Joyner et al. 1987), while the absolute yolk weight continuously increases with age (Suk and Park, 2001). The yolk is the main target tissue within the egg compartments, as approximately 90% and 99% of the deposited PFOA and PFOS egg concentrations, respectively, are transferred to the yolk (Su et al., 2017). Consequently, one would expect that laying hens build up again higher PFAS body burdens and lower elimination capacities from around 16 months of age onwards, with larger quantities of PFAS that can be transferred to a fewer number of eggs. Unfortunately, the age of the laying hens in the category “old” was still relatively young (33 ± 12 (SD) months of age) and the sample size was too low ($N = 10$) to properly test this hypothesis in the present study.

Laying hens that were fed an obligate diet of kitchen leftovers tended to contain higher egg PFOS and PFOA concentrations. Crop uptake of PFAS from contaminated soil has been shown to be an important entrance pathway to the terrestrial food chain (Lechner and Knapp, 2011; Liu et al., 2019). Contrary to other organic pollutants, PFAS accumulate both in vegetative and root parts of plants, which are dominated by short-chain PFAS and long-chain PFAS, respectively (Ghisi et al., 2019). Both plant tissues are frequently provided as leftovers to laying hens of private owners. This was also supported by the fact that these compounds were frequently detected in the chicken eggs. Moreover, many volunteers simultaneously cultivated their own plant crops besides the housing of chickens, which can contain relatively high PFAS concentrations compared to commercial feed as they are grown in less controlled conditions (Liu et al., 2019; Önel et al., 2018). Additionally, numerous carboxylates that were detected in the eggs are also typically found in rain water, which may be a contributing PFAS source as drinking water to the laying hens (Lu et al., 2018). Nevertheless, soil has also been identified as a major exposure source of organic pollutants to laying hens (Sioen et al., 2008; Waegeneers et al., 2009), including PFAS (Death et al., 2021). Besides self-cultivated crops, other potential food sources can be a significant source of contamination to

domestic chickens (e.g. fat leftovers of meat and cheese crusts), which should be considered in future studies.

2.5.3 Human health risk indications

Overall, consumption of HPE may contribute to a large extent to the intake of PFAS in humans. For all age groups, the TWI of 4.4 ng/kg bw per week (for the sum of PFHxS, PFOS, PFOA and PFNA) was exceeded ($\geq 67\%$ of the locations) in every buffer zone up till 10 km from the plant site (Table 2.2) at a consumption rate of two eggs per week. Similarly, the MTR of PFOS (43.8 ng/kg bw per week) was frequently exceeded within 4 km from the plant site, in particular for young children up to 9 years old.

The present study indicates that PFAS exposure in the Flemish population, both nearby (<2 km) large fluorochemical industry and in a 10 km radius from this point source, should be of high concern. Both health criteria (TWI and MTR) were frequently exceeded both closely and more remotely from the fluorochemical plant, and often to a great extent in the case of the TWI. Besides HPEs, the potential intake of PFAS via other sources, including commercial food (eg. fish, meat and offal food), self-cultivated vegetables, atmospheric dust and water, can be important additional pathways of human PFAS exposure (Herzke et al., 2013; Liu et al., 2019; Pasecnaja et al., 2022; Xu et al., 2021b). Likely, the total PFAS intake via multiple exposure pathways will be higher than the estimations made in the present study. Therefore, health effects due to PFAS intake via HPE cannot be excluded, especially on the immune system, for which human epidemiological evidence exists to date (EFSA, 2020; Grandjean et al., 2020; Sunderland et al., 2019). Although the underlying mode of action is still largely unknown, epidemiological studies have found strong indications that the immune system, on which the TWI criterion is based, is a major toxic endpoint of PFAS in humans (EFSA, 2020; Grandjean et al., 2020; Sunderland et al., 2019). In light of the SARS CoV 2 pandemic, for which increased severity of COVID-19 disease outcome has been associated with elevated PFBA plasma concentrations (Grandjean et al., 2020), it remains extremely important to further biomonitor PFAS and assess human exposure risks.

2.5.4 Future research perspectives

Our study, which aimed at examining the PFAS distribution in HPE, has several limitations which give rise to new research directions/questions that need to be tackled. Firstly, PFAS have the potential for air dispersion (Galloway et al., 2020) and knowing that the prevailing wind in most areas in Flanders is either northwest (0-90°) or southwest (180-270°) (Toparlar et al., 2018), higher egg PFAS concentrations are expected in gardens oriented towards these particular directions. Therefore, additional locations in missing wind directions will be sampled in successive monitoring campaigns to elaborate on this hypothesis. Secondly, our results demonstrate for the first time that housing conditions and biological factors can play a significant role in the exposure of PFAS to free-ranging laying hens. Future studies should consider relevant factors that may affect the PFAS exposure in laying hens. For instance, soil characteristics, scratching area and density (number of hens/m²), vegetation coverage and shape of the chicken enclosure can (in)directly influence the bioavailability and exposure of organic pollutants to laying hens (Sioen et al., 2008; Waegeneers et al., 2009). Ultimately, this may result in remedial measures for inhabitants to reduce exposure to PFAS via self-cultivated food consumption. Finally, extensive research considering multiple self-cultivated food items other than HPE (vegetables and fruit), as well as relevant exposure sources to laying hens (soil, rain water and key prey items, such as earthworms) should be considered in future PFAS monitoring campaigns.

2.6 Conclusion

The present study detected numerous PFAS in HPE, both nearby (<2 km) and up to 10 km from a major known point source. PFOS was the dominant compound and present in relatively high concentrations, compared to other European studies on PFAS in food. PFOS concentrations steeply declined with increasing distance from the fluorochemical plant in Antwerp. By comparing our results to previous studies in the same study area, maximum PFOS concentrations seem to have declined over the years, probably resulting from the phase-out. Nevertheless, the present findings indicate that human exposure to PFAS via consumption of HPE can be relatively high, even for compounds that have been phased-out decades ago in Europe. Potential health risks with respect to currently established health guidelines cannot be excluded, as the tolerable weekly intake threshold was often exceeded in every examined buffer zone.



Chapter 3: Prediction of perfluoroalkyl acids (PFAAs) in homegrown eggs: insights into abiotic and biotic factors affecting bioavailability and derivation of potential remediation measures

This chapter was published in *Environment International*:

Lasters, R., Van Sundert, K., Groffen, T., Buytaert, J., Eens, M. & Bervoets, L. (2023). Prediction of perfluoroalkyl acids (PFAAs) in homegrown eggs: Insights into abiotic and biotic factors affecting bioavailability and derivation of potential remediation measures. *Environment International*. 181: 108300-108313. <https://doi.org/10.1016/j.envint.2023.108300>.

3.1 Abstract

Homegrown eggs from free-ranging laying hens often contain elevated concentrations of perfluoroalkyl acids (PFAAs). However, it is unclear which factors contribute to these relatively large exposure risk scenarios. Moreover, existing bioavailability and modeling concepts of conventional organic pollutants cannot be generalized to PFAAs due to their different physicochemical soil interactions. Therefore, there is an urgent need for empirical models, based on real-world data, to provide insights into how (a)biotic factors affect the bioavailability to eggs. To this end, 17 targeted analytes were analyzed in abiotic (i.e. rainwater, soil; both $N = 101$) matrices and homegrown eggs ($N = 101$), which were sampled in 101 private gardens across Flanders (Belgium) in 2019, 2021 and 2022. Various soil characteristics were measured to evaluate their role in affecting PFAA bioavailability to the eggs. Finally, PFAAs were measured in potential feed sources (i.e. homegrown vegetable and earthworm pools; respectively $N = 49$ and $N = 34$) of the laying hens to evaluate their contribution to the egg burden. Modeling suggested that soil was a major exposure source to laying hens, accounting for 16-55% of the total variation in egg concentrations for dominant PFAAs. Moreover, concentrations in vegetables and earthworms for PFBA and PFOS, respectively, were significantly positively related with corresponding egg concentrations. Predictive models based on soil concentrations, total organic carbon (TOC), pH, clay content and exchangeable cations were successfully developed for major PFAAs, providing possibilities for time- and cost-effective risk assessment of PFAAs in homegrown eggs. Among other soil characteristics, TOC and clay content were related with lower and higher egg concentrations for most PFAAs, respectively. This suggests that bioavailability of PFAAs to the eggs is driven by complex physicochemical interactions of PFAAs with TOC and clay. Finally, remediation measures were formulated that are readily applicable to lower PFAA exposure via homegrown eggs.

3.2 Introduction

Production of self-cultivated food in private gardens has become increasingly popular over recent years (Illieva et al., 2022). Especially, housing of free-ranging laying hens for the production of homegrown eggs has gained worldwide popularity due to its intrinsic economic, nutritional and ecological benefits for humans (Padhi, 2016). However, the presence of organic contaminants in private gardens can pose a significant risk to human health as these can easily enter the food-chain through their bioaccumulative properties, which is also the case for per- and polyfluoroalkylated substances (PFAAs).

Compared to the majority of organic pollutants, PFAAs are exceptional in terms of physicochemical properties. These organofluorine compounds have fully fluorinated alkyl chains characterized by strong hydrophobic C-F bonds and a lipophobic ionizable acid group, making them very relevant for a wide range of industrial and commercial applications (Buck et al., 2011; Glüge et al., 2020). However, these properties also result in a very large persistence to degradation combined with a relatively large environmental mobility, varying with the alkyl chain length and type of acid group (Buck et al., 2011). Additionally, their proteinophilic nature leads to a large affinity with protein-rich tissues, including eggs (Wang et al., 2019), while food has generally been identified as the major human exposure source of PFAAs (Roth et al., 2020).

Biomonitoring studies have consistently linked PFAA intake via homegrown egg consumption with elevated human serum PFAA concentrations (Colles et al., 2020) and potential health risks (Lasters et al., 2022; Wang et al., 2019), the latter even in rural areas under very modest egg consumption scenarios (chapter 2, Lasters et al., 2022). Over the last decade, epidemiological studies have increasingly associated human exposure to specific PFAAs, mostly perfluorooctane sulfonic acid (PFOS) and perfluorooctanoic acid (PFOA), with various adverse health outcomes (Fenton et al., 2021; Shearer et al., 2021). Although there is still ongoing scientific debate about the degree of (mixture) toxicity for many PFAAs to humans at environmentally relevant concentrations (Ducatman et al., 2022), elevated exposure to PFOS and PFOA has consistently been linked with increased cholesterol levels, immune suppression (e.g. decreased vaccination response), thyroid disease and cancer (liver, kidney and testicular cancer) (Fenton et al., 2021; Grandjean et al., 2020; Shearer et al., 2021).

In order to decrease PFAA bioaccumulation in homegrown eggs and reduce potential health risks to humans, it is essential to understand how abiotic and biotic factors may affect the bioavailability of these compounds to laying hens and ultimately humans. However, very little knowledge exists on the bioavailability of PFAAs to food from animal origin and the majority of studies is largely limited to plant crop species and performed under experimental conditions, as recently reviewed by Adu et al. (2023). These studies have identified that the soil forms the main sink of PFAAs and that soil physicochemical properties play a decisive role in the bioavailability to terrestrial organisms. In a field experiment on a crop species (common bean, *Phaseolus vulgaris* Linnaeus), Knight et al. (2021) have shown that the bioavailable soil PFAA fraction to plants is largely influenced by the physicochemical properties of both the soil (organic matter, pH, clay content, soil electrical conductivity and cation exchange capacity (CEC)) and the PFAA properties (chain length and functional group). It is likely that these physicochemical properties also play a crucial role in the bioavailability of PFAAs to free-ranging laying hens.

Free-ranging laying hens are geophagous animals that can be directly exposed to pollutants through ingestion of contaminated soil particles (Kijlstra, 2004), which can make up to 40% of their diet (Jurjanz et al., 2015). Homegrown eggs from free-ranging laying hens have been shown to contain elevated PFAA concentrations compared to commercial eggs (Zafeiraki et al., 2016) and eggs from hens housed primarily in indoor conditions (Gazzotti et al., 2021; Mikolajczyk et al., 2022). Grazing of laying hens in outdoor conditions can result in significantly increased soil levels of organic matter, electrical conductivity and CEC (Soares et al., 2022). These soil characteristics can differently affect the bioavailability of PFAAs in the soil, depending on their type of binding interaction with the soil fractions (e.g. clay and organic matter) (Cai et al., 2022). For these reasons, homegrown eggs are an ideal study matrix for examining the role of PFAA bioavailability in the soil on the accumulation in the eggs.

PFAAs dominantly adsorb onto the organic matter and clay fraction via relatively strong hydrophobic and weak electrostatic interactions, respectively (Cai et al., 2022; Li et al., 2018a). Therefore, it can be expected that soil organic matter content and clay content would decrease and increase the bioavailability of PFAAs in the soil to the eggs. Moreover, soil properties can affect the binding interaction type (hydrophobic vs electrostatic) of PFAAs and, hence, also the bioavailability of PFAAs in the soil to the eggs. Higher pH and CEC levels may be associated with increased

bioavailability by increasing deprotonation of pH-dependent surface charges on the clay matrix fraction. Consequently, relatively weak electrostatic interactions between PFAAs and the clay matrix may increase through bridging of PFAAs with CEC fractions (exchangeable mineral and metal cations) (Cai et al., 2022; 2023), which may result in a higher fraction of PFAAs sorbed onto the clay. As soon as soil particles are ingested by the laying-hen, the low pH values in their glandular stomach (ranging from 3-4) (Waegeneers et al., 2009) should theoretically result in large protonation of the clay surface charges, which can result in increased absorption and thus larger bioavailability to the eggs.

Furthermore, biotic components of the terrestrial ecosystem within the private gardens, which may serve as feed items to the laying hens, such as invertebrates (e.g. earthworms) and crop food leftovers, are hypothesized to result in higher egg PFAA burdens. Likewise, rain water, which can be provided as drinking water to the laying hens, may also be related with higher egg PFAA concentrations. However, to the best of our knowledge, no studies have been performed to date that have evaluated the relationships between any of these (a)biotic factors and the bioaccumulation of PFAS in homegrown eggs.

From various perspectives, it is of the utmost importance to characterize these possible relationships and to predict homegrown egg PFAA concentrations, based on these multiple factors. Firstly, preventive what-if risk scenarios can potentially be modeled that may estimate the human exposure risk when free-ranging laying hens would be introduced. Secondly, identification of soil physicochemical properties that potentially affect the bioavailability of PFAAs to the laying hens may enable the opportunity to manipulate these soil physicochemical properties to ultimately lower human exposure. From a fundamental toxicological point of view, existing concepts of processes that affect the bioavailability for conventional organic pollutants cannot be generalized to PFAAs, due to their complex and very different physicochemical interactions with soil matrices (Sigmund et al., 2022). Therefore, there is also an urgent need for empirical models under real-world field conditions that can provide invaluable fundamental knowledge about the interaction of PFAAs with major environmental media, such as soil.

The main objective of this study was to develop and evaluate predictive empirical models for environmentally relevant PFAA concentrations in homegrown eggs, taking into account the

potential influence of corresponding soil concentrations, rain water concentrations and multiple soil physicochemical properties (total organic carbon (TOC), clay content, pH, CEC and soil electrical conductivity). Secondly, an explanatory analysis was conducted to gain mechanistic insights into potential associations between these abiotic variables and the egg PFAA concentrations. Finally, relationships between the feed items of the free-ranging laying hens (i.e. pools of self-cultivated vegetables and earthworms) and the egg concentrations were tested to assess their role in the possible transfer of PFAAs to the eggs.

3.3 Materials and methods

3.3.1 Volunteer recruitment

Eligible volunteers that met the major study criterium (i.e. private garden with at least two free-ranging laying hens of \geq six months old) were selected throughout Flanders (Belgium) via existing social networks, such as call ups in community groups of Facebook and existing informal contacts. All the personal data were treated confidentially in accordance with the latest privacy regulations (General Data Protection Regulation, GDPR). The privacy policy department of the University of Antwerp approved the data management plan. Each volunteer provided explicit approval for the processing of their data within the context of the research objectives in this study by means of an informed consent. The personal results were communicated to each volunteer via a short report containing background information on PFAAs, a consumption advice based on their individual results and general strategies that may lower overall PFAA exposure.

3.3.2 Sample collection

Paired environmental and biota samples were collected from 101 private gardens during the summer period of 2019 ($N = 33$), 2021 ($N = 58$) and 2022 ($N = 10$) across Flanders. These samples were collected at various distances within a radius of 25 km from a major fluorochemical plant in Antwerp (Belgium), based on the previously reported spatial distribution of PFAA concentrations in homegrown eggs (Lasters et al., 2022). In this way, a geographically diverse dataset could be obtained with a large contrast in the variables of interest, which was essential for the later data analysis of the predictive model. At all private gardens, a representative composite sample of the top soil layer (three subsamples in polypropylene (PP) tubes from 0-5 cm depth) in the chicken

enclosure, rain water (50 ml in PP tube), and homegrown eggs (two independent egg samples) were collected. Additionally, free-living earthworms (*Lumbricus terrestris* L), i.e. two separate pools of, respectively, three adult (= with clitellum) and three juvenile (= without clitellum) individuals in PP tubes and homegrown vegetables (pool of minimally two crop species in PP containers) were sampled in, respectively, 49 and 34 of the private gardens. For each monitoring period, the same standardized sample collection protocol was used for each matrix (detailed in SI: section 3.1) to minimize sampling bias.

Sample matrices were selected so as to explain a maximum amount of variation in egg PFAA concentrations, both at the compound and concentration level. Rain water and soil were selected as both are two major environmental media which can contain a wide variety of PFAA compounds (Liu et al., 2015; Pike et al., 2021). Moreover, rain water is often provided as a drinking water source to free-ranging laying hens (Chung et al., 2020), while the soil is a major feeding source to free-ranging laying hens (Jurjanz et al., 2015). Earthworms and homegrown vegetables can be important feed sources to free-ranging laying hens (Clark et al., 1995). Earthworms can accumulate very large concentrations of long-chain PFAAs (Munoz et al., 2020), while homegrown vegetables are usually enriched with short-chain PFAAs (Liu et al., 2023). Therefore, these potential feed sources were considered to be optimal candidate matrices to comprise most variation in PFAA exposure of the free-ranging laying hens and, hence, accumulation into the eggs. The PFAA concentrations can vary among vegetable species (Liu et al., 2023). Therefore, the vegetable samples were pooled to even out this potential variation. Further details on the collection methodology of these samples are given in the supplementary information (SI section 3.1).

3.3.3 Sample processing

The fresh soil samples were mixed thoroughly by hand and divided in separate aliquots for analyses of PFAAs and physicochemical soil characteristics (SI section 3.2). The homegrown eggs were homogenized with a stainless steel kitchen mixer and pooled into one sample. The earthworms were depurated for ± 24 h in PP containers (height: 8.8 cm, diameter: 12 cm), after which they were rinsed with MQ-water and homogenized with a TissueLyser. The edible parts of the crops were washed with MQ-water, after which they were mixed with a steel kitchen mixer. In between the mixing of each biotic sample, the kitchen mixer and TissueLyser were thoroughly cleaned with acetonitrile (ACN). All the samples were preserved at -20°C for later analyses.

3.3.4 Soil physicochemical characteristics

Both fresh and oven-dried soil samples were analyzed for various soil physicochemical characteristics and nutrients, including pH_{KCl} , clay content, TOC, total P/N, inorganic P (PO_4^{3-})/N (NH_4^+ and NO_3^-) fractions, electrical conductivity and exchangeable base cations (mineral cations: Ca^{2+} , Mg^{2+} , K^+ , Na^+ ; metal cations: Fe^{3+} , Mn^{2+} and Al^{3+}). The methodological procedures for the measurement of these soil parameters are detailed in the supplementary information (SI section 3.2).

3.3.5 PFAA chemical extraction

For the extraction of the samples, different protocols were used depending on the matrix type. Abiotic matrices, including oven-dried soil (0.30 ± 0.01 g) and unfiltered rain water (10 ± 0.1 mL) samples, were extracted following the protocol described by Groffen et al. (2019c). The biotic matrices, which comprised homogenized pooled samples of eggs (0.30 ± 0.01 g), earthworms (0.15 ± 0.01 g) and vegetables (0.30 ± 0.01 g), were extracted following the procedure of Powley et al. (2005). In brief, the biotic samples were extracted based on solvent extraction using ACN, and were cleaned-up with graphitized Envicarb carbon powder and the abiotic samples were extracted using solid-phase extraction with weak-anion exchange (WAX) cartridges. Details of both extraction methodologies are described in the supplementary information (SI section 3.3).

3.3.6 Quality control and quality assurance

During the homogenization of the biotic samples, solvent blanks (= 10 mL of ACN) were included every 10 samples to check for cross contamination between the samples. For the extraction, one procedural blank (= 10 mL ACN spiked with 10 ng of mass-labeled perfluoroalkyl carboxylic acid (PFCA) and perfluoroalkyl sulfonic acid (PFSA) mixture (Internal Standard, ISTD; MPFAC-MXA, Wellington Laboratories, Guelph, Canada) was included per 15 samples to verify any contamination during the extraction. In the case of batch contamination, the procedural blank values were subtracted from the subsequently measured samples. During the PFAA analysis, instrumental blanks (ACN) were regularly injected to rinse the columns and prevent cross contamination across the samples. Sadia et al. (2020) reported the presence of taurodeoxycholic acid (TDCA), a bile acid that shares the same diagnostic transition with PFOS (i.e. 499->80) and thus could affect the

quantified PFOS concentrations. However, full removal of TDCA was observed with a purification step during the extraction process using graphitized carbon at a ratio of 1:8 (mass graphitized carbon:mass chicken egg sample) (Sadia et al., 2020). In the present study, a ratio of 1:6 was used in the purification step which ensured removal of TDCA from the samples. This was also confirmed with the additional monitoring of the 499->99 transition unique for PFOS, as calculated concentrations based on this transition were not significantly different from those calculated with the 499->80 transition ($P = 0.57$, paired-Wilcox test).

Calibration curves were prepared by adding a constant amount of the ISTD to varying concentrations of an unlabeled PFAA mixture. The serial dilution of this mixture was performed in ACN. A linear regression function with highly significant linear fit (all $R^2 > 0.98$; all $P < 0.001$) described the ratio between concentrations of unlabeled and labeled PFAAs. Individual PFAAs were quantified using their corresponding ISTD with exception of perfluoropentanoic acid (PFPeA), perfluoroheptanoic acid (PFHpA), perfluorotridecanoic acid (PFTrDA), perfluorotetradecanoic acid (PFTeDA), perfluorobutane sulfonic acid (PFBS), perfluorodecane sulfonic acid (PFDS), hexafluoropropylene oxide-dimer acid (HFPO-DA) and sodium dodecafluoro-3H-4,8-dioxanonoate (NaDONA). These analytes were all quantified using the ISTD of the compound closest in terms of functional group and size (Table S3.1), which was validated by Groffen et al. (2021).

The samples from the three monitoring campaigns (i.e. 2019, 2021 and 2022) were analyzed separately in each of their respective years. Potential variation in the instrumental analyses among these years was taken into account by spiking all the samples with a constant quantity (i.e. 10 ng) of ISTD. For the calculation of the concentration, the peak response area of the unlabeled targeted analyte was normalized to the peak response area of the corresponding labeled compound present in the ISTD. In this way, potential variation in extraction efficiency and instrumental analyses among the samples was corrected.

3.3.7 Chemical analysis

In total 11 perfluoroalkyl carboxylic acids (PFCAs) (perfluorobutanoic acid (PFBA), PFPeA, perfluorohexanoic acid (PFHxA), PFHpA, PFOA, perfluorononanoic acid (PFNA), perfluorodecanoic acid (PFDA), perfluoroundecanoic acid (PFUnDA), perfluorododecanoic acid (PFDoDA), PFTrDA and

PFTeDA), four perfluoroalkyl sulfonic acids (PFSAs) (PFBS, perfluorohexane sulfonic acid (PFHxS), PFOS and perfluorodecane sulfonic acid (PFDS)) and two emerging fluoroether analytes (NaDONA and HFPO-DA or GenX) were targeted using ultrahigh performance liquid chromatography (ACQUITY, TQD, Waters, Milford, MA, USA) coupled to a tandem quadrupole (TQD) mass spectrometer (UPLC-MS/MS), operating in negative electrospray ionization. The different target analytes were separated using an ACQUITY UPLC BEH C18 VanGuard Precolumn (2.1 × 50 mm; 1.7 μm, Waters, USA). The mobile phase solvents consisted of ACN- and HPLC-grade water, which were both dissolved in 0.1% HPLC-grade formic acid. The solvent gradient started at 65% of water to 0% of water in 3.4 min and back to 65% water at 4.7 min. The flow rate was set to 450 μL/min and the injection volume was 6 μL. PFAA contamination that might originate from the LC-system was retained by insertion of an ACQUITY BEH C18 pre-column (2.1 × 30 mm; 1.7 μm, Waters, USA) between the solvent mixer and the injector. The target PFAA analytes were identified and quantified based on multiple reaction monitoring (MRM) of the diagnostic transitions that are displayed in Table S3.1. Limits of quantification (LOQs) were calculated for each detected analyte, in matrix, as the concentration corresponding to a peak signal-to-noise ratio of 10.

3.3.8 Data processing

The raw dataset consisted of PFAA concentrations from all detected compounds in eggs, soil, rain water, juvenile earthworm pools, adult earthworm pools and vegetable pools along with the soil physicochemical characteristics (TOC, clay content, pH, exchangeable base cations and soil electrical conductivity) from both monitoring campaigns of 2019 and 2021. The dataset from 2022 was only used as validation dataset for the predictive modeling (see further in 3.3.9.). Prior to the regression analyses, this raw dataset was split into three sub datasets of paired data (Fig. S3.1), ranging from the most quantitative dataset to the most qualitative dataset (i.e. dataset containing most independent datapoints and least number of variables, and vice versa). In this way, both models with hypothetically the largest predictive power (most quantitative dataset) as well as models with the largest explanatory power (most qualitative dataset) could be selected for the regression analyses.

Exchangeable base cations were considered as separate variables for the later statistical analyses as these are known to influence the soil adsorption behavior of PFAAs in a different way, depending on their amount of charges and cation type (cf. mineral vs. metal) (Campos-Pereira et al., 2020),

and hence may also affect the bioavailability to the laying hens in a different way. For every sub dataset, PFAA compounds with $\leq 50\%$ detection frequency in any matrix were omitted to minimize left-skewness and prediction inaccuracy, which resulted in a paired dataset for nine PFAAs (PFOS, PFBA, PFOA, PFNA, PFDA, PFUnDA, PFDoDA, PFTTrDA and PFTTeDA). For repeatedly sampled locations in 2019 and 2021 ($N = 7$), one independent datapoint was obtained by calculating the average of the variable values from both years to avoid pseudoreplication.

3.3.9 Data analyses

3.3.9.1 Predictive modeling

All the statistical analyses were done in R (version 4.2) and the graphical visualization was conducted in GraphPad Prism (version 9.0). The most quantitative dataset (Fig. S3.1; dataset A) of the monitoring campaigns in 2019 and 2021 was used to evaluate the predictability of PFAA concentrations in homegrown eggs ($N = 89$), as this dataset contained the largest sample size and data contrast relative to the number of predictors. Hereby, the chance of overfitting the predictive model is reduced and the robustness of model predictions is increased. Positively skewed continuous variables were log-transformed as this stabilized the variation in the residual distribution of the datapoints. Model diagnostic plots were run to evaluate model assumptions including linearity, as well as normality and homoscedasticity of the residuals. Variance inflation factors (VIFs) were calculated for all the significant predictors to assess the degree of collinearity among them. If VIF was ≥ 5 , the variable with the lowest partial R^2 was excluded from the model following Akinwande et al. (2015). For all the selected variables, the VIFs ranged between 1.00 and 2.31 indicating no significant multicollinearity problems (Table S3.4 and Table S3.5). Regression tree plots (package 'tree') and 3D surface plots (package 'mgcv') were used to identify any potential meaningful interactions among the predictor variables.

For each of the nine PFAAs, multiple regression models were constructed with egg concentrations as the dependent variable and the corresponding soil concentrations, soil physicochemical characteristics and rain water concentrations as independent predictor variables. A stepwise backward selection procedure was used to obtain the best-fit model using the Akaike information criterion (AIC), followed by stepwise elimination of predictors with the highest non-significant P -value ($P \geq 0.1$). This reduction process continued until only significant ($P \leq 0.05$) variables remained

in the final model (Steyerberg, 2009). The variable soil concentrations always remained in the model as continuous covariate to have real-world based models. A two-way interaction term between pH and clay content was added to each model for the following reasons: (1) changing pH values can affect the amount of pH-dependent surface charges on the binding sites of clay minerals, which can result in altered PFAA adsorption strength (Nguyen et al., 2020) and hence change the bioavailability of PFAAs to the laying hens; (2) models with inclusion of the interaction term systematically exhibited lower prediction error (lower AIC value) than models with only the main effects of pH and clay content.

Quality metrics were computed for the regression models to assess their overall predictive performance, as outlined by Steyerberg et al. (2010). Goodness-of-fit parameters were constructed which comprised the model fit (adjusted total R^2), the mean absolute error (MAE) and the root mean squared error (RMSE) of the residuals. The uncertainty of the mean slope and individual predictions were captured with, respectively, a 95% confidence interval (CI) and/or prediction interval (PI). The models were calibrated using both an internal validation and an external validation approach to test the degree of similarity between the measured and predicted egg PFAA concentrations. This was done through 10-fold cross-validation with repeatedly random selection of the test sets, after which these predictions were combined with those of the original model and regressed to the measured egg concentrations. Additionally, the performance of the model predictions was externally tested on an entirely new validation dataset of homegrown eggs ($N = 10$) from a monitoring campaign in 2022, which was conducted within the same season but in different private gardens as compared to the ones in 2019 and 2021.

3.3.9.2 Explanatory analysis

Descriptive statistics were computed for the main soil physicochemical properties of the chicken enclosures (Table 3.1). In addition, Pearson correlation tests were performed among the soil physicochemical characteristics to better understand their relationships (Fig. S3.2), which was useful as general background information for the interpretation of the further analyses and given that soil properties in the chicken enclosure usually show a distinct pattern (Soares et al., 2022). The quantitative dataset (Fig. S3.1; dataset A) was used to test significant associations between soil PFAA concentrations, soil physicochemical characteristics (i.e. explanatory variables) and egg PFAA concentrations (i.e. response variable). The dataset was mean-centered and standardized to

harmonize the variables and to enable valid comparisons among them. Tree plots were constructed for each of the nine PFAAs to visualize the associations between the tested explanatory variables and the outcome variable. Parameter estimates were reported as standardized Cohen’s effect sizes and 95% CIs.

Table 3.1: Descriptive statistics (geometric mean, standard deviation (SD) and min. – max. range) of the soil physicochemical characteristics in the top soil (0-5 cm) composite samples from the chicken enclosures of private gardens ($N = 89$) in Flanders (Belgium). The soil solid components include the total organic carbon content (TOC), total organic nitrogen (TON), total organic phosphorus (TOP) and clay content. The measured physicochemical properties are pH_{KCl}, soil electrical conductivity (in $\mu\text{S}/\text{cm}$), exchangeable cations (mineral base cations: Ca^{2+} , Mg^{2+} , K^+ , Na^+ and metal cations: Fe^{3+} , Al^{3+} , Mn^{2+} in meq/100 g of dry weighed soil) and the inorganic N (NH_4^+ and NO_3^- , in mg/kg) and P (PO_4^{3-} , in mg/kg) fractions. Note that the N and P (in)organic fractions could only be measured on the soil samples of 2021 and 2022.

Soil physicochemical property	Min	Mean	SD	Max
TOC (%)	2.1	2.78	2.68	15.5
TON (mg/kg dw)	820	4790	2368	15577
TOP (mg/kg dw)	762	1967	615	3585
Clay content (%)	0.933	2.02	0.604	3.84
pH _{KCl}	5.23	6.58	0.461	7.54
Soil electrical conductivity	41.5	310	32.9	1261
Ca^{2+} (meq/100 g soil dw)	4.06	15.9	5.82	37.3
Mg^{2+} (meq/100 g soil dw)	0.498	2.72	1.55	7.89
K^+ (meq/100 g soil dw)	0.235	2.49	1.64	7.66
Na^+ (meq/100 g soil dw)	0.027	0.429	0.615	3.98
Fe^{3+} (meq/100 g soil dw)	0.005	0.024	0.018	0.092
Al^{3+} (meq/100 g soil dw)	0.008	0.052	0.032	0.245
Mn^{2+} (meq/100 g soil dw)	0.024	0.134	0.102	0.747
NH_4^+ (mg/kg dw)	0.28	62.3	96.8	440
NO_3^- (mg/kg dw)	2.49	216	213	1238
PO_4^{3-} (mg/kg dw)	0.207	20.7	33.1	196

The qualitative dataset (Fig. S3.1; dataset B) was used to evaluate any significant relationships between the egg PFAA concentrations and the PFAA concentrations in the earthworm pools (juveniles and adults, two separate explanatory variables) and in the vegetable pools. Hereby, the soil PFAA concentrations which explained most variation in the corresponding egg concentrations, based on the partial R^2 of the previous analysis, were controlled for by retaining soil PFAAs as a continuous covariate in these models. A two-way interaction term was tested between the

earthworm PFAA concentrations and soil PFAA concentrations as earthworms may synergistically decrease or increase the bioavailability of PFAAs to terrestrial organisms and hence the egg concentrations (Hickman and Reid, 2008). An interaction term between PFAA concentrations in earthworm pools and vegetable pools was not included in the model to prevent oversaturation of the models, as the number of statistical tests was high relative to the sample size ($N = 34$) of the qualitative dataset.

3.4 Results

3.4.1 Matrix profile and concentrations

An overview of the profile and mean concentrations of all detected PFAAs in each of the examined abiotic and biotic matrices are shown in Fig. 3.1. PFOS was the dominant compound in both the soil, homegrown eggs, adult and juvenile earthworms (Fig. 3.1a-c, mean: 4.61 ng/g dry weight (dw), 32.1 ng/g wet weight (ww), 38.1 ng/g ww and 54.7 ng/g ww, respectively). On the other hand, PFOA and PFBA were the major compounds in rain water and in the vegetable pools (Fig 1a-c, mean: 34.0 ng/l and 0.483 ng/g ww, respectively). The polyfluoroalkyl compounds HFPO-DA (GenX) and NaDONA were never detected in any of the samples. In total nine PFAAs (PFOS, PFBA, PFOA, PFNA, PFDA, PFUnDA, PFDoDA, PFTTrDA and PFTTeDA) could be detected in > 50% of the samples across all the matrices. These PFAAs were selected for the predictive modeling (see further section 3.4.2).

In chicken enclosure soil and rain water, up to 13 and 11 PFAAs could be quantified with a mean total sum concentration of 9.45 ng/g dw and 138 ng/l, respectively (Fig. 3.1a, Fig. 3.1b). In chicken enclosure soil, three PFAAs (i.e. PFOS, PFBS and PFOA) contributed for > 62% of the total mean sum concentration. The composition of rainwater was dominated by PFOA (= 34.0 ng/l), PFBA (= 31.5 ng/l) and PFHxA (26.5 ng/l), which together accounted for > 59% of the total mean sum concentration (Fig. 3.1b). In the biotic matrices, 12 (vegetable pools), 13 (both homegrown eggs and adult earthworms), 12 (juvenile earthworms) targeted PFAAs could be detected (Fig. 3.1c). The highest total mean sum concentrations were found in juvenile earthworms (= 93.1 ng/g ww), followed by adult earthworms (= 72.9 ng/g ww), homegrown eggs (= 47.3 ng/g ww) and vegetable pools (= 3.78 ng/g ww) (Fig. 3.1c). In all the animal matrices, PFOS and long-chain PFCA (PFDoDA,

PFTrDA and PFTeDA) were the dominant compounds, whereas short-chain compounds (PFBA, PFPeA and PFHxA) contributed most to the profile of the vegetable pools (Fig. 3.1c).

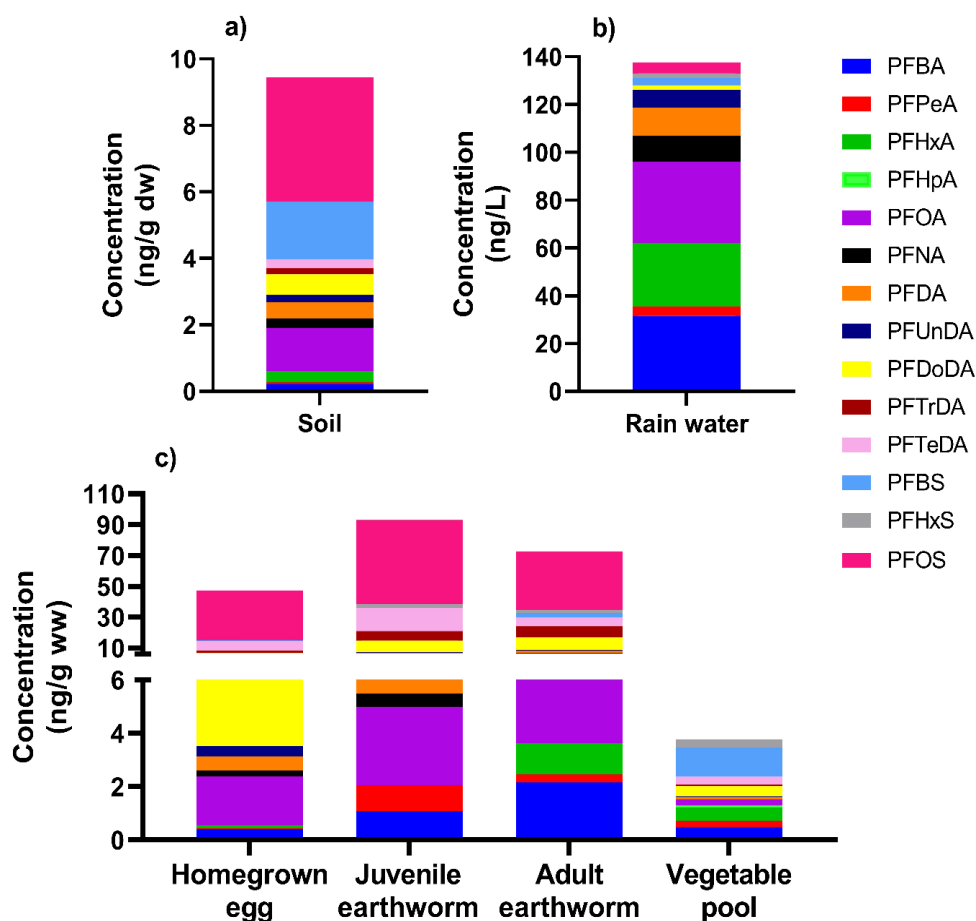


Fig. 3.1: Overview of the arithmetic mean concentrations of all detected PFAAs in (a) the top soil layer (0-5 cm) of the chicken enclosure soil (in ng/g dry weight (dw)), (b) rain water (in ng/l) and (c) homegrown eggs, juvenile earthworms, adult earthworms and vegetable pools (in ng/g wet weight (ww)) from the private gardens ($N = 89$) in Flanders (Belgium).

3.4.2 Predictive modeling

The descriptive statistics of the soil physicochemical properties in the chicken enclosure are provided in Table 3.1. The total organic matter fractions (TOC, total organic nitrogen (TON) and total organic phosphorous (TOP)) and pH were strongly variable among the chicken enclosures, while the clay content exhibited a relatively narrow range (min. – max.: 0.933 – 3.84 %). From the measured exchangeable base cations, Ca^{2+} showed the highest relative soil exchange capacity (15.9 ± 5.82 meq/100 g soil). PFOS, PFBA and the C_{9-14} carboxylates were all found at quantifiable concentrations in every target matrix (Table 3.2).

Table 3.2: Overview of the arithmetic mean concentrations of all detected PFAAs in (a) the top soil layer (0-5 cm) of the chicken enclosure soil (in ng/g dry weight (dw)), (b) rain water (in ng/l) and (c) homegrown eggs, juvenile earthworms, adult earthworms and vegetable pools (in ng/g wet weight (ww)) from the private gardens (*N* = 89) in Flanders (Belgium). For each matrix, the arithmetic mean \pm standard error (SE) is given along with the minimum (min.) and maximum (max.) range of the PFAA concentrations. LOQ = limit of quantification.

Chicken enclosure soil (ng g ⁻¹ dw)	PFAAs								
	PFOS	PFBA	PFOA	PFNA	PFDA	PFUnDA	PFDoDA	PFTTrDA	PFTeDA
LOQ	0.072	0.11	0.079	0.13	0.133	0.139	0.171	0.178	0.23
Min. - max. range	0.080 - 29.5	<LOQ - 3.60	0.290 - 6.15	<LOQ - 1.20	<LOQ - 1.45	<LOQ - 0.627	<LOQ - 2.48	<LOQ - 1.82	<LOQ - 1.07
Mean \pm SE	3.74 \pm 0.610	0.224 \pm 0.049	1.31 \pm 0.104	0.279 \pm 0.027	0.491 \pm 0.037	0.217 \pm 0.016	0.623 \pm 0.058	0.189 \pm 0.025	0.256 \pm 0.031
Rain water (ng l⁻¹)									
LOQ	0.301	1.35	1.63	0.738	1.32	1.28	1.4	1.47	1.51
Min. - max. range	<LOQ - 79.7	<LOQ - 604	<LOQ - 329	<LOQ - 421	<LOQ - 55.8	<LOQ - 86.7	<LOQ - 14.1	<LOQ - 28.5	<LOQ - 17.5
Mean \pm SE	4.61 \pm 1.32	31.5 \pm 9.18	34.0 \pm 6.61	10.7 \pm 1.32	11.9 \pm 1.24	7.34 \pm 1.46	2.04 \pm 0.127	<LOQ \pm LOQ	<LOQ \pm <LOQ
Homegrown eggs (ng g⁻¹ ww)									
LOQ	0.073	0.111	0.128	0.098	0.185	0.142	0.141	0.194	0.222
Min. - max. range	0.860 - 571	<LOQ - 3.72	<LOQ - 8.13	<LOQ - 1.20	<LOQ - 2.34	<LOQ - 3.78	0.187 - 21.9	<LOQ - 12.3	0.240 - 147
Mean \pm SE	32.1 \pm 9.34	0.404 \pm 0.063	1.84 \pm 0.284	0.223 \pm 0.026	0.525 \pm 0.049	0.386 \pm 0.052	3.07 \pm 0.397	1.54 \pm 0.194	6.42 \pm 1.74
Earthworm pools (ng g⁻¹ ww)									
Adult									
LOQ	0.518	0.35	0.146	0.167	0.626	0.124	0.782	0.336	0.335
Min. - max. range	2.42 - 320	<LOQ - 21.6	0.439 - 5.91	<LOQ - 2.15	<LOQ - 4.26	0.133 - 1.81	1.64 - 31.0	1.36 - 28.2	0.723 - 30.7
Mean \pm SE	38.1 \pm 7.78	2.17 \pm 0.482	2.57 \pm 0.194	0.391 \pm 0.051	1.54 \pm 0.108	0.649 \pm 0.046	8.21 \pm 0.927	7.26 \pm 0.760	5.66 \pm 0.725
Juvenile									
Min. - max. range	1.65 - 451	<LOQ - 10.1	<LOQ - 72.3	<LOQ - 10.8	<LOQ - 11.2	<LOQ - 3.22	<LOQ - 57.5	0.888 - 28.5	1.90 - 79.8
Mean \pm SE	54.7 \pm 12.3	1.08 \pm 0.241	2.95 \pm 1.37	0.491 \pm 0.205	1.33 \pm 0.208	0.646 \pm 0.083	7.33 \pm 1.19	6.09 \pm 0.682	15.2 \pm 2.07
Vegetable pools (ng g⁻¹ ww)									
LOQ	0.028	0.118	0.11	0.044	0.078	0.021	0.232	0.067	0.028
Min. - max. range	<LOQ - 0.259	<LOQ - 5.16	<LOQ - 1.42	<LOQ - 0.063	<LOQ - 0.461	<LOQ - 0.073	<LOQ - 1.28	<LOQ - 0.407	0.090 - 1.03
Mean \pm SE	<LOQ \pm <LOQ	0.483 \pm 0.162	0.235 \pm 0.038	<LOQ \pm <LOQ	0.084 \pm 0.013	0.028 \pm 0.003	0.377 \pm 0.037	0.074 \pm 0.013	0.282 \pm 0.036

The significant predictors and best-fit predictive equations of the final multiple regression models are summarized for nine PFAAs (PFOS, PFBA, PFOA, PFNA, PFDA, PFUnDA, PFDoDA, PFTrDA and PFTeDA) in Table 3.3. The soil concentration was the best single predictor of the corresponding egg concentrations for PFOS ($P < 0.001$, $R^2_{\text{partial}} = 42.2$) and the C₄₋₉ carboxylates ($P < 0.001$, $R^2_{\text{partial}} = 16.3$ -55.3%), while it was only marginally significant for the C₁₀₋₁₄ carboxylates ($P < 0.1$, $R^2_{\text{partial}} \leq 2.8\%$). Moreover, exchangeable Mn²⁺ ($P < 0.01$, $R^2_{\text{partial}} = 3.8$ -27.3%), exchangeable Fe³⁺ ($P < 0.01$, $R^2_{\text{partial}} = 2.4$ -11.3%), and the two-way interaction term pH:clay content ($P < 0.01$, $R^2_{\text{partial}} = 2.4$ -5.5%) and TOC ($P < 0.05$, $R^2_{\text{partial}} = 2.7$ -5.0%) were significant predictors of egg concentrations. Rain water concentrations and soil electrical conductivity did not significantly contribute to explaining variation in the egg concentrations for any compound ($P > 0.05$), both in single linear regression as well as in the multiple regression models controlling for the other significant predictors.

All the best-fit predictive equations showed a highly significant linear fit ($P \leq 0.01$), but varied in quality of prediction accuracy and precision of the egg concentrations (Fig. 3.2). The explained variation in egg concentrations, reflected by the adjusted R^2 values, ranged from 9.12% for PFDoDA to 66.6% for PFOA (Table 3.3). Importantly, the best predictive models were obtained for PFOS, PFOA and PFNA which together dominantly contributed for >75% to the total measured egg PFAA burden. The model quality metrics for PFOS, PFOA and PFNA were good to very good, with a MAE of 0.58, 0.28 and 0.07, respectively (Table 3.3). Moreover, robust and accurate predictions could be made for the models of these compounds, as the slopes of the predicted egg concentrations and measured egg concentrations did not significantly differ (two-sample t-tests, $P > 0.05$), both with the external validation approach (Fig. 3.2, Table S3.2) and the internal cross-validation approach (Fig. S3.3).

The predictive performance for the regression models of the other compounds (PFBA and $\geq C_{10}$ carboxylates) performed less well, with relatively low adjusted R^2 values ranging from 9.12% to 37.1% (Table 3.3). For PFDA and the C₁₂₋₁₄ carboxylates, most prediction error was caused by relatively large overall model-predicted underestimation of the measured egg concentrations and variation in the predictions of measured egg concentrations in the lower part of the concentration range (Fig. 3.2, range 0 - 1 log ng/g ww). This was also reflected in the quality metric values (Table 3.3, low RMSE and MAE) of these compounds and relatively large deviations in the cross-validation slopes for predictions within this lower concentration range (Fig. S3.2).

Table 3.3: Overview of the multiple regression modeling output for the prediction of homegrown egg concentrations (response variable) with respect to nine PFAAs (PFOS, PFBA, PFOA, PFNA, PFDA, PFUnDA, PFDoDA, PFTrDA and PFTeDA), taking into account the corresponding soil concentrations and significant soil physicochemical characteristics as predictor variables. The mathematic equations of the best-fit multiple regression models are provided along with the model quality metrics (AIC = Akaike information criterion; RMSE = root mean square error of the residuals; MAE = mean absolute error of the model predictions) to estimate the predictive performance of these models.

Response variable	Equation best-fit model	Model quality metrics				
		Model significance level	Adjusted R^2	AIC value	RMSE	MAE
Log egg PFOS concentrations	$36.6 + 1.07 * \log \text{soil PFOS} + 23.2 * \log \text{Fe}^{3+} - 0.934 * \log \text{TOC} - 37.2 * \log \text{clay content} - 17.5 * \log \text{pH} + 5.52 * \log \text{Mn}^{2+} - 7.92 * \log \text{Al}^{3+} + 18.7 * \log \text{pH}:\log \text{clay content}$	$P < 0.0001$ $F_{8,80} = 19.0$	62.1	-28.5	0.77	0.58
Log egg PFBA concentrations	$8.41 + 0.633 * \log \text{soil PFBA} - 9.44 * \log \text{clay content} - 3.98 * \log \text{pH} + 1.11 * \log \text{Mn}^{2+} - 0.174 * \log \text{Ca}^{2+} + 4.75 * \log \text{pH}:\log \text{clay content}$	$P < 0.0001$ $F_{6,82} = 7.21$	29.8	-240	0.23	0.18
Log egg PFOA concentrations	$-4.30 + 0.799 * \log \text{soil PFOA} + 25.6 * \log \text{Fe}^{3+} + 2.10 * \log \text{pH} - 2.96 * \log \text{Al}^{3+} - 0.251 * \log \text{Mg}^{2+}$	$P < 0.0001$ $F_{5,83} = 36.1$	66.6	-145	0.41	0.28
Log egg PFNA concentrations	$5.25 + 0.672 * \log \text{soil PFNA} + 2.04 * \log \text{Fe}^{3+} - 0.104 * \log \text{TOC} - 5.19 * \log \text{clay content} - 2.53 * \log \text{pH} + 0.399 * \log \text{Mn}^{2+} + 2.56 * \log \text{pH}:\log \text{clay content}$	$P < 0.0001$ $F_{7,81} = 21.5$	61.9	-389	0.10	0.07
Log egg PFDA concentrations	$8.86 + 0.063 * \log \text{soil PFDA} + 5.08 * \log \text{Fe}^{3+} - 0.255 * \log \text{TOC} + 0.882 * \log \text{Mn}^{2+} - 4.16 * \log \text{pH} - 8.97 * \log \text{clay content} + 4.50 * \log \text{pH}:\log \text{clay content}$	$P < 0.0001$ $F_{7,81} = 3.06$	25.8	-252	0.22	0.17
Log egg PFUnDA concentrations	$9.79 - 0.0008 * \log \text{soil PFUnDA} + 4.93 * \log \text{Fe}^{3+} + 1.13 * \log \text{Mn}^{2+} - 10.0 * \log \text{clay content} - 4.74 * \log \text{pH} - 0.235 * \log \text{Mg}^{2+} - 2.16 * \log \text{Al}^{3+} + 5.15 * \log \text{pH}:\log \text{clay content}$	$P < 0.0001$ $F_{8,80} = 7.46$	37.1	-273	0.19	0.14
Log egg PFDoDA concentrations	$1.86 + 0.319 * \log \text{soil PFDoDA} - 0.602 * \log \text{TOC} + 2.28 * \log \text{Mn}^{2+}$	$P < 0.05$ $F_{3,85} = 3.90$	9.12	-87	0.58	0.45
Log egg PFTrDA concentrations	$21.1 + 0.315 * \log \text{soil PFTrDA} - 0.560 * \log \text{TOC} + 1.83 * \log \text{Mn}^{2+} - 17.4 * \log \text{clay content} - 10.0 * \log \text{pH} + 8.95 * \log \text{pH}:\log \text{clay content}$	$P < 0.001$ $F_{6,82} = 5.22$	22.3	-136	0.43	0.34
Log egg PFTeDA concentrations	$38.0 + 0.187 * \log \text{soil PFTeDA} - 0.728 * \log \text{Mg}^{2+} + 5.13 * \log \text{Mn}^{2+} - 37.4 * \log \text{clay content} - 6.81 * \log \text{Al}^{3+} - 18.5 * \log \text{pH} + 19.1 * \log \text{pH}:\log \text{clay content}$	$P < 0.0001$ $F_{7,81} = 6.54$	30.6	-44.8	0.74	0.61

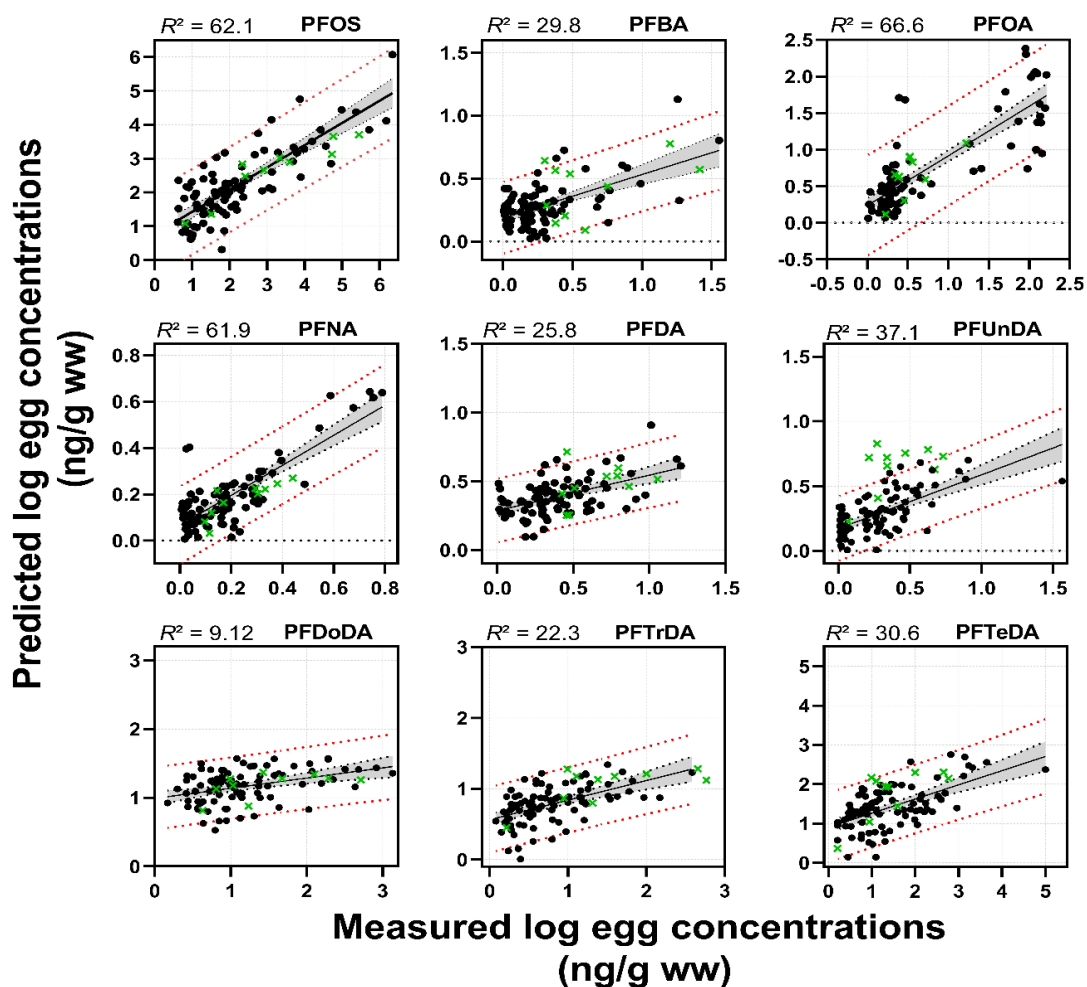


Fig. 3.2: Multiple regression plots showing the model-predicted concentrations (in $\log \text{ng g}^{-1}$ wet weight (ww) in homegrown eggs of 2021 (training dataset, black dots; $N = 89$) and 2022 (validation dataset, green crosses; $N = 10$) as a function of the measured homegrown egg concentrations (in ng g^{-1} ww, log-scale) for nine PFAAs. The adjusted R^2 value of each best-fit model is provided. The black solid line and grey band represent, respectively, the linear regression curve and 95% confidence interval of the average model-predicted log egg concentrations. The red dotted line represent the 95% prediction intervals.

On the other hand, the prediction uncertainty for PFUnDA and PFBA egg concentrations was mainly due to the large leverage from a few outliers, which was evident from the low adjusted R^2 values, but still good quality metric values (Table 3.3, e.g. low MAE and RMSE). Moreover, new predictions based on the external validation dataset fell within the 95% prediction interval of the regression curve (Fig. 3.2).

3.4.3 Explanatory analysis

The soil concentrations were positively and strongly associated with the egg concentrations for PFOS, PFBA, PFOA and PFNA (all $P < 0.01$ and large mean effect sizes of ≥ 0.35 units). For the C₁₀₋₁₂ carboxylates and PFTeDA, only a modestly significant relationship could be observed between the soil concentrations and egg concentrations ($P < 0.05$), while these associations were not significant for the other two carboxylates (all $P > 0.05$, Table S3.3). Lower amounts of soil TOC were significantly related with higher egg concentrations for PFOS ($P < 0.01$) and C₉₋₁₄ carboxylates ($P < 0.01$), except for PFUnDA (Fig. 3.3). For TON, only weak negative associations were found with PFUnDA egg concentrations (effect size of -0.13, $P < 0.05$), whereas higher TOP was associated with lower egg concentrations for PFBA and PFOS (resp. effect size of -0.19 to -0.29, $P < 0.05$).

The opposite relationship was observed for the main effects of both clay content and pH, as higher values of both variables were related with higher egg concentrations for most PFAAs (all $P < 0.05$), but in a contrasting way (Fig. 3.3). Indeed, the effect size of the positive relationship between pH and the egg concentrations was highly significant and very similar, in terms of effect size magnitude, for most compounds (apart from PFDoDA and PFTrDA, all $P < 0.05$ and range of mean effect sizes 0.22 – 0.38). On the other hand, the main effect of clay content was significantly and positively associated with the egg concentrations for most PFAAs ($P < 0.05$), but the effect size magnitude of this relationship tended to increase with increasing alkyl chain-length (Fig. 3.3). Similarly, the significantly positive two-way interaction term between pH and clay content indicated a combined synergistic relationship of these two variables with the egg concentrations (Fig. S3.5), except for PFOA and PFDoDA.

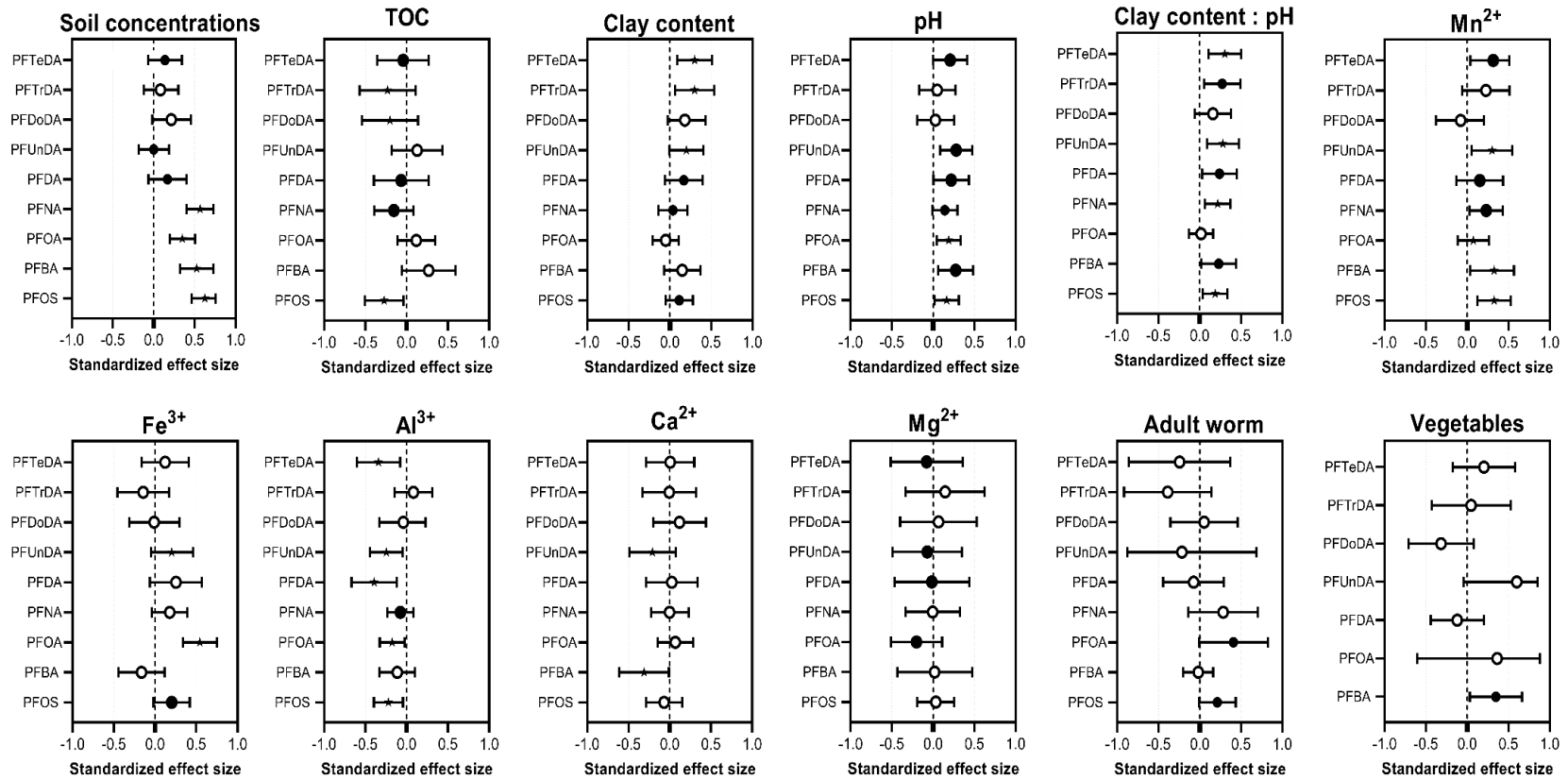


Fig. 3.3: Standardized effect size estimates and 95% confidence intervals (CIs) of the relationships between the dependent variable (= homegrown egg concentrations for nine PFAAs) and relevant explanatory variables (soil concentrations, total organic carbon (TOC), clay content, pH, two-way interaction term of clay content * pH, exchangeable metal cations (Mn^{2+} , Fe^{3+} and Al^{3+}) and exchangeable mineral cations (Ca^{2+} and Mg^{2+}), based on the outcome of the predictive regression models. Rain water PFAA concentrations, soil electrical conductivity, exchangeable Na^+ and K^+ are not shown as none of these explanatory variables was significantly related with any of the egg PFAA concentrations. Symbols represent the significance level of the relationship between the independent and dependent variable (asterisk : $P < 0.01$; filled circle: $P \leq 0.05$; hollow circle: $P \geq 0.05$ or not significant)

For the exchangeable cations, various significant relationships were found between egg PFAA concentrations and di-/tri-valent exchangeable cations, but in a contrasting way (Fig. 3.3). With respect to the exchangeable metal cations, most PFAAs showed significantly positive relationships between Mn^{2+} and egg concentrations (Fig. 3.3). Notably, Mn^{2+} was also strongly positively correlated with soil clay content (Pearson $R = 0.68$, $P < 0.01$; Fig. S3.2) and significantly positive interaction terms between Mn^{2+} and clay content were found (Fig. S3.5). Moreover, higher Fe^{3+} was strongly related with higher egg PFOA concentrations (mean effect size of 0.55, $P < 0.01$; Fig. 3.3), while this metal cation was also positively associated with higher PFOS and PFUnDA egg concentrations ($P < 0.05$; Fig. 3.3). Remarkably, and in contrast to Mn^{2+} and Fe^{3+} , the metal cation Al^{3+} was strongly negatively related with egg concentrations for most PFAAs ($P < 0.05$; Fig. 3.3). Moreover, Al^{3+} was strongly positively correlated with TOC content (Pearson $R = 0.51$, $P < 0.01$; Fig. S3.2). Likewise, this negative relationship was also found between mineral cations (Mg^{2+} and Ca^{2+}) and PFAA egg concentrations, but for less compounds and often less strong relationships compared to those found for Al^{3+} (Fig. 3.3). Lastly, monovalent exchangeable mineral cations K^+ and Na^+ were unrelated with egg PFAA concentrations.

PFOS was the dominant compound in homegrown eggs, earthworms and in the chicken enclosure soil, while PFBA was the major compound detected in vegetables (Table 3.2). For PFOS and PFOA, significantly positive relationships could be observed between adult worm concentrations and egg concentrations (both $P \leq 0.05$), whereas the relationships for the other compounds were not significant (all $P > 0.05$). For PFBA, the vegetable concentrations were significantly associated with the corresponding egg concentrations ($P < 0.05$) but not for the other compounds (all $P > 0.05$). Interestingly, juvenile worms contained significantly higher PFOS and PFTeDA concentrations than adult worms, while the reverse was true for PFBA and PFOA (two-sample t-tests; all $P < 0.05$).

3.5 Discussion

3.5.1 Matrix profile and concentrations

From the 17 targeted analytes, up to 13 PFAAs could be detected in the soil from the chicken enclosure (Fig. 3.1). Compared to general soil data at non-suspected sites across Europe, the mean soil concentrations for the Σ PFCA and Σ PFSA in the chicken enclosure (Σ PFCA = 3.58 ng/g dw;

Σ PFSA = 7.66 ng/g dw) largely exceeded the mean concentrations of soil for the Σ PFCAs and Σ PFSA in Europe, respectively 1.00 ng/g dw and 0.808 ng/g dw (Rankin et al., 2016). Moreover, the soil short-chain PFAAs concentrations of the present study were similar to those in residential garden soil from Minnesota (USA), which were sampled both nearby and remotely from a fluorochemical waste disposal site (Scher et al., 2018). However, soil PFOS and PFOA concentrations of the present study were more than twice as high as those reported by Scher et al. (2018). In rainwater, PFOA and PFBA were the major compounds with concentrations ranging between <LOQ- 329 ng/l and <LOQ-604 ng/l, respectively (Table 3.2). The rainwater concentrations for most detected compounds were in the same order of magnitude as those reported in some urban regions, as recently meta-analyzed by Cousins et al. (2022). Notably, trifluoroacetic acid is frequently the most abundant compound detected in rainwater (Pike et al., 2021), which was not included as a targeted analyte in the present study.

The homegrown egg concentrations of the present study were among the highest ever reported in homegrown chicken eggs (Gazzotti et al., 2021; Su et al., 2017; Wang et al., 2019), especially for PFOS, which was the dominant compound in the eggs with concentrations ranging between 0.860-571 ng/g ww (Table 3.2). The current European regulatory limits for PFOS (= 1.0 ng/g ww), PFOA (= 0.30 ng/g ww) and PFNA (= 0.70 ng/g ww) concentrations in commercial eggs (EC, 2022) were exceeded in 94%, 76% and 25% of the egg samples. This clearly confirms previous findings that homegrown egg consumption can be a major PFAA exposure source presenting potential health risks to humans (chapter 2, Lasters et al., 2022).

Likewise, PFOS was the dominant compound in the earthworms, with concentrations ranging between 1.65-451 ng/g ww and 2.42-320 ng/g ww in juvenile and adult life-stages (Table 3.2). This is in agreement with other studies on earthworms at aqueous film-forming foam impacted sites, which found large accumulation of PFOS, although at concentrations more than 100x higher compared to those of the present study (Munoz et al., 2020; Rich et al., 2015). The vegetable pool concentrations were dominated by PFBA (range: <LOQ - 5.16 ng/g ww), which is in agreement with other studies that examined PFAAs in field-grown vegetables (Liu et al., 2023; Scher et al., 2018). However, long-chain PFCAs were frequently detected in the vegetable pool samples at quantifiable concentrations (range: <LOQ - 1.28), while these compounds were rarely reported in field-grown vegetables at other sites (Liu et al., 2023; Scher et al., 2018).

3.5.2 Predictive modeling

To the best of our knowledge, no studies have been conducted that evaluated the predictability of PFAA concentrations in (homegrown) food, which makes it difficult to compare the obtained predictive models of the present study with literature data. Based on the extensive set of applied quality metrics to evaluate the model performance, good predictive models were obtained in terms of robustness (successful internal and external validation, resp. Fig. S3.4 and Fig. 3.3), precision and accuracy (relatively high adjusted R^2 , low MAE, Table 3.3) for prominent PFAAs (e.g. PFOS, PFOA and PFNA). These three compounds are often major contributors to the total PFAA content in dietary food (Klenow et al., 2013; chapter 2, Lasters et al., 2022), which is considered to be the most important exposure source of bioaccumulative long-chain PFAAs to the general human population (Roth et al., 2020). Consequently, they are very frequently detected in humans at concentrations associated with potential health risks (Colles et al., 2020; Fenton et al., 2021; Richterova et al., 2023).

For most PFAAs, the soil concentration was the most important predictor of their corresponding egg concentrations, which is in agreement with studies on other persistent organic pollutants, such as dioxins and polychlorinated biphenyls (PCBs), that also exhibit strong soil adsorption properties and hence a relatively large exposure risk to free-ranging laying hens (Waegeneers et al., 2009; Windal et al., 2009). Importantly, for these aforementioned classic organic pollutants, the soil concentration could often be used as a single predictor for egg concentrations (Schoeters and Hoogenboom, 2006; Waegeneers et al., 2009), whereas this is clearly not the case for PFAAs. In the present study, predictions often significantly improved by adding additional physicochemical properties to the models (Table S3.3), which clearly demonstrates the complex and distinct sorption behavior of PFAAs compared to other groups of organic pollutants. Therefore, the present study highlights the necessity of evaluating multiple parameters to adequately predict PFAA accumulation in terrestrial organisms.

The established predictive models for PFOS, PFOA and PFNA in the present study show promising potential for effective usage in monitoring and human risk assessment of PFAAs. Importantly, the construction of these models was underpinned by a large dataset ($N = 89$) and thoroughly validated (Fig. 3.3, Fig. S3.3) across a large geographical range, resulting in a well-covered contrast for most of the examined variables. Therefore, the models for those compounds that showed good overall

performance (e.g. PFOS, PFOA and PFNA) should be sufficiently accurate for large-scale application by regulatory agencies for decision-making processes to rapidly estimate the exposure risk via consumption of homegrown eggs in any given private garden of Flanders. Since soil is present in virtually every private garden, it enables the development of what-if risk scenarios that could clarify which exposure risk would be posed to the owners when free-ranging laying hens would be introduced. Furthermore, soil data of PFAA concentrations have become increasingly available over the last years in several countries (Brusseau et al., 2020), including in Flanders (City of Antwerp, 2021; Department Environment and Health, 2022b; Flemish Environment Agency, 2022a) due to intensified (ongoing) monitoring efforts, which could potentially be inserted into the models. In this way, the available soil data can be complementarily used together with the models to evaluate conditional human exposure risk scenarios with respect to homegrown egg consumption. Within this particular context, the models should at least include some basic soil parameters for the aforementioned PFAA (e.g. soil concentration, pH and clay content and their interaction effect), of which the first one can increasingly be adopted from existing soil databanks and the latter two are relatively low in cost and readily measurable (Wäldchen et al., 2012).

As a general remark, it should also be noted that the relative weight of a predictive model in decision-making processes should be in proportion to the amount of verification and validation of the model (Ellis, 2012). Therefore, the potential application of these models on a global scale should be interpreted with caution. For instance, some gardens in tropical climate regions can be characterized by much higher clay content ranges than those measured in Flanders (Akihiko and Wagai, 2017), which may result in an increased uncertainty of the model predictions. Moreover, for the remaining compounds (i.e. PFBA and C₁₀₋₁₄ carboxylates), which performed considerably less well than the aforementioned compounds (PFOS, PFOA and PFNA), some of the constructed predictive models in the present study have to be considered as an interim step for which future revision is highly recommended.

Clearly, soil concentrations and the other examined predictors did explain much less variation in egg concentrations for these compounds (min.-max. range total R^2 : 9.12 – 37.1%). This poor model performance is probably due to the lower variability of the concentration range for these compounds (e.g. often one order of magnitude difference between lower and higher order concentrations), which would make it intrinsically more difficult to predict the variability in egg

concentrations. However, it cannot be ruled out that other potential exposure sources than the soil could contribute to explaining additional variation in egg PFAA concentrations, such as inhalation of contaminated dust. The enclosures of laying hens are known for the accumulation of fine, airborne particulate dust matter, through preening, molting of feathers and deposition of fecal residues (Maffia et al., 2021; Viegas et al., 2013), to which PFAAs in theory can be adsorbed (Gustafsson et al., 2022). Prior to and during the timing of sample collection for the present study, these compounds were actively emitted (Peters et al., 2022) and circulating (Department Environment and Health, 2022a) in the atmosphere for a substantial part of the study area. For these reasons, it can be hypothesized that laying hens, through soil scratching and dust bathing behavior, can be substantially exposed to contaminated dust particles via inhalation.

Based on preliminary calculations with available literature data (detailed for PFDoDA as an example in section 3.6 of the SI), the contribution of PFAA intake via dust inhalation would be much lower than via soil consumption. Even for the worse-case scenario of dust intake, the intake (i.e. 0.120 ng/day) would be almost 8x lower than the intake (i.e. 0.945 ng/day) via a modal soil consumption scenario. However, we could not take into account the additional intake of dust via typical free-ranging laying hen behavioral activities, e.g. dust-bathing and feather preening behavior. Therefore, the above calculations for dust inhalation are probably still an underestimation of the total exposure via dust. It would be beneficial that future modeling efforts quantify these potentially important PFAA exposure sources.

Another important exposure source that may likely explain additional variation of the egg concentrations is feed of the laying hens other than earthworms and vegetables, which were considered in the present study. Notably, the explained variation in egg PFBA and PFOS concentrations substantially improved when the predictive models were run with the homegrown vegetables and adult earthworms as additional, significant predictors for PFBA and PFOS, respectively (e.g. total adjusted R^2 for PFBA increased from 29.8 to 43.9%). This result is in agreement with other studies on PFAAs (chapter 2, Lasters et al., 2022) and dioxins (Kijlstra, 2004; Waegeneers et al., 2009) in homegrown eggs. Together, these results indicate that homegrown vegetables and adult earthworms can be an important exposure source of PFBA and PFOS to free-ranging laying hens, respectively.

Lastly, it should be noted that seasonal fluctuations with respect to some of the soil physicochemical characteristics and grazing patterns of the free-ranging laying hens may affect the model outcomes. Nevertheless, soil TOC, pH and exchangeable cation levels usually vary only to a small extent within sites (Soares et al., 2022) and the variation among private gardens was relatively large in the present study due to the large spatial range that was considered. Therefore, it is unlikely that fluctuations in soil physicochemical characteristics would significantly alter the outcome of the modeling. Nevertheless, it is known that seasonal variation in grazing patterns and activity of free-ranging laying hens can be relatively large as longer days and warmer temperatures in the summer period result in more outside foraging and feeding activity (Ferreira et al., 2022; Taylor et al., 2017). Therefore, one might expect that soil and water intake would be higher in summer compared to spring (i.e. the onset of the egg-laying cycle) and may result in higher intake of PFAAs during summer. However, to the best of our knowledge, this has not yet been investigated and thus remains speculative.

3.5.3 Explanatory analysis

In line with the expectations, soil physicochemical characteristics that should result in lower (e.g. TOC) and higher (e.g. clay content, pH, exchangeable cations) bioavailability were often associated with lower and higher egg concentrations, respectively (Fig. 3). While TOC and clay content are often identified as the dominant soil solid components governing PFAA adsorption and retention in the soil matrix (Li et al., 2018a; Millinovic et al., 2015), their association with egg concentrations was consistently negative and positive for all the compounds, respectively. Therefore, given that the soil could also be identified as a major exposure source to the laying-hens, it is likely that opposite associations for TOC and clay content with egg concentrations result from adsorption affinity differences of PFAAs with both matrices (Li et al., 2018a; Cai et al., 2022), resulting in bioavailability differences. Consequently, the degree of PFAA absorption from the digestive tract to the systemic circulation may be altered and hence also the accumulation in the eggs.

Strong hydrophobic interactions dominate the PFAA adsorption onto TOC, whereas weaker and more reversible, electrostatic interactions are predominant on the clay fraction (Li et al., 2018a). Furthermore, the sorption reversibility on TOC decreases with increasing alkyl chain-length, whereas PFOS typically shows almost negligible reversibility, once adsorbed onto the TOC matrix (Millinovic et al., 2015). Therefore, it is hypothesized that TOC-adsorbed PFAAs could largely not be

absorbed from the digestive tract into the eggs, ultimately leading to lower egg concentrations. This is reflected in the present study as the largest effect size between TOC and egg concentrations was observed for more hydrophobic compounds with high sorption coefficients, such as PFOS (Fig. 3.3). Furthermore, as PFOS and many of the long-chain carboxylates have been phased-out (UNEP, 2019), a substantial proportion of environmental contamination of these compounds originates from historical pollution (chapter 2, Lasters et al., 2022). However, polyfluorinated precursor compounds, which are still being produced, can be biotransformed to PFBA and PFOA (Dhore and Murthy, 2021; Prevedouros et al., 2006). This may additionally explain the absence of relationships between the soil solid components and PFBA as well as PFOA.

On the other hand, the positive relationship between clay content and egg PFAA concentrations could be explained by weak, reversible electrostatic interactions resulting in successful absorption of PFAAs from the digestive tract to the eggs. All the examined PFAAs in the present study have such low pKa values that they are dominantly present in their anionic form under modal environmental conditions (Goss, 2008). Therefore, the charged nature of the electrostatic interaction between PFAAs and clay particles implies that the ad-/desorption is largely prone to pH changes, in contrast to the dominant hydrophobic interactions of PFAAs with TOC. As soon as soil particles are ingested by the laying-hen, the low pH values in their glandular stomach (ranging from 3-4) (Waegeneers et al., 2009) should theoretically result in large protonation of the clay surface charges, which can result in increased absorption. This is also in agreement with another study on PCB exposure to piglets, which has reported a much larger retention of pollutants in the digestive tract by TOC, compared to clay, resulting in lower bioavailability to adipose tissue (Delannoy et al., 2015).

The suggested higher bioavailability to the eggs of ingested PFAAs adsorbed to the clay content, is further supported by the observed significantly positive interaction between clay content and pH linked with higher egg concentrations. Higher pH levels result in increased deprotonation of pH-dependent surface charges on the clay mineral and TOC surface, which promotes binding of positively charged di- and trivalent cations onto the clay matrix (Wang et al., 2023). On their turn, these cations can interact with negatively charged PFAAs via cation bridging and ligand exchange mechanisms (Li et al., 2018a; You et al., 2010). Indeed, exchangeable Mn^{2+} and Fe^{3+} were positively correlated with egg concentrations for major PFAAs (Fig. 3.3) and also showed strong positive

interactions with clay content and pH, respectively (Fig. S3.5). Moreover, exchangeable Mn^{2+} correlated strongly and significantly with clay content while no significant correlations were found between these cations and TOC (Fig. S3.2). This could imply that the PFAA fraction sorbed to the clay content is larger than the fraction sorbed to the TOC, which would also explain the larger statistical effect sizes of the relationships between clay content and most PFAAs (Fig. 3.3) Notably, the statistical interaction effect between pH and clay content tended to increase with increasing chain-length, which may indicate that electrostatic sorption increases with increasing chain-length (Cai et al. 2022). Then, when the ingested clay particles are absorbed from the digestive tract to the liver, a proportionally larger amount of longer chain PFAAs may be transferred to the eggs.

Unexpectedly, for the exchangeable mineral cations (Ca^{2+} and Mg^{2+}) and Al^{3+} , which nevertheless show similar electrostatic interactions as described earlier for the metal cations (Li et al., 2018a), significantly negative associations were found with egg concentrations for several compounds. The soil chemistry of the chicken enclosures in the present study could be characterized by a mean pH of 6.58, combined with large concentrations of exchangeable Ca^{2+} and PO_4^{3-} (resp. mean 15.9 meq/100 g soil and 20.7 mg/kg soil). Under these specific soil conditions, which are typical for soils impacted by grazing of laying-hens (Soares et al., 2022), formation of precipitated $CaPO_4^{3-}$ and $MgPO_4^{3-}$ complexes is promoted (Shen et al., 2011). These complexes can potentially repulse PFAAs through competition for binding sites (Qian et al., 2017), leading indirectly to lower bioavailability to the laying-hens and hence lower egg concentrations. This hypothesis is partly supported by the observed positive and strong correlation between Ca^{2+} and PO_4^{3-} (Fig. S2), although such correlations with PO_4^{3-} were absent for Mg^{2+} and Al^{3+} . However, all of these three cations were significantly positively correlated with TOC (Fig. S3.2). Therefore, it is also plausible that the negative associations between these exchangeable cations and egg concentrations are, in fact, a reflection of the negative relationship between TOC and egg concentrations. In other words, soils with higher TOC levels also contained higher exchangeable Ca^{2+} , Mg^{2+} and Al^{3+} levels.

In conclusion, although the sorption behavior of PFAAs with soil solid components has been relatively well described (Cai et al., 2022), very little is known to date on how these soil ad- and desorption mechanisms can affect bioavailability of PFAAs in terrestrial organisms, including laying-hens. Nevertheless, it is well known for other pollutants (e.g. metals, PCBs and dioxins) that varying amounts of organic matter, clay content and other soil characteristics can have a profound effect

on the bioavailability to geophageous animals (Delannoy et al., 2015; Waegeneers et al., 2009; Zhang et al., 2019). Due to the amphiphilic properties of PFAAs, the present study emphasizes that multiple soil properties may affect the bioavailability of these compounds to terrestrial organisms. Evidently, the interplay of the suggested mechanistic soil interactions in the present study should be further elucidated under controlled lab conditions. With respect to the electrostatic clay content-PFAA interactions, this can be achieved by *in vitro* digestion models with simulated pH conditions of those found in the chicken stomach (pH = 3-4) and in the digestive tract (pH = 6.5) (Waegeneers et al., 2009). Alternatively, but more demanding from a practical point of view, semi-controlled lab experiments could be conducted with exposure of chickens to equally spiked soil concentrations but varying soil physicochemical properties. Within this setting, measurements in faeces and eggs of the exposed chickens could further elucidate to which extent PFAAs are bioavailable to the eggs.

3.5.4 Potential remediation implications

In comparison to eggs from commercial origin, which often contain non-detectable PFAA concentrations (Zafeiraki et al., 2016), it is clear that homegrown eggs are generally more susceptible to PFAA contamination. The present study shows that the soil can play both directly (i.e. food source) and indirectly (i.e. through soil-PFAA physicochemical interactions and as medium for prey, such as earthworms) a crucial role in this exposure context. Particularly, as the clay mineral fraction is associated with higher egg PFAA accumulation, it could be useful to introduce a sand parcel within the chicken enclosure as a readily applicable and relatively cheap measure. PFAAs show only very weak interactions with quartz (SiO₂), the main component of sand, which are readily desorbed with rainfall (Helling et al., 2016). In addition, sandy soils tend to contain lower amounts of soil invertebrates, including earthworms (Bedano et al., 2016), which could be identified as a significant exposure source of some PFAAs to the laying hens. Thus, considering that soil and soil physicochemical characteristics often explained >50% of the total variation in egg concentrations of abundant PFAAs in eggs, implementation of these measures could result in a substantial decrease in homegrown egg concentrations.

Notably, rain water PFAA concentrations were not significantly related with egg concentrations for any of the compounds in the present study. Although most target PFAAs were frequently detected in rain water, relatively low concentrations (mean ranged from <LOQ – 0.034 ng/ml, Table 3.2) were

measured compared to the soil or feed concentrations. Moreover, laying hens have an average drinking water intake of 185 ml per day (Howard, 1975), while soil and feed intake during foraging can be up to 35 g per day (Kijlstra, 2004), which implies that the intake of PFAAs via water would be negligibly small compared to the feed. Furthermore, it should be noted that some chicken owners did also provide tap water to the laying hens, especially during dry summer periods at the time of sampling. Nevertheless, it should be noted that the relative importance of exposure sources to terrestrial biota is generally site-specific. In the present study, a considerable part of the locations had been prone to industrial emissions and deposition onto the soil, which may have masked the role of water in the PFAA exposure to the free-ranging laying hens. In study areas with another PFAA contamination history, rain water can still be an important exposure source, for instance at study sites with accidental release of PFAAs into the air.

3.6 Conclusions

In the present study, we successfully developed and validated empirical models that accurately predict homegrown egg concentrations for some environmentally widespread and abundant PFAAs, e.g. PFOS, PFOA and PFNA. Based on these model outcomes, we proposed regulatory implications as part of time and cost-effective risk assessment of PFAAs in homegrown food, which is a dominant human exposure source of PFAAs. The present study highlighted that soil can be a major exposure source of PFAAs to free-ranging laying hens and that accumulation in homegrown eggs from soil intake is highly dependent on the internal bioavailability of the compounds, which is likely influenced by the interaction type (hydrophobic versus electrostatic) of PFAAs with the soil component (organic versus mineral composition) and potentially governed by the soil pH and exchangeable cations. The constructed predictive models of the present study can be further refined in future research efforts with additional data of other potential exposure pathways (e.g. dust ingestion and inhalation) and by evaluating the applicability of the models in regions with other PFAA contamination sources. Important local remediation measures were formulated to substantially lower the PFAA exposure to free-ranging laying hens and hence lower human exposure via homegrown egg consumption.



Chapter 4: Per- and perfluoroalkyl substances in homegrown crops: accumulation and human exposure risk

This chapter is under review as a research article in *Chemosphere*. Author list:

Lasters, R., Groffen, T., Eens, M. & Bervoets, L. (under review).

4.1 Abstract

Homegrown crops can present a significant exposure source of per- and polyfluoroalkyl substances (PFAS) to humans. Field studies studying PFAS accumulation in multiple vegetable food categories and examining the potential influence of soil characteristics on vegetable bioavailability under realistic exposure conditions are very scarce. Crop PFAS accumulation depends on a complex combination of factors. The physicochemical differences among the numerous PFAS makes risk assessment very challenging. Thus, simplification of this complexity into key factors that govern crop PFAS accumulation is critical. This study analyzed 29 targeted legacy, precursor and emerging PFAS in the vertical soil profile (0-45 cm depth), rainwater and edible crop parts of 88 private gardens, at different distances of a major fluorochemical plant. Gardens closer to the plant site showed higher soil concentrations which could be linked with historical and recent industrial emissions, while substantial PFOS concentrations in rainwater close to the plant site may be associated with local major road infrastructure works. Most compounds showed little variation along the soil depth profile, regardless of the distance from the plant site, which could be due to gardening practices. Annual crops consistently accumulated higher sum PFAS concentrations than perennials. Highest concentrations were observed in vegetables, followed by fruits and walnuts. Single soil-crop relationships were weak, which indicated that other factors (e.g. porewater) may be better measures of bioavailability in homegrown crop accumulation. Regression models, which additionally considered soil characteristics showed limited predictive power (all $R^2 \leq 35\%$), mainly due to low variability in crop concentrations. Human dietary intake estimations revealed that the crop exposure risk was similar nearby and remotely from the plant site, although overall contribution to dietary exposure can be relatively large. The tolerable weekly intake was frequently exceeded with respect to fruit and vegetable consumption, thus potential health risks cannot be ruled out.

4.2 Introduction

Per- and polyfluoroalkyl substances (PFAS) are a diverse group of synthetic aliphatic compounds that have at least one fully fluorinated methyl or methylene carbon atom (Wang et al., 2021). Their C-F bonds provide very high stability against (a)biotic degradation, hydrophobic and lipophobic properties making them valuable in various applications. Large-scale examples are fluoropolymer production (e.g. Teflon), electroplating, textile impregnation, firefighting foams and food packaging papers among many others (Glüge et al., 2020). However, these same properties make PFAS highly resistant to environmental degradation (Buck et al., 2011), leading to widespread global detection in environment and biota, including humans (Byns et al., 2022; De Silva et al., 2021; Lasters et al., 2021; Sims et al., 2022). Both research on laboratory animals and epidemiological studies over the past decade have linked PFAS exposure to various health risks, such as liver damage, immune system disruption, neurotoxicity, and cancer (Fenton et al., 2021; Grandjean et al., 2020; Lilienthal et al., 2017).

Food is a major PFAS exposure source to humans and recent scientific evaluations in commercial food concluded that seafood, eggs and fruits contributed most to the dietary exposure (EFSA, 2020; Pasecnaja et al., 2022). Production of homegrown food has become increasingly popular in many countries. Nonetheless, only few monitoring studies pointed out that homegrown food can have a large contribution to human exposure to chemicals (Brown et al., 2020; chapter 2, Lasters et al., 2022). For instance, weekly consumption of two homegrown chicken eggs was associated with an exceedance of the tolerable weekly intake (TWI) of 4.4 ng/kg bodyweight (EFSA, 2020) in $\geq 67\%$ of the sampled private gardens ≤ 10 km from a fluorochemical plant (chapter 2, Lasters et al., 2022). Nevertheless, studies on other popular homegrown produce in realistic field settings, such as annual and perennial crops, are still limited.

Most studies on PFAS accumulation in crops have been conducted in controlled soil experiments or hydroponic settings, often considering (very) high PFAS concentrations and a limited number of plant species, as recently reviewed (Xu et al., 2022; Wang et al., 2020). Mechanisms of PFAS uptake, accumulation and translocation in plants are very complex and depend on multiple factors. Among these, plant-specific characteristics, the molecular structure of the PFAS compound, soil physicochemical and biotic conditions play major roles in governing these mechanisms (Adu et al.,

2023; Mei et al., 2021). Long-chain PFAS tend to retain in below-ground parts (e.g. roots and tubers), while short-chain PFAS tend to accumulate in above-ground parts after being taken up by roots and transported through active and passive pathways (Ghisi et al., 2019; Mei et al., 2021). Moreover, accumulated sum PFAS concentrations are generally higher in vegetables than in fruits and cereal crops (Ghisi et al., 2019), while concentrations within crops are usually highest in leaves, followed by roots, shoots and fruiting parts (Liu et al., 2023; Xu et al., 2022). However, discrepancies in these general patterns have been observed between experimental work and field studies (Adu et al., 2023).

Another potentially important and somewhat overlooked factor in crop accumulation is the soil depth profile of PFAS. Long-chain PFAS tend to reside in the topsoil layer, while short-chain PFAS contribute more to the PFAS profile in deeper soil layers (Brusseau et al., 2020; Gan et al., 2022). The functional root depth of plants is species-specific and plants can adjust their root systems to take up resources at different soil depths throughout their life-stages (Peng and Chen, 2021). This implies that plants may be exposed to different PFAS, depending on their species-specific root depth and life-stage, which is a factor rarely taken into account for plant uptake studies in the field.

To the best of our knowledge, field studies considering the aforementioned factors in realistic exposure scenarios for a large variety of homegrown crops are very scarce (Liu et al., 2023). One major problem is that gathering of comprehensive field data on various site-specific parameters is costly and labor-intensive. PFAS comprises millions of chemicals which makes it unlikely that plant uptake of all these compounds can be evaluated (Adu et al., 2023). Predictive models linking soil and crop concentrations, considering critical soil characteristics impacting bioavailability, offer a potential solution (Xiang et al., 2023). Recently, simpler models predicting PFAS in certain crops relied on plant part concentrations and/or soil organic matter (SOM) as parameters (Felizeter et al., 2021; Liu et al., 2023). Yet, these models were limited, focusing on a few annual crop species, compounds, and soil parameters across specific sites (agricultural fields or lysimeters with spiked soil).

In this study, the accumulation of 29 targeted PFAS was compared among the edible parts of a large variety of crop categories (i.e. both annual and perennial species), grown in private gardens along distance gradient from a fluorochemical plant in Zwijndrecht, Belgium. Additionally, the PFAS

profile and concentrations in the soil of these gardens was assessed along a depth range of 0-45 cm. Moreover, empirical regression models were constructed which aimed to identify soil characteristics that may affect crop bioavailability and to predict PFAS concentrations in crops. Hereby, the soil concentrations, rainwater concentrations and a broad set of soil physicochemical characteristics were taken into account as model variables. Furthermore, the dietary intake and potential health risks to humans from consuming crops were evaluated according to existing health guidelines.

4.3 Materials and methods

4.3.1 Study area

Private gardens can exhibit large variation in crop species and soil characteristics, due to the highly variable cultivation practices and features among individual gardens (Egerer et al., 2017; Tresch et al., 2018). From this perspective, they can represent a promising study system to develop broadly applicable predictive models, which have the additional advantage that they provide a direct link with human exposure risk. The selected study area was the province of Antwerp (Belgium), in which a major fluorochemical plant is situated (Fig. S4.1). Through sampling at various distances from this plant site, a large variation in environmental concentrations and in soil characteristics was expected which may improve the predictive model performance (Groffen et al., 2019b; chapter 3, Lasters et al., 2023).

4.3.2 Volunteer recruitment

Potential study volunteers were recruited via existing social networks, such as call ups in community groups of Facebook and existing informal contacts. The following criteria had to be met in order to be eligible for study participation: 1) presence of vegetable cultivation in an open-field garden segment; 2) no usage of pesticides and 3) no replacement of main soil bedding material during the cultivation period. All personal information was handled confidentially according to the current privacy regulations of the General Data Protection Regulation (GDPR). The University of Antwerp's privacy policy department endorsed the data management plan of the study. Each participant explicitly consented to their data being processed for the research objectives through an informed consent. Individualized findings were communicated to volunteers via concise reports, including

background details on PFAS, personalized consumption advice based on their results, and general strategies to reduce overall PFAS exposure.

4.3.3 Sample collection

Rainwater ($N = 68$), soil ($N = 264$) and crop ($N = 197$) samples were collected in 88 private gardens during the summer (July until September) periods of 2019, 2021 and 2022 across the region of Antwerp (Fig. S4.1) within a radius of 0.5-30 km from a major fluorochemical plant in Antwerp, which is a well-known PFAS hotspot (Groffen et al., 2019b; chapter 2, Lasters et al., 2022). Both private gardens with suspected contamination from this point source as well as non-suspected sites, based on the PFAS hotspot map of Flanders (Department Environment and Health, 2022a), were selected for the sample collection.

The rainwater samples (± 50 ml) were collected in polypropylene (PP) tubes from rainwater casks, rainwater wells or open drinking water beakers (PP), depending on the availability and the source of irrigation that the volunteers used for watering of the crops. Soil samples of each ± 50 g were collected in 88 private gardens from three depth layers (0-5 cm, 5-25 cm and 25-45 cm; each $N = 88$) of the vegetable garden segment with a stainless-steel gouge drill and stored in separate PP tubes. The three subsamples of each depth layer were sampled at the growing spot of one annual vegetable plant, from which the edible parts were collected to have paired samples for the later predictive modeling. Additionally, the edible parts of maximally three other crop species, depending on the availability, were harvested. This resulted in the collection of shoot vegetables ($N = 34$), fruit vegetables ($N = 29$), leaf vegetables ($N = 19$), root vegetables ($N = 13$), legumes ($N = 6$), herbs ($N = 4$), small fruits ($N = 37$), large fruits ($N = 36$) and walnuts ($N = 19$) (Table S4.1). Minimally three replicate samples, preferably in the middle and at both edges of the vegetable segment, were collected manually with nitril gloves and stored in PP tubes.

4.3.4 Sample processing

The field-collected soil samples in the PP tubes were manually shaken and thoroughly mixed. An aliquot of 5.0 g from each subsample was oven-dried at 70°C for at least 72 hours and further analyzed for all targeted PFAS (Table S4.2). The remaining soil of the subsamples of the three depth layers was thoroughly mixed and aliquots of about 20 g from this pooled sample taken for further

analyses of various soil physicochemical characteristics and nutrients (see 4.3.6). The edible parts of the crop samples were thoroughly washed with milli-Q water in the lab, except for the walnuts. Then, each of the vegetable samples received a pretreatment according to the conventional requirements for human consumption (Table S4.1). The replicate samples were pooled and homogenized with a stainless-steel kitchen mixer (Bosch, type MSM65PER), which was thoroughly washed with acetonitrile (ACN) and milli-Q water in between the samples to prevent cross-contamination. The homogenates were stored in the fridge at $-20\text{ }^{\circ}\text{C}$ for later PFAS extraction and analysis.

4.3.5 PFAS analysis

The oven-dried soil ($0.30 \pm 0.01\text{ g}$) and rainwater ($10 \pm 0.1\text{ mL}$) samples were extracted using weak anion exchange solid phase extraction according to a validated procedure for abiotic samples described by Groffen et al. (2019c). The vegetable samples ($0.30 \pm 0.01\text{ g}$) were subjected to a clean-up step extraction procedure using graphitized carbon powder, following the protocol by Powley et al. (2005) with minor modifications. Full descriptions of both extraction methodologies, the quality control and assurance throughout the chemical extraction and analyses are provided in the supplementary information (SI section 4.3 and 4.4). Ultrahigh performance liquid chromatography (ACQUITY, TQD, Waters, Milford, MA, USA) coupled to a tandem quadrupole (TQD) mass spectrometer (UPLC-MS/MS), operating in negative electrospray ionization-mode was used for detection of peak signal for all the targeted analytes.

4.3.6 Soil physicochemical characteristics

Various soil physicochemical characteristics were measured including pH_{KCl} , clay content, TOC, total P/N, inorganic P (PO_4^{3-})/N (NH_4^+ and NO_3^-) fractions, electrical conductivity and exchangeable base cations (mineral cations: Ca^{2+} , Mg^{2+} , K^+ , Na^+ ; metal cations: Fe^{3+} , Mn^{2+} and Al^{3+}). Detailed descriptions of the methodological procedures for the analysis of those soil characteristics can be found in the supplementary information (SI section 4.5).

4.3.7 Data processing

The final raw dataset was split into three subsets of data to statistically test the formulated study hypotheses: dataset 1 consisted of all the soil data ($N = 264$) for comparison among the three soil depth layers (i.e. 0-5 cm, 5-25 cm and 25-45 cm), dataset 2 contained all the data ($N = 197$) of the crop PFAS concentrations for comparison of the crop categories and dataset 3 comprised the paired data of the PFAS in crop, soil, rainwater and soil characteristics ($N = 68$) which was used for the regression modeling.

The soil concentrations in every soil depth layer followed a strong distance gradient with respect to the fluorochemical plant in Antwerp, while no such gradient was observed for the vegetable food concentrations (Fig. S4.2). The distance from the plant site was taken into account as a controlling fixed factor (two subcategories: “ ≤ 4 km” and “ > 4 km”) in the later statistical comparisons of the soil concentrations (see section 4.3.9). Only compounds that could be quantified in $\geq 50\%$ of the samples in all the matrices (i.e. rainwater, each soil depth layer and in each crop category or subcategory (in the case of vegetables) were used for further statistical analyses. For those compounds, replacement concentration values were assigned to concentrations that were $< \text{LOQ}$, following a maximum likelihood estimation method (Villanueva, 2005; Lasters et al., 2022). No statistically significant differences in PFAS concentrations were found among the sampling years for the soil depth layers or the vegetable food (one-way ANOVAs, all $P > 0.05$). Hence, the sampling year was not considered as a controlling variable in further statistical analyses and the data of all the years were merged.

4.3.8 Human exposure risk

The evaluation of potential PFAS intake from vegetable-based foods comprised vegetables, fruits, and walnuts. Estimations were based on the average weekly consumption in Flanders, corresponding to 1015 g for vegetables and 770 g for fruits (De Ridder et al., 2016). For walnuts, given the absence of specific intake data, a weekly consumption of 175 g was considered in alignment with the recommended quantity advised by the Flemish health advisory board (De Hoge Gezondheidsraad, 2003). Assessments of PFAS intake through crops and walnuts were categorized into age groups, acknowledging that younger individuals typically exhibit a higher relative PFAS intake per kilogram of bodyweight compared to adults. Mean body weight values were extracted

from the latest food consumption datasets of the Belgian population (Van der Heyden et al., 2018), calculations were conducted for age intervals: 3-5, 6-9, 10-13, 14-17, and 18-64 years old. Data differentiation for males and females was provided for the latter age groups due to substantial weight variations between sexes within these categories. Ultimately, the estimated weekly intake (EWI) of PFAS was computed using the formula outlined below by Lasters et al. (2022).

$$EWI \left(\frac{ng}{kg} bw \right) = \frac{crop\ consumption\ (g/week) \times crop\ PFAS\ concentration\ (ng/g\ ww)}{body\ weight\ (kg)}$$

Subsequently, the estimated weekly intake (EWI) was compared with two commonly utilized health guideline benchmarks concerning the maximum acceptable PFAS intake through food. The first benchmark, the tolerable weekly intake value (TWI: 4.4 ng/kg bw per week), accounts for the combined levels of PFHxS, PFOS, PFOA, and PFNA, as outlined by the EFSA CONTAM Panel in 2020. The second health guideline value, known as the maximum tolerable risk values (MTR), specifies 43.8 ng/kg bw per week for PFOS and 87.5 ng/kg bw per week for PFOA. These two health criteria are established based on distinct toxicity measures: one centered around a sensitive toxic endpoint (i.e. reduced antibody response to vaccination in infants) and the other emphasizing a more critical endpoint (i.e. liver hypertrophy in rats). This approach is designed to ensure a comprehensive assessment of potential risks associated with PFAS intake.

4.3.9 Statistical analysis

All the statistical analyses were conducted in R (version 4.2.3) and visualization was done in GraphPad (version 9.0.0). Linear mixed effect models (LMMs) were used to compare PFAS concentrations among the soil depth layers and among the vegetable food categories (Table S4.1). One LMM was built with soil depth layer and distance zone from the plant site as fixed factors and another LMM was constructed with food category as fixed factor. For both LMMs, the private garden identity was included as a random factor. In this way, the potential within-site correlation due to repeatedly sampled food items and the non-independent nature of three soil layer samples originating from the same garden were taken into account. Post-hoc pairwise comparisons between the food and soil depth layer subcategories were performed using estimated (Bonferroni corrected) marginal means with the ‘emmeans’ package.

Multiple linear regression (MLR) models were built with the paired dataset to evaluate the soil-crop relationships and predictability of crop PFAS concentrations, taking into account the soil physicochemical characteristics. The root uptake of PFAS in plants has been suggested to be the main uptake pathway in plants (Xu et al., 2022), thus soil concentration was hypothesized to be an important influencing variable of crop concentrations. Moreover, the root system can be differently distributed throughout the soil depth profile, depending mainly on the plant species (Weaver and Bruner, 1927) and the prevailing soil characteristics *in situ* (Fan et al., 2016). Therefore, a comparative procedure was performed prior to the actual modeling for selection of the best “soil concentration” predictor variable.

To this end, five homologous MLR models were fitted with an identical model structure containing the same explanatory variables (i.e. soil concentrations, rainwater concentrations and soil physicochemical characteristics), but with another measure for the soil concentration: 0-5 cm, 5-25 cm, 25-45 cm, mean concentration of the three soil depth layers and the plant species-specific root density layer. The latter variable was derived from existing literature data for all the relevant vegetable crops (Table S4.5) and is detailed in the SI section 4.7. Then, the soil measure from the model with the lowest Akaike Information Criterion (AIC) value from those five MLR models was chosen as the best predictor of crop PFAS concentrations and used for further modeling.

Contrary to the expectations, prior MLRs indicated that rainwater was not a significant predictor variable (all $P > 0.05$), nor did it explain any variation in crop PFAS concentrations. This could be due to several reasons: firstly, the rainwater was only sporadically used for watering the vegetable garden. Most of the gardeners combined irrigation of their vegetable garden with rainwater from casks and tap water, while others used collected rainwater solely for their ornamental garden. Secondly, the measured rainwater concentrations were often below the LOQ for many compounds which may have obscured a potential relationship (Table S4.8). Furthermore, the rainwater concentrations may represent a snapshot at the period of sampling while rainwater concentrations can substantially vary over time, depending on the type of precipitation formation and atmospheric dust circulation (Olney et al., 2023; Peters et al., 2022).

Final MLRs were constructed for nine PFAS (i.e. PFBA, PFPeA, PFHxA, PFOA, PFDA, PFUnDA, PFDoDA, PFTTrDA and PFTeDA) with the soil concentration and soil physicochemical characteristics

as explanatory variables. Full models were reduced with stepwise backward model selection procedures using the AIC value, followed by subsequent elimination of predictors with the highest non-significant value ($P > 0.05$). This model reduction process proceeded until only significant explanatory variables ($P \leq 0.05$) were left in the best-fit model which was used for the predictive modeling (Steyerberg, 2009). Predictability of the measured crop PFAS concentrations was evaluated with model performance and validation criteria adopted from Lasters et al. (2023) and are fully described in the SI section 4.8.

4.4 Results and Discussion

4.4.1 General PFAS soil depth profile

An overview of the soil physicochemical characteristics is presented in Table 4.1. The pH of the soils among the private gardens was variable and could be characterized as acidic to neutral (min.-max. range: 3.80-7.14). Moreover, large variation of total organic nitrogen (TON), total organic phosphorus (TOP), soil electrical conductivity and exchangeable Ca^{2+} could be observed. However, the absolute clay content and TOC values were low in overall (clay percentage: 0.831-3.74%) (Table 4.1) in comparison with typical values (min.-max. clay content: 7.9-38.9% and min.-max. TOC: 1.3-13.8%) reported for private gardens (Bester et al., 2013; Tresch et al., 2018).

Table 4.1: Descriptive statistics (mean, min.-max. range and standard deviation (SD)) of the soil physicochemical characteristics in the pooled soil samples of the three soil depth layers of the vegetable gardens (N = 71). The measured soil solid components include the total organic carbon content (TOC), total organic nitrogen (TON), total organic phosphorus (TOP) and clay content. The analyzed physicochemical properties are pH_{KCl} , soil electrical conductivity (in $\mu\text{S}/\text{cm}$), exchangeable cations (mineral base cations: Ca^{2+} , Mg^{2+} , K^+ , Na^+ and metal cations: Fe^{3+} , Al^{3+} , Mn^{2+} in $\text{meq}/100\text{ g}$ of dry weighed soil), saturation of exchangeable base cations (%), the inorganic N (NH_4^+ and NO_3^- , in mg/kg) and P (PO_4^{3-} , in mg/kg) fractions. Note that these physicochemical soil characteristics could only be measured in the soil samples of 2021 and 2022

Soil physicochemical property	Min.	Mean	Max.	SD
pH_{KCl}	3.80	5.99	7.14	0.766
Clay (%)	0.831	2.03	3.74	0.629
TOC (%)	1.33	3.32	6.89	1.38
TON (mg/kg dw)	486	2035	5823	1126
TOP (mg/kg dw)	221	1003	2444	460
NH_4^+ (mg/kg dw)	0.026	10.7	25.1	5.84
NO_3^- (mg/kg dw)	0.051	14.0	89.7	13.7

PO ₄ ³⁻ (mg/kg dw)	0.070	2.61	14.7	2.82
Soil electrical conductivity (in μS/cm)	1.16	300	1261	224
Ca ²⁺ (meq/100 g of dw soil)	2.91	15.4	37.3	5.97
K ⁺ (meq/100 g of dw soil)	0.129	2.11	6.82	1.36
Mg ²⁺ (meq/100 g of dw soil)	0.260	2.29	6.23	1.19
Na ⁺ (meq/100 g of dw soil)	0.022	0.511	2.95	0.693
Al ³⁺ (meq/100 g of dw soil)	0.010	0.054	0.148	0.025
Fe ³⁺ (meq/100 g of dw soil)	0.006	0.018	0.056	0.010
Mn ²⁺ (meq/100 g of dw soil)	0.010	0.101	0.506	0.075
Saturation exchangeable base cations (%)	17.2	76.8	99.5	19.9

Generally, a diverse array of compounds could be detected in every soil depth layer, comprising emerging and precursor compounds from the fluorochemical plant (Fig. 4.1, Table S4.7). The upper 0-5 cm soil layer contained the largest number of PFAS, up to 20, while 18 and 19 compounds could be observed in the 5-25 cm and 25-45 cm depth layers, respectively (Table S4.7). This widespread and heterogeneous distribution of PFAS in the soil is in alignment with recent review reports of monitoring studies in surface soil (Brusseu et al., 2020; Rankin et al., 2016). These findings highlight the role of this environmental compartment as a major reservoir for PFAS, not only in industrially impacted residential areas but also in rural areas (Brusseu et al., 2020; Sörengard et al., 2022; Wang et al., 2023).

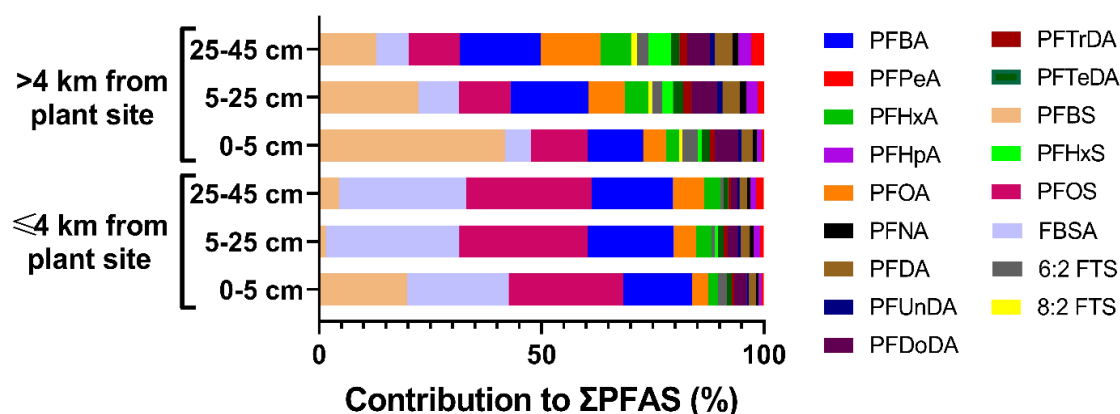


Fig. 4.1: Relative contribution (%) of all the quantified PFAS to the Σ PFAS in every soil depth layer (0-5 cm, 5-25 cm and 25-45 cm) of the vegetable garden segment from private gardens, situated ≤ 4 km ($N = 30$) and >4 km ($N = 58$) from a major fluorochemical plant site in Antwerp (Belgium). PFHpS, PFDS and 9Cl-PF3ONS are not included as their mean contribution was $<LOQ$.

Soil Σ PFAS concentrations showed no significant differences across depth layers, ranging from 24.1 ng/g dry weight (dw) in the 0-5 cm layer to 21.0 ng/g dw in the 25-45 cm layer near the plant site (Fig. 4.2, Fig. S4.4). Further away from the plant site, the same pattern was observed in the corresponding soil layers although the absolute concentrations were lower, ranging from 12.6 to 9.57 ng/g dw (Fig. 4.2). For PFOS and PFTeDA, slightly higher concentrations were found in the 0-5 cm layer compared to the 25-45 cm layer (Fig. 4.3, both $P < 0.05$). Soil composition and PFAS leaching behavior influence the vertical distribution under natural conditions. Organic matter in the upper soil layer enhances the sorption of compounds with strong soil affinity (e.g. PFTeDA and PFOS) (Gan et al. 2022; Wellmitz et al., 2023). However, all the other quantified compounds showed very little variation along the depth profile with no differences in soil concentrations (Fig. S4.3), as opposite to findings from previous studies (Brusseau et al., 2020; Gan et al. 2022; Groffen et al., 2019d; Wellmitz et al., 2023). This may be primarily due to the very different site-specific characteristics in the present study (i.e. private garden) compared to those studies, which were mostly done at contaminated public sites and forestry areas (Brusseau et al., 2020; Gan et al. 2022; Wellmitz et al., 2023).

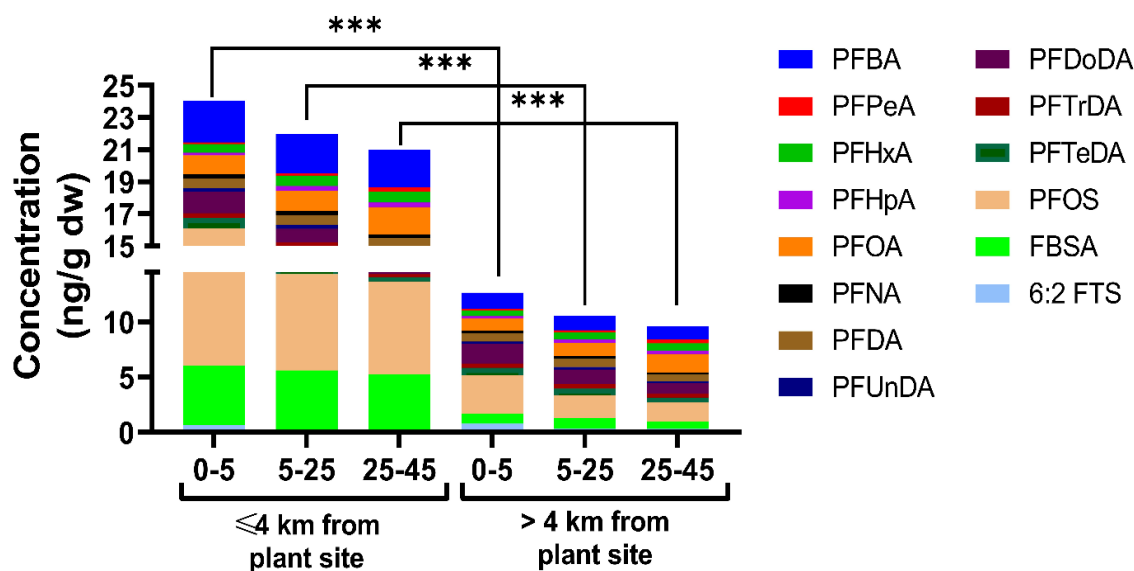


Fig. 4.2: Overview of the mean PFAS (ng/g dry weight) concentrations in every soil depth layer (0-5 cm, 5-25 cm and 25-45 cm) of the vegetable garden segment from private gardens, situated ≤ 4 km ($N = 30$) and >4 km ($N = 58$) from a major fluorochemical plant site in Antwerp (Belgium). For every soil layer, the Σ PFAS concentration in private gardens within 4 km from the plant site were significantly (all $P \leq 0.001$) higher compared to their corresponding soil layer in private gardens situated > 4 km from the plant site.

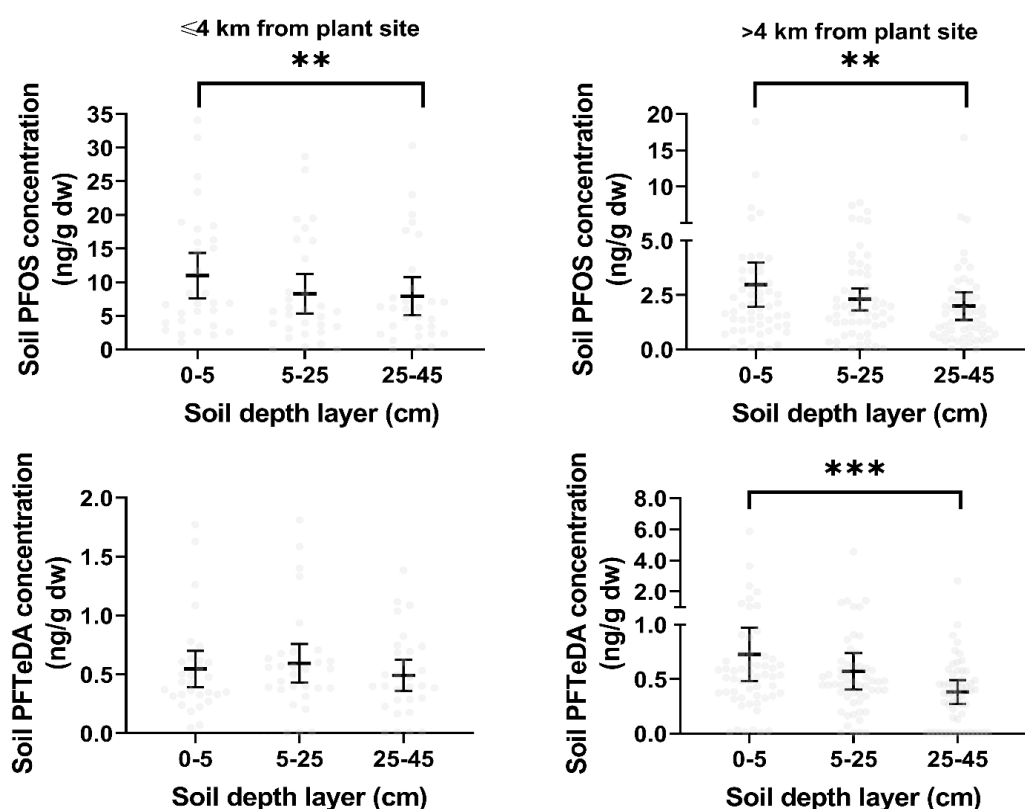


Fig. 4.3: Comparison of the mean PFOS (upper graphs) and PFTeDA (lower graphs) concentrations (ng/g dry weight) among the three examined soil depth layers (0-5 cm, 5-25 cm and 25-45 cm) of the vegetable garden segment from private gardens, situated ≤ 4 km ($N = 30$) and >4 km ($N = 58$) from a major fluorochemical plant site in Antwerp (Belgium). The error bar represents the lower and upper 95% confidence interval. **: $P \leq 0.01$; ***: $P \leq 0.001$.

Soil of vegetable garden segments often receives various human soil management practices, involving physical maintenance processes (e.g. mulching, tillage and planting) and addition of soil amendment products (e.g. compost, fertilizer and potting mixes). These actions can thoroughly mix up the (sub)surface soil layers, potentially disrupting any spontaneous downward migration and leaching of PFAS across the depth. Importantly, short-chain PFAS (e.g. PFBA and PFBS) largely contributed into soils remotely from the plant site (Fig. 4.1), whereas Lasters et al. (2023) (chapter 3) reported dominant contributions of long-chain compounds to the PFAS profile in chicken enclosure soils. This distinct profile in vegetable garden soil may be explained by the substantial amounts of short-chain PFCAs and their precursors present in various commercial soil amendment products. These precursor compounds can transform into various short-chain PFCA end-products under ambient soil conditions, especially in the presence of root-exudate-associated microorganisms in the plant rhizosphere (Lazcano et al., 2020; Just et al., 2022). It would be interesting to study whether the application frequency and amount would effectively change the

PFAS profile and concentrations in the soil and how this may affect uptake in crops. These findings also highlight that considerable spatial differences in PFAS profile and concentrations can exist even within small land parcels, emphasizing the role of functional usage in shaping the site-specific PFAS contamination profile.

4.4.2 Soil PFAS depth profile and concentrations along the distance gradient

Close to the plant site (≤ 4 km), PFOS and FBSA were the largest contributors, accounting together for 48.6%, 58.9%, and 56.8% of the total PFAS in soil layers of 0-5 cm, 5-25 cm, and 25-45 cm, respectively (Fig. 4.1). The mean soil Σ PFAS concentrations were significantly higher closer to the plant site than further away and for every soil layer (Fig. 4.2: all $P < 0.001$, $F_{1,84} = 21.8$). Post hoc comparisons clarified that this difference was mainly due to significantly higher soil concentrations of PFBA, PFOA, PFOS, and FBSA in gardens close to the plant site (Fig. 4.2, all $P < 0.01$). Moreover, these compounds were positively and significantly intercorrelated close to the plant site in every soil layer (Fig. S4.5, all $R \geq 0.41$, $P < 0.05$), which indicates that they originate from a common pollution source.

Previous monitoring studies have also found increased concentrations of these compounds (except FBSA, which was not included before as targeted analyte) closer to this plant site in soil, rainwater and biotic matrices (Groffen et al., 2019b; chapter 2, Lasters et al., 2022; chapter 3, Lasters et al., 2023). The elevated soil contamination of PFOS and PFOA in private gardens nearby the plant site can be linked with historical emissions, as these compounds were used on a large scale for fluoropolymer production and industrial applications, until their phase-out from 2002 onwards (De Silva et al., 2021; Gaber et al., 2023). In addition, PFOS was the main active ingredient in early generation aqueous film forming foam (AFFF) formulations, which have been extensively used at test locations nearby the fluorochemical plant site (Li et al., 2023). The potential contribution of AFFF contamination is expected to be low in gardens, as the contamination spread of such discharges is usually local and primarily to the surface- and groundwater (Reinikainen et al., 2022), however, it cannot be ruled out.

Likewise, the rainwater PFOS concentrations followed the same exponentially decreasing trend with increasing distance from the plant site as observed for soil (Fig. S4.3). Since PFOS has been phased-out decades ago, its prominent presence in wet deposition is likely not originating directly

from an active source(s). Alternatively, it could be that atmospheric degradation of PFOS precursors (e.g. PFOSA and PFOSAA), which were recently detected in dry and wet deposition samples within the same study area (Peters et al., 2022), might result in increased rainwater concentrations. Moreover, the concentrations reported by Peters et al. (2022) were associated with proximity to local major road infrastructure works (i.e. Oosterweel Link, one of the largest ongoing public construction works in Europe. Although speculative, this suggests that large-scale physical disturbance of the topsoil layer (e.g. excavation and transport) may contribute to recirculating PFOS-adsorbed dust particles into the air, after which they are deposited again via rainwater. However, more research is needed on data of environmental matrices before and after these construction works to elaborate this hypothesis.

The elevated soil concentrations of PFBA and FBSA closer to the plant site (Fig. 4.2) are probably a reflection of the industrial production shift towards precursors and short-chain PFAS in response to the phase-out of long-chain legacy PFAS (De Silva et al., 2021; Dhore and Murthy, 2021). The highest rainwater concentrations were also observed in the gardens closest to the plant site (Fig. S4.3), with concentrations up to 384 and 708 ng/L for PFBA and FBSA, respectively. The present study is one of the first to report the widespread presence of FBSA in soil, rainwater and crops (Table S4.7-S9). This compound is the main precursor of post-2002 fluorinated surfactant products (e.g. Scotchgard fabric protector) (Chu et al., 2016). Notably, Chu et al. (2016) detected FBSA in 32 out of 33 freshwater fish samples collected from Canada and the Western Scheldt (Belgium), with the highest concentrations (80.12 ng/g wet weight (ww)) found in one flounder (*Platichthys flesus*) from the Western Scheldt. It is noteworthy that the 3M company is situated on the bank right next to this tidal river and recent monitoring of PFAS in fish near the mouth of this river suggested that wastewater discharge by 3M might be related with PFAS concentrations in the fish (Byns et al., 2022). Recent research has demonstrated the bioaccumulation potential of FBSA in mammals (Dewapriya et al., 2023) and it exhibited higher toxicity in zebrafish larvae, compared to other short-chain PFAS (Dewapriya et al., 2023; Rericha et al., 2022). Despite these findings, literature reports of this compound in the environment remain limited, thus more data are needed of this relatively unknown compound to elucidate the potential exposure risk to humans.

Further away from the plant site (>4 km), the soil PFAS profile was very scattered with PFBS and PFBA as major constituents, contributing together for 54.3%, 39.8%, and 31.0% to the total PFAS

from the upper to the deepest layer (Fig. 4.1). This is in agreement with another study that investigated PFAS distribution in residential areas at non-suspect sites in China (Li et al., 2020). Correlations among PFBA, PFOA, PFOS and FBSA were mostly absent for every soil depth layer (Fig. S4.5), which is in contrast with soil close to the plant site. On the contrary, significant and positive relationships were frequently observed between pairs of long-chain PFCAs (C_{9-14}) ($R \geq 0.32$, $P < 0.001$) and ratios of homologue pairs were between 1 and 6, which is typically associated with atmospheric transport of precursors (e.g. fluorotelomer alcohols (FTOHs)) and oxidation to long-chain PFCAs (Rankin et al., 2016). Together, these results suggest that these gardens are relatively more affected by diffuse sources (e.g. runoff, atmospheric long-range transport and deposition), rather than point sources (Chen et al., 2018; Li et al., 2020) and reflect the current usage of short-chain homologues as substitutes for their long-chain counterparts (De Silva et al., 2021; Dhore and Murthy, 2021). This finding further indicates that long-range transport and degradation of precursors may be a non-negligible pathway in sites without any nearby point source (Chen et al., 2018).

4.4.3 General PFAS profile and concentrations in crops

The mean crop sum PFAS concentrations are presented in Fig. 4.4 and ranged from <LOQ to 4.76 ng/g ww. These concentrations were much lower (i.e. 1-3 orders of magnitude) compared to those in crops cultivated on agricultural soils up to 10 km away from a major fluorochemical industrial park in China (Liu et al., 2019; Liu et al., 2023). On the other hand, the Σ PFAS concentrations in the homegrown crops are ± 3 to 10 times higher than pooled vegetable and fruit products from commercial origin randomly sampled across Europe, which fell within the min.-max. range of <LOQ-0.450 ng/g ww (EFSA, 2020; Pérez et al., 2014; Herzke et al., 2013). Nevertheless, reported agricultural soil concentrations in literature for European countries are often also higher than those in vegetable garden soil of the present study (Costello and Lee, 2020; Ghisi et al., 2019). This difference in accumulated crop concentrations between agricultural and private gardens has also been reported for metals (Douay et al., 2013), which generally behave opposite to PFAS in terms of soil sorption behavior and hence bioavailability to crops. Therefore, site-specific differences in terms of soil management practices (e.g. nutrient supply) and cultivation strategies (e.g. planting density and cultivation intensity) may be important generalizable determinants for crop accumulation of pollutants in general.

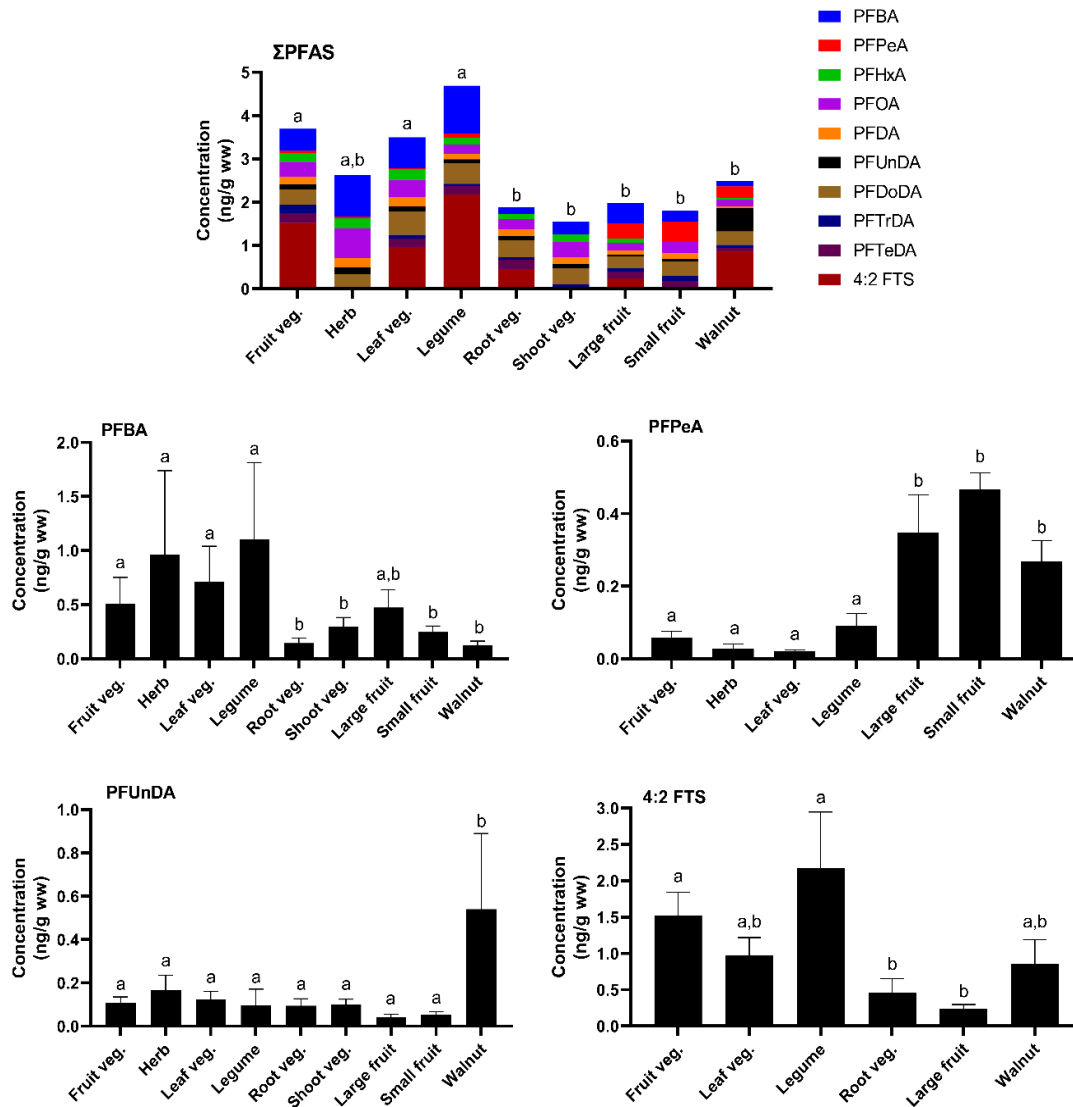


Fig. 4.4: Mean PFAS concentrations (in ng/g wet weight) in the edible parts of fruit vegetables ($N = 29$), herbs ($N = 4$), leaf vegetables ($N = 19$), legumes ($N = 6$), root vegetables ($N = 12$), shoot vegetables ($N = 35$), large fruits ($N = 36$), small fruits ($N = 37$) and walnuts ($N = 19$). Letters denote statistically significant differences of total PFAS concentrations (upper graph) and PFBA, PFPeA, PFUnDA and 4:2 FTS concentrations (lower graphs) among crop categories. The error bars represent the standard errors.

To the best of our knowledge, only one study reported data from homegrown crops of seven targeted PFAS in annual vegetable crops, within and outside a groundwater contaminated area (Scher et al., 2018). Regardless of the proximity towards the contaminated area, these authors reported that PFBA was detected in >50 % of the crop samples, whereas all the other targeted compounds exhibited very low detection frequencies (<10%). Similar concentrations were found for PFBA (median: 0.068 ng/g ww) in the crops compared to those in the present study (median: 0.102 ng/g ww), although all the other compounds accumulated to higher concentrations in the

present study for the same crop categories. This difference among study results demonstrates the importance of species- and site-specific characteristics, soil contamination origin and soil physicochemical characteristics to explain plant PFAS accumulation. This may also explain the finding that crop concentrations did not show the same distance gradient towards the plant site that was observed for soil (Fig. S4.2).

4.4.4 Crop- and compound-specific PFAS accumulation

Perennial crop categories showed a larger number of quantifiable compounds (i.e. 18-21) than annual crops (i.e. 9-19) and sporadic detection of emerging substitute perfluoroalkyl ether compounds (e.g. PF50HxA, 11Cl-PF3OUdS, and PFEESA), which were not found in any of the annual crops (Table S4.9). The longer lifespan and extensively developed root system of perennial crops enable greater soil volume exploitation, which would increase the uptake probability of PFAS (Vico and Brunzell, 2018). In contrast, annual crops have more limited root systems and are harvested within shorter growth cycles (Minoli et al., 2022).

The \sum PFAS concentrations were significantly higher in annual crops (e.g. fruit vegetables, leaf vegetables and legumes) compared to all the perennial crop categories, root vegetables and shoot vegetables (Fig. 4.4, all $P < 0.05$, $F_{8,181} = 4.14$). Elevated concentrations in annual plants were mainly driven by significantly higher concentrations of PFBA and 4:2 FTS (Fig. 4.4, both $P < 0.05$). This clear distinction aligns with the differences in life-history strategy between annual and perennial plants. Annual crops are fast-growing plants that exhibit higher relative growth rates, transpiration rates, nutrient and water uptake than perennial plants (Lundgren and Des Marais, 2020), which can be related with higher accumulation than perennial crops. Other field studies have also found larger accumulated PFAS concentrations in annual plants (Groffen et al., 2023a: in nettles; He et al., 2023: in weeds).

Additionally, it could possibly be that the lower sum PFAS concentrations in perennials may additionally be the result of PFAS removal through yearly leaf shedding, which may act as an excretion pathway that is absent in annual crops. This pathway has been demonstrated for metals (Thakur et al., 2016; Yan et al. 2020) and it would be of interest in future research to investigate whether this mechanism also holds true with respect to PFAS. Likewise, the secondary thickness growth of perennials may also represent an extra sequestration route of PFAS in perennial crops.

Gobelius et al. (2017) found large contributions of PFAS in the bark (>30 % of the total tree burden) of silver birch (*Betula pendula*).

The mean Σ PFAS concentrations in the crops ranged from 1.55 ng/g ww in shoot vegetables to 4.69 ng/g ww in legumes (Fig. 4.4). The tendency for relatively high uptake of PFAS in legumes has also been confirmed in other studies (Blaine et al., 2014; Knight et al., 2021). Legumes, belonging to the Fabaceae plant family, commonly do not possess hypodermal Casparian strips (Perumalla et al., 1990), which typically serve as barriers hindering the apoplastic movement of ionized substances (Naseer et al., 2012). The absence of these strips has consistently been linked with dramatically increased transfer of short-chain PFAS from roots to above-ground plant tissues (Mei et al., 2021).

Finally, some compound-specific differences among the individual plant categories could be observed (Fig. 4.4). Contrary to the observed pattern for the Σ PFAS, PFPeA showed a significantly larger accumulation in perennial crops than in annual crops (Fig. 4.4, $P < 0.01$). This result was unexpected as PFPeA has a similar accumulation potential as PFBA, for which significantly higher concentrations were found in annual crops (Fig. 4.4). It could be that this finding is a result of differences in the root depth system, as perennial plants can develop both deeper roots (up to 3.3 m) and larger lateral root spreads (up to 7.7 m) than annuals which are mostly restricted to <0.4 m of soil depth (Costantini et al., 2016). Unfortunately, no samples were obtained from deeper soil layers to verify this hypothesis. Following this reasoning, one would also expect a higher accumulation of PFBA in perennial crops, which has similar soil leaching behavior as PFPeA (Gan et al., 2022). Since the opposite was true, this result should be carefully interpret (Fig. 4.4).

In walnuts, significantly higher PFUnDA concentrations were found than in all the other crop categories (Fig. 4.4, $P < 0.05$). Unlike the fruit components of smaller and tree fruits, primarily composed of water and sugars, nuts contain significantly higher quantities of (lipo)proteins, constituting approximately 13.6-25.7% of the total walnut content, respectively (Jiang et al., 2021; Kafkas et al., 2020). Long-chain PFAS, such as PFUnDA are known to be favorably deposited in protein-rich tissues (Wen et al., 2016), which may explain their tendency for accumulation in nuts. Nevertheless, it is unexpected that this pattern was only observed for PFUnDA and not for other long-chain carboxylates. Moreover, Groffen et al. (2023a) reported rather high PFBA concentrations (up to ± 7 ng/g ww) in nuts of *Quercus robur*, instead of PFUnDA. Moreover, it remains unclear how

long-chain PFAS are translocated all the way from the roots to the fruit parts in perennial crops. In theory, this is a very unfavourable transport pathway, especially for less-mobile long-chain PFAS, since much longer transport distances and multiple biological barriers have to be crossed, compared to annual plants. Therefore, it cannot be ruled out that this result may be an (analytical) artifact, thus more field data on PFAS accumulation in walnuts are needed to verify its ecotoxicological significance. This is one of the very first studies to report PFAS in perennial crops and more field data are needed to better understand these crop-specific accumulation patterns. Moreover, mechanistic uptake studies in semi-controlled field experiments would be very useful to unravel these particular accumulation patterns.

While PFBS and PFOS were major contributors to the sum PFAS in the soil, their concentrations in the crop categories were often <LOQ in over 50% of the samples (Table S4.9). This result has also been consistently found in other field studies examining PFAS accumulation in plants (Groffen et al., 2023a; He et al., 2023). PFASs exhibit greater sorption affinity to the soil than their corresponding homologue PFCAs (Knight et al., 2021), making them less bioavailable for uptake and subsequent translocation to edible plant parts. Short-chain PFAS (i.e. 4:2 FTS, PFBA, PFPeA and PFHxA) showed the largest contribution to the Σ PFAS in the majority of crop categories, except for root and shoot vegetables (Fig. 4.4). Many crop uptake studies in soil have consistently found that short-chain PFAS are preferably transferred to above-ground plant compartments primarily via passive diffusion through the xylem (Blaine et al., 2014; Felizeter et al., 2021). Conversely, long-chain PFAS tend to be sorbed largely onto and into the below-ground plant organs (Adu et al., 2023), which can explain their larger contribution in the root vegetables (Fig. 4.4).

The relatively large contribution of long-chain compounds in shoot vegetables contrasts with previous findings (Costello and Lee, 2020; Xu et al., 2022). Moreover, Liu et al. (2019) found among the highest concentrations in celery and leek stems from heavily contaminated agricultural soil, which is opposite to our study where shoot vegetables exhibited among the lowest concentrations (Fig. 4.4). This difference might be due to the large number of collected rhubarb (*Rheum rhabarbarum*) petioles, constituting 26 out of 34 samples for the shoot vegetables. Short-chain PFAS are typically most enriched in leaf tissues, largely driven by the water transpiration stream (Felizeter et al., 2014). Rhubarb has an exceptionally high water transpiration stream factor, relatively high growth- and transpiration rate for its biomass (Aubert and Schwitzguébel, 2004).

Therefore, it is possible that this species accumulates the majority of short-chain PFAS in its leaves instead of the petiole. Unfortunately, leaves from rhubarb were not analyzed in this study as this fell beyond the original scope of the study objectives. Notably, rhubarb has already been suggested as a potential hyperaccumulator of organic pollutants and metals, which is promising for phytoremediation (Aubert and Schwitzguébel, 2004; Yang et al., 2022). It would be valuable to explore its phytoremediation potential for PFAS in future studies.

Notably, the precursor FBSA showed large contributions to the PFAS profile in the soil while 4:2 FTS was never detected in any of the soil samples (Table S4.7; Fig. 4.4). However, 4:2 FTS was nevertheless found at relatively high concentrations in most of the crop categories, while FBSA and its end-degradation product (i.e. PFBS) were <LOQ in more than 50% of the samples for every crop category. Similarly, 6:2 FTS and 8:2 FTS were found in the soil samples but not in any of the crop categories, while their end-degradation products (e.g. short-chain PFCAs) were frequently present in the crops (Fig. 4.4). Together, these findings highlight that biotransformation pathways among precursors in plants can greatly differ and that even very small structural differences (e.g. one methyl group in the alkyl chain) within the same molecule can dramatically affect PFAS uptake in crops. This is especially relevant given that the fluorochemical production strategy has shifted increasingly towards the manufacturing of these precursor compounds and new substitute PFAS (e.g. perfluoroalkyl ether acids with insertion of one ether bond in the alkyl chain) (Dhore and Murthy, 2021). Moreover, these precursors and substitute compounds have been shown to be as similarly persistent and (even more) toxic than legacy PFAS (Rericha et al., 2022; Zhang et al., 2021b). Therefore, new analytical methods including suspect screening and total oxidizable precursor assay (TOPA) will become indispensable in future plant accumulation studies in complex, real-world field conditions (Liu et al., 2019).

4.4.5 Modeling of PFAS soil-crop relationships

Prior to the predictive modeling with the soil physicochemical properties, the best soil predictor variable was selected using regression models, based on the five measures of soil concentration (SI section 4.7). For four long-chain PFCAs, significant soil-crop relationships were found (Table 4.2, all $P < 0.05$) with the species-specific (i.e. soil depth of maximum root intensity) soil layer (PFDA, PFTTrDA and PFTTeDA) or with the mean soil concentration (PFUnDA). This may suggest that species-specific root depth can be a non-negligible factor for uptake studies in different crop species.

However, the overall explained variation in crop concentrations by the soil was very low and no soil-crop relationships were observed for the short-chain PFAS and PFOA (Table 4.2, all $R^2 \leq 3.00$ and $P > 0.05$). This finding is in agreement with Scher et al. (2018), who also reported no soil-crop relationships in homegrown vegetables for PFBA at comparable concentrations as those in the present study.

This result is probably a reflection of the partitioning behavior of PFAS between soil and porewater. Compounds need to be present in the bioavailable porewater fraction in order to be taken up by the roots and translocated to the edible plant parts (Blaine et al., 2014). Long-chain compounds exhibit strong sorption to soil and higher soil concentrations are needed to reach a given porewater concentration, compared to the more hydrophilic short-chain compounds (Felizeter et al., 2020; Wellmütz et al., 2023). Since the soil concentrations for most PFAS were relatively low in the present study (Fig. S4.2), one might expect that the largest fraction of long-chain PFAS would be present in the soil. Reversely, the more hydrophilic compounds (e.g. short-chain PFAS and PFOA) would be mostly partitioned in the bioavailable porewater fraction. Therefore, porewater may be a better direct measure in future crop accumulation studies than soil, at least for sites with relatively low

Table 4.2: Comparison of the relationship between the pooled crop PFAS concentrations and the five candidate soil PFAS concentration predictor variables (i.e. soil concentration at 0-5 cm depth, 5-25 cm depth, 25-45 cm depth, the species-specific soil layer (derived from the values in Table S5) and the mean soil concentration of the three depth layers), based on the model AIC value. The soil concentration predictor variable with the lowest AIC value (in gray) was selected for inclusion in the final predictive models for each of the compounds.

	AIC-value					Model significance level	Adjusted R^2
	0-5 cm	5-25 cm	25-45 cm	Species-specific layer	Mean soil conc.		
PFBA	58.3	57.9	58.8	59.7	56.0	$P > 0.05$	1.95
PFPeA	2.15	1.38	1.73	1.85	2.27	$P > 0.05$	3.00
PFHxA	-49.0	-49.5	-50.2	-50.9	-51.4	$P > 0.05$	0.94
PFOA	-20.5	-22.5	-22.2	-23.1	-22.2	$P > 0.05$	1.15
PFDA	-137	-136	-155	-157	-138	$P < 0.05$	5.65
PFUnDA	-140	-154	-142	-145	-150	$P < 0.001$	29.9
PFDoDA	-60.1	-61.8	-60.6	-60.0	-60.6	$P > 0.05$	2.96
PFTrDA	-153	-153	-153	-154	-153	$P < 0.001$	16.4
PFTeDA	-69.9	-69.5	-69.8	-70.0	-69.5	$P < 0.01$	9.42

soil contamination. This hypothesis is supported by a recent study of Liu et al. (2023) who examined PFAS accumulation in a relatively large set of crops, grown in agricultural fields. These authors reported much stronger soil-crop relationships than in the present study, whereas the soil and crop concentrations were two to three orders of magnitude higher. Finally, it should be mentioned that some of the collected crop species (e.g. rhubarb, cucumber, pumpkin) have their maximum root intensity at depths well below the examined soil depth range of 0-45 cm (Table S4.5), which may also have caused the weak relationships between the soil and crop concentrations.

Table 4.3: Regression models showing the relationship between the pooled crop concentrations and the corresponding soil concentrations, taking into account the significant soil physicochemical characteristics. The response variable and predictor variables are given on a log-basis.

Response variable	Best-fit regression model	Model significance level	Adjusted R^2
PFBA crops	$-0.178 + 0.146 * \log \text{PFBA soil} - 0.310 * \log \text{Mg}^{2+} + 0.409 * \log \text{clay content} + 3.37 * \log \text{Al}^{3+}$	$P < 0.05$, $F_{4,64} = 2.81$	9.62
PFPeA crops	$0.076 + 0.151 * \log \text{PFPeA soil}$	$P > 0.05$, $F_{1,67} = 3.10$	3.00
PFHxA crops	$-0.265 + 0.113 * \log \text{PFHxA soil} + 0.183 * \log \text{clay content} + 8.25 * \log \text{Fe}^{3+}$	$P < 0.001$, $F_{3,65} = 9.83$	28.0
PFOA crops	$0.409 + 0.019 * \log \text{PFOA soil} - 0.178 * \log \text{Mg}^{2+}$	$P > 0.05$, $F_{2,66} = 3.63$	7.25
PFDA crops	$-0.576 + 0.226 * \log \text{PFDA soil} + 3.60 * \log \text{Fe}^{3+} + 0.076 * \log \text{Porg}$	$P < 0.001$, $F_{5,63} = 6.52$	19.6
PFUnDA crops	$-0.080 + 0.303 * \log \text{PFUnDA soil} + 0.062 * \log \text{clay content}$	$P < 0.001$, $F_{2,66} = 17.5$	34.6
PFDoDA crops	$0.338 - 0.082 * \log \text{PFDoDA soil}$	$P > 0.05$, $F_{4,64} = 3.07$	2.96
PFTTrDA crops	$-0.195 + 0.193 * \log \text{PFTTrDA soil} + 3.27 * \log \text{Fe}^{3+} + 0.152 * \log \text{clay content}$	$P < 0.001$, $F_{3,65} = 9.05$	26.2
PFTeDA crops	$0.062 + 0.141 * \log \text{PFTeDA soil} + 0.160 * \log \text{clay content} - 0.072 * \log \text{Mg}^{2+} - 0.080 * \log \text{NH}_4^+ + 0.043 * \log \text{NO}_3^-$	$P < 0.001$, $F_{5,63} = 5.90$	26.5

The best-fit model equations were established for nine PFAS, taking into account the soil physicochemical characteristics, and the significant predictors are given in Table 4.3. Generally, these could be ranked from most to least important: exchangeable metal cations (Fe^{3+} or Al^{3+}), clay content, soil concentrations and exchangeable Mg^{2+} . The model adjusted R^2 values generally improved for most compounds, with explained variation ranging between 3 to 35% (Table 4.3), compared to the single soil-concentration models (Table 4.2). This result reinforces the previously discussed findings that multiple soil physicochemical characteristics are important contributors to explain bioavailability of PFAS to crops rather than the soil concentrations (Xu et al., 2022).

Nevertheless, the overall explained variation in crop concentrations and predictability (Fig. 4.5) was low. One major reason for this contrasting result is probably that the measured crop and soil concentrations were low and lacked sufficient variation, which makes it intrinsically more challenging to predict accumulation. This is exemplified by the small concentration range of the measured crop concentrations and right-skewed distribution of the concentration values (Fig. 4.5, $\geq 75\%$ of the datapoints fell within the log 0.0-0.3 ng/g ww range for all compounds). Likewise, the variation of some major soil characteristics (e.g. TOC and clay content) that are known to be important soil parameters in governing bioavailability of PFAS in crops (Searce et al., 2023), showed also little variation and a small range (Table 4.1). Lastly, other potentially important abiotic factors were not taken into account, such as porewater available fraction, which may simply be a better predictor on itself than the soil, especially for short-chain PFAS (Felizeter et al., 2020; Wellmütz et al., 2023) and in low-exposure scenarios (see also end of the previous discussion section).

Moreover, the vegetable categories were merged to increase the sample size, which was necessary to enable the development of multiple regression models. This pragmatic strategy intended to obtain a generalizable prediction of PFAS concentrations in crops, given that a large series of crop species and private gardens in various land types (industrial, urban and rural) were sampled. However, the potential downside of this approach may be that some of the species-specific characteristics were overlooked and compromised the prediction accuracy. Although variability in root depth among the species was taken into account and turned out to be a significant factor (Table 4.2), PFAS uptake in plants is very complex and also strongly depends on a wide range of other species-specific characteristics. These factors include intrinsic morphological and

physiological properties, such as lipid and protein content, root morphology (e.g. tap versus fibrous root system), presence/absence of plant uptake barriers (e.g. Casparian strips) and differences in primary translocation mechanisms among edible plant parts (e.g. phloem transport in fruit vegetables versus xylem transport in leaf vegetables) (Adu et al., 2023; Felizeter et al., 2021; Wen et al., 2016). Lastly, plant life-stages and maturation stage of the fruit at time of sampling could also influence the accumulated compounds and concentrations in crops (McDonough et al., 2021).

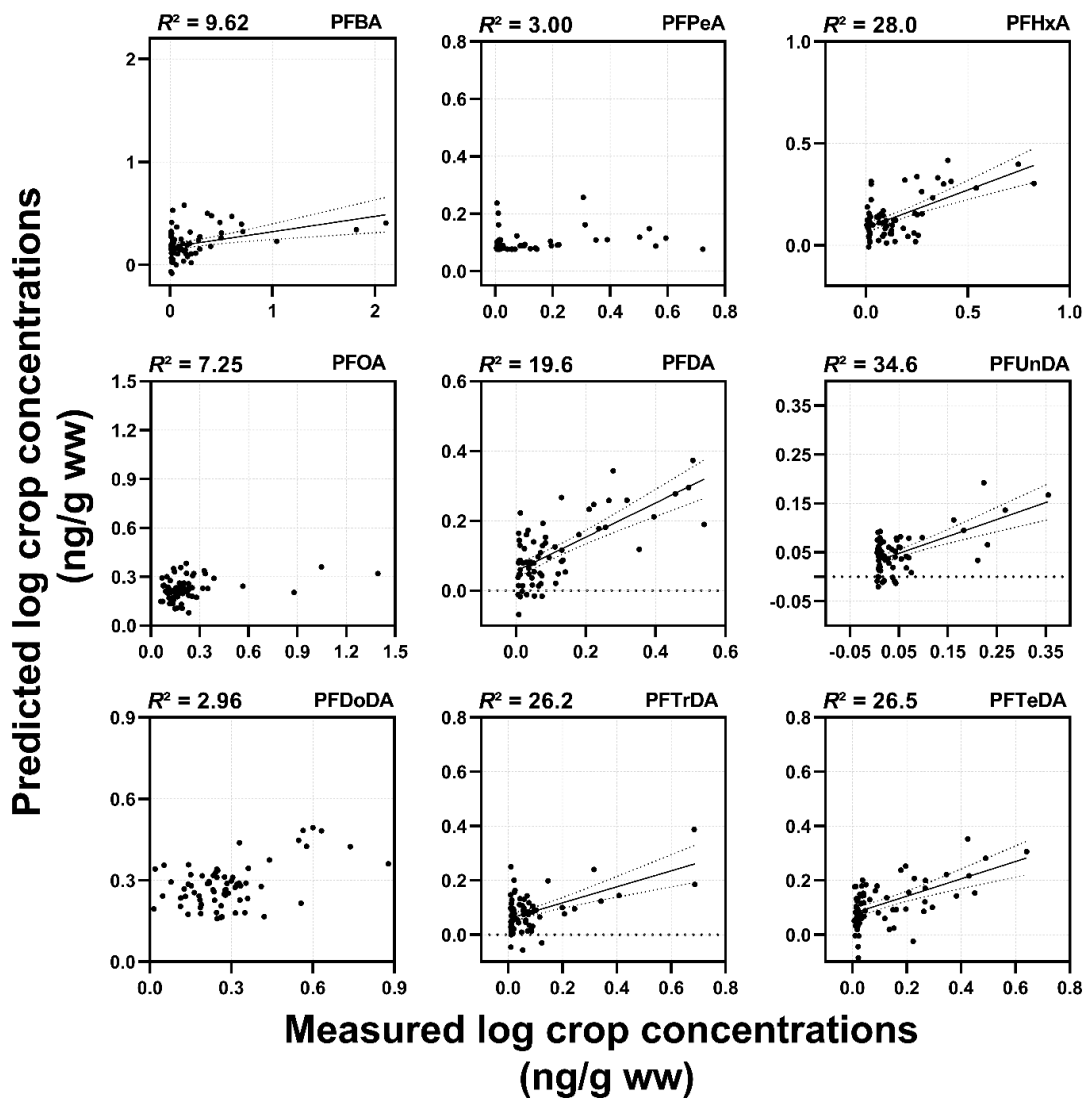


Fig. 4.5: Regression plots between the model-predicted crop concentrations and the measured crop concentrations, in log ng/g wet weight, for nine targeted analytes ($N = 69$). The total adjusted R^2 value is given of each best-fit model. The black solid line represents significant ($P < 0.05$) regression curves and the dotted lines denote the 95% confidence intervals.

The importance of species-specific characteristics in predicting PFAS in crops is also highlighted by previous work that examined the predictability of PFAS in homegrown eggs of free-ranging chickens (chapter 3; Lasters et al., 2023). Free-ranging chickens experience multiple exposure pathways, including the intake of soil, feed (i.e. kitchen waste, invertebrates), water and inhalation of contaminated dust (chapter 2; Lasters et al., 2022), whereas the exposure pathways in plants is primarily restricted to root uptake and, to a minor extent, leaf absorption of deposited dust (Ghisi et al., 2019; Wang et al., 2020). Despite the more complex exposure of PFAS in chickens,

considerably more variation (i.e. range R^2 : 9-67%) in egg concentrations could be explained for all the corresponding compounds and good predictability could be achieved for some compounds (chapter 3, Lasters et al., 2023), based on models with the same predictor variables as in the present study. These findings highlight that the development of successful predictive models in crops (i.e. various species and plant matrices) is much more complex than for homegrown chicken eggs (i.e. one species and one matrix).

Lastly, site-specific characteristics can further challenge the development of predictive models for crops and this may be an important determinant for explaining the difference in model performance among functionally different sites. For instance, Liu et al. (2023) developed reasonably good predictive models for some PFAS in crops grown in an agricultural field. Compared to agricultural fields, private gardens are multifunctional land areas and prone to a complex combination of variable gardening practices. The type and amount of added soil amendment products and fertilizers may affect the input and composition of dissolved organic matter (McDowell, 2003), plant growth rate and root exudate activity (Zhou et al., 2020) which can affect PFAS uptake as well (Qi et al., 2022; Xiang et al., 2020). Therefore, the present study elaborates on earlier indications that predictive models for pollutant uptake in plants may only be generalized and applied to sites with similar land-use and functional background (Boshoff et al., 2014).

Based on the predictive models, some significant relationships were observed between some of the predictors (e.g. exchangeable Fe^{3+} , exchangeable Mg^{2+} and clay content) and crop PFAS accumulation (Table 4.3). Although the statistical direction sign of these relationships was consistent among the models, they were inconsistent among the individual compounds and the model significance was low or even absent (Table 4.3: e.g. PFOA). Moreover, the majority of studies examining potential links between soil characteristics and plant PFAS accumulation are restricted to SOM and pH (Liu et al., 2023; Xiang et al., 2023), while one other study found that these soil characteristics were largely unrelated with plant accumulation (Groffen et al., 2023a). These conflicting results address the urgency to conduct studies on crops under semi-controlled field conditions using realistic exposure concentrations, comparable to those found in the present study. Moreover, inclusion of other and (potentially) better measures of crop bioavailability under these exposure scenarios (e.g. porewater, as also earlier discussed) are needed to disentangle the factors affecting crop accumulation.

4.4.6 Human exposure risk estimation

The mean and max. intake amount for the sum of four EFSA PFAS (PFHxS, PFOS, PFOA and PFNA) through consumption of vegetables, fruits and walnuts is shown for every age group in Table 4.4. The intake amount of these four PFAS was largest for consumption of vegetables, followed by fruits and walnuts. The mean intake was ± 1.7 and 11 times higher for the consumption of vegetables (age 3-5 year: mean 23.8 ng/kg bw per week), compared to fruits (age 3-5 year: mean 13.3 ng/kg bw per week) and walnuts (age 3-5 year: mean 1.91 ng/kg bw per week), respectively (Table 4.4).

The strict MTR health guideline for PFOS and PFOA was exceeded in the young age groups (3-5 and 6-9 years age) for vegetable consumption in 3.81 % and 0.95% of the locations, respectively. When the amount of fruit intake was added, this slightly increased to an exceedance of <6.55 % for PFOA while this remained the same for PFOS, which could be attributed to the very low accumulation of PFOS in the crops. The MTR health guideline was never exceeded in any of the consumption scenarios for walnuts and fruits (Table 4.4). On the other hand, the mean weekly PFAS intake via consumption of vegetables and fruits frequently exceeded the EFSA health guidelines in 21.1% of the locations, while this was only sporadically the case for walnuts (Table 4.4). Specifically, the mean intake exceeded the EFSA health guideline on average nearly 5 times in the sensitive age group 3-5 years and 7.5 times in that age group when the contribution via fruit consumption was taken into account (Table 4.4).

Table 4.4: Weekly PFAS intake through consumption of vegetables, fruits and walnuts for various age groups. The consumption scenario was based on the average weekly intake of the Flemish population for the corresponding food category. The intake was based on the sum of four compounds (PFHxS, PFOS, PFOA and PFNA). The percentage of sampling locations above the sensitive health guideline, which corresponds to the tolerable weekly intake (TWI: 4.4 ng/kg bodyweight per week) of the European Food Safety Authority (EFSA) is provided, along with the percentage of sampling locations above the critical maximum tolerable risk (MTR) for PFOA (87.5 ng/kg bw per week) and PFOS (43.8 ng/kg bw per week).

Vegetables	Intake parameters (ng/kg bw per week)				Percentage locations above health guideline (%)			
	Age group (years)	Min.	Median	Mean	Max.	EFSA TWI	MTR	
							PFOA	PFOS
3-5	3.55	12.1	23.8	174	95.3	3.81	0.953	
6-9	2.63	8.94	17.6	129	91.6	1.91	0	
10 - 13	1.71	5.79	11.4	83.5	71.0	0	0	
14-17 Male	1.07	3.65	7.20	52.6	38.3	0	0	
Female	1.21	4.11	8.10	59.2	44.9	0	0	
18-64 Male	0.839	2.85	5.62	41.1	29.9	0	0	
Female	1.01	3.44	6.79	36.5	36.5	0	0	
Fruits	Intake parameters (ng/kg bw per week)				Percentage locations above health guideline (%)			
Age group (years)	Min.	Median	Mean	Max.	EFSA TWI	MTR		
						PFOA	PFOS	
3-5	0.698	8.86	13.3	67.7	92.9	0	0	
6-9	0.517	6.56	9.82	50.1	81.7	0	0	
10 - 13	0.335	4.25	6.36	32.5	52.1	0	0	
14-17 Male	0.211	2.86	4.01	20.5	23.9	0	0	
Female	0.237	3.01	4.51	23.0	23.9	0	0	
18-64 Male	0.165	2.09	3.13	16.0	21.1	0	0	
Female	0.199	2.53	3.78	19.3	23.9	0	0	
Walnuts	Intake parameters (ng/kg bw per week)				Percentage locations above health guideline (%)			
Age group (years)	Min.	Median	Mean	Max.	EFSA TWI	MTR		
						PFOA	PFOS	
3-5	0.314	1.74	1.91	5.11	11.8	0	0	
6-9	0.233	1.29	1.42	3.78	0	0	0	
10 - 13	0.151	0.833	0.917	2.45	0	0	0	
14-17 Male	0.095	0.525	0.578	1.55	0	0	0	
Female	0.107	0.591	0.650	1.74	0	0	0	
18-64 Male	0.074	0.410	0.451	1.21	0	0	0	
Female	0.090	0.495	0.545	1.46	0	0	0	

The combined mean intake of these vegetable food items was 5.5 times lower than the estimated mean intake of two homegrown eggs in residents living within a 2 km radius from the same fluorochemical plant (chapter 2, Lasters et al., 2022). The consumption of eggs is often higher than two eggs per week and the bioaccessibility (i.e. PFAS fraction effectively absorbed from the human digestive tract into the systemic circulation) of PFAS from animal-derived food intake is higher than for vegetable food, especially for foods relatively high in protein content (Zhu et al., 2023). Therefore, the PFAS intake risk via homegrown eggs is generally larger than for homegrown crops and this risk seems to increase closer to main PFAS point sources, while such a gradient is not observed for vegetable food items (Fig S4.2). Recently, the EFSA assessed that the European population in nearly all age groups exceeds the TWI health guideline, based on food intake from commercial origin (EFSA, 2020). The total estimated intake via commercial food ranged from 3 to 70 ng/kg bw per week in adult age groups (EFSA, 2020). Furthermore, the present study shows that the consumption of homegrown crops can potentially be a relatively large contributor to dietary PFAS exposure in humans. The EFSA TWI was frequently exceeded, especially concerning vegetable and fruit consumption. Therefore, potential health risks due to PFAS exposure via homegrown food in general cannot be ruled out.

4.5 Conclusion

To the best of our knowledge, this is one of the very first studies that documented PFAS accumulation for a large range of PFAS in a wide variety of homegrown crops in real-world field conditions. Our results showed that PFAS concentrations and profiles differed substantially depending on the distance from the fluorochemical plant. Vertical soil profiles, however, showed less variation likely due to soil management practices.

The total PFAS concentrations in the homegrown crops consisted largely of short-chain PFAS (4:2 FTS, PFBA, PFPeA and PFHxA) and were highest in vegetables, followed by fruits and walnuts. Moreover, total accumulated concentrations were consistently higher in annual crops compared to perennial crops, which may be related with morphological and physiological differences between these plant taxa. Within the vegetable category, relatively higher concentrations could be observed in legumes and leaf vegetables. Multiple regression models taking into account soil concentrations and soil physicochemical characteristics showed modest model performance ($R^2 \leq 0.35$) for most

compounds, which could be mainly attributed to a low range and variability in observed crop concentrations. Clay content and the exchangeable metal cation Fe^{3+} appeared to play a significant role in explaining variation of accumulated PFAS concentrations in crops. The human intake estimations showed that homegrown crops, in particular vegetables, can have a relatively large contribution to the dietary exposure of PFAS. Moreover, the intake risk was similar between residents close to the plant site and those further away. The tolerable weekly intake was frequently exceeded with respect to vegetable and fruit consumption, thus potential health risks cannot be ruled out.



Chapter 5: Dynamic spatiotemporal changes of per- and polyfluoroalkyl substances (PFAS) in private gardens at different distances from a fluorochemical plant

This chapter was published in *Environmental Pollution*:

Lasters, R., Groffen, T., Eens, M. & Bervoets, L. (2024). Dynamic spatiotemporal changes of per- and polyfluoroalkyl substances (PFAS) in soil and eggs of private gardens at different distances from a fluorochemical plant. *Environmental Pollution*. 346: 123613-123624. <https://doi.org/10.1016/j.envpol.2024.123613>.

5.1 Abstract

Homegrown food in private gardens has been identified as an important human exposure source of per- and polyfluoroalkyl substances (PFAS). However, very little is known about the spatiotemporal distribution of these chemicals in private gardens. Nevertheless, this is crucial knowledge to allow more accurate site-specific risk assessment, identification of new potential sources and to evaluate the effectiveness of regulations. The present study evaluated spatiotemporal changes of legacy and emerging PFAS in surface soil from vegetable gardens ($N = 78$) and chicken enclosures ($N = 102$), as well as in homegrown eggs ($N = 134$) of private gardens, across the Province of Antwerp (Belgium). Hereby, the potential influence of the wind orientation and distance towards a major fluorochemical plant was examined. Short-chain PFAS and precursor concentrations were higher in vegetable garden soil compared to chicken enclosure soil and homegrown eggs, while the reverse was true for long-chain sulfonates and C_{11-14} carboxylates. Short-term (2018/2019-2022) temporal changes were mostly absent in vegetable garden soil, while changes in chicken enclosure soils oriented S-SW nearby (<4 km) the fluorochemical plant were characterized by a local, high-concentration plume. Moreover, soil from chicken enclosures oriented SE and remotely from the plant site was characterized by a widespread, diffuse but relatively low-concentration plume. Long-term data (2010-2022) suggest that phaseout and regulatory measures have been effective in declining PFOS and PFOA concentrations at private gardens nearby the plant site, but had limited effect remotely from the plant site, warranting further rapid regulation and remediation measures. Further monitoring efforts are needed to allow long-term comparison for multiple PFAS and better distinction from potential confounding variables, such as variable emission outputs and variability in wind patterns.

5.2 Introduction

Per- and polyfluoroalkyl substances (PFAS) are a very diverse group of synthetic aliphatic compounds, in which the alkyl chain is completely and partly fluorinated, respectively (Buck et al., 2011). Since the 1940s, these compounds have been used in many industrial applications and commercial products due to their exceptional water-, oil- and stain- repellent properties (Kissa, 2001). The widespread and intensive usage of PFAS combined with their highly persistent, bioaccumulative and mobile properties have resulted in global contamination of virtually every environmental compartment and organism on earth (Cousins et al., 2020; Giesy and Kannan, 2002).

Over the past two decades, growing biomonitoring and experimental evidence has associated elevated exposure to PFAS, in particular perfluorooctane sulfonic acid (PFOS) and perfluorooctanoic acid (PFOA), with various toxic health effects on organisms (De Silva et al., 2021; Letcher et al., 2010), including humans (Fenton et al., 2021). Consequently, the main fluorochemical producing companies have phased-out PFOS, PFOA and related long-chain compounds from 2002 onwards (3M Company, 2000). Moreover, formal restriction of PFOS and PFOA was imposed in 2009 and 2015, respectively, at the Stockholm Convention and has currently been ratified by 152 countries (UNEP, 2019). In response, the fluorochemical industry has shifted its production strategy towards the increased manufacturing of short-chain PFAS, precursor chemicals (Dhore and Murthy, 2021), and the development of new substitute emerging PFAS which are considered to be as similarly persistent and toxic as the legacy PFAS (Brendel et al., 2018; Munoz et al., 2019). Currently, the European Chemicals Agency is evaluating a broad restriction proposal of several countries to ban all PFAS in production and usage purposes across Europe (ECHA, 2023). However, even if emissions would cease in the future, it will still take decades to centuries for degradation and reversal of PFAS contamination in the environment (Cousins et al., 2022; Wang et al., 2015). Therefore, monitoring and evaluating temporal trends in the environment and biota will remain important for their accurate risk assessment.

Within this context, the soil is such an important environmental compartment to monitor as it represents a major sink and long-term reservoir for many PFAS (Brusseau et al., 2020; Liu et al., 2015). In parallel, the soil represents an important cultivation medium in many countries for the production of food, which is generally the most important exposure source of PFAS to the human

population (Roth et al., 2020; Vestergren and Cousins, 2013). Therefore, both short-term and long-term monitoring of PFAS in soil and in food is essential to characterize the potential ongoing risks of human exposure to PFAS. Furthermore, it is imperative to evaluate the effectiveness of regulatory measures for some long-chain PFAS and the possible consequences of PFAS industrial production shifts towards short-chain PFAS and precursors on their potential accumulation in these matrices (Land et al., 2018). To the best of our knowledge, no studies to date have examined spatiotemporal trends in self-cultivated food and in garden soil, despite its utter direct importance regarding human risk assessment of PFAS. Moreover, potential differences of PFAS contamination within gardens due to functionally different areas (e.g. chicken enclosure versus vegetable segment) have not been studied.

Previous monitoring studies in Flanders (Belgium) have reported globally among the highest PFAS concentrations in environmental media and biota, including homegrown chicken eggs, nearby a main fluorochemical plant in Antwerp (Groffen et al., 2017; chapter 2, Lasters et al., 2022; Lopez-Antia et al., 2019). However, potential spatiotemporal trends and wind orientation in function of this major point source may greatly affect the exposure risk to biota and humans, while it may improve the accuracy of risk assessment. Additionally, it may help to unravel potential new point sources, which is crucial in a densely populated and strongly industrialized region such as Flanders (Verbruggen, 1997), and can enhance our understanding of the environmental fate and distribution of PFAS. Furthermore, few data exist on spatiotemporal trends in (a)biotic matrices across Europe and the study designs are often limited, both in terms of spatiotemporal scale and selected targeted analytes (Land et al., 2018).

In the present study, the PFAS profile and concentrations within private gardens was examined with respect to vegetable garden soil, chicken enclosure soil and homegrown eggs. Secondly, potential short-term (2018/2019-2022) spatiotemporal changes of 29 targeted PFAS (legacy-, emerging-, and precursor PFAS) were investigated in these matrices, nearby and remotely from a major fluorochemical plant, throughout the Province of Antwerp (Belgium). Hereby, it was also tested whether private gardens oriented towards the dominant wind direction from this plant site, during the examined time period (2018-2022), were associated with higher egg concentrations. Moreover, potential local changes in PFAS soil concentrations were examined in repeatedly sampled private gardens before and after major road infrastructure works (i.e. Oosterweel Link, henceforth

abbreviated as OW). This road infrastructure project is among the largest road work projects ever undertaken in Flanders (Belgium) and a major part of it has been conducted within vicinity (<4 km) of the 3M fluorochemical plant (Peters et al., 2022). Recent air deposition measurements during the road works have suggested spreading of PFAS via blowing dust from the OW site (Peters et al., 2022). Lastly, long-term (2010-2022) temporal changes of PFOS and PFOA concentrations in chicken enclosure soil and in homegrown eggs were investigated.

5.3 Materials and Methods

5.3.1 Data collection

Five subsamples from the top soil layer (0-5 cm), each consisting of ± 20 g soil, were collected with a stainless steel gouge drill. This resulted in approximately 100 g of pooled soil samples in private gardens across the Province of Antwerp (Belgium) from both the chicken enclosure and vegetable garden segment during the summer period of 2019 (resp. $N = 34$ and $N = 20$), 2021 (resp. $N = 58$ and $N = 45$) and 2022 (resp. $N = 10$ and $N = 13$). Pools of whole egg content from two individual eggs were sampled from free-ranging laying hens in 2019 ($N = 34$), 2021 ($N = 58$) and 2022 ($N = 10$) at the same moment. All the soil samples were collected from uncovered outdoor areas and the eggs originated from free-ranging laying hens with unlimited access to an outdoor enclosure.

The sampling locations were selected along a distance gradient from a known major fluorochemical point source in Antwerp (3M), including private gardens both nearby (<4 km range) this point source and remotely (>4 km range) from it across the province of Antwerp (Fig. S5.1). The distance boundary of 4 km was based on previous monitoring studies in this area showing that most of the variation in PFAS concentrations falls within 4 km from this point source (Groffen et al., 2017; Lasters et al., 2022; Lopez-Antia et al., 2019). Moreover, top layer (0-5 cm) soil samples from repeatedly sampled chicken enclosures ($N = 7$) and vegetable gardens ($N = 6$) were collected in 2019 and 2021 nearby (<4 km range) this point source (Fig. S5.1). This provided the opportunity to test whether local intensive road infrastructure works of the OW, which have begun in 2020, could be associated with temporal changes within these gardens. Moreover, the interactive PFAS map of Flanders (Department Environment and Health, 2022b) was consulted to verify private gardens that

were situated within vicinity of any known local PFAS source (e.g. firefighting facilities, military training sites and airports), which was not the case.

In addition to the sample collection, additional data were adopted from published monitoring studies of the same study area to increase the robustness of the later statistical analyses and to enable examination of long-term (2010-2022) trends for PFOS and PFOA. To this end, data of D'Hollander et al. (2011) on topsoil PFOS concentrations from chicken enclosures ($N = 29$) were adopted along with data of PFOS and PFOA concentrations in homegrown eggs ($N = 29$) from 2010. Moreover, data of 16 PFAS in homegrown eggs ($N = 35$) from 2018 were adopted from Lasters et al. (2022). The soil and egg samples in these studies were collected and pre-treated in the same standardized way as in the current study, which resulted in statistically comparable datasets.

5.3.2 Sample pre-treatment

The fresh soil samples were transferred to polypropylene (PP) tubes and oven-dried at 70°C. The whole egg content of the homegrown eggs was beaten and homogenized in a PP container (rinsed a priori with acetonitrile (ACN) with a stainless steel kitchen mixer and pooled into one homogenate sample. The kitchen mixer was thoroughly rinsed with ACN in between every location. All the samples were stored at -20°C for further chemical analyses of all targeted PFAS (see Table S5.1).

5.3.3 PFAS chemical extraction

About 0.30 g of soil or egg sample was weighed on a precision balance to the nearest 0.01 g (Mettler Toledo, Zaventem, Belgium). Briefly, the weighed samples were spiked with 10 ng of mass-labelled internal standard mixture (ISTD, MPFAC-MXA, Wellington Laboratories, Guelph, Canada). Details on the chemical composition of the ISTD are provided in Table S5.1. Then, 10 ml of the extraction solvent (HPLC-grade ACN) was added to each sample, after which they were thoroughly vortex-mixed and sonicated during three times 10 min. After shaking overnight on a shaking plate (135rpm, room temperature, GFL3 020, VWR International, Leuven, Belgium), the samples were centrifuged (4 °C, 10 min, 2400 rpm, 1037 *g*, Eppendorf centrifuge 5804R, rotor A-4-44) and the supernatant was brought over to a new 15 mL PP tube. The soil samples were extracted using solid-phase extraction based on the principle of weak-anion exchange, according to the protocol described by Groffen et al. (2019c) with small adjustments. The egg samples were extracted with a clean-up step

extraction using graphitized carbon powder following the protocol described by Powley et al. (2005) with minor modifications. Full descriptions of both extraction methodologies are provided in the supplementary information (SI section 5.1).

5.3.4 PFAS chemical analysis

For the PFAS analyses, in total 29 analytes were targeted in all the samples. Ultrahigh performance liquid chromatography (ACQUITY, TQD, Waters, Milford, MA, USA) coupled to a tandem quadrupole (TQD) mass spectrometer (UPLC-MS/MS), operating in negative electrospray ionization-mode was used for detection of peak signal for all the targeted analytes. The different targeted PFAS were separated using an ACQUITY UPLC BEH C18 VanGuard Precolumn (2.1 × 50 mm; 1.7 μm, Waters, USA). The mobile phase solvents consisted of ACN and HPLC grade water, which were both dissolved in 0.1% HPLC-grade formic acid. The solvent gradient started at 65% of water to 0% of water in 3.4 min and back to 65% water at 4.7 min. The flow rate was set to 450 μL/min and the injection volume was 6 μL (partial loop). PFAS contamination that might originate from the LC-system was retained by insertion of an ACQUITY BEH C18 pre-column (2.1 × 30 mm; 1.7 μm, Waters, USA) between the solvent mixer and the injector. The targeted PFAS analytes were detected and quantified based on multiple reaction monitoring (MRM) of the diagnostic transitions, which are displayed in Table S5.1 as validated by Groffen et al. (2019c; 2022).

5.3.5 Quality control and quality assurance

During the homogenization of the biotic samples, solvent blanks (= 10 mL of ACN) were included every 10 samples to check for cross-contamination between the samples. During the extraction, one procedural blank (= 10 mL ACN spiked with 10 ng of ISTD solution) was included per 15 samples to verify any contamination during the extraction. During instrumental analysis, solvent blanks (ACN) were regularly injected to rinse the columns and prevent cross-contamination across injections. In the case of batch contamination, the procedural blank values were subtracted from the subsequently measured samples. For the clean-up of the egg samples, 50 mg of graphitized activated carbon powder was used per 0.30 g egg sample to remove the PFOS-interferent analyte taurodeoxycholic acid (TDCA) from the extract, as validated by Sadia et al. (2020).

Calibration curves were prepared by adding a constant amount of the ISTD to varying concentrations of an unlabelled PFAS mixture. The serial dilution of this mixture was performed in ACN. A linear regression function with highly significant linear fit (all $R^2 > 0.98$; all $P < 0.001$) described the ratio between concentrations of unlabelled and labelled PFAS. The individual compounds were quantified using their corresponding ISTD except for compounds of which no ISTD was present. These analytes were all quantified using the ISTD of the compound closest in terms of functional group and size (Table S5.1), which was validated by Groffen et al. (2019c; 2022).

5.3.6 Data processing

Limits of quantification (LOQs) were calculated in matrix for each detected analyte and considered as the concentration corresponding to a peak signal-to-noise ratio of 10. For all the compounds, LOQs are provided for chicken enclosure soil, vegetable garden soil and homegrown eggs in Table S5.2-4, respectively. For every matrix, a common LOQ was assigned among the sampling years which corresponded to the maximum LOQ among all the years combined to reduce bias in studying the actual temporal trends, following Jouanneau et al. (2020). For PFAS that were <LOQ, replacement concentration values were assigned according to the maximum likelihood estimation method (De Solla et al., 2012; Villanueva, 2005). For the linear discriminant analysis (see section 5.3.7), concentration values of the various detected PFAS compounds were centred and standardized to obtain equal mean and standard deviations.

The distance of the private gardens from the point source was considered as a categorical variable and divided into two sub-categories: ≤ 4 km from the plant site and >4 km from the plant site, henceforth also referred to as “nearby the plant site” and “remotely from the plant site”, respectively. The precise geographical location of the adopted data from private gardens of 2010 could not be verified as these data were reported at sub-municipal level by D’Hollander et al. (2011). Hence, the distance from the plant site could not be accurately quantified for these samples. In the results and discussion section, “large-scale” refers to both distance categories, while “small-scale” refers only to private gardens “nearby the plant site”. The orientation of each private garden relative to the plant site in Antwerp was assessed following the conventional eight-division classification system of wind direction (Yannopoulos, 2011), resulting in the following wind orientation sectors: N (337.5° to 22.5°), NE (22.5° to 67.5°), E (67.5° to 112.5°), SE (112.5° to 157.5°), S (157.5° to 202.5°), SW (202.5° to 247.5°), W (247.5° to 292.5°) and NW (292.5° to 337.5°).

5.3.7 Statistical analysis

The statistical analyses and data visualizations were performed in the R program version 4.2.3 (R Core Team, 2023) and in GraphPad Prism version 9. The threshold level for significance testing was set at $P \leq 0.05$ for statistical significance testing. Descriptive statistics (geometric mean and min.-max. range) were computed for all detected PFAS in the top soil (chicken enclosure and vegetable garden) and in homegrown eggs for every sampling year and considering the distance category from the major fluorochemical point source in Antwerp (Table S5.1-S5.3). The Shapiro Wilk's test was conducted to verify normality assumptions of the data, and the data were $\log(x+1)$ transformed to meet normality assumptions of the residuals.

Firstly, multivariate linear discriminant analysis (LDA) was conducted to better understand the general PFAS profile and concentration characterization across the three matrices, but also to explore whether separate clusters could be identified according to the wind orientation towards the plant site, based on the explained variation in PFAS concentrations by the two first linear discriminant functions (i.e. LD1 and LD2). Compounds that were <50% of the LOQ in any matrix were excluded from the linear discriminant analysis to enable valid matrix comparisons for commonly detected compounds.

Then, several two-way ANOVA models with distance category from the plant site and matrix type were ran to evaluate specific significant differences in PFAS concentrations among the matrices according to the distance from the plant site. Another two-way ANOVA model, with sampling year and distance category from the major fluorochemical plant both as fixed factors, was constructed to test specific temporal differences for each matrix. After formal ANOVA testing, post-hoc Tukey's HSD multiple comparison tests were conducted to examine which specific pairs of sub-variables were significantly different. The variable sampling year was considered as a factor in these analyses as it could not be assumed that time behaved linear between the relatively large time gap of the period from 2010 to 2018 and the relatively small sample size. For private gardens that were repeatedly sampled among the years, only the measurement from the first sampling year was included to avoid pseudoreplication in this analysis.

For each matrix, spatiotemporal differences were tested with ANCOVA linear models, containing the wind orientation towards the plant site and sampling year as a fixed factor, as well as the

distance from the plant site as a continuous covariate. Then, significant differences in the spatiotemporal distribution of PFAS concentrations among the three matrices were further interpreted by means of the package “openair” in R (Carslaw, 2019; Carslaw and Ropkins, 2012). Hereby, the function windRose was firstly used to plot the frequency of both wind direction and wind speed in the study area during the sampling years 2019, 2021 and 2022. To this end, meteorological time-series data of these wind parameters were adopted from the open-source databank of the Flemish Environment Agency (Flemish Environment Agency, 2022b). Then, the polarPlot function was used to visually plot the PFAS concentrations of each matrix towards the plant site using Gaussian kernel smoothing, which apportions the observed mean concentration of a pollutant to sectors defined by distance and orientation towards the plant site (Henry et al., 2009). Furthermore, it is also an effective way to visualize spatiotemporal trends while anonymizing the individual location of the private gardens.

Lastly, to test the hypothesis whether the OW road works may influence local soil concentrations in nearby private gardens, repeated paired data of private gardens from 2019 and 2021 nearby the plant site were selected from the original dataset. Then, paired t-tests were conducted to test for potential differences between both sampling years within the same private gardens. Lastly, Pearson correlation tests were conducted for the paired data between the nearest distance from the OW road works site and the soil PFAS concentrations.

5.4 Results and discussion

5.4.1 PFAS profile and concentration patterns within private gardens

For clarification and readability reasons, the terms “chicken enclosure soil”, “vegetable garden soil” and “homegrown eggs” are henceforth referred to as “chicken soil”, “garden soil” and “eggs”, respectively.

From the 29 targeted PFAS, up to 15 and 20 analytes could be detected in the chicken soil and garden soil, respectively (Table S5.2-S5.3). In every soil sample, at least five PFAS compounds could be detected which strongly varied in terms of composition among the samples, regardless of the distance from the major fluorochemical plant. This widespread and heterogeneous presence of PFAS in soil is in agreement with other large-scale PFAS monitoring studies in surface soil,

demonstrating that this environmental compartment is a major reservoir for PFAS, both in residential areas that are industrially impacted and in sites without any known nearby source (Brusseau et al., 2020; Söregard et al., 2022).

Compared to general soil data at non-suspected sites across Europe, the mean concentrations for the Σ PFCA_s and Σ PFSA_s in the chicken soil (Σ PFCA_s = 3.58 ng/g dw; Σ PFSA_s = 7.66 ng/g dw) and garden soil (Σ PFCA_s = 7.38 ng/g dw; Σ PFSA_s = 7.99 ng/g dw) largely exceeded the mean concentrations of soil for the same Σ PFCA_s and Σ PFSA_s in Europe, respectively 1.00 ng/g dw and 0.808 ng/g dw (Rankin et al., 2016). For most compounds, the soil concentration range fell within the same order of magnitude compared to previous local soil measurements in nature areas nearby the fluorochemical plant site in Antwerp (Groffen et al., 2019b; 2019c).

In the eggs, up to 16 compounds could be detected (Table S5.4) including PFHpA, PFHxS and PFDS, whereas these compounds were <LOQ in the chicken soil. The egg concentrations of the present study were among the highest ever reported in homegrown chicken eggs (Gazzotti et al., 2021; Su et al., 2017; Wang et al., 2019), especially for PFBS and PFOS (Table S5.4). This confirms earlier findings that homegrown egg consumption can be a major PFAS exposure source presenting potential health risks to humans (chapter 2, Lasters et al., 2022). Together, these results indicate that the general PFAS contamination burden in the Province of Antwerp is among the highest compared to other regions in Europe, which is in agreement with the recently established PFAS pollution map of Europe (Le Monde, 2023) and may be linked with the large degree of industrialization in the densely populated Flanders (Verbruggen, 1997).

The linear discriminant analysis showed that most variation in PFAS concentrations for soil and eggs could be explained by the linear discriminant function 1 (LD1) and linear discriminant function 2 (LD2), which together explained >84% of the total variation in PFAS concentrations (Fig. 5.1). Clearly, the variation in PFAS concentrations was better explained by the matrix type than the distance (nearby or remotely) from the fluorochemical plant site, indicated by the large overlap of clusters between samples nearby the plant site and remotely from the plant site (Fig 5.1). Importantly, regardless of the matrix type, increased concentrations in private gardens nearby the fluorochemical plant site in Antwerp were primarily caused by significantly higher concentrations of FBSA, PFBA, PFBS, PFHxS, and PFOS (Fig. 5.1, Table S5.2-S5.3). This finding supports the outcome

of earlier PFAS monitoring studies in this area which also found indications that historical industrial emissions have been an important source of phased-out PFHxS and PFOS (Groffen et al., 2019b, 2019c). Moreover, the present study affirms early indications that precursor compounds, such as FBSA, as well as short-chain PFBS and PFBA can also be linked with recent industrial emissions (Dhore and Murthy, 2021).

The multivariate analysis revealed large differences between the garden and chicken soil, in terms of PFAS profile and concentrations (Fig 5.1). The vector loadings emphasized that garden soil was distinguished from the chicken soil by distinct clustering of significantly higher concentrations for PFBA, PFHpA, PFHxA, FBSA, and 6:2 FTS (all $P < 0.01$, Fig. 5.1-2). This supports our hypothesis that vegetable gardens are enriched with these compounds through intensive soil management and frequent addition of soil amendment products (compost and potting mixes) by gardeners, which are known to be enriched with short-chain PFCAs and precursors of PFCAs (Sivaram et al., 2022). Additionally, these PFCA precursors (FTSs, di-PAPs and FOSA) can be partly transformed into various short-chain PFCA end-products under ambient soil conditions (Lazcano et al., 2020), especially in the presence of root exudate associated microorganisms in the plant rhizosphere (Just et al., 2022). Lastly, the typical PFAS profile in the garden soil can also be explained through the frequent supply of irrigation water, which is known to largely contain short-chain PFCAs and precursors, due to their relatively high water solubility and mobility (Scher et al., 2018; Zhang et al., 2021a). To the best of our knowledge, the present study is the first that examined and identified relatively large differences in PFAS contamination within private garden sections (Fig. 5.1-2), depending on their functional usage. Therefore, comparisons with literature data should be interpreted with caution as the precise origin of the soil is rarely specified.

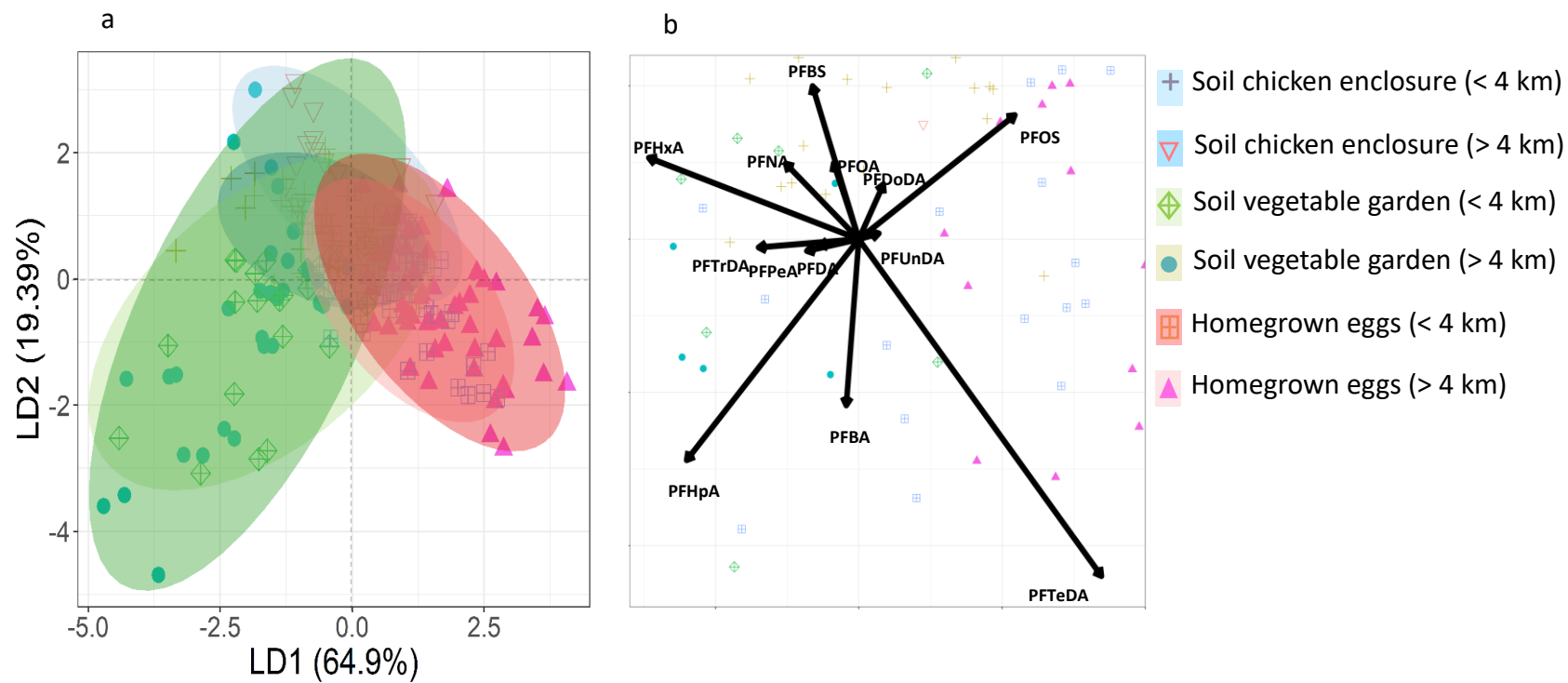


Fig. 5.1: (a) Multivariate linear discriminant analysis of PFAS concentrations clustered according to the matrix type (soil chicken enclosure, soil vegetable garden and homegrown eggs) and distance from the plant site (<4 km or >4km range from the fluorochemical plant site in Antwerp (Belgium)), based on the two first linear discriminant functions LD1 and LD2, which explained 64.9% and 19.4% of the total variation in PFAS concentrations, respectively. (b) Biplot showing the factor loadings and scores of each PFAS compound, indicated by the vector arrows. Symbols and colours represent different matrix types and different distance categories.

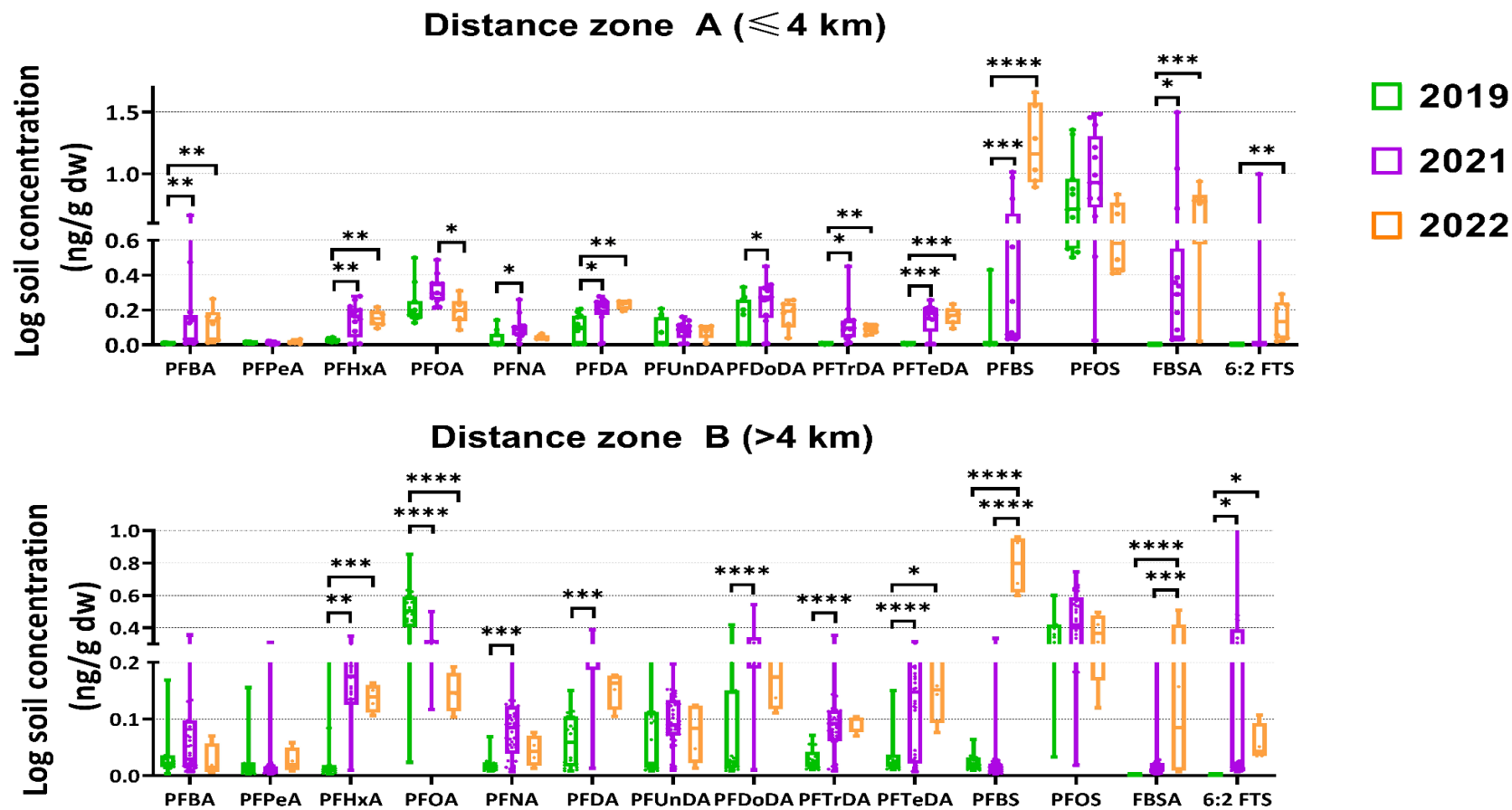


Fig. 5.2a: Short-term temporal trends of PFAS concentrations in the top soil layer of chicken enclosures (in ng/g dry weight) from private gardens nearby (≤ 4 km) and remotely (>4 km) from the major fluorochemical plant in Antwerp (Belgium) from the time period 2019 – 2022. Box whiskers denote the log min.-max. concentrations and significant differences between years are shown with asterisks (*: $P \leq 0.05$; **: $P \leq 0.01$; ***: $P \leq 0.001$; ****: $P \leq 0.0001$).

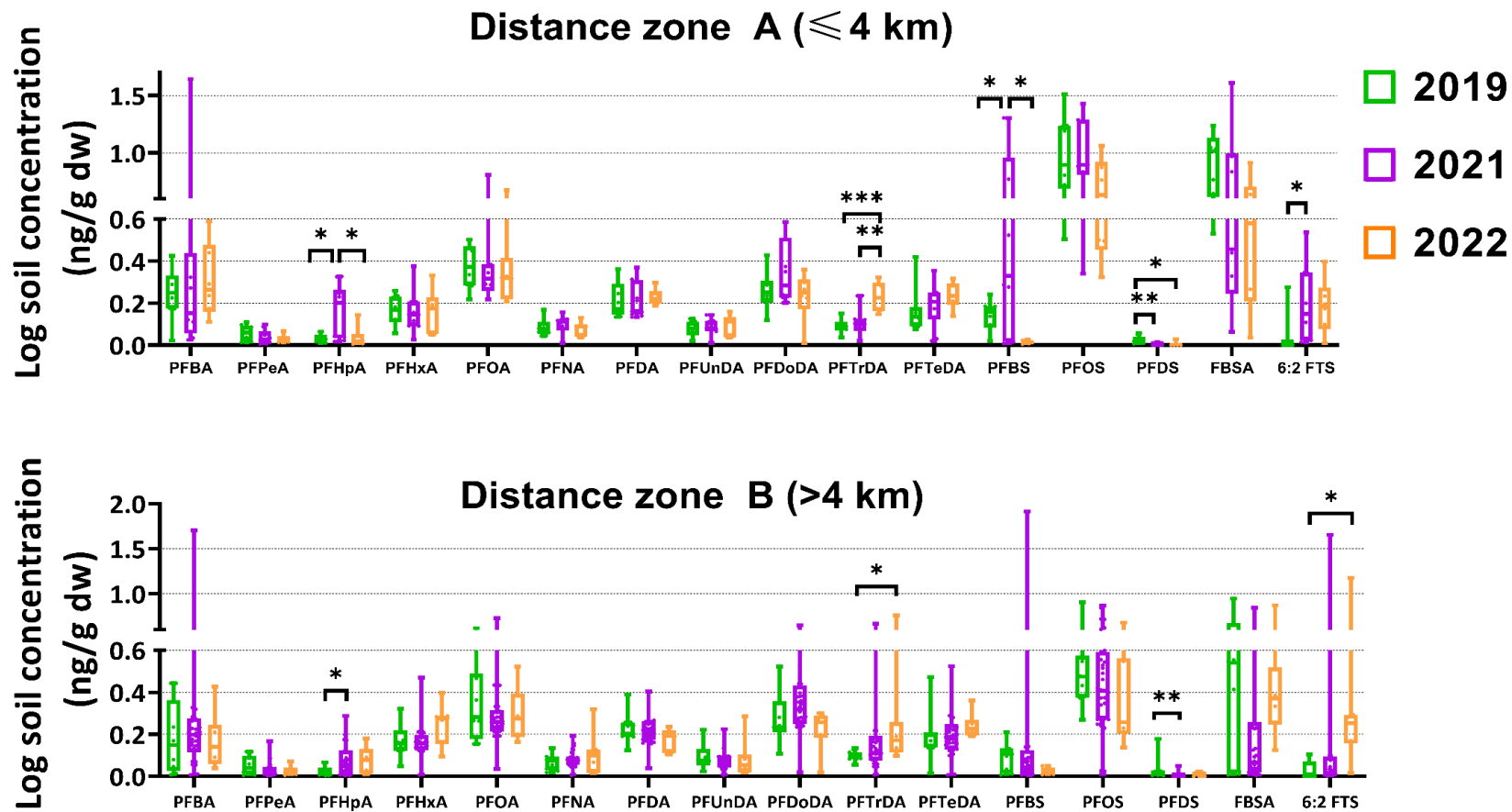


Fig. 5.2b: Short-term temporal trends of PFAS concentrations in the top soil layer of vegetable gardens (in ng/g dry weight) from private gardens nearby (≤ 4 km) and remotely (>4 km) from the major fluorochemical plant in Antwerp (Belgium) from the time period 2019 – 2022. Box whiskers denote the log min.-max. concentrations and significant differences between years are shown with asterisks (*: $P \leq 0.05$, **: $P \leq 0.01$, ***: $P \leq 0.001$, ****: $P \leq 0.0001$).

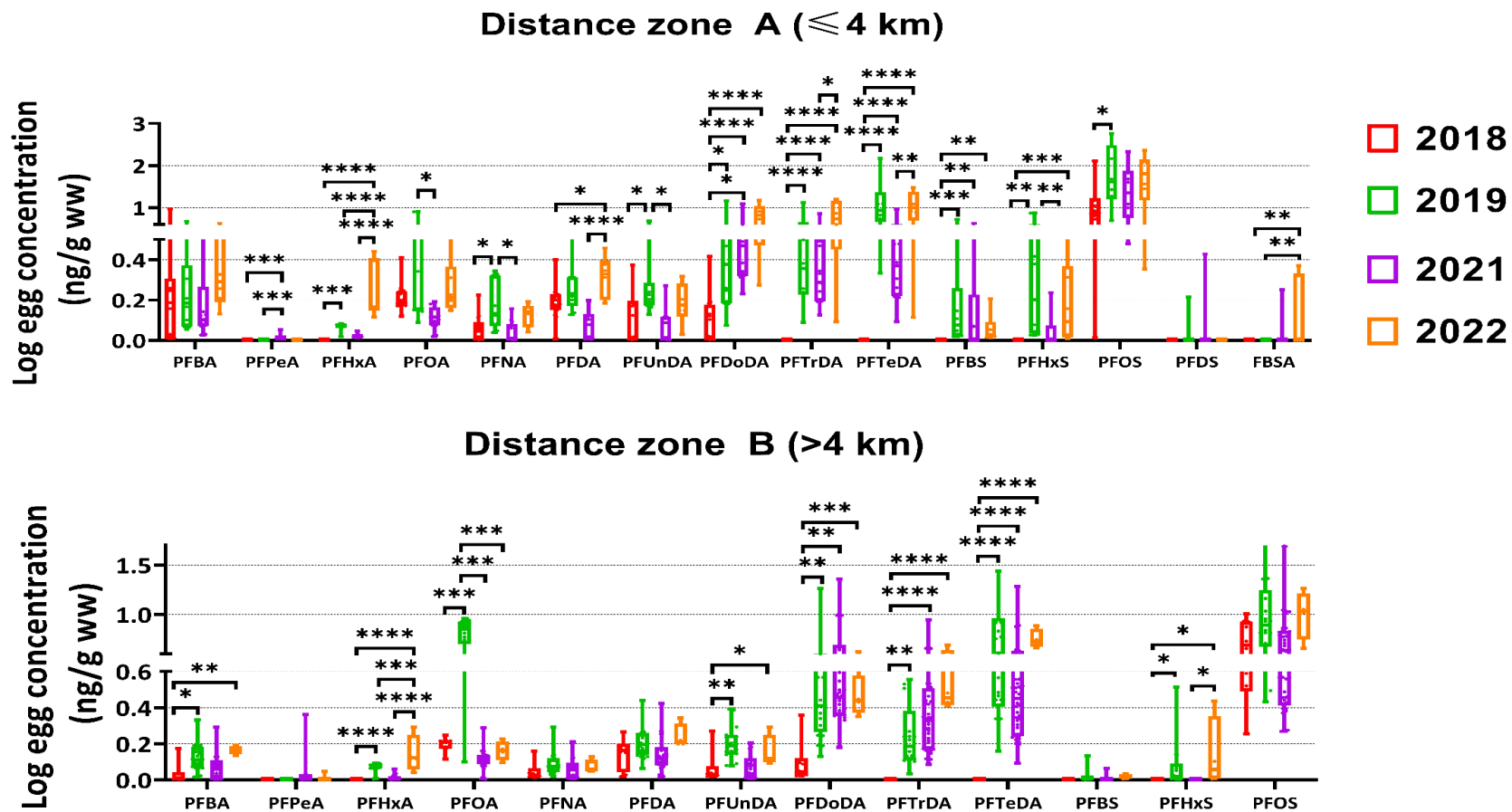


Fig. 5.2c: Short-term temporal trends of PFAS concentrations in homegrown eggs (in ng/g wet weight) from private gardens nearby (≤ 4 km) and remotely (>4 km) from the major fluorochemical plant in Antwerp (Belgium) from the time period 2019 – 2022. Box whiskers denote the log min.-max. concentrations and significant differences between years are shown with asterisks (*: $P \leq 0.05$, **: $P \leq 0.01$, ***: $P \leq 0.001$; ****: $P \leq 0.0001$).

Except for FBSA, which was found at low concentrations and only nearby the plant site, no targeted precursor compounds were detected in the eggs (Table S5.4). Moreover, from the precursor compounds that were primarily detected in the present study (i.e. 6:2 FTS and FBSA), significantly lower concentrations were consistently observed in the chicken soil compared to the garden soil ($P < 0.01$, Fig. 5.2a and Fig. 5.2b). On the other hand, end-degradation products of these precursors, which are PFBS and a mixture of C₄₋₆ PFCAs for FBSA and 6:2 FTS, respectively (Méndez et al., 2022; Sivaram et al., 2022), were frequently found in the chicken soil and eggs, while PFBS was the main compound that could be attributed for the distinct cluster of chicken soil from the multivariate analyses. Together, these results suggest that these precursor compounds can be readily biotransformed to their respective end products, which has been demonstrated experimentally for related precursors of PFSA (Kowalczyk et al., 2020) and PFCAs (Chen et al., 2020) in laying hens.

In contrast to the garden soil, higher PFBS and PFOS concentrations were related with the separate clustering of chicken soil and eggs (Fig. 5.1b) and significantly higher concentrations were found in eggs for C₉₋₁₄ PFCAs and most PFSA, especially PFOS (all $P < 0.05$, Fig. 5.2c). This suggests that chicken enclosure soil is an important exposure source of long-chain PFSA and PFCAs to the laying hens. Free-ranging laying hens are geophagous animals that are known to be particularly susceptible for exposure to pollutants via ingestion of contaminated soil particles (Waegeneers et al., 2009). PFSA and long-chain PFCAs generally exhibit stronger sorption affinity towards the soil and larger bioaccumulation potential compared to short-chain PFAS (Brendel et al., 2018).

5.4.2 Short-term spatiotemporal trends (2018/2019-2021)

5.4.2.1 Large-scale changes in PFAS concentrations

Dynamic short-term temporal increases in PFAS concentrations were most evident in the chicken soil and eggs for short-chain compounds (PFBA, PFHxA and PFBS) and long-chain PFCAs (C₁₀ and C₁₂₋₁₄), as well as for the precursors FBSA and 6:2 FTS (all $P < 0.01$, Fig. 5.2a and Fig. 5.2c). On the other hand, almost no differences were observed among years for PFOA and PFOS. In fact, apart from decreasing concentrations of PFOA and PFDS in the chicken soil remotely from the plant site and in the garden soil, respectively, concentrations of most compounds increased (i.e. chicken soil and eggs) or remained stable (i.e. garden soil) from 2018/2019 – 2022, depending on the matrix type (Fig. 5.2a-c).

The majority of temporal studies in abiotic matrices, which are mainly limited to sediment and water, as reviewed by Land et al. (2018), have reported similar increasing trends of long-chain PFCAs and precursors over time, while no clear trends have been observed for PFOS and PFOA. The observed temporal changes in eggs are partly in line with other monitoring studies in free-living birds, which observed no clear changes in PFOS and PFOA concentrations over time, while increased concentrations were reported for some long-chain PFCAs in predatory birds of relatively high trophic levels (Bustnes et al., 2022; Miller et al., 2015), including in buzzard liver samples from Flanders (Groffen et al., 2023b). However, these changes are often less consistent and for fewer compounds than those found in the present study. While dynamic changes of PFAS have also been observed in other studies within a small time frame (Meng et al., 2022), the present study supports the earlier proposed hypothesis that ecosystems show a lagged response to environmental changes in pollutant concentrations (De Silva et al., 2020), according to the trophic level of organisms. In other words, organisms on lower trophic levels which have closer exposure to environmental media (e.g. dust, water and soil), such as free-ranging laying hens, seem to respond relatively fast to environmental PFAS changes, while organisms which are on a relatively high trophic level, such as apex predatory birds, have a lagged response.

Both nearby and remotely from the plant site, the concentrations of most short-chain PFAS and the precursors significantly increased in chicken soil (PFBS, PFHxA, FBSA and 6:2 FTS), garden soil (PFHpA and 6:2 FTS) and eggs (PFHxA) over time (all $P < 0.05$, Fig. 5.2a-c), which is in line with the recent shift of the fluorochemical industry towards increased production of these compounds (Dhore and Murthy, 2021; Munoz et al., 2019). Interestingly, the relative increase of these compounds tended to be larger in private gardens nearby the fluorochemical plant site in Antwerp (Fig. 5.2a-c), which further supports that the PFAS production shift may be an important driver of the observed temporal trends for these PFAS. Notably, PFBS was the short-chain compound with the largest, relative increase over time in chicken soil, both nearby and remotely from the plant site (Fig. 5.2a). Likewise, FBSA (i.e. precursor of PFBS) concentrations also strongly increased in chicken soil. On the other hand, FBSA was only sporadically detected in eggs while PFBS concentrations did significantly decrease only in this matrix (all $P < 0.05$, Fig. 5.2c). This finding confirms the earlier findings that biotransformation of FBSA to PFBS is probable (Chen et al., 2020) and may explain this specific temporal pattern.

The long-chain PFCAs (C_{12} - C_{14}) significantly increased from 2019 to 2022 in chicken soil and eggs both nearby and remotely from the plant site (all $P < 0.05$, Fig. 5.2a and Fig. 5.2c). Apart for PFTrDA, no such trends were observed for long-chain PFCAs in the garden soil (all $P > 0.05$, Fig. 5.2b). Contrarily to the short-chain PFCAs and precursor compounds, the relative increases for these long-chain PFCAs were rather uniform over time between private gardens nearby the plant site and those located remotely from it. Moreover, the majority of samples for every matrix fell within the range of 1/1 to 6/1 ratio for both the homologue pairs of PFDA/PFUnDA and PFDoDA/PFTrDA in every sampling year at private gardens further away from the plant site and, with few exceptions, also for private gardens nearby the fluorochemical plant site (Table S5.5). Fluorotelomer degradation typically leads to relatively consistent homologue ratios of deposited PFCAs over time and can be a useful tool for further elucidation of potential precursor degradation (Rankin et al., 2016; Prevedouros et al., 2006). Homologue ratios of PFCAs ranging between 1/1 to 6/1 are typical for atmospheric transport of FTOHs precursors and subsequent oxidation, while ratios above 8/1 are indicative for direct PFCA emissions and/or biological degradation (Rankin et al., 2016). Therefore, it is likely that atmospheric oxidation of PFCA precursor compounds, such as fluorotelomer alcohols (FTOHs), may be an important driving pathway for explaining the increase of long-chain C_{10-14} PFCAs (Styler et al., 2013).

Ratios above 8/1 for the homologue pair PFOA/PFNA were observed for chicken soil and egg samples, with a decreasing mean ratio from 2019 to 2022 in chicken soil (Table S5.5). These results further strengthen the hypothesis that atmospheric oxidation of precursors is a plausible mechanism for the elevated C_{10-14} PFCA concentrations found in the present study. On the other hand, PFOA and PFNA probably originate from historical emissions and consumer products, but also from biological transformation of precursors as often high PFOA/PFNA concentration ratios were found for chicken soil and eggs. Since the scope of the present study was restricted to two precursor compounds (FBSA and 6:2 FTS), future monitoring efforts should include FTOHs as targeted analytes to further elucidate this hypothesis.

In contrast to what is observed for chicken soil, short-term temporal changes were largely absent in the garden soil (Fig. 5.2b). This difference may be explained by functional differences in human soil management practices between these two garden segments. Frequent physical disturbance of the top soil layer and addition of soil amendments in the garden soil may mask environmental

changes in PFAS concentrations (Sivaram et al., 2022; Gerardu et al., 2023), while such soil manipulations and disturbances are limited in chicken enclosures. Consequently, the chicken soil may provide a better reflection of potential environmental changes in PFAS concentrations than garden soil. Regarding the eggs, similar directions of temporal changes were observed as for the chicken soil in the present study, although the magnitude of change was often larger and more explicit (Fig. 5.2a and Fig. 5.2c). This finding also provides evidence that free-ranging laying hens, due to their close relatively small home-range and close proximity to humans, can be ideal bioindicators of pollutants in residential areas (Lasters et al., 2022; Zergui et al., 2023).

5.4.2.2 Influence wind orientation towards point source

Meteorological data showed dominant NW-N and N-NE wind currents (>50%) in the region near the fluorochemical plant in Antwerp from 2019 to 2021, respectively (Fig. S5.2). Nearby the plant site, concentrations of soil and eggs, in private gardens oriented S-SW from the plant site, were often significantly higher for PFBA, PFBS, PFHxS, PFOS and FBSA in recent years (2021 and 2022) (all $P < 0.05$, Fig. S5.2-S5.4). These high but relatively local pollution plumes sharply decreased with increasing distance from the plant site (Fig. S5.2-S5.4). Recently, aerial and dust deposition measurements in the same distance zone from this plant site also confirmed strong but local distance gradients for some of these compounds (Peters et al., 2022). Moreover, a similar spatial pattern has been described by monitoring studies within the same study area in soil (Groffen et al., 2019d), isopods (Groffen et al., 2019b) and bird eggs (Lasters et al., 2022). Together, these findings strongly indicate that direct historical emissions from the fluorochemical plant, followed by atmospheric deposition, likely explain the typical plume pattern for these compounds.

For 2021, consistently elevated concentrations of long-chain PFCAs (C_{11-14}) were observed downwind in chicken soil remotely from the plant site in S-SE direction (all $P < 0.05$, Fig. S5.2), suggesting long-range atmospheric transport and oxidation of precursor compounds. It is difficult to fingerprint potential sources to explain this pattern. Nevertheless, it is likely that these elevated concentrations originate from distant, diffuse constant sources rather than local stack sources, given that the contamination area is relatively widespread (Gerardu et al., 2023; Peters et al., 2022). Moreover, the ratios of PFCA homologue pairs fell within the typical range for precursor oxidation (Rankin et al., 2016), both nearby and remotely from the fluorochemical plant site (Table S5.5; chicken soil 2021). Unfortunately, no private gardens could be sampled in 2019 and 2022 from

these areas to evaluate whether these trends would be confirmed. Therefore, future PFAS monitoring programs in these particular areas would be helpful for further identification of potential source types.

Remarkably, a strong peak of PFOA concentrations in 2019 was followed by a steep decrease in 2021 (Fig. 5.2a and Fig. 5.2c). This could be attributed to a cluster of private gardens which were sampled ± 9 km away and oriented N-NE from the fluorochemical plant site (soil chicken enclosure, Fig. S5.2b; homegrown eggs, Fig. S5.4b). It is not possible to identify the precise source of this elevated PFOA concentration, based on the present study data. However, this pattern was observed in both the soil and the eggs, which may suggest a common source. Although speculative, it should be noted that these private gardens were all situated E-SE within 3 km from a large waste incineration plant. Waste incinerators, such as the one in the study area of the present study (Department Environment and Health, 2022a) and elsewhere (Gerardu et al., 2023; Liu et al., 2021b), have been identified as active sources of diffuse environmental contamination of complex PFAS mixtures. Indeed, the input material for incineration can range diversely from PFAS-containing household and consumer products to industrial waste products. Hence, emissions can strongly vary in terms of concentrations and compounds (Liu et al., 2021b). It would be useful to install passive air samplers in private gardens within a E-SE distance gradient from this potential source to continuously monitor PFAS in circulating air and dust samples to evaluate whether this hypothesis would be supported.

It should be noted that, on the long-term, wind currents in Flanders are mainly originating from the S-SW directions, implying that private gardens located N-NE nearby the plant site would also have relatively higher PFAS concentrations compared to other private gardens at comparable site distance, but in another orientation. Recent investigations in this study area, based on dust deposition data (Peters et al., 2022), have indeed found indications that N-NE located sites from the fluorochemical plant may receive relatively larger PFAS inputs via historical aerial deposition. However, it was practically impossible to investigate such long-term wind effect in the present study for private gardens as the N-NE region nearby the plant site almost exclusively consists of industrial area and is also intersected by the Scheldt river. Finally, it cannot be ruled out that short-term changes in industrial emission releases may also affect the interpretation of the results. However, if emissions would have been variable, then one might expect variable statistical effects

(mix of increases and decreases of concentrations) or no differences among the years, which was not the case based on the data of the present study (Fig. 5.2). Nonetheless, systematic air measurements with passive air sampling stations during one year, within vicinity of point (e.g. fluorochemical plant) and diffuse PFAS sources (e.g. waste incinerator), would be helpful to quantify potential emission variation and to further disentangle this potential confounding variable.

5.4.2.3 Small-scale changes in PFAS concentrations (2019-2021)

For repeatedly sampled chicken enclosures nearby the plant site in 2019 and 2021, mean soil concentrations were significantly higher in 2021 compared to 2019 for FBSA, PFOS, PFHxA and C₁₀₋₁₄ PFCAs (all $P < 0.05$, Fig. 5.3). For PFBA, a similar trend was observed, albeit just not significant ($P = 0.06$). For repeatedly sampled gardens in 2019 and 2021 nearby the plant site, mean soil concentrations were significantly higher for PFHpA and 6:2 FTS in 2021 compared to 2019 (both $P < 0.05$, Fig. 5.3), while an increasing trend was observed for PFBS ($P = 0.08$). On the other hand, FBSA concentrations were significantly lower in 2021 than in 2019 ($P < 0.05$, Fig. 5.3). For all the other compounds, no significant changes in garden soil concentrations between both years were observed (all $P > 0.05$). Importantly, the temporal changes in long-chain PFCA and precursor concentrations were largely in line with those observed in the large-scale dataset (see previous section 5.4.3.1) and mostly for the chicken soil (Fig. 5.3), which may be due to previously discussed differences in soil management and practices between these two garden segments.

Moreover, further correlation analyses of the repeatedly sampled chicken enclosures in 2021 revealed that PFBA concentrations were strongly and significantly negatively correlated with the nearest distance from the OW road work site ($P < 0.05$, $R_{2021} = -0.83$; Fig. S5.5), while this trend was absent in 2019. The same pattern could also be observed for the soil PFOS concentrations (both $P < 0.001$, $R_{2019} = -0.93$ and $R_{2021} = -0.98$, Fig. S5.5) and the precursor compounds FBSA and 6:2 FTS (FBSA: $P < 0.05$, $R_{2021} = -0.85$ and 6:2 FTS: $P < 0.05$, $R_{2021} = 0.98$; Fig. S5.5), both which were not detected in 2019. The other compounds did not show any significant correlations (all $P > 0.05$).

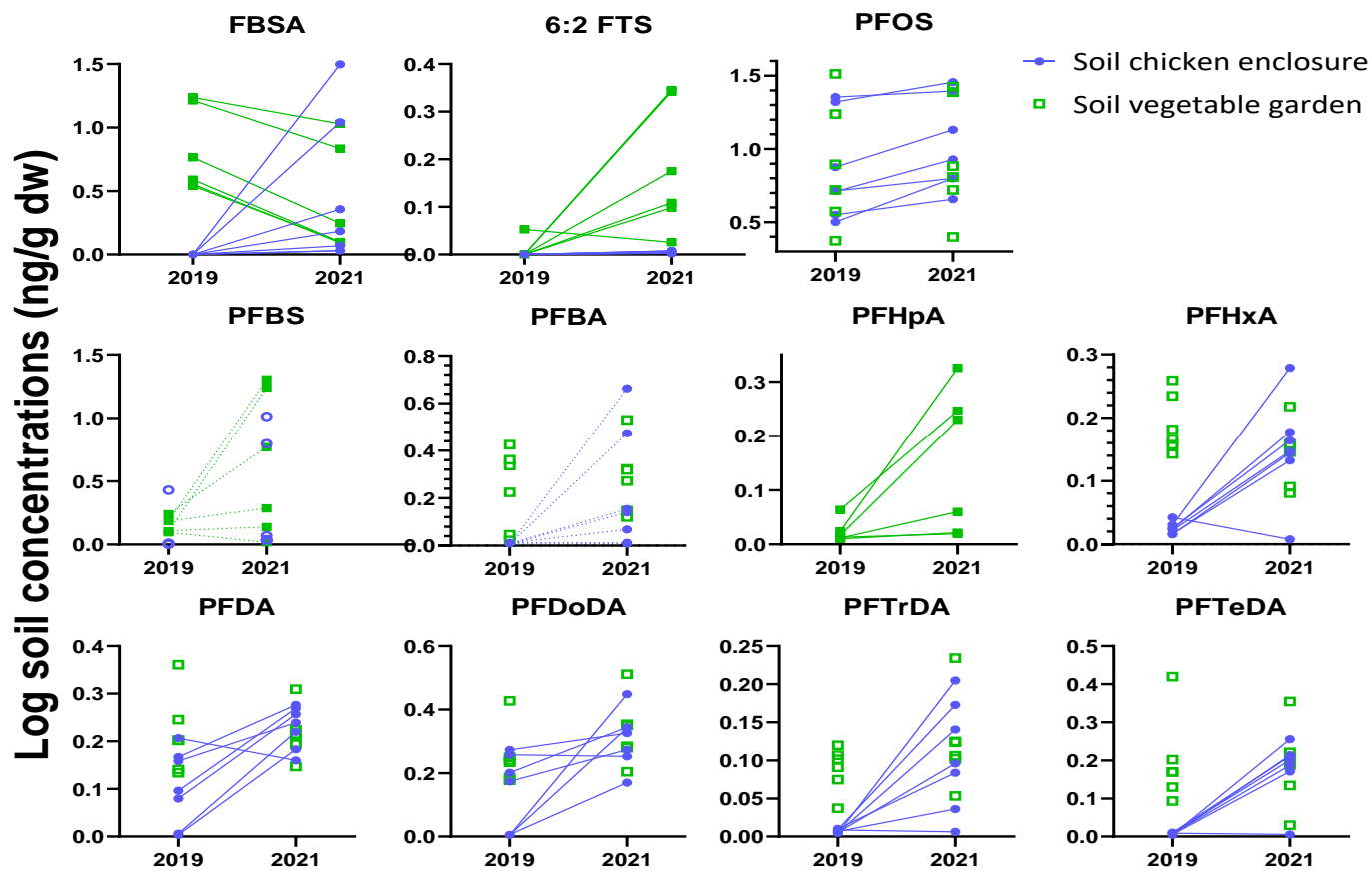


Fig. 5.3: Local short-term temporal changes in soil PFAS concentrations (in ng/g dw) of repeatedly sampled private gardens in 2019 (before the Oosterweel road works) and in 2021 (during the Oosterweel road works) within 4 km from the fluorochemical plant site in Antwerp (Belgium). The blue circles and green rectangles represent top soil layer data of repeatedly sampled chicken enclosures ($N = 7$) and vegetable gardens ($N = 6$), respectively. Solid lines denote statistically significant ($P < 0.05$) concentration changes from 2019 to 2021.

Together, these results suggest that soil disturbance and transfer activities on the OW road work site may be associated with higher local soil concentrations. Peters et al. (2022) conducted atmospheric air and dust measurements near this OW road work site and also demonstrated elevated concentrations of PFBS and PFOS closer to the site compared to background measurements. Moreover, higher amounts of PFAS deposition were observed on rainy days, indicating that wet deposition is an important route of atmospheric deposition (Peters et al., 2022; Pfothner et al., 2022). PFAS can be adsorbed onto fine and coarse dust fractions, which can act as vehicles for both long-range and short-range transport of PFAS, if these fractions become airborne due to physical disturbance (Liu et al., 2021b; Peters et al., 2022). This implies that OW could contribute to this process. Moreover, construction of asphalt roads have been intensively conducted on the OW site, which have also been associated with increased volatilization of PFAS into the air (Bastow et al., 2022). This may also explain the finding that correlations with distance from the road work site were mostly found for short-chain PFAS, which are more volatile than their long-chain homologues (Brunn et al., 2023). Evidently, the wind orientation of the private gardens towards the OW construction site can also play a significant role hereby. Unfortunately, this could not be properly investigated due to the irregular shape of this area and the limited sample size of this repeated dataset.

5.4.3 Long-term spatiotemporal trends: soil and homegrown eggs (2010-2022)

Nearby the fluorochemical plant site, a clear significant decline of PFOS concentrations in chicken soil, and for both PFOS and PFOA in eggs, was found for the long-term dataset from 2010 to 2022 (all $P < 0.05$, Fig. 5.4). However, remotely from the plant site, PFOS and PFOA concentrations in these matrices remained unchanged during this time period (all $P > 0.05$, Fig. 5.4). Consequently, the industrial phase-out of these compounds and regulatory measures (3M Company, 2000) did not appear to have an effect further away from the plant site, but only largely affected private gardens nearby the plant site. Moreover, based on the short-term dataset, PFOS and PFOA concentrations nearby the plant site remained unchanged during the last years (2018/2019-2022), which may also indicate that the effect of the regulatory measures and phase-outs on environmental and biota concentrations may have faded over recent years, similar to what other temporal studies have

reported for long-term (> 10 year timeframe) datasets (Jouanneau et al., 2020; Land et al., 2018; Pereira et al., 2021).

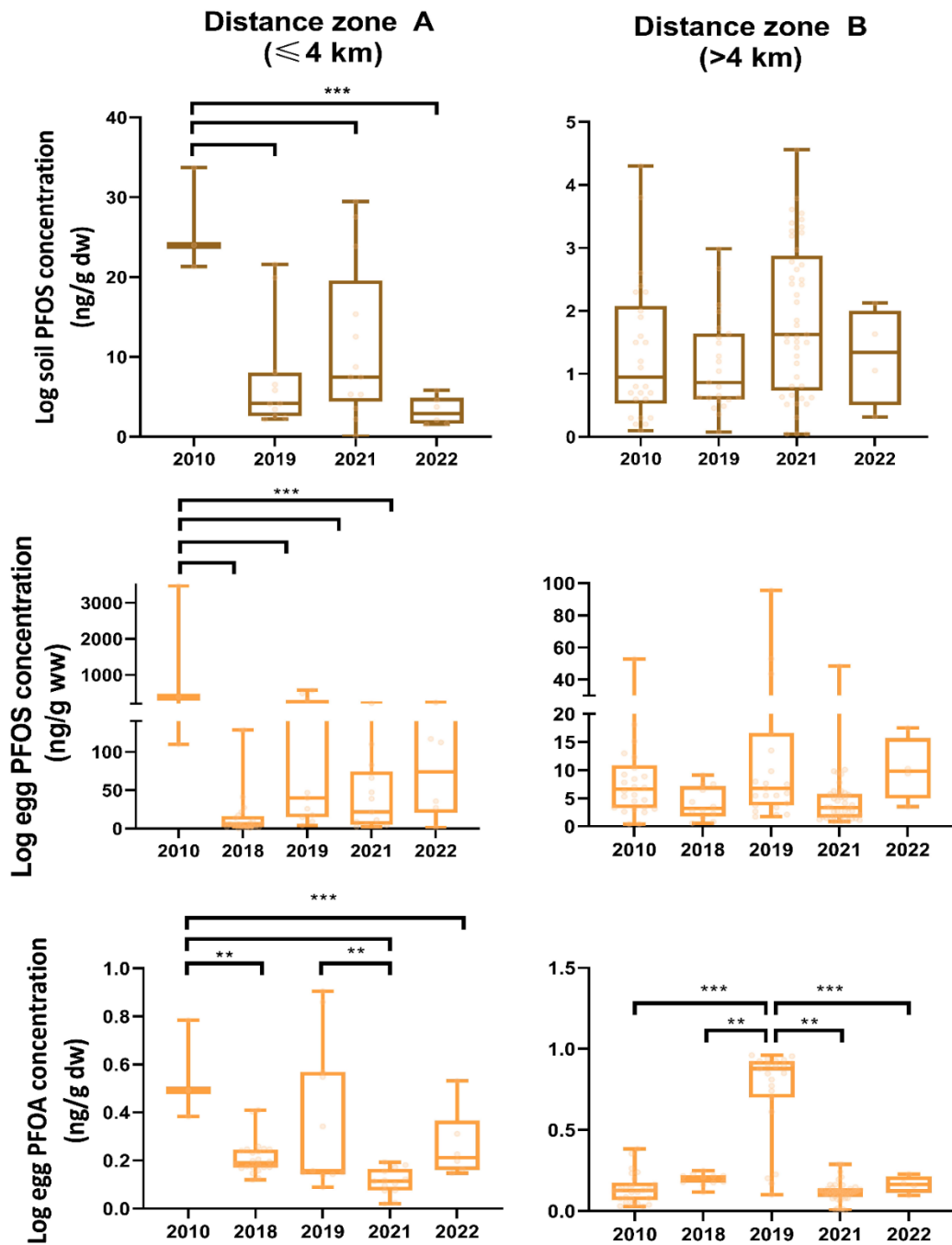


Fig. 5.4: Long-term temporal trends of PFOS and/or PFOA concentrations in the top soil layer of chicken enclosures (in ng/g dry weight; upper graphs) and homegrown eggs (in ng/g wet weight; lower graphs) within 4 km and outside 4 km range from the major fluorochemical point source in Antwerp (Belgium) from the time period 2010 – 2022. Box whiskers denote the log min.-max. concentrations and significant differences between years are shown with asterisks (*: $P \leq 0.05$, **: $P \leq 0.01$; ***: $P \leq 0.001$).

Long-term temporal monitoring studies of PFOS and PFOA at non-suspect sites have often reported mixed results. The majority also shows an absence of changes over the long-term for soil (Land et al., 2018), while unchanged (Eriksson et al., 2016), decreasing (Wang et al., 2022) or even increasing trends (Land et al., 2018) have been observed in bird eggs. Differences in site-specific environmental conditions and historical PFAS emissions, both in terms of quality and quantity, are likely to explain these contrasting results across countries as well as the species' ecology, e.g. marine vs terrestrial birds (Jouanneau et al., 2020; Land et al., 2018). Moreover, a temporal investigation of PFAS in buzzard livers, randomly sampled across Flanders, also did not find any significant concentration changes of PFOS and PFOA from 2000 to 2021 (Groffen et al., 2023b). Therefore, in densely populated and industrialized areas with large historical emission outputs, such as Flanders (Verbruggen, 1997), it remains important to continuously monitor temporal trends for PFOS and PFOA, which are still widespread and abundant in the environment.

Remarkably, the rate of decrease for PFOS from 2010 to 2022 in chicken soil and eggs was very similar (Fig. 5.4), suggesting again that soil is a major PFAS exposure source for laying hens and strongly correlates with PFAS accumulation in the eggs (Lasters et al., 2022). Although median PFOA concentrations in eggs were five times lower than PFOS in 2010, the decrease over time was proportionally slower than for PFOS while the reverse could be expected. Provided that the soil is a dominant exposure source of PFAS to the laying hens and that PFOA leaches much faster from the surface soil to the groundwater than PFOS (Gerardu et al., 2023), one would expect a faster decrease in PFOA concentrations over time in eggs. This could imply that other sources than the soil are important for PFOA exposure to laying hens, e.g. rain water (Cousins et al., 2022) and vegetable leftovers which can contain considerable concentrations of PFOA (Li et al., 2019). Alternatively, this relative difference in decreasing rate can also be explained by the fact that PFOS had already been phased-out much earlier in 2002, while this was only the case for PFOA in 2015 (UNEP, 2019).

Evidently, biological factors, such as inter-individual age differences, may also affect egg PFAS concentrations and could also hinder the interpretation of temporal changes in egg concentrations. However, age had only a minor influence on egg concentrations (Lasters et al., 2022) and more than 70% of the laying-hens in the present study was distributed between one and three years old, thus effects of age differences is expected to be negligible. Moreover, the present study showed that dynamic, short-term temporal trends observed for the chicken soil were often very similar

compared to those in eggs, especially for long-chain PFCAs (C₁₁₋₁₄). Importantly, these specific compounds are actual by-products of PFOA production and should therefore, in parallel, have remained stable or decreased over time, which was clearly not the case. Based on the current body of evidence, it is obvious that former restrictions are not sufficient to further reduce the environmental concentrations of these persistent and toxic substances. Therefore, in view of the ongoing and, for some PFAS, even increasing impact on the environment and related health concerns of PFAS, rapid regulatory actions are crucial, particularly in regions with a relatively high chemical footprint, such as Flanders.

5.5 Conclusion

To the best of our knowledge, our study is the first to demonstrate large differences within private gardens, both in terms of PFAS profile and concentrations. Apparently, vegetable garden soils were being much less affected by environmental changes of PFAS concentrations compared to chicken enclosure soil, probably due to functional differences in soil management processes. Dynamic short-term temporal trends, taking into account wind orientation towards a major PFAS point source, were observed in soil and eggs across a relatively large spatial scale. However, further monitoring efforts are needed in the coming years to allow long-term comparison and better distinction from potential confounding variables, which could not be ruled out due to the relatively small-time frame of the present study.

Long-term data show that PFOS and PFOA concentrations in soil and homegrown eggs have declined within 4 km range from a major fluorochemical plant compared to 2010, probably due to phase-out and regulatory measures. However, concentrations of these two major PFAS remained largely unchanged further away from the plant site and generally stagnated during recent years. The present study provided various lines of indications that temporal changes may be caused by direct recent and historical emissions of legacy PFAS as well as atmospheric precursor oxidation and subsequent degradation to legacy PFAS, as well as precursor biotransformation. These short-term changes appeared to be partly dependent on the wind orientation towards potential point sources, which requires further investigation. Future measurements of precursors via Total Oxidizable Precursor Assay (TOPA) in abiotic and biotic matrices, combined with non-target and suspect screening, would be insightful to further elaborate these hypotheses.



Chapter 6: General discussion and future research perspectives

6.1 Homegrown food: general accumulation patterns

Based on the outcome of chapters 2 and 4, a basic paradigm of PFAS accumulation in homegrown food could be developed, as illustrated in Fig. 6.1. The large PFAS accumulation in eggs, which contained on average 3-4 fold higher concentrations than in vegetable food, adds to the evidence that eggs have a high propensity for accumulating PFAS (Groffen et al., 2019a; Lasters et al., 2019). Previous research has attributed this finding to the very large binding affinity of PFAS to phospho- and lipoproteins in the yolk (Bangma et al., 2022; Wang et al., 2019). The present thesis adds to this evidence that higher egg concentrations are probably also a result of the multiple exposure sources that free-ranging laying hens encounter and their relatively high trophic position. As geophageous animals, they are highly susceptible for accumulation of PFAS in eggs (e.g. PFOS and long-chain PFCAs) via contaminated soil consumption.

This was supported by the large variation explained by soil concentrations in the empirical models of chapter 3, the higher soil concentrations of these compounds in the chicken enclosure and the parallel distance trend observed with soil concentrations relative to the fluorochemical plant (chapter 5). Additionally, PFAS in other feed sources (e.g. vegetable and earthworm pools) were also significantly associated with corresponding egg concentrations, indicating the biomagnification potential to higher concentrations in chickens. On the other hand, plant-based food is on a lower trophic level decreasing its biomagnification potential and the uptake of PFAS in plant-based food is mainly restricted to one exposure source, which is root uptake of PFAS from the porewater (Adu et al., 2023) and may explain the lower overall accumulation in crops.

Partly in parallel to the present thesis project, a human biomonitoring project was launched in the summer period of 2022, during which soil (i.e. chicken enclosure and garden soil) and homegrown food (i.e. eggs and plant-based food) were collected from private gardens within a 5 km distance

buffer zone (chapter 2) from the same fluorochemical plant (Consortium UAntwerpen et al., 2023). The soil samples were collected using different depth layers (0-10 cm layer versus 0-5 cm layer in my thesis project) and soil quantities (500 g versus 100 g in my thesis project) which hampers the comparability of these study results with those of the present thesis project. However, the homegrown food samples were also collected in the same season (i.e. summer) and analyzed in the same lab using similar extraction methods as those from the present thesis project, which enables a comparison between both studies.

As expected, the concentrations were generally in the same order of magnitude and similar for dominant compounds (e.g. PFOS and PFOA) between my thesis project and the human biomonitoring project (Consortium UAntwerpen et al., 2023). Nevertheless, the eggs from the biomonitoring project showed higher concentrations of long-chain PFCAs ($\geq C_{10}$) than those analyzed in my thesis project from all the sampling years. Interestingly, egg concentrations of these particular long-chain PFCAs mostly increased from 2018 to 2022 (chapter 5), which may be linked with atmospheric degradation of precursor compounds (e.g. FTOHs). Moreover, generally higher PFBS concentrations were found in the eggs and crops of the human biomonitoring study. This might be explained by the higher contribution of dust deposition close to the fluorochemical plant, as elevated PFBS concentrations were also found in circulating dust samples within 3 km from the plant site (Peters et al., 2022). Additionally, chapter 5 showed that both large within- and among garden variation can exist in PFAS profile and concentrations. Therefore, differences in garden-specific characteristics (e.g. functional usage, soil physicochemical properties) between both studies may also result in different bioavailability scenarios and hence accumulation differences in the food. This is also exemplified in both my thesis project and the human biomonitoring project, as large discrepancies could be observed between soil and crop concentrations. For instance, very low 4:2 FTS concentrations were observed in the soil and high concentrations in the crops (chapter 4), while the same pattern was observed for PFBS in the human biomonitoring project (Consortium UAntwerpen et al., 2023).

My thesis and the human biomonitoring project are among the first studies to examine PFAS accumulation in such a broad set of homegrown crop categories, including annual and perennial crops, under realistic field conditions. Therefore, an opportunistic sampling strategy was chosen to maximize generation of novel knowledge on PFAS accumulation in multiple crop categories.

However, the potential drawback of this approach was that the accumulation pattern for a few of the examined crop categories was dependent on the availability in a given garden. The shoot vegetable category was primarily composed of rhubarb, which may accumulate the largest PFAS fraction in the leaves (cf. chapter 4). Moreover, only very little data could be obtained on other shoot vegetables (e.g. leek and celery), which have shown relatively high accumulation potential in previous studies (Liu et al., 2019; Liu et al., 2023). For instance, flower vegetables (e.g. cauliflower and broccoli) that showed relatively high bioaccumulation potential (Scher et al., 2018) could not be sampled due to general absence in the private gardens at time of sampling. Therefore, the bioaccumulation schedule of Fig. 6.1 serves as a basic proxy for homegrown crop accumulation, subject to further refinement as monitoring efforts proceed.

In order to overcome this limitation in the future, it would be interesting to simultaneously introduce a consistent set of seedlings from these main crop categories in the private gardens at the beginning of the growth season. Additionally, this stratified sampling design should ideally be implemented in those gardens that showed minimal contrast in terms of soil physicochemical characteristics. In this way, the sample size can potentially be increased, while the potential influence of confounding factors affecting accumulation, such as soil characteristics (Searce et al., 2023), plant life-stage and fruit maturation stage (McDonough et al., 2021) can be reduced. Alternatively, this approach could also be useful in a semi-controlled greenhouse experiment: this may even further reduce the influence of confounding factors and also enabling the assessment of perennial crop categories, which may not be feasible for introduction in private gardens. This latter setting may also be ideal for studying the transport mechanisms of PFAS transport to the edible parts of perennial crops, which remains poorly understood and is important, given that chapter 4 showed consistent accumulation differences between perennial and annual crops.

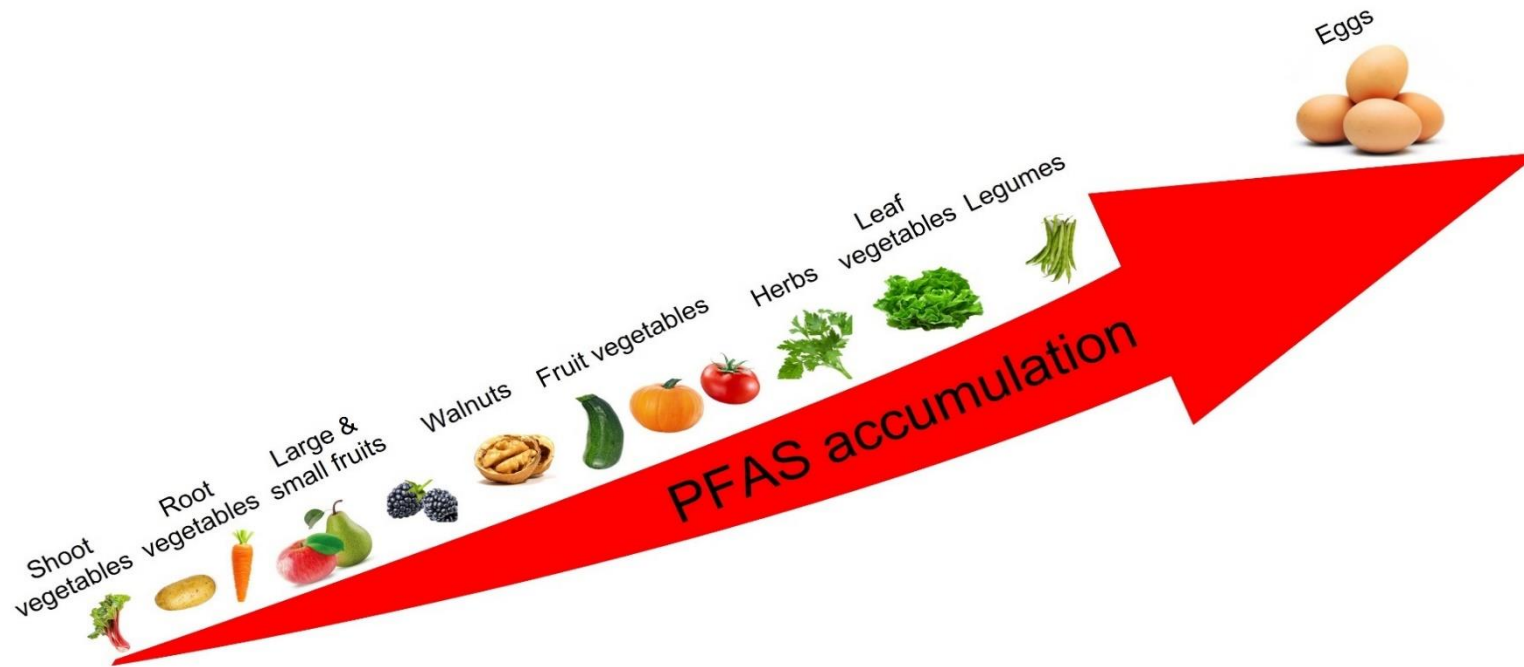


Fig. 6.1: Illustration of the examined food categories in my thesis, ranked from low to high according to the total PFAS accumulation in their edible parts. This figure was made based on the outcome of chapters 2 and 4.

From a broader perspective, it is remarkable that the observed PFAS concentrations in all the homegrown food categories were 1-3 orders of magnitude higher (chapters 2 and 4) than those in corresponding food products from commercial origin in Europe (EFSA, 2020; Pérez et al., 2014; Herzke et al., 2013). Regarding eggs, this difference can be primarily explained by the larger intake of contaminated soil and increased contribution from non-controlled feed sources (e.g. earthworms and crops), as demonstrated in chapters 2 and 3. However, this same argument cannot be made with respect to vegetable crops as PFAS exposure is mainly restricted to uptake via the roots under common environmental conditions (Adu et al., 2023). Moreover, reported soil concentrations in the vegetable garden segment were often lower than those in common agricultural soils (Costello and Lee, 2020; Ghisi et al., 2019), while food processing and packaging may additionally contribute to elevated concentrations in commercial food (Lerch et al., 2023). This suggests that site-specific differences in terms of crop cultivation strategies (e.g. planting density and cultivation intensity) between private gardens and agricultural settings may be an important overarching determinant for accumulation differences between crops from private and commercial origin. Therefore, it would be interesting in future research to test whether higher planting density and cumulative, intensive crop rotation cycles which are typical for agricultural soils may decrease the accumulated concentrations in individual crops due to dilution across a larger number of crops and depletion of the bioavailable fraction over time, respectively.

6.2 Influence of local abiotic and biotic factors on food concentrations

The developed empirical models of the chicken eggs support the established experimental evidence that sorption mechanisms between PFAS and the soil solid phases can strongly affect their bioavailability (Cai et al., 2022; Li et al., 2018b). Additionally, my thesis highlights the importance of the clay content, pH, their synergistic interaction and exchangeable cations with respect to bioavailability, as discussed in chapter 3. This is different compared to the majority of other POPs (i.e. PCBs and dioxins) which primarily interact via hydrophobic interactions (Sigmund et al., 2022). Moreover, the contribution of local feed sources to the eggs was revealed in chapter 2 and further unraveled in chapter 3, as concentrations in earthworms and homegrown crops were related with higher egg concentrations for long-chain and short-chain PFAS, respectively. This result also

emphasizes the importance of short-chain and long-chain PFAS accumulation in animals from plant-derived food and animal-derived food, respectively (Vorst et al., 2021).

Categorical survey data from chapter 2 showed that younger laying hens (<1 year old) and those fed with an obligate diet of kitchen leftovers tend to contain higher egg PFAS concentrations, which was corroborated in the human biomonitoring project (Consortium UAntwerpen et al., 2023). These survey results provided novel insights on potential exposure sources of PFAS to laying hens, but were also partly useful as a proof-of-concept to select relevant targeted matrices (e.g. homegrown crops) in the later sampling campaigns for the modeling in chapter 3. Nevertheless, it might be useful to actually measure PFAS in pools of kitchen leftovers in future research. In this way, one can quantify the actual contribution of this potential PFAS source to the egg concentrations and the predictive model performance (cf., chapter 3) would potentially further improve. Moreover, it would also be insightful to examine potential differences in PFAS concentrations among individual types of kitchen leftovers (e.g. vegetable waste, meat, dairy products and (shell)fish). In this way, remediation measures may be formulated to further lower exposure via egg consumption. Ideally, this should be tested in a standardized way through introduction of laying hens with similar properties (i.e. same origin, age and breed) to the volunteers' gardens (cf. as earlier discussed for the crops in section 6.1).

As opposed to the eggs, the modeling of the crops showed that soil concentrations and soil characteristics were not important determinants for explaining crop accumulation, which was largely in disagreement with the literature (Liu et al., 2023; Scarce et al., 2023). There are several possible reasons why no meaningful models could be obtained for the crop accumulation, which should be considered in future research. Firstly, models could not be constructed for the individual crop species as the sample size was too low ($N < 10$) and, therefore, crops were pooled within categories with the aim of obtaining generalizable models. However, despite the efforts to correct for species-specific root length using literature data, important other species-specific traits (e.g. fine roots versus tap roots, absence versus presence of plant barriers such as Casparian strips) that affect crop accumulation (Scarce et al., 2023) were neglected in this way, which may have obscured statistical relationships. As previously discussed, a semi-controlled field experiment could be an alternative way to overcome this issue, due to opportunistic sampling.

Moreover, the relatively low variability in crop and soil concentrations may also be a primary cause of the weaker models obtained for the crops. This was also manifested in chapter 3 for the egg models, in which compounds that showed low intrinsic variability in concentrations showed decreased overall significance of the model parameters and predictive performance. Therefore, it might be interesting to include additional datapoints for both the crop and egg models from other hotspot sites with high concentrations, but different PFAS contamination patterns (e.g. private gardens near firefighting facilities, airports, textile- and paper industry). For instance, the spatiotemporal results from chapter 5 revealed that a cluster of private gardens, close to the airport in Deurne, showed elevated concentrations of 6:2 FTS.

Importantly, dust deposition and subsequent leaf absorption may be a relevant exposure pathway of PFAS for crops, especially nearby fluorochemical production sources (e.g. fluorochemical plant in Antwerp), as PFAS can be directly emitted into the air (Liu et al., 2019). Moreover, short-chain PFAS and precursors, which showed a relatively high tendency to accumulate in crops (chapter 4), are also typically present at relatively high concentrations in air and circulating dust (Jin et al., 2018; Peters et al., 2022). For instance, PFBA contributed for >50 % of the total PFAS concentration in the dust fraction nearby the fluorochemical plant in Antwerp (Peters et al., 2022). However, it is difficult to compare and link the aerial data from Peters et al. (2022) with my thesis project as the time periods of monitoring were different and aerial PFAS data will likely vary considerably over time, due to variation in emission outputs and fluctuations in weather (e.g. rain and wind) dynamics. Therefore, it would be useful to install passive air samplers in private gardens within a gradient from aerial emission sources and continuously monitor PFAS in both the air and crops at regular time intervals and fixed distances to further evaluate the potential role of this exposure pathway for crops.

Lastly, it could be that soil is not the best measure of crop PFAS accumulation and that porewater may represent a better measure of the bioavailable PFAS fraction (Felizeter et al., 2020), especially in relatively low soil concentration scenarios. Indeed, at relatively low soil concentrations, the majority of the short-chain PFAS fraction (e.g. chapter 4: PFBA and 4:2 FTS), which show the largest crop accumulation potential (Adu et al., 2023), may be present in the porewater due to their relatively high hydrophilicity (Blaine et al., 2014; Felizeter et al., 2020). Unfortunately, it was not feasible to comprise porewater measurements within the timeframe of my thesis project.

Nevertheless, the finding in chapter 4 that 4:2 FTS was one of the dominant compounds in the crops but barely detected in the garden soil, further motivates the inclusion of PFAS porewater measurements in future research.

6.3 Potential human exposure risks

Based on the calculated homegrown food intake levels of chapters 2 and 4, previous indications that homegrown food can be a major exposure source to humans were affirmed (Colles et al., 2020; 2022; Consortium UAntwerpen et al., 2023). In fact, the combined intake of homegrown food frequently exceeded the current TWI health guideline of the EFSA and this was the case both close to the fluorochemical plant and further away. Moreover, the MTR guideline, based on a more severe health endpoint (e.g. liver damage), was also frequently exceeded for PFOS intake via egg consumption within 2 km from the plant site, as shown in chapter 2. These results were based on modest consumption scenarios and other exposure pathways (e.g. intake of commercial food, drinking water and dust) were not taken into account, highlighting the need for urgent regulatory measures of PFAS.

This pressing need for further action on a large scale becomes further clear when the overall concentrations in the homegrown eggs and vegetables are compared to the European maximum levels (MLs) for the same food categories from commercial origin (Table 6.1).

Table 6.1: The percentage exceedance of the maximum/indicative levels (ng/g ww), established by the European commission (EU, 2022), in all the egg, vegetable and fruit samples of the present thesis project.

Food type	Compound	Maximum level (ng/g ww)	Exceedance (%)
Eggs	PFHxS	0.3	10.5
	PFOS	1	95.5
	PFOA	0.3	79.9
	PFNA	0.7	5.20
	Total sum EFSA-4	1.7	92.5
Indicative level (ng/g ww)			
Vegetables and fruits	PFHxS	0.015	12.6
	PFOS	0.01	19.8
	PFOA	0.01	99.5
	PFNA	0.015	29.4

With respect to the eggs, the ML for the sum of the EFSA-4 compounds (cf. TWI) would be exceeded in 92.5% of the samples, mainly driven by the relatively high PFOS concentrations. For the vegetables and the fruits, the MLs were exceeded to lesser extent although the ML for PFOA would be exceeded in nearly all the vegetable and fruit samples.

Additionally, it should be noted that these MLs and the available health guideline values (i.e. TWI and MTR) used for the exposure assessment in chapters 2 and 4 are only applicable for the EFSA-4 PFAS (i.e. PFHxS, PFOS, PFOA and PFNA). Although these four compounds are meaningful for exposure assessment of eggs, they are of less relevance for the exposure assessment of vegetables and fruits. Chapter 4 showed clearly that short-chain PFAS and some precursors tend to enrich in vegetables and fruits, for which no health guidelines are officially available. This implies that the PFAS intake levels for plant-based food items may give a large underestimation of the potential exposure risk when comparing to the current health guidelines. Therefore, future health guidelines should be developed for additional PFAS to further improve the risk assessment. Hereby, it would be helpful to group individual compounds as much as possible, following the European drinking water guidelines, to facilitate policymaking and action.

The present thesis project clearly showed that complex mixtures of PFAS were present in all the food matrices. Therefore, humans are exposed to mixtures of PFAS which is in another important consideration in risk assessment. Recently, there have been promising efforts to take into account the exposure to PFAS mixtures, e.g. by using relative potency factors (Bil et al., 2020). It predicts the combined effect for a given toxic endpoint (e.g. liver toxicity) resulting from exposure to a mixture of chemicals by concentration addition, taking the relative potency into account of the individual compounds in that mixture. However, this approach assumes that the compounds show similar toxicity profiles and no synergistic effects in the mixture. Although this may hold true for PFAA congeners, other PFAS are structurally very diverse compounds with likely varying toxicity. Furthermore, they can have synergistic effects rather than additive effects for certain health endpoints (Pierozan et al., 2023). Therefore, more toxicity data are needed for more PFAS to validate the applicability of relative potency factors to them as well.

Clearly, proper risk assessment of PFAS has become very complex and should not be further complicated. Therefore, a realistic regulatory strategy of PFAS in compliance with feasible phase-

out timings for major industrial branches that produce or use PFAS (Glüge et al., 2020) should be developed as soon as reasonably possible. This will allow gradual elimination of PFAS from non-essential towards essential applications (Cousins et al., 2019; 2022). This statement is further strengthened by the temporal trend results from chapter 5, which indicated that detection frequency and concentrations of emerging PFAS (e.g. precursors and short-chain PFCAs) increased over the last years. In parallel, concentrations of phased-out legacy compounds (i.e. PFOA and PFOS), levelled off throughout that period. Moreover, the spatiotemporal results in chapter 5 indicated that the elevated exposure risk via eggs could be related with both historical and recent industrial emissions, especially for FBSA, PFBA, PFOS and PFOA. This was evident from the stacked point source influence up to around 4 km in W-SW orientation towards the plant site, while remote sites (>10 km away) in SE direction from the plant site were related slightly elevated long-chain PFCA concentrations, probably from diffuse sources (i.e. atmospheric transport and precursor oxidation into long-chain PFCAs).

Moreover, this thesis also emphasized the importance of local point sources as elevated soil PFAS concentrations could be observed in repeatedly sampled gardens during large road infrastructure works (i.e. Oosterweel) nearby the 3M plant site, in comparison with measurements prior to the start of those works. This was especially evident for those compounds that were linked with historical pollution (e.g. phased-out PFOS) from this plant site and measurements in circulating dust also pointed in the same direction (Peters et al., 2022). However, the limited amount of repeated data on private gardens did not allow to effectively characterize the contribution from this potential local source. Elsewhere, elevated 6:2 FTS concentrations could be observed in private gardens around the airport in Deurne and a recent study has found elevated concentrations in influent wastewater from the catchment area in that same region (Jeong et al., 2022).

Following this, the results from chapter 5 clearly show that the PFAS contamination profile and concentrations in private gardens are often site-specific with even large differences possible within gardens (e.g. long-chain PFAS chicken enclosure soil versus short-chain PFAS garden soil). Furthermore, the human intake estimations in chapters 2 and 3 were likely underestimations as they were based on only a limited number of targeted analytes and 1% or less of the known PFAS is currently analyzed in human biomonitoring studies (EFSA, 2020). Therefore, refined monitoring strategies using an arrowhead approach combining non-target and suspect screening, extractable

organic fluorine and TOPA, followed by conventional site-specific targeted analysis (Cousins et al., 2020), will become indispensable to enhance risk assessment.

Based on the results of my thesis (i.e. chapter 2 and 3) and those reported in human serum by the human biomonitoring project (Consortium UAntwerpen et al., 2023), eggs from free-ranging laying hens may be a valuable matrix to conduct such a monitoring approach in private gardens. Indeed, the eggs of free-ranging laying hens might enable a quick *in situ* characterization of the human exposure risk (i.e. biomonitor). The consumption of homegrown eggs has consistently been associated with increased human blood serum concentrations of PFOS, PFOA and PFNA (Colles et al., 2020; Consortium UAntwerpen et al., 2023), while these compounds were dominant in eggs (chapter 2) and human blood (Consortium UAntwerpen et al., 2023). Moreover, with regard to PFOS, the soil concentrations were strongly correlated with the corresponding egg concentrations (cf. chapter 3). Therefore, eggs may also be a good bioindicator for this major and omnipresent compound. Finally, chapter 5 showed that the short-term and long-term changes of PFOS concentrations in soil were in agreement with those in the eggs, further supporting their bioindicator potential for this compound.

Hereby, significant associations were reported between serum PFOS, PFNA and PFDA levels and biomarkers of immune and sex endocrine disruption in teenagers, which further highlights the need for human biomonitoring. One major knowledge gap in this study and many other human biomonitoring studies is the potential confounding and interaction of PFAS with other pollutants and stressors. This will become highly important in the future, as emerging evidence makes increasingly clear that these interactions can affect the environmental fate and behaviour of PFAS (Mahmoudnia et al., 2022; Parashar et al., 2023) and may enhance human toxicity (Pan et al., 2023). It has even been suggested that PFAS may enhance climate positive feedback loops. For instance, global warming may be accelerated through the transfer of PFAS from the ocean water to sea-spray aerosols in the ocean, which increases the cloud albedo and consequently the temperature (MacLeod et al., 2014). Therefore, a multistressor approach will become very important in the near future to increase our understanding of human health risks (Richardson et al., 2023).

6.4 Potential remediation and mitigation measures

It is promising that the predictive models in chapter 3 showed reliable and accurate prediction of PFAS in the eggs, which was the matrix that represented the largest relative human exposure risk, based on the intake estimations from chapters 2 and 4. The outcome of the predictive models for major compounds (e.g. PFOS, PFOA and PFNA) in the eggs may be potentially helpful tools for human risk assessment. It should be stressed that the construction of these models was underpinned by a large robust dataset ($N = 89$), thorough validation process and large variation in PFAS concentrations and soil composition among private gardens that were situated in industrial, urban and rural areas. Therefore, these models show potential for large-scale applicability for estimation of what-if risk exposure scenarios when laying hens would be introduced in a given private garden. Currently, many soil PFAS investigations in residential areas have already been conducted in Flanders (City of Antwerp, 2021; Department and Health, 2022b; Flemish Environment Agency, 2022a) and would only require the measurement of the most important soil characteristics (i.e. pH and clay content) and insert these variable values, together with the soil concentrations, into the models. In this way, policy makers can be able to not only provide information on the actual soil contamination profile, but also on the implications with respect to homegrown egg consumption risk.

The results of my thesis appear to suggest that manipulation of soil characteristics in the chicken enclosure may be a potential way of lowering egg PFAS accumulation. Indeed, as the soil concentration and the clay mineral fraction were associated with higher egg PFAA accumulation, it could be useful to introduce a sand parcel within the chicken enclosure as a readily applicable and relatively cheap measure. PFAS show only very weak interactions with quartz, the main component of sand, which are readily desorbed with rainfall (Hellsing et al., 2016). In addition, sandy soils tend to contain lower amounts of soil invertebrates, including earthworms (Bedano et al., 2016), which could be identified as a significant exposure source of some PFAAs to the laying hens. Thus, implementation of these measures could result in a substantial decrease in egg concentrations. Ideally, this should be verified in existing private gardens by measuring egg concentrations before and after the inclusion of this sand parcel. Furthermore, it can be further investigated what dimensions (e.g. depth and surface area) would be ideal for maximizing remediation efficiency of such a parcel.

Unfortunately, the model output of the crops is not very helpful for risk assessment as previously discussed. Alternatively, the bioaccumulation schedule in Fig. 6.1 may be useful as an illustrative tool to easily inform citizens on the relative exposure risk of various homegrown crop categories. The ranking of the vegetable categories in this schedule was largely in agreement with previous studies (Liu et al., 2019; Liu et al., 2023). However, it should be noted that Liu et al. (2019) reported higher PFAS concentrations in shoot vegetables, compared to my thesis results. As discussed in chapter 4, this can be explained by differences in the examined species within this category (e.g. shoot vegetables mainly consisted of rhubarb leaf petioles in the present thesis) and site-specific differences in soil conditions and characteristics. The latter argument is also supported by the finding of Liu et al. (2023) that predictive models for plants could successfully be developed for one agricultural site. On the other hand, the models in my thesis (cf. chapter 4), which were based on multiple sites with probably much higher variability in terms of soil conditions, did perform less well. Moreover, data on edible parts from perennial crops (i.e. fruits and nuts) were not included in those studies (Liu et al., 2019; Liu et al., 2023). Importantly, it should be stressed that this schedule would benefit from inclusion of more data from shoot vegetables, legumes and herbs due to low sample sizes for these categories ($N < 10$).

In addition to the results already mentioned in chapter 2, the effect of egg boiling on PFAS concentrations was tested with small batches of spiked commercial egg samples, which did not show any significant changes in concentrations after boiling (detailed in textbox 6.1 and Fig. 6.1). By contrast, steaming of crops has been shown to reduce concentrations of short-chain PFCAs and increase those of long-chain PFAS, which was possibly due to volatilization loss and precursor degradation, respectively (Liu et al., 2023). This difference could be related with the different matrix composition, as eggs may retain PFAS much stronger due to the strong hydrophobic interactions with lipoproteins (Bangma et al., 2022), which is supported by the finding that crops with higher protein contents showed much lower reduction in PFAS concentrations after steaming (Liu et al., 2023). Clearly, these results show that processing of food can have major implications with respect to human exposure risk. Therefore, it would be useful to further elucidate the potential effect of other processing methods (e.g. frying, grilling) in the future.

Textbox 6.1:

The effect of egg boiling on the concentrations of 12 PFAAs in eggs was tested (see Fig 6.1.) a set of six aliquots (0.3 g) from a commercial egg, which were spiked with 10 ng of a 1:1 mixture of STD:ISTD, after which three were boiled for 5 min. No significant differences were observed between the raw and boiled treatment (Fig. 6.1, $P > 0.05$, two-sample t-test).

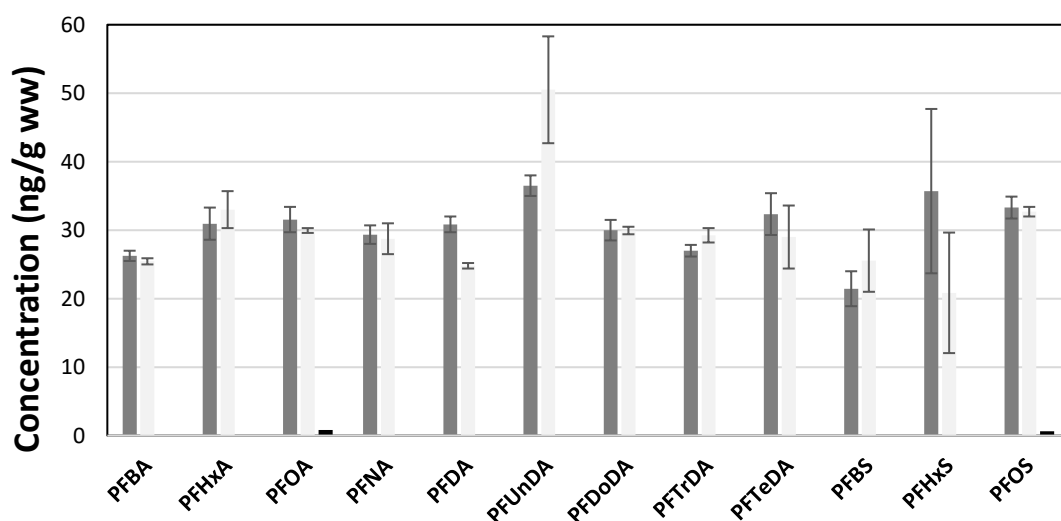


Fig. 6.1: Mean concentrations (in ng/g wet weight) of raw (dark gray) and boiled (light gray) whole egg aliquots which were spiked with 10 ng of a 1:1 mixture of unlabeled standard mix:labeled internal standard mix. Black bars for PFOA and PFOS represent background concentrations. Error bars represent standard deviations. Sample mass: 0.3 g; $N = 3$.

Finally, it is noteworthy that earthworms were able to accumulate relatively high PFAS concentrations, in particular of PFOS and long-chain PFCAs, which is in agreement with literature reports (Munoz et al., 2020; Rich et al., 2015). Currently, studies on cost-effective and practical ways of soil remediation are receiving increased attention (Shahsavari et al., 2021). In this regard, phytoremediation has been put forward as a potential strategy for remediation of mainly short-chain PFAS from low-contaminated soils (Nassazzi et al., 2023). From this perspective, it might be an interesting new research avenue to evaluate whether earthworms and hyperaccumulating plants (cf., potentially rhubarb, as hypothesized in chapter 4) can both be used in a complementary way to further enhance remediation potential in gardens. Moreover, earthworms can potentially increase the bioavailability of PFAS to plants (Hickman and Reid, 2008), and vice versa (Zhao et al., 2014). Given that contamination profiles considerably differed between vegetable garden soil (e.g. primarily short-chain PFAS) and chicken enclosure soil (e.g. primary long-chain PFAS) as shown in chapter 5, the need for cost-effective and practical remediation approaches in gardens that are inclusive for multiple compounds is strongly needed. This is especially relevant within the local context of the current costly and laborious remediation strategy of private gardens around the 3M fluorochemical plant, as contaminated soil is simply excavated and replaced (ERM, 2022).

6.5 Risk communication and perception

The transfer of scientifically correct communication in a clear way to the broad public and policy makers are key for effective implementation of the previously discussed remediation and mitigation measures. Within my PhD, I had the privilege to get insights in this challenging aspect of science through the personal interactions with the study volunteers during the sampling campaigns, media disseminations and presentations of research results for policy institutes (e.g. OVAM). Moreover, the risk communication survey of the human biomonitoring project found that study participants showed among the highest confidence in scientists as information source (Consortium UAntwerpen et al., 2023). This enabled me as a scientist to increase the impact of my research and to strengthen the scientific knowledge of the broad public, which is especially relevant at a time when disinformation has become widespread (O'Grady and Mangina, 2024).

During my interactions with the study volunteers, it became clear that people tended to focus on the legal debate of the PFAS contamination problem and often narrowed the complexity of this problem down to the production plant of the 3M Company in Zwijndrecht (Antwerp). In this regard,

it was a thankful opportunity for me to broaden their perspective by explaining that local factors (e.g. functional usage and soil properties) in gardens are often more drivers of food contamination than the distance of their garden towards this point source. Bringing these nuances as a scientist required extra time and effort, but led to multiple benefits: volunteers got a more comprehensive understanding of the exposure risk, showed a more constructive attitude towards the (chaotic) public debate about the PFAS contamination crisis in Flanders, and were more engaged in the study outcomes as a trusting relationship could be established with many of the volunteers. This latter one often resulted in more challenging questions from the volunteers, which provided me more insights, fulfilment and motivation to persevere in my PhD trajectory.

From these personal exchanges with the volunteers, it became clear to me that there are large benefits of direct, personal communication for both parties (i.e. study participant and researcher). However, the drawback of this approach included that the reach-out of information was limited. Therefore, I regularly devoted myself to public (online) presentations and media appearances during my PhD to overcome this limitation. In this particular format, I could also make use of visual aids to explain PFAS and the remediation measures in a simplified yet accessible way. I had strongly the impression that this way of scientific communication attracted people that felt otherwise hesitant to ask questions, which again broadened the impact and reach-out of my research. Additionally, these public appearances also (in)directly caught the attention of other scientists which facilitated collaboration, reproducibility, and transparency of study results. In this regard, the PFAS@Home study (Colles et al., 2022) and the human biomonitoring study (Consortium UAntwerpen et al., 2023) are excellent examples as their set-up was facilitated through public communication of my PhD research. Considering these multiple benefits, it is highly recommended to devote time in future study projects for risk communication to enhance the public perception towards science, while science itself can also become more effective and enriched through it.

6.6 General conclusions

Despite the central paradigm that food is the major exposure source of PFAS to humans, very little is known about the distribution and exposure potential of PFAS in homegrown food. Therefore, the main objective of the present thesis project was to assess the accumulation in a large variety of homegrown food categories and the related human exposure risk. Hereby, abiotic and biotic factors

in the private gardens were examined that may affect the bioavailability in the homegrown food. To this end, an extensive network of 135 volunteering gardeners was set-up to collect and analyze the data of these food matrices and factors.

I could show that multiple PFAS are omnipresent in homegrown food and can accumulate to concentrations in the food that frequently exceed available health guidelines, even under modest consumption scenarios and especially with regard to egg intake. Within the crop category, higher accumulation was noticed in annual crops in comparison to perennial crops, potentially linked with differences in terms of life-history strategies between these two plant taxa. Large spatial and temporal differences in soil PFAS profile and concentrations were found within private gardens, suggesting that site-specific characteristics and functional usage play a major role in shaping local PFAS contamination differences. Predictive models could be constructed for some major PFAS in eggs, which show promising potential for applicability in risk assessment by policy makers. Moreover, mitigation and remediation measures could be formulated that should be readily usable for private gardeners to ultimately lower PFAS exposure via homegrown food.

PFAS pollution in gardens within ± 4 km from the fluorochemical plant in Antwerp could be strongly linked with both historical and recent fluorochemical emissions. On the other hand, diffusive mechanisms (e.g. atmospheric transport) and site-specific soil management may be mainly affecting levels at gardens further away from point sources. The accumulation in chicken eggs was generally higher closer to the major fluorochemical plant, although soil characteristics (e.g. SOM, clay content and pH) could strongly affect this pattern. Conversely, the PFAS accumulation in the crops was not affected by the distance from the plant site and soil characteristics played only a minor role in governing crop accumulation. Long-term declining concentrations in soil and eggs could be observed for PFOS and PFOA, although this trend stagnated over recent years and was less manifested for PFOA. Short-term increases of short-chain and long-chain PFAS concentrations could be observed, mainly in the soil from the chicken enclosure, requiring further regulation steps and monitoring efforts.

Bibliography

3M Company (2000). Phase-out plan for POSF-based products. US EPA Administrative Record AR226 – 0600. <https://www.regulations.gov/document?D=EPA-HQ-OPPT-2002-0051-0006>. Accessed 13th of June 2021.

3M Company (2021). Milieuverklaring 2020. 3M Zwijndrecht productiesite. <https://omgeving.vlaanderen.be/sites/default/files/2021-11/3M%20Milieuverklaring%202020%20Zwijndrecht.pdf>. Accessed 11th of December 2023.

Adu, O., Ma, X. & Sharma, V. K. (2023). Bioavailability, phytotoxicity and plant uptake of per- and polyfluoroalkyl substances (PFAS): A review. *Journ. Haz. Mat.* 447: 130805-130815.

Ahrens, L. & Bundschuh, M. (2014). Fate and effects of poly- and perfluoroalkyl substances in the aquatic environment: A review. *Env. Tox. Chem.* 33: 1921-1929.

Akihiko, I. & Wagai, R. (2017). Global distribution of clay-size minerals on land surface for biogeochemical and climatological studies. *Sci. Data.* 4: 170103-170113.

Akinwande, M. O., Dikko, H. G. & Samson, A. (2015). Variance Inflation Factor: As a Condition for the Inclusion of Suppressor Variable(s) in Regression Analysis. *Open Journ. Stat.* 5: 754-767.

Ali, A. B. A., Campbell, D. L. M. & Siegford, J. M. (2020). A risk assessment of health, production, and resource occupancy for 4 laying hen strains across the lay cycle in a commercial-style aviary system. *Poultry Sci.* 99: 4672-4684.

Ames, G. K. (2006). Growing Blackberries in Missouri. Bulletin No. 39. Missouri State University: pp 1-28. <https://ag.missouristate.edu/MtnGrv/Files/B39GrowingBlackberriesinMissouri.pdf>. Accessed 18th of September 2023.

ATSDR (2021). Toxicological profile for perfluoroalkyls. <https://www.atsdr.cdc.gov/toxprofiles/tp200.pdf>. Accessed 11th of December 2023.

Aubert, S. & Schwitzguébel, J. (2004). Screening of plant species for the phytotreatment of wastewater containing sulphonated anthraquinones. *Wat. Res.* 38: 3569-3575.

Bangma, J., Guillette, T. C., Bommarito, P. A., Ng, C., Reiner, J. L., et al. (2022). Understanding the dynamics of physiological changes, protein expression, and PFAS in wildlife. *Env. Int.* 159: 107037-107048.

Bar-On, Y. M., Phillips, R. & Milo, R. (2018). The biomass distribution on Earth. *Proc. Nat. Acad. Sci.* 115: 6506-6511.

Bastow, T. P., Douglas, G. B. & Davis, G. B. (2022). Volatilization Potential of Per- and Poly-fluoroalkyl Substances from Airfield Pavements and during Recycling of Asphalt. *Env. Tox. Chem.* 41: 2202-2208.

Bedano, J. C., Domínguez, A., Arolfo, R. & Wall, L. G. (2016). Effect of Good Agricultural Practices under no-till on litter and soil invertebrates in areas with different soil types. *Soil Till. Res.* 158: 100-109.

Bester, P. K., Lobnik, F., Erzen, I., Kastelec, D. & Zupan, M. (2013). Prediction of cadmium concentration in selected home-produced vegetables. *Ecotox. Env. Saf.* 96: 182-190.

Bil, W., Zeilmaker, M., Fragki, S., Lijzen, J., Verbruggen, E., et al. (2020). Risk Assessment of Per- and Polyfluoroalkyl Substance Mixtures: A Relative Potency Factor Approach. *Env. Tox. Chem.* 40: 859-870.

Blaine, A. C., Rich, C. D., Sedlacko, E. M., Hyland, K. C., Stushnoff, C., et al. (2014). Perfluoroalkyl acid uptake in lettuce (*Lactuca sativa*) and strawberry (*Fragaria ananassa*) irrigated with reclaimed water. *Env. Sci. Techn.* 48: 14361-14368.

Borzenkova, I., Zorita, E., Borisova, O., Kalnina, L., Kisieliene, D., et al. (2015). Chapter: Climate Change During the Holocene (Past 12,000 Years). *Sec. Assess. Clim. Change Balt. Sea Bas.* pp. 25-49. Springer, New York: USA.

Boshoff, M., De Jonge, M., Scheifler, R. & Bervoets, L. (2014). Predicting As, Cd, Cu, Pb and Zn levels in grasses (*Agrostis* sp. and *Poa* sp.) and stinging nettle (*Urtica dioica*) applying soil–plant transfer models. *Sci. Tot. Env.* 493: 862-871.

Brendel, S., Fetter, É., Staude, C., Vierke, L. & Biegel-Engler, A. (2018). Short-chain perfluoroalkyl acids: environmental concerns and a regulatory strategy under REACH. *Env. Sci. Eur.* 30: 9-19.

Briels, N., Ciesielski, T. M., Herzke, D. & Jaspers, V. L. B. (2018). Developmental toxicity of perfluorooctanesulfonate (PFOS) and its chlorinated polyfluoroalkyl ether sulfonate alternative F-53B in the domestic chicken. *Env. Sci. Techn.* 52: 12859-12867.

Brown, J. B., Conder, J. M., Arblaster, J. A. & Higgins, C. P. (2020). Assessing Human Health Risks from Per- and Polyfluoroalkyl Substance (PFAS)-Impacted Vegetable Consumption: A Tiered Modeling Approach. *Env. Sci. Techn.* 54: 15202-15214.

Brunn, H., Arnold, G., Körner, W., Rippen, G., Steinhäuser, K. G., et al. (2023). PFAS: forever chemicals—persistent, bioaccumulative and mobile. Reviewing the status and the need for their phase out and remediation of contaminated sites. *Env. Sci. Eur.* 35: 20-69.

Brusseau, M. L., Anderson, R. H. & Guo, B. (2020). PFAS Concentrations in Soils: Background levels versus Contaminated Sites. *Sci. Tot. Env.* 740: 140017-140024.

Buck, R. C., Franklin, J., Berger, U., Conder, J. M., Cousins, I. T., et al. (2011). Perfluoroalkyl and polyfluoroalkyl substances in the environment: terminology, classification, and origins. *Integr. Env. Assess. Manag.* 7: 513-541.

Buck, R. C., Korzeniowski, S. H., Laganis, E. & Adamsky, F. (2021). Identification and classification of commercially relevant per- and poly-fluoroalkyl substances (PFAS). *Integr. Env. Assess. Manag.* 17: 1045-1055.

Buekers, J., Verheyen, V., Remy, S., Covaci, A., Colles, A., et al. (2021). Combined chemical exposure using exposure loads on human biomonitoring data of the 4th Flemish Environment and Health Study (FLEHS-4). *Int. Journ. Hyg. Env. Health.* 238: 113849-113859.

Bustnes, J. O., Bårdsen, B. J., Herzke, D., Bangjord, G., Bourgeon, S., et al. (2022). Temporal trends of organochlorine and perfluorinated contaminants in a terrestrial raptor in Northern Europe over 34 years (1986-2019). *Env. Tox. Chem.* 41: 1508-1519.

Buytaert, J., Eens, M., Elgawad, H. A., Bervoets, L., Beemster, G., et al. (2023). Associations between PFAS concentrations and the oxidative status in a free-living songbird (*Parus major*) near a fluorochemical facility. *Env. Poll.* 335: 122304.

Byns, C., Teunen, L., Groffen, T., Lasters, R. & Bervoets, L. (2022). Bioaccumulation and trophic transfer of perfluorinated alkyl substances (PFAS) in marine biota from the Belgian North Sea: Distribution and human health risk implications. *Env. Poll.* 311: 119907-119918.

Cai, W., Navarro, D. A., Du, J., Srivastava, P., Cao, Z., et al. (2023). Effect of heavy metal co-contaminants on the sorption of thirteen anionic per- and poly-fluoroalkyl substances (PFAS) in soils. *Sci. Tot. Env.* 905: 167188-167196.

Cai, W., Navarro, D. A., Du, J., Ying, G., Yang, B., et al. (2022). Increasing ionic strength and valency of cations enhance sorption through hydrophobic interactions of PFAS with soil surfaces. *Sci. Tot. Env.* 817: 152975-152982.

Campos-Pereira, H., Kleja, D. B., Sjostedt, C., Ahrens, L., Klysubun, W., et al. (2020). The adsorption of per- and polyfluoroalkyl Substances (PFASs) onto ferrihydrite is governed by surface charge. *Env. Sci. Techn.* 54: 15722-15730.

Capoccia, S., Masters, M. & Risser, S. (2018). Urban Chickens as a Pathway for Human Illness: An Examination of Knowledge, Behavior and Risk. *Urb. Sci.* 2: 25-37.

Carslaw, D. C. (2019). The openair manual – open-source tools for analysing air pollution data. Manual for version 2.6-6, University of York.

Carslaw, D. C. & Ropkins, K. (2012). *Openair* – An R package for air quality data analysis. *Env. Mod. Soft.* 28: 52-61.

Chen, D., Zhao, Y., Xu, W., Pan, Y., Wei, Q., et al. (2020). Biotransformation and tissue bioaccumulation of 8:2 fluorotelomer alcohol in broiler by oral exposure. *Env. Poll.* 267: 115611-115621.

Chen, H., Yao, Y., Zhao, Z., Wang, Y., Wang, Q., et al. (2018). Multimedia Distribution and Transfer of Per- and Polyfluoroalkyl Substances (PFASs) Surrounding Two Fluorochemical Manufacturing Facilities in Fuxin, China. *Env. Sci. Techn.* 52: 8263-8271.

Christiansen, J. S., Thorup-Kristensen, K. & Kristensen, H. L. (2006). Root development of beetroot, sweet corn and celeriac, and soil N content after incorporation of green manure. *Journ. Hortic. Sci. Biotechn.* 81: 831-838.

Chu, S., Letcher, R. J., McGoldrick, D. J. & Backus, S. M. (2016). A New Fluorinated Surfactant Contaminant in Biota: Perfluorobutane Sulfonamide in Several Fish Species. *Env. Sci. Techn.* 50: 669-675.

Chung, E. L. T., Nayan, N., Kamalludin, M. H., Alghirani, M. M., Jesse, F. E. A., et al. (2020). The effects of alkaline water and rainwater on the production and health performance of commercial broilers under tropical conditions. *Thai Journ. Vet. Med.* 50: 65-73.

Church, A., Mitchell, R., Ravenscroft, N. & Stapleton, L. M. (2015). 'Growing your own': A multi-level modelling approach to understanding personal food growing trends and motivations in Europe. *Ecol. Econ.* 110: 71-80.

City of Antwerp. (2021). Bodemonderzoek Volkstuinen 2021. Available from: <https://www.antwerpen.be/info/onderzoeken-pfas-pfos>. Accessed 20th of May 2023.

Clark, M. S., Gage, S. H., Delind, L. B. & Lenington, M. (1995). The compatibility of domestic birds with a nonchemical agroecosystem. *Journ. Altern. Agric.* 10: 114-121.

Colin, G. S., Butler, L. D. & Kidd, M. T. (2020). Chapter 20 - Reproductive management of poultry. *Animal Agriculture*. Academic Press, Massachusetts: USA. pp. 349-366.

Colles, A., Bierkens, J., Jacobs, G., Govarts, E., Van Holderbeke, M., et al. (2022). Per- en polyfluoralkylstoffen in en rond de woning. Verantwoordelijke uitgever Departement Omgeving, Vlaams Planbureau voor Omgeving, versie november 2022, studie in opdracht van Departement Omgeving en OVAM.

Colles, A., Bruckers, L., Den Hond, E., Govarts, E., Morrens, B., et al. (2020). Perfluorinated substances in the Flemish population (Belgium): Levels and determinants of variability in exposure. *Chemosphere*. 242: 125250-125260.

Consortium UAntwerpen, VITO, PIH, UHasselt & VUB. (2023). Jongerenstudie HBM - omgeving 3M – Resultatenrapport, in opdracht van het Departement Omgeving, Vlaams Planbureau voor Omgeving, 219p.

Cornelis, C., D'Hollander, W., Roosens, L., Covaci, A., Smolders, R., et al. (2012). First assessment of population exposure to perfluorinated compounds in Flanders, Belgium. *Chemosphere*. 86: 308-314.

Costantini, E. A. C., Branquinho, C., Nunes, A., Schwilch, G., Stavi, I., et al. (2016). Soil indicators to assess the effectiveness of restoration strategies in dryland ecosystems. *Sol. Earth*. 7: 397-414.

Costello, M. C. S. & Lee, L. S. (2020). Sources, fate, and plant uptake in agricultural systems of per- and polyfluoroalkyl substances. *Curr. Poll. Rep.* 9: 1-21.

Cousins, I. T., DeWitt, J. C., Glüge, J., Goldenman, G., Herzke, D., et al. (2020). Strategies for grouping per- and polyfluoroalkyl substances (PFAS) to protect human and environmental health. *Env. Sci: Proc. Imp.* 22: 1444-1460.

Cousins, I. T., Goldenman, G., Herzke, D., Lohmann, R., Miller, M., et al. (2019). The concept of essential use for determining when uses of PFASs can be phased out. *Env. Sci.: Proc. Imp.* 21: 1803-1815.

Cousins, I. T., Johansson, J. H., Salter, M. E., Sha, B. & Scheringer, M. (2022). Outside the Safe Operating Space of a New Planetary Boundary for Per- and Polyfluoroalkyl Substances (PFAS). *Env. Sci. Techn.* 56: 11172-11179.

D'Hollander, W., de Bruyn, L., Hagenaaers, A., de Voogt, P. & Bervoets, L. (2014). Characterisation of perfluorooctane sulfonate (PFOS) in a terrestrial ecosystem near a fluorochemical plant in Flanders, Belgium. *Env. Sci. Poll. Res.* 21: 11856-11866.

D'Hollander, W., de Voogt, P. & Bervoets, L. (2011). Accumulation of perfluorinated chemicals in Belgian home-produced chicken eggs. *Org. Comp.* 73: 917-920.

D'Hollander, W., Herzke, D., Huber, S., Hajslova, J., Pulkrabova, J., et al. (2015). Occurrence of perfluorinated alkylated substances in cereals, salt, sweets and fruit items collected in four European countries. *Chemosphere*, 129: 179-185.

Darimont, C. T., Fox, C. H., Bryan, H. M. & Reimchen, T. E. (2015). The unique ecology of human predators. *Science*. 349: 858-860.

Dauwe, T., Van de Vijver, K., De Coen, W. & Eens, M. (2007). PFOS levels in the blood and liver of a small insectivorous songbird near a fluorochemical plant. *Env. Int.* 33: 357-361.

De Hoge gezondheidsraad (2003). Food recommendations for Belgium. Revised version 2030 (brochure). Ministry of social affairs, public health and environment, Brussel. Last consulted at 22/06/2021 on www.health.fgov.be.

De Ridder, K., Lebacqz, T., Ost, C., Teppers, E. & Brocatus, L. (2016). Rapport 4: De consumptie van voedingsmiddelen en de inname van voedingsstoffen. Voedselconsumptiepeiling 2014-2015. In: Teppers E., Tafforeau J. (ed.).

De Silva, A. O., Armitage, J. M., Bruton, T. A., Dassuncao, C., Heiger-Bernays, W. (2021). PFAS Exposure Pathways for Humans and Wildlife: A Synthesis of Current Knowledge and Key Gaps in Understanding. *Env. Tox. Chem.* 40: 631-657.

De Solla, S. R., de Silva, A. O. & Letcher, R. J. (2012). Highly elevated levels of perfluorooctane sulfonate and other perfluorinated acids found in biota and surface water downstream of an international airport, Hamilton, Ontario, Canada. *Env. Int.* 39: 19–26.

Death, C., Bell, C., Champness, D., Milne, C., Reichman, S., et al. (2021). Per- and polyfluoroalkyl substances (PFAS) in livestock and game species: A review. *Sci. Tot. Env.* 774: 144795-144806.

Delannoy, M., Fournier, A., Dan-Badjo, A. T., Schwarz, J., Lerch, S., et al. (2015). Impact of soil characteristics on relative bioavailability of NDL-PCBs in piglets. *Chemosphere.* 139: 393-401.

Department Environment & Health. (2022a). Case: monitoring PFAS schouwemissies uit draaitrommeloven (DTO2) van Indaver NV. Rapport LUCHT. pp. 1-16.

Department Environment & Health. (2022b). PFAS in Flanders: reports of the PFAS Commissioner. Available from: <https://www.vlaanderen.be/en/pfas-in-flanders>. Accessed 20th of May 2023.

Dewapriya, P., Nilsson, S., Gorji, S. G., O'Brien, J. W., Bräunig, J., et al. (2023). Novel Per- and Polyfluoroalkyl Substances Discovered in Cattle Exposed to AFFF-Impacted Groundwater. *Env. Sci. Techn.* 57: 13635-13645.

Dhore, R. & Murthy G. S. (2021). Per/polyfluoroalkyl substances production, applications and environmental impacts. *Bior. Techn.* 341: 125808-125817.

Ding, G. & Peijnenburg, W. (2013). Physicochemical Properties and Aquatic Toxicity of Poly- and Perfluorinated Compounds. *Crit. Rev. Env. Sci. Techn.* 43: 598-678.

Douay, F., Pelfrêne, A., Planque, J., Fourrier, H., Richard, A., et al. (2013). Assessment of potential health risk for inhabitants living near a former lead smelter. Part 1: metal concentrations in soils, agricultural crops, and homegrown vegetables. *Env. Mon. Assess.* 185: 3665-3680.

Dragovic, S., Spalevic, V., Radojevic, V., Cicmil, M., Uscumlic, M., et al. (2012). Importance of chemical and microbiological water quality for irrigation in organic food production. *Agric. For.* 55: 83-102.

Ducatman, A., LaPier, J., Fuoco, F. & DeWitt, J. C. (2022). Official health communications are failing PFAS-contaminated communities. *Env. Health.* 21: 51-69.

EC (2022). Amending Regulation (EC) No 1881/2006 as regards maximum levels of perfluoroalkyl substances in certain foodstuffs. Official Journ. of the EU. <https://eur-lex.europa.eu/legal-content/EN/TXT/PDF/?uri=CELEX:32022R2388>. Accessed 5th of October 2023.

EFSA (2020). Risk to human health related to the presence of perfluoroalkyl substances in food. EFSA Journ. 18: 1-391.

Egerer, M. H., Philpott, S. M., Liere, H., Jha, S., Bichler, P., et al. (2017). People or place? Neighborhood opportunity influences community garden soil properties and soil-based ecosystem services. Int. Journ. Biod. Sci., Ecos. Serv. Manag. 14: 32-44.

Ellis, G. (2012). Chapter 13 – Model Development and Verification. Contr. Syst. Des. Guide (4th edition). pp. 261-282. Elsevier: The Netherlands.

Eriksson, U., Roos, A., Lind, Y., Hope, K., Ekblad, A., et al. (2016). Comparison of PFASs contamination in the freshwater and terrestrial environments by analysis of eggs from osprey (*Pandion haliaetus*), tawny owl (*Strix aluco*), and common kestrel (*Falco tinnunculus*). Env. Res. 149: 40-47.

ERM (2022). Eerste gefaseerd bodemsaneringsproject. <https://multimedia.3m.com/mws/media/22295330/rap-by-erm-for-zone-1a-report-2022.pdf>. Accessed 15th of December 2023.

EU. (2022). Commission recommendation of 24 August 2022 on the monitoring of perfluoroalkyl substances in food. Off. Journ. Eur. Un. 221/105.

European Chemicals Agency. (2023). ECHA publishes PFAS restriction proposal. Available from: <https://echa.europa.eu/-/echa-publishes-pfas-restriction-proposal>. Accessed 25th of April 2023.

Fan, J., McConkey, B., Wang, H. & Janzen, H. (2016). Root distribution by depth for temperate agricultural crops. Field Crops Res. 189: 68-74.

Fedorenko, M., Alesio, J., Fedorenko, A., Slitt, A. & Bothun, G. D. (2021). Dominant entropic binding of perfluoroalkyl substances (PFASs) to albumin protein revealed by ¹⁹F NMR. Chemosphere. 263: 1-9.

Felizeter, S., Jüring, H., Kotthoff, M., De Voogt, P. & McLachlan, M. S. (2021). Uptake of perfluorinated alkyl acids by crops: results from a field study. *Env. Sci: Proc. Imp.* 23: 1158-1170.

Felizeter, S., McLachlan, M. S. & De Voogt, P. (2014). Root uptake and translocation of perfluorinated alkyl acids by three hydroponically grown crops. *Journ. Agric. Food Chem.* 15: 3334-3342.

Felizeter, S., Jüring, H., Kotthoff, M., De Voogt, P. & McLachlan, M. S. (2020). Influence of soil on the uptake of perfluoroalkyl acids by lettuce: A comparison between a hydroponic study and a field study. *Chemosphere.* 260: 127608-127615.

Fenton, S. E., Ducatman, A., Boobis, A., DeWitt, J. C., Lau, C., et al. (2021). Per- and Polyfluoroalkyl Substance Toxicity and Human Health Review: Current State of Knowledge and Strategies for Informing Future Research. *Env. Tox. Chem.* 40: 606-630.

Ferreira, V. H. B., Simoni, A., Germain, K., Letierrier, C., Lansade, L., et al. (2022). Foraging Behavior Shows Individual-Consistency Over Time, and Predicts Range Use in Slow-Growing Free-Range Male Broiler Chickens. *Front. Vet. Sci.* 7: 1-12.

Flemish Environment Agency. (2022a). Databank PFAS explorer. Available from: <https://www.dov.vlaanderen.be/portaal/?module=pfasverkenner>. Accessed 20th of May 2023.

Flemish Environment Agency (2022b). Meteorological measurements wind direction, wind speed and precipitation. Available from: <https://www.waterinfo.be/Meetreeksen>. Accessed 29th of March 2023.

Fort, F, Volaire, F, Guilioni, L, Barkaoui, K., Navas, M., et al. (2017). Root traits are related to plant water-use among rangeland Mediterranean species. *Func. Ecol.* 31: 1700-1709.

Gaber, N., Bero, L. & Woodruff, T. J. (2023). The Devil they Knew: Chemical Documents Analysis of Industry Influence on PFAS Science. *Ann. Glob. Health.* 37: 1-17.

Gaines, L. G. T. (2022). Historical and current usage of per- and polyfluoroalkyl substances (PFAS): A literature review. *Amer. Journ. Ind. Med.* 66: 353-378.

Galhena, D. H., Freed, R. & Maredia, K. M. (2013). Home gardens: a promising approach to enhance household food security and wellbeing. *Agric. Food Sec.* 2: 8-21.

Galloway, J. E., Moreno, A. V. P., Lindstrom, A. B., Strynar, M. J., Newton, S., et al. (2020). Evidence of Air Dispersion: HFPO–DA and PFOA in Ohio and West Virginia Surface Water and Soil near a Fluoropolymer Production Facility. *Env. Sci. Techn.* 54: 7175-7184.

Gan, C., Peng, M., Liu, H. & Yang, J. (2022). Concentration and distribution of metals, total fluorine, per- and poly-fluoroalkyl substances (PFAS) in vertical soil profiles in industrialized areas. *Chemosphere.* 302: 134855-134864.

Gazzotti, T., Sirri, F., Ghelli, E., Zironi, E., Zampiga, M., et al. (2021). Perfluoroalkyl contaminants in eggs from backyard chickens reared in Italy. *Food Chem.* 362: 130178-130207.

Gebbink, W. A., Ullah, S., Sandblom, O. & Berger, U. (2013). Polyfluoroalkyl phosphate esters and perfluoroalkyl carboxylic acids in target food samples and packaging—method development and screening. *Env. Sci. Poll. Res.* 20: 7949-7958.

Gerardu, T., Dijkstra, J., Beeltje, H., van Duivenbode, A. V. R. & Griffioen, J. (2023). Accumulation and transport of atmospherically deposited PFOA and PFOS in undisturbed soils downwind from a fluoropolymers factory. *Env. Adv.* 11: 100332-100342.

Ghisi, R., Vamerali, T. & Manzetti, S. (2019). Accumulation of perfluorinated alkyl substances (PFAS) in agricultural plants: A review. *Env. Res.* 169: 326-341.

Giesy, J. P. & Kannan, K. (2001). Global Distribution of Perfluorooctane Sulfonate in Wildlife. *Env. Sci. Techn.* 35: 1339-1342.

Giesy, J.P. & Kannan, K. (2002). Perfluorochemical surfactants in the environment: These bioaccumulative compounds occur globally, warranting further study. *Env. Sci. Techn.* 36: 146A-152A.

Glüge, J., Scheringer, M., Cousins, I. T., DeWitt, J. C., Goldenman, G., et al. (2020). An overview of the uses of per- and polyfluoroalkyl substances (PFAS). *Env. Sci.: Proc. Imp.* 22: 2345-2373.

Gobelius, L., Lewis, J. & Ahrens, L. (2017). Plant Uptake of Per- and Polyfluoroalkyl Substances at a Contaminated Fire Training Facility to Evaluate the Phytoremediation Potential of Various Plant Species. *Env. Sci. Techn.* 51: 12602-12610.

Goodrum, P. E., Anderson, J. K., Luz, A. L. & Ansell, G. K. (2020). Application of a Framework for Grouping and Mixtures Toxicity Assessment of PFAS: A Closer Examination of Dose-Additivity Approaches. *Tox. Sci.* 179: 262-278.

Goss, K. (2008). The pKa Values of PFOA and Other Highly Fluorinated Carboxylic Acids. *Env. Sci. Techn.* 42: 456-458.

Grandjean, P., Timmermann, C. A. G. T., Kruse, M., Nielsen, F., Vinholt, P. J., et al. (2020). Severity of COVID-19 at elevated exposure to perfluorinated alkylates. *PLoS ONE*. 15: 1-12.

Grgas, D., Petrina, A., Stefanac, T., Beslo, D. & Dragicevic, T. L. (2023). A Review: Per- and Polyfluoroalkyl Substances—Biological Degradation. *Toxics*. 11: 446-463.

Groffen, T., Bervoets, L. & Eens, M. (2023b). Temporal trends in PFAS concentrations in livers of a terrestrial raptor (common buzzard; *Buteo buteo*) collected in Belgium during the period 2000-2005 and in 2021. *Env. Res.* 216: 114644-114650.

Groffen, T., Bervoets, L., Jeong, Y., Willems, T., Eens, M., et al. (2021). A rapid method for the detection and quantification of legacy and emerging per- and polyfluoroalkyl substances (PFAS) in bird feathers using UPLC-MS/MS. *Journ. Chrom. B*. 1172: 122653-122659.

Groffen, T., Eens, M. & Bervoets, L. (2019b). Do concentrations of perfluoroalkylated acids (PFAAs) in isopods reflect concentrations in soil and songbirds? A study using a distance gradient from a fluorochemical plant. *Sci. Tot. Env.* 657: 111-123.

Groffen, T., Lasters, R., Bervoets, L., Prinsen, E. & Eens, M. (2020). Are Feathers of a Songbird Model Species (The Great Tit, *Parus major*) Suitable for Monitoring Perfluoroalkyl Acids (PFAAs) in Blood Plasma. *Env. Sci. Techn.* 54: 9334-9344.

Groffen, T., Lasters, R., Lemière, F., Willems, T., Eens, M., et al. (2019c). Development and validation of an extraction method for the analysis of perfluoroalkyl substances (PFASs) in environmental and biotic matrices. *Journ. Chrom. B.* 1116: 30-37.

Groffen, T., Lasters, R., Lopez-Antia, A., Prinsen, E., Bervoets, L., et al. (2019a). Limited reproductive impairment in a passerine bird species exposed along a perfluoroalkyl acid (PFAA) pollution gradient. *Sci. Tot. Env.* 652: 718-728.

Groffen, T., Lopez-Antia, A., D'Hollander, W., Prinsen, E., Eens, M., et al. (2017). Perfluoroalkylated acids in the eggs of great tits (*Parus major*) near a fluorochemical plant in Flanders, Belgium. *Env. Poll.* 228: 140-148.

Groffen, T., Prinsen, E., Stoffels, O. D., Maas, L., Vincke, P., et al. (2023a). PFAS accumulation in several terrestrial plant and invertebrate species reveals species-specific differences. *Env. Sci. Poll. Res.* 30: 23820-23835.

Groffen, T., Rijnders, J., Verbrigghe, N., Verbruggen, E., Prinsen, E., et al. (2019d). Influence of soil physicochemical properties on the depth profiles of perfluoroalkylated acids (PFAAs) in soil along a distance gradient from a fluorochemical plant and association with soil microbial parameters. *Chemosphere.* 236: 124407-124417.

Gustafsson, A., Bergman, A. & Weiss, J. M. (2022). Estimated daily intake of per- and polyfluoroalkyl substances related to different particle size fractions of house dust. *Chemosphere* 303: 135061-135069.

Harding-Marjanovic, K. C., Houtz, E. F., Yi, S., Field, J. A., Sedlak, D. L, et al. (2015). Aerobic Biotransformation of Fluorotelomer Thioether Amido Sulfonate (Lodyne™) in AFFF-Amended Microcosms. *Env. Sci. Techn.* 49: 7666-7674.

He, Q., Yan, Z., Qian, S., Xiong, T., Grieger, K. D., et al. (2023). Phytoextraction of per- and polyfluoroalkyl substances (PFAS) by weeds: Effect of PFAS physicochemical properties and plant physiological traits. *Journ. Haz. Mat.* 454: 131492-131501.

Heiri, O., Lotter, A. & Lemcke, G. (2001). Loss on Ignition as a Method for Estimating Organic and Carbonate Content in Sediments: Reproducibility and Comparability of Results. *Journ Paleol.* 25: 101-110.

Hekster, F. M., De Voogt, P., Pijnenburg, A. M. C. M. & Laane, R. W. P. M. (2002). Perfluoroalkylated substances. Aquatic environmental assessment. RIKZ rapport nr.2000.043.

Hellsing, M. S., Josefsson, S., Hughes, A. V. & Ahrens, L. (2016). Sorption of perfluoroalkyl substances to two types of minerals. *Chemosphere.* 159: 385-391.

Henry, B. J., Carlin, J. P., Hammerschmidt, J. A., Buck, R. C., Buxton, L. W., et al. (2018). A critical review of the application of polymer of low concern and regulatory criteria to fluoropolymers. *Integr. Env. Assess. Manag.* 14: 316-334.

Henry, R., Norris, G. A., Vedantham, R. & Turner, J. R. (2009). Source Region Identification Using Kernel Smoothing. *Env. Sci. Techn.* 43: 4090-4097.

Herzke, D., Huber, S., Bervoets, L., D'Hollander, W., Hajslova, J., et al. (2013). Perfluorinated alkylated substances in vegetables collected in four European countries; occurrence and human exposure estimations. *Env. Sci. Poll. Res.* 20: 7930-7939.

Hickman, Z. A. & Reid, B. J. (2008). Earthworm assisted bioremediation of organic contaminants. *Env. Int.* 34: 1072-1081.

Hoff, P. T., Van Campenhout, K., Van de Vijver, K., Covaci, A., Bervoets, L., et al. (2005). Perfluorooctane sulfonic acid and organohalogen pollutants in liver of three freshwater fish species in Flanders (Belgium): relationships with biochemical and organismal effects. *Env. Poll.* 137: 324-333.

Holmström, K. E. & Berger, U. (2008) Tissue Distribution of Perfluorinated Surfactants in Common Guillemot (*Uria aalge*) from the Baltic Sea. *Env. Sci. Techn.* 42: 5879-5884.

Hopcroft, P. O., Valdes, P. J., Shuman, B. N., Toohey, M. & Sigl, M. (2023). Relative importance of forcings and feedbacks in the Holocene temperature conundrum. *Quat. Sci. Rev.* 108322-108335.

Houba, V. J. G., van der Lee, J. J., Novazamsky, I. & Waling, I. (1989). *Soil and plant analysis, part 5*. Wageningen Agricultural University, Wageningen.

Howard, B. R. (1975). Water Balance of the Hen During Egg Formation. *Poultry Sci.* 54: 1046-1053.

Illieva, R. T., Cohen, N., Israel, M., Specht, K., Fox-Kämper, R., et al. (2022). The Socio-Cultural Benefits of Urban Agriculture: A Review of the literature. *Land.* 11: 622-643.

ITRC (Interstate Technology & Regulatory Council). (2023). *PFAS Technical and Regulatory Guidance Document and Fact Sheets PFAS-1*. Washington, D.C.: Interstate Technology & Regulatory Council, PFAS Team.

Jaspers, V. L. B., Covaci, A., Deleu, P. & Eens, M. (2009). Concentrations in bird feathers reflect regional contamination with organic pollutants. *Sci. Tot. Env.* 407: 1447-1451.

Jeddi, M. Z., Hopf, N. B., Louro, H., Viegas, S., Galea, K. S., et al. (2022). Developing human biomonitoring as a 21st century toolbox within the European exposure science strategy 2020–2030. *Env. Int.* 168: 107476-107496.

Jeong, Y., Da Silva, K. M., Iturraspe, E., Fujii, Y., Boogaerts, T., et al. (2022). Occurrence and contamination profile of legacy and emerging per- and polyfluoroalkyl substances (PFAS) in Belgian wastewater using target, suspect and non-target screening approaches. *Journ. Haz. Mat.* 437: 129378-129387.

Jiang J., Liang L., Ma, Q. & Zhao, T. (2021). Kernel Nutrient Composition and Antioxidant Ability of *Corylus* spp. in China. *Front. Plant Sci.* 12: 690966-690978.

Jin, H., Shan, G., Zhu, L., Sun, H. & Luo, Y. (2018). Perfluoroalkyl Acids Including Isomers in Tree Barks from a Chinese Fluorochemical Manufacturing Park: Implication for Airborne Transportation. *Env. Sci. Techn.* 52: 2016-2024.

Johnson, G. R. (2022). PFAS in soil and groundwater following historical land application of biosolids. *Wat. Res.* 211: 118035-118043.

Johnston, R., Jones, K. & Manley, D. (2018). Confounding and collinearity in regression analysis: a cautionary tale and an alternative procedure, illustrated by studies of British voting behaviour. *Qual. Quant.* 52: 1957-1976.

Jouanneau, W., Bårdsen, B., Herzke, D., Johnsen, T. V., Eulaers, I., et al. (2020). Spatiotemporal Analysis of Perfluoroalkyl Substances in White-Tailed Eagle (*Haliaeetus albicilla*) Nestlings from Northern Norway-A Ten-Year Study. *Env. Sci. Techn.* 54: 5011-5020.

Joyner, C. J., Peddie, M. J. & Taylor, T. G. (1987). The effect of age on egg production in the domestic hen. *Gen. Comp. Endocrin.* 65: 331-336.

Jurjanz, S., Germain, K., Juin, H. & Jondreville, C. (2015). Plant and soil intake by organic broilers reared in tree- or grass-covered plots as determined by means of n-alkanes and of acid-insoluble ash. *Animal: Int. Journ. Animal Biosci.* 9: 888-898.

Just, H., Göckener, B., Lämmer, R., Wiedemann-Krantz, L., Stahl, T., et al. (2022). Degradation and Plant Transfer Rates of Seven Fluorotelomer Precursors to Perfluoroalkyl Acids and F-53B in a Soil-Plant System with Maize (*Zea mays* L.). *Journ. Agric. Food Chem.* 70: 8920-8930.

Kafkas, E., Attar, S. H., Gundesli, M. A., Ozcan, A. & Ergun, M. (2020). Phenolic and Fatty Acid Profile, and Protein Content of Different Walnut Cultivars and Genotypes (*Juglans regia* L.) Grown in the USA. *Int. Journ. Fruit Sci.* 20: 1711-1720.

Kijlstra, A. (2004). The role of organic and free range poultry production systems on the dioxin levels in eggs. *Proc. 3rd SAFO works.* pp. 83-90.

Kissa, E. (2001). Fluorinated surfactants and repellents. *Surfactants science series.* vol. 97, pp. 640. CRC Press, New York: USA.

Klenow, S., Heinemeyer, G., Brambilla, G., Dellatte, E., Herzke, D., et al. (2013). Dietary exposure to selected perfluoroalkyl acids (PFAAs) in four European regions. *Food Addi. Cont. A.* 30: 2141-2151.

Knight, E. R., Bräunig, J., Janik, L. J., Navarro, D. A., Kookana, R. S., et al. (2021). An investigation into the long-term binding and uptake of PFOS, PFOA and PFHxS in soil-plant systems. *Journ. Haz. Mat.* 404: 124065-124075.

Kowalczyk, J., Göckener, B., Eichhorn, M., Kotthoff, M., Bücking, M., et al. (2020). Transfer of Per- and Polyfluoroalkyl Substances (PFAS) from Feed into the Eggs of Laying Hens. Part 2: Toxicokinetic Results including the Role of Precursors. *Journ. Agric. Food Chem.* 68: 12539-12548.

Kudryavtseva, A., Shelepchikov, A. & Brodskiy, E. S. (2020). Free-range chicken eggs as a bioindicator of dioxin contamination in Vietnam, including long-term Agent Orange impact. *Emerg. Cont.* 6: 114-123.

Land, M., de Wit, C. A., Bignert, A., Cousins, I. T., Herzke, D., et al. (2018). What is the effect of phasing out long-chain per and polyfluoroalkyl substances on the concentrations of perfluoroalkyl acids and their precursors in the environment? A systematic review. *Env. Evid.* 7: 4-35.

Lang, J. R., Allred, B. M., Field, J. A., Levis, J. W. & Barlaz, M. A. (2017). National estimate of per- and polyfluoroalkyl substance (PFAS) release to US municipal landfill leachate. *Env. Sci. Techn.* 51: 2197-2205.

Lasters, R., Groffen, T., Lopez-Antia, A., Bervoets, L. & Eens, M. (2019). Variation in PFAA concentrations and egg parameters throughout the egg-laying sequence in a free-living songbird (the great tit, *Parus major*): Implications for biomonitoring studies. *Env. Poll.* 246: 237-248.

Lasters, R., Groffen, T., Bervoets, L. & Eens, M. (2021). Perfluoroalkyl acid (PFAA) profile and concentrations in two co-occurring tit species: distinct differences indicate non-generalizable results across passerines. *Sci. Tot. Env.* 761: 143301-143309.

Lasters, R., Groffen, T., Eens, M., Coertjens, D., Gebbink, W. A., et al. (2022). Home-produced eggs: An important human exposure pathway of perfluoroalkylated substances (PFAS). *Chemosphere.* 308: 136283-136294.

Lasters, R., Van Sundert, K., Groffen, T., Buytaert, J., Eens, M., et al. (2023). Prediction of perfluoroalkyl acids (PFAAs) in homegrown eggs: Insights into abiotic and biotic factors affecting bioavailability and derivation of potential remediation measures. *Env. Int.* 181: 108300-108313.

Lau, C., Anitole, K., Hodes, C., Lai, D., Pfahles-Hutchens, A. & Seed, J. (2007). Perfluoroalkyl acids: a review of monitoring and toxicological findings. *Tox. Sci.* 99: 366-394.

Lazcano, R. K., Choi, Y. J., Mashtare, M. L. & Lee, L. S. (2020). Characterizing and Comparing Per- and Polyfluoroalkyl Substances in Commercially Available Biosolid and Organic Non-Biosolid-Based Products. *Env. Sci. Techn.* 54: 8640-8648

Le Monde. (2023). 'Forever pollution': Explore the map of Europe's PFAS contamination. Available from: https://www.lemonde.fr/en/les-decodeurs/article/2023/02/23/forever-pollution-explore-the-map-of-europe-s-pfas-contamination_6016905_8.html. Accessed 1st of June 2023.

Lebacqz, T. (2015). Antropometrics (BMI). Voedselconsumptiepeiling 2014-2015. Report 1: WIV-ISP, Brussel.

Lechner, M. & Knapp, H. (2011). Carryover of Perfluorooctanoic Acid (PFOA) and Perfluorooctane Sulfonate (PFOS) from Soil to Plant and Distribution to the Different Plant Compartments Studied in Cultures of Carrots (*Daucus carota ssp. Sativus*), Potatoes (*Solanum tuberosum*), and Cucumbers (*Cucumis Sativus*). *Journ. Agric. Food Chem.* 59: 11011-11018.

Lerch, M., Fengler, R., Mbog, G., Nguyen, K. H. & Granby, K. (2023). Food simulants and real food – What do we know about the migration of PFAS from paper based food contact materials? *Food Pack. Shelf Life.* 35: 100992-10103.

Letcher, R. J., Bustnes, J. O., Dietz, R., Jenssen, B. M., Jörgensen, E. H., et al. (2010). Exposure and Effects Assessment of Persistent Organohalogen Contaminants in Arctic Wildlife and Fish. *Sci. Tot. Env.* 408: 2995-3043.

Li, F., Fang, X., Zhou, Z., Liao, X., Zou, J., et al. (2018a). Adsorption of perfluorinated acids onto soils: Kinetics, isotherms, and influences of soil properties. *Sci. Tot. Env.* 649: 504-514.

Li, H., Junker, A. L., Wen, J., Ahrens, L., Sillanpää, M., et al. (2023). A recent overview of per- and polyfluoroalkyl substances (PFAS) removal by functional framework materials. *Chem. Eng. Journ.* 452: 139202-139215.

Li, J., He, J., Niu, Z. & Zhang, Y. (2020). Legacy per- and polyfluoroalkyl substances (PFASs) and alternatives (short-chain analogues, F-53B, GenX and FC-98) in residential soils of China: Present implications of replacing legacy PFASs. *Env. Int.* 135: 105419-105426.

Li, P., Oyang, X., Zhao, Y., Tu, T., Tian, X., et al. (2019). Occurrence of perfluorinated compounds in agricultural environment, vegetables, and fruits in regions influenced by a fluorine-chemical industrial park in China. *Chemosphere.* 225: 659-667.

Li, Y., Oliver, D. P. & Kookana, R. S. (2018b). A critical analysis of published data to discern the role of soil and sediment properties in determining sorption of per and polyfluoroalkyl substances (PFASs). *Sci. Tot. Env.* 628: 110-120.

Lilienthal, H., Dieter, H. H., Hölzer, J. & Wilhelm, M. (2017). Recent experimental results of effects of perfluoroalkyl substances in laboratory animals - Relation to current regulations and guidance values. *Int. Journ. Hyg. Env. Health.* 220: 766-775.

Lin, Y., Capozzi, S. L., Lin, L. & Rodenburg, L. A. (2021a). Source apportionment of perfluoroalkyl substances in Great Lakes fish. *Env. Poll.* 290: 118047-118054.

Liu, L., Qu, Y., Huang, J. & Weber, R. (2021a). Per- and polyfluoroalkyl substances (PFASs) in Chinese drinking water: risk assessment and geographical distribution. *Env. Sci. Eur.* 33: 6-17.

Liu, S., Liu, Z., Tan, W., Johnson, A. C., Sweetman, A. J., et al. (2023). Transport and transformation of perfluoroalkyl acids, isomer profiles, novel alternatives and unknown precursors from factories to dinner plates in China: New insights into crop bioaccumulation prediction and risk assessment. *Env. Int.* 172: 107795-107811.

Liu, S., Lu, Y., Xie, S., Wang, T., Jones, K. C., et al. (2015). Exploring the fate, transport and risk of Perfluorooctane Sulfonate (PFOS) in a coastal region of China using a multimedia model. *Env. Int.* 85: 15-26.

Liu, S., Zhao, S., Liang, Z., Wang, F., Sun, F., et al. (2021b). Perfluoroalkyl substances (PFASs) in leachate, fly ash, and bottom ash from waste incineration plants: Implications for the environmental release of PFAS. *Sci. of the Tot. Env.* 795: 148468-148475.

Liu, Y., Qi, F., Fang, C., Naidu, R., Duan, L., Dharmarajan, R., et al. (2020). The effects of soil properties and co-contaminants on sorption of perfluorooctane sulfonate (PFOS) in contrasting soils. *Env. Techn. Innov.* 19: 100965-100977.

Liu, Z., Lu, Y., Song, X., Jones, K., Sweetman, A. J., et al. (2019). Multiple crop bioaccumulation and human exposure of perfluoroalkyl substances around a mega fluorochemical industrial park, China: Implication for planting optimization and food safety. *Env. Int.* 127: 671-684.

Lopez-Antia, A., Groffen, T., Lasters, R., AbdElgawad, H., Sun, J., et al. (2019). Perfluoroalkyl acids (PFAAs) concentrations and oxidative status in two generation of great tits inhabiting a contamination hotspot. *Env. Sci. Techn.* 53: 1617-1626.

Lu, G., Jiao, X., Piao, H., Wang, X., Chen, S., et al. (2018). The extent of the impact of a fluorochemical industrial park in eastern China on adjacent rural areas. *Arch. Env. Cont. Tox.* 74: 484-491.

Lu, M., Cagnetta, G., Zhang, K., Huang, J. & Yu, G. (2017). Mechanochemical mineralization of “very persistent” fluorocarbon surfactants – 6:2 fluorotelomer sulfonate (6:2FTS) as an example. *Sci. Rep.* 7: 17180-17189.

Lundgren, M. R. & Des Marais, D. L. (2020). Life History Variation as a Model for Understanding Trade-Offs in Plant–Environment Interactions. *Curr. Biol.* 30: 180-189.

MacLeod, M., Breitholtz, M., Cousins, I. T., de Wit, C. A., Persson, L. M., et al. (2014). Identifying Chemicals That Are Planetary Boundary Threats. *Env. Sci. Techn.* 48: 11057-11063.

Maffia, J., Aarnink, A. J. A., Ploegaert, J. P. M., Dinuccio, E., Paolo, B., et al. (2021). Assessing particulate matter (PM₁₀) emissions from outdoor runs in laying hen houses by integrating wind tunnel and lab-scale measurements. *Biosci. Eng.* 210: 1-12.

Mahmoudnia, A., Mehrdadi, N., Baghdadi, M. & Moussavi, G. (2022). Change in global PFAS cycling as a response of permafrost degradation to climate change. *Journ. Haz. Mat. Adv.* 5: 100039.

McDonough, A. M., Bird, A. W., Freeman, L. M., Luciani, M. A. & Todd, A. K. (2021). Fate and budget of poly- and perfluoroalkyl substances in three common garden plants after experimental additions with contaminated river water. *Env. Poll.* 285: 117115-117122.

McDowell, W. H. (2003). Dissolved organic matter in soils—future directions and unanswered questions. *Geoderma.* 113: 179-186.

Mei, W., Sun, H., Song, M., Jiang, L., Yongtao, L., et al. (2021). Per- and polyfluoroalkyl substances (PFASs) in the soil-plant system: Sorption, root uptake, and translocation. *Env. Int.* 156: 106642-106650.

Méndez, V., Holland, S., Bhardwaj, S., McDonald, J., Khan, S., et al. (2022). Aerobic biotransformation of 6:2 fluorotelomer sulfonate by *Dietzia aurantiaca* J3 under sulfur-limiting conditions. *Sci. Tot. Env.* 829: 154587-154596.

Meng, L., Lu, Y., Wang, Y., Ma, X., Li, J., et al. (2022). Occurrence, Temporal Variation (2010–2018), Distribution, and Source Appointment of Per- and Polyfluoroalkyl Substances (PFAS) in Mollusks from the Bohai Sea, China. *ACS EST Water.* 2: 195-205.

Mikolajczyk, S., Pajurek, M. & Warenik-Bany, M. (2022). Perfluoroalkyl substances in hen eggs from different types of husbandry. *Chemosphere.* 303: 134950-134955.

Miller, A., Elliott, J. E., Elliott, K. H., Lee, S. & Cyr, F. (2015). Temporal trends of perfluoroalkyl substances (PFAS) in eggs of coastal and offshore birds: Increasing PFAS levels associated with offshore bird species breeding on the Pacific coast of Canada and wintering near Asia. *Env. Tox. Chem.* 34: 1799-1808.

Miller, M. E., Hamann, M. & Kroon, F. J. (2020). Bioaccumulation and biomagnification of microplastics in marine organisms: A review and meta-analysis of current data. *PLoS ONE.* 15: 1-25.

Millinovic, J., Lacorte, S., Vidal, M. & Rigol, A. (2015). Sorption behavior of perfluoroalkyl substances in soils. *Sci. Tot. Env.* 511: 63-71.

Minoli, S., Jägermeyr, J., Assend, S., Urfels, A. & Müller, C. (2022). Global crop yields can be lifted by timely adaptation of growing periods to climate change. *Nat. Comm.* 13: 7079-7088.

Munoz, G., Desrosiers, M., Vetter, L., Vo Duy, S., Jarjour, J., et al. (2020). Bioaccumulation of Zwitterionic Polyfluoroalkyl Substances in Earthworms Exposed to Aqueous Film-Forming Foam Impacted Soils. *Env. Sci. Techn.* 54: 1687-1697.

Munoz, G., Liu, J., Duy, S. V. & Sauvé, S. (2019). Analysis of F-53B, Gen-X, ADONA, and emerging fluoroalkylether substances in environmental and biomonitoring samples: A review. *Trends Env. Anal. Chem.* 23: 1-10.

Naseer, S., Lee, Y., Lapierre, C. & Geldner, N. (2012). Casparian strip diffusion barrier in *Arabidopsis* is made of a lignin polymer without suberin. *Biol. Sci.* 109: 10101-10106.

Nassazzi, W., Wu, T., Jass, J., Lai, F. Y. & Ahrens, L. (2023). Phytoextraction of per- and polyfluoroalkyl substances (PFAS) and the influence of supplements on the performance of short-rotation crops. *Env. Poll.* 333: 122038-122046.

Nelson, D. W. & Sommers, L. E. (1996). Total carbon, organic carbon and organic matter. *Methods of soil analysis part 3. Chemical methods.*

Newman, M. C. (2001). *Fundamentals of Ecotoxicology*. 3rd edition. CRC Press, Florida: USA.

Ng, C., Cousins, I. T., DeWitt, J. C., Glüge, J., Goldenman, G., et al. (2021). Addressing Urgent Questions for PFAS in the 21st Century. *Env. Sci. Techn.* 55: 12755-12765.

Nguyen, T. M. H., Bräunig, J., Thompson, J., Kabiri, S., Navarro, D. A., et al. (2020). Influences of Chemical Properties, Soil Properties, and Solution pH on Soil–Water Partitioning Coefficients of Per- and Polyfluoroalkyl Substances (PFASs). *Env. Sci. Techn.* 54: 15883-15892.

Niu, Y. F., Chai, R. S., Jin, G. L., Wang, H., Tang, C. X., et al. (2013). Responses of root architecture development to low phosphorus availability: a review. *Ann. Bot.* 112: 391-408.

O’Grady, M. & Mangina, E. (2024). Citizen scientists-practices, observations, and experience. *Hum. Soc. Sci. Comm.* 11: 469-477.

Olney, S., Jones, M., Rockwell, C., Collins, R. D., Bryant, J. D., et al. (2023). Influence of convective and stratiform precipitation types on per- and polyfluoroalkyl substance concentrations in rain. *Sci. Tot. Env.* 890: 164051-164061.

Önel, S. E., Sungur, S. & Köroglu, M. (2018). Determination of perfluorooctanoic acid (PFOA) and perfluorooctane sulfonic acid (PFOS) in livestock feeds. *South Afric. Journ. Animal Sci.* 45: 1042-1048.

Padhi, M. K. (2016). Importance of Indigenous Breeds of Chicken for Rural Economy and Their Improvements for Higher Production Performance. *Scientifica 2016*: 1-9.

Pan, Y., Mei, J., Jiang, J., Xu, K., Gao, X., et al. (2023). PFAS in PMs might be the escalating hazard to the lung health. *Nano Res.* 23: 1-21.

Panieri, E., Baralic, K., Djukic-Cosic, D., Buha Djordjevic, A. & Saso, L. (2022). PFAS Molecules: A Major Concern for the Human Health and the Environment. *Toxics.* 10: 44-98.

Papadopoulou, E., Padilla-Sanchez, J. A., Collins, C. D., Cousins, I. T., Covaci, A., et al. (2016). Sampling strategy for estimating human exposure pathways to consumer chemicals. *Emerg. Cont.* 2: 26-36.

Parashar, N., Mahanty, B. & Hait, S. (2023). Microplastics as carriers of per- and polyfluoroalkyl substances (PFAS) in aquatic environment: interactions and ecotoxicological effects. *Wat. Emerg. Cont. Nanopl.* 2: 15-35.

Park, K., Barghi, M., Lim, J., Ko, H., Nam, H., et al. (2021). Assessment of regional and temporal trends in per- and polyfluoroalkyl substances using the Oriental Magpie (*Pica serica*) in Korea. *Sci. Tot. Env.* 793: 148513-148519.

Pasecnaja, E., Bartkevics, V. & Zacs, D. (2022). Occurrence of selected per- and polyfluorinated alkyl substances (PFASs) in food available on the European market – a review on levels and human exposure assessment. *Chemosphere.* 287: 132378-132391.

Pelch, K. E., Reade, A., Kwiatkowski, C. F., Merced-Nieves, F. M., Cavalier, H., et al. (2022). The PFAS-Tox Database: A systematic evidence map of health studies on 29 per- and polyfluoroalkyl substances. *Env. Int.* 167: 107408-107422.

Peng, S. & Chen, H. Y. (2021). Global responses of fine root biomass and traits to plant species mixtures in terrestrial ecosystems. *Glob. Ecol. Biog.* 30: 289-304.

Pereira, M. G., Lacorte, S., Walker L. A. & Shore, R. F. (2021). Contrasting long term temporal trends in perfluoroalkyl substances (PFAS) in eggs of the northern gannet (*Morus bassanus*) from two UK colonies. *Sci. Tot. Env.* 754: 141900-141909.

Pérez, F., Llorca, M., Köck-Schulmeyer, M., Skrbic, B., Oliveira, L. S., et al. (2014). Assessment of perfluoroalkyl substances in food items at global scale. *Env. Res.* 135: 181-189.

Pérez, F., Nadal, M., Navarro-Ortega, A., Fàbrega, F., Domingo, J. L., et al. (2013). Accumulation of perfluoroalkyl substances in human tissues. *Env. Int.* 59: 354-362.

Persson, L., Almroth, B. M. C., Collins, C. D., Cornell, S., de Wit, C. A., et al. (2022). Outside the Safe Operating Space of the Planetary Boundary for Novel Entities. *Env. Sci & Techn.* 56: 1510-1521.

Perumalla, C. J., Peterson, C. A. & Enstone, D. E. (1990). A survey of angiosperm species to detect hypodermal Casparian bands. I. Roots with a uniseriate hypodermis and epidermis. *Bot. Journ. Linn. Soc.* 103: 93-112.

Peters, J., Berghmans, P., Jacobs, G., Voorspoels, S., Spruyt, M., et al. (2022). Studie naar PFAS in lucht en deposities in de omgeving van 3M en Zwijndrecht. Vito-Health: pp. 1-77.

Pfotenhauer, D., Sellers, E., Olson, M., Praedel, K. & Shafer, M. (2022). PFAS concentrations and deposition in precipitation: An intensive 5-month study at National Atmospheric Deposition Program – National trends sites (NADP-NTN) across Wisconsin, USA. *Atm. Env.* 291: 119368-119379.

Pierozan, P., Kosnik, M. & Karlsson, O. (2023). High-content analysis shows synergistic effects of low perfluorooctanoic acid (PFOS) and perfluorooctane sulfonic acid (PFOA) mixture concentrations on human breast epithelial cell carcinogenesis. *Env. Int.* 172: 107746-107759.

Pike, K. A., Edmiston, P. L., Morrison, J. J. & Faust, J. A. (2021). Correlation Analysis of Perfluoroalkyl Substances in Regional U.S. Precipitation Events. *Wat. Res.* 190: 116685-116694.

Post, G. B. (2021). Recent US State and Federal Drinking Water guidelines for Per- and Polyfluoroalkyl Substances. *Env. Tox. Chem.* 40: 550-563.

Powley, C. R., George, S. W., Ryan, T. W. & Buck, R. C. (2005). Matrix effect-free analytical methods for determination of perfluorinated carboxylic acids in environmental matrixes. *Anal. Chem.* 77: 6353-6358.

Prevedouros, K., Cousins, I. T., Buck, R. C. & Korzeniowski, S. H. (2006). Sources, fate and transport of perfluorocarboxylates. *Env. Sci. Techn.* 40: 32-44.

Qi, Y., Cao, H., Pan, W., Wang, C. & Liang, Y. (2022). The role of dissolved organic matter during Per- and Polyfluorinated Substance (PFAS) adsorption, degradation, and plant uptake: A review. *Journ. Haz. Mat.* 436: 129139-129151.

Qian, J., Shen, M., Wang, P., Wang, C., Hou, J., et al. (2017). Adsorption of perfluorooctane sulfonate on soils: Effects of soil characteristics and phosphate competition. *Chemosphere.* 168: 1383-1388.

Ragnarsdóttir, O., Abdallah, M. A. & Harrad, S. (2022). Dermal uptake: An important pathway of human exposure to perfluoroalkyl substances? *Env. Poll.* 307: 119478-119491.

Rankin, K., Mabury, S. A., Jenkins, T. M. & Washington, J. W. (2016). A North American and global survey of perfluoroalkyl substances in surface soils: Distribution patterns and mode of occurrence. *Chemosphere.* 161: 333-341.

Ravindran, B., Mupambwa, H. A., Silwana, S. & Pearson, N. S. M. (2017). Assessment of nutrient quality, heavy metals and phytotoxic properties of chicken manure on selected commercial vegetable crops. *Heliyon* 3: 1-17.

Reinikainen, J., Perkola, N., Äystö, L & Sorvari, J. (2022). The occurrence, distribution, and risks of PFAS at AFFF-impacted sites in Finland. *Sci. Tot. Env.* 829: 154237-154242.

Rericha, Y., Cao, D., Truong, L., Simonich, M. T., Field, J. A., et al. (2022). Sulfonamide functional head on short-chain perfluorinated substance drives developmental toxicity. *iScience*. 25: 103789-103803.

Rich, C. D., Blaine, A. C., Hundal, L. & Higgins, C. P. (2015). Bioaccumulation of Perfluoroalkyl Acids by Earthworms (*Eisenia fetida*) Exposed to Contaminated Soils. *Env. Sci. Techn.* 49: 881-888.

Richardson, K., Steffen, W., Lucht, W., Bendtsen, J., Cornell, S. E., et al. (2023). Earth beyond six of nine planetary boundaries. *Sci. Adv.* 9: 1-17.

Richterova, D., Govarts, E., Fabelova, L., Rausova, K., Rodriguez, M. L., et al. (2023). PFAS levels and determinants of variability in exposure in European teenagers – Results from the HBM4EU aligned studies (2014-2021). *Int. Journ. Hyg. Env. Health*. 247: 114057-114066.

Rockström, J., Steffen, W., Noone, K., Persson, A., Chapin, F. S., et al. (2009). Planetary Boundaries: Exploring the Safe Operating Space for Humanity. *Ecol. & Soc.* 14: 1-33.

Roopnarine, P. D. (2014). Humans are apex predators. *Proc. Nat. Acad. Sci.* 111: 1.

Roth, K., Imran, Z., Liu, W. & Petriello, M. C. (2020). Diet as an Exposure Source and Mediator of Per- and Polyfluoroalkyl Substance (PFAS) Toxicity. *Front. Tox.* 2: 1-15.

Sadia, M., Yeung, L. W. Y. & Fiedler, H. (2020). Trace level analyses of selected perfluoroalkyl acids in food: Method development and data generation. *Env. Poll.* 263: 113721-113729.

Scaramozzino, P., Battisti, S., Desiato, R., Tamba, M., Fedrizzi, G., et al. (2019). Application of a risk-based standardized animal biomonitoring approach to contaminated sites. *Env. Mon. Assess.* 191: 526-538.

Scearce, A. E., Goossen, C. P., Schattman, R. E., Mallory, E. B. & MaCrae, J. D. (2023). Linking drivers of plant per- and polyfluoroalkyl substance (PFAS) uptake to agricultural land management decisions. *Biointerphases*. 18: 1-8.

Schenk, H. J. & Jackson, R. B. (2002). Rooting depths, lateral root spreads and below-ground/above-ground allometries of plants in water-limited ecosystems. *Journ. Ecol.* 90: 480-494.

Scher, D. P., Kelly, J. E., Huset, C. A., Barry, K. M., Hoffbeck, R. W., et al. (2018). Occurrence of perfluoroalkyl substances (PFAS) in garden produce at homes with a history of PFAS-contaminated drinking water. *Chemosphere.* 196: 548-555.

Scheringer, M., Johansson, J. H., Salter, M. E., Sha, B. & Cousins, I. T. (2022). Stories of Global Chemical Pollution: Will We Ever Understand Environmental Persistence? *Env. Sci. Techn.* 56: 17498-17501.

Schiavone, C. & Portesi, C. (2023). PFAS: A Review of the State of the Art, from Legislation to Analytical Approaches and Toxicological Aspects for Assessing Contamination in Food and Environment and Related Risks. *Appl. Sci.* 13: 6696-6721.

Schoeters, G. & Hoogenboom, R. (2006). Contamination of free-range chicken eggs with dioxins and dioxin-like polychlorinated biphenyls. *Mol. Nutr. Food Res.* 50: 908-914.

Schroeder, T., Bond, D. & Foley, J. B. (2021). PFAS soil and groundwater contamination via industrial airborne emission and land deposition in SW Vermont and Eastern New York State, USA. *Env. Sci.: Proc. Imp.* 23: 291 – 301.

Schultes, L., Vestergren, R., Volkova, K., Westberg, E., Jacobson, T., et al. (2018). Per- and polyfluoroalkyl substances and fluorine mass balance in cosmetic products from the Swedish market: implications for environmental emissions and human exposure. *Env. Sci.: Proc. Imp.* 20: 1680-1690.

Schymanski, E. L., Zhang, J., Thiessen, P. A., Chirsir, P., Kondic, T., et al. (2023). Per- and polyfluoroalkyl substances (PFAS) in PubChem: 7 million and growing. *Env. Sci. Techn.* 44: 16918-16928.

Sedlmaier, N., Hoppenheidt, K., Krist, H., Lehmann, S., Lang, H., et al. (2009). Generation of avian influenza virus (AIV) contaminated fecal fine particulate matter (PM_{2.5}): Genome and infectivity detection and calculation of immission. *Vet. Microb.* 139: 156-164.

Shahsavari, E., Rouch, D., Khudur, L. S., Thomas, D., Aburto-Medina, A., et al. (2020). Challenges and Current Status of the Biological Treatment of PFAS-Contaminated Soils. *Front. Bioeng. Biotechn.* 8: 602040-602054.

Sharma, S.P., Leskovar, D. I., Crosby, K. M. & Volder, A. (2017). Root growth dynamics and fruit yield of melon (*Cucumis melo* L) genotypes at two locations with sandy loam and clay soils. *Soil Till. Res.* 168: 50-62.

Shatalov, V., Dutchak, S., Fedyunin, M., Mantseva, E., Strukov, B, et al. (2003). Chapter: Persistent Organic Pollutants. *Pers. Org. Poll. Env.* pp. 1-22. Met. Synth. Centre, Moscow: Russia.

Shearer, J. J., Callahan, C. L., Calafat, A. M., Huang, W., Jones, R. R., et al. (2021). Serum Concentrations of Per- and Polyfluoroalkyl Substances and Risk of Renal Cell Carcinoma. *Journ. Nat. Canc. Inst.* 113: 580-587.

Shen, J., Yuan, L., Zhang, J., Li, H., Bai, Z., et al. (2011). Phosphorus Dynamics: From Soil to Plant. *Plant Phys.* 156: 997-1005.

Sigmund, G., Arp, H. P. H., Aumeier, B. M., Bucheli, T. D., Chefetz, B., et al. (2022). Sorption and Mobility of Charged Organic Compounds: How to Confront and Overcome Limitations in Their Assessment. *Env. Sci. Techn.* 56: 4702-4710.

Sims, J. L., Stroski, K. M., Kim, S., Killeen, G., Ehalt, R., et al. (2022). Global occurrence and probabilistic environmental health hazard assessment of per- and polyfluoroalkyl substances (PFASs) in groundwater and surface waters. *Sci. Tot. Env.* 816: 151535-151547.

Sioen, I., Bilau, M., Van Overmeire, I., Eppe, G., Waegeneers, N., et al. (2008). Intake of dioxins and dioxin-like PCBs consuming home produced versus commercial eggs. *Org. Comp.* 70: 1483-1485.

Sivaram, A. K., Panneerselvan, L., Surapaneni, A., Lee, E., Kannan, K., et al. (2022). Per- and polyfluoroalkyl substances (PFAS) in commercial composts, garden soils and potting mixes of Australia. *Env. Adv.* 7: 100174-1001781.

Smit, A. L., Booij, R. & Van der Werf, A. (1996). The spatial and temporal rooting pattern of Brussels sprouts and leeks. *Neth. Journ. Agric. Sci.* 44: 57-72.

Soares, P. R., Pato, R. L., Dias, S. & Santos, D. (2022). Effects of Grazing Indigenous Laying Hens on Soil Properties: Benefits and Challenges to Achieving Soil Fertility. *Sustainability.* 14: 3407-3425.

Sonne, C., Desforges, J., Gustavson, K., Bossi, R., Bonefeld-Jørgensen, E. C., et al. (2023). Assessment of exposure to perfluorinated industrial substances and risk of immune suppression in Greenland and its global context: a mixed-methods study. *The Lancet: Plan. Health.* 7: 570-579.

Sörengard, M., Kikuchi, J., Wiberg, K. & Ahrens, L. (2022). Spatial distribution and load of per- and polyfluoroalkyl substances (PFAS) in background soils in Sweden. *Chemosphere.* 295: 133944-133950.

Steffen, W., Crutzen, P. J. & McNeill, J. R. (2007). The Anthropocene: Are Humans Now Overwhelming the Great Forces of Nature. *Ambio.* 36: 614-621.

Stephens, R. D., Petreas, M. X. & Hayward, D. G. (1995). Biotransfer and bioaccumulation of dioxins and furans from soil: chickens as a model for foraging animals. *Sci. Tot. Env.* 175: 253-273.

Steyerberg, E. W. (2009). *Clinical Prediction Models: A Practical Approach to Development, Validation, and Updating.* Springer, New York: USA.

Steyerberg, E. W., Vickers, A., Cook, N. R., Gerds, T., Gonen, M., et al. (2010). Assessing the performance of prediction models: a framework for some traditional and novel measures. *Epidemiology* 21: 128-138.

Styler, S. A., Myers, A. L. & Donaldson, D. J. (2013). Heterogeneous photooxidation of fluorotelomer alcohols: a new source of aerosol-phase perfluorinated carboxylic acids. *Env. Sci Techn.* 47: 6358-6367.

Su, H., Shi, Y., Lu, Y., Wang, P., Zhang, M., et al. (2017). Home produced eggs: An important pathway of human exposure to perfluorobutanoic acid (PFBA) and perfluorooctanoic acid (PFOA) around a fluorochemical industrial park in China. *Env. Int.* 101: 1-6.

Suk, Y. O. & Park, C. (2001). Effect of Breed and Age of Hens on the Yolk to Albumen Ratio in Two Different Genetic Stocks. *Poultry Sci.* 80: 855-858.

Sunderland, E. M., Hu, X. C., Dassuncao, C., Tokranov, A. K., Wagner, C. C., et al. (2019). A review of the pathways of human exposure to poly- and perfluoroalkyl substances (PFASs) and present understanding of health effects. *Journ. Exp. Sci. Env. Epid.* 29: 131-147.

Taylor, P. S., Hemsworth, P. H., Groves, P. J., Gebhardt-Henrich, S. G. & Rault, J. (2017). Ranging Behaviour of Commercial Free-Range Broiler Chickens 2: Individual Variation. *Animals.* 7: 55-63.

Thakur, S., Singh, L., Wahid, Z. A., Siddiqui, M. F., Atnaw, S. M., et al. (2016). Plant-driven removal of heavy metals from soil: uptake, translocation, tolerance mechanism, challenges, and future perspectives. *Env. Mon. Ass.* 188: 1-11.

Thorup-Kristensen, K. (2001). Root Growth and Soil Nitrogen Depletion by Onion, Lettuce, Early Cabbage and Carrot. *Act. Hortic.* 563: 201-206.

Toparlar, Y., Blocken, B., Maiheu, B. & van Heijst, G. J. F. (2018). Impact of urban microclimate on summertime building cooling demand: A parametric analysis for Antwerp, Belgium. *Appl. Energy.* 228: 852-872.

Tresch, S., Moretti, M., Le Bayon, R., Mäder, P., Zanetta, A., et al. (2018). A Gardener's Influence on Urban Soil Quality. *Front. Env. Sci.* 6: 1-17.

UNEP. (2019). Chemicals listed in Annex A and Annex B. Available from: <https://www.pops.int/Implementation/Alternatives/AlternativestoPOPs/ChemicalslistedinAnnexA/tabid/5837/Default.aspx>. Accessed 4th of October 2023.

Van der Heyden, J., Nguyen, D., Renard, F., Scohy, A., Demarest, S., et al. (2018). Belgian health research 2018. Brussel, Belgium: Sciensano; Report number: 2019/14.440/89. www.gezondheidsenquête.be. Accessed 22nd of June 2021.

Van der Jagt, A. P. N., Szaraz, L. R., Delshammar, T., Cvejić, R., Santos, A., et al. (2017). Cultivating nature-based solutions: The governance of communal urban gardens in the European Union. *Env. Res.* 159: 264-275.

Van Overmeire, I., Pussemier, L., Hanot, V., De Temmerman, L., Hoenig, M., et al. (2006). Chemical contamination of free-range eggs from Belgium. *Food Add. Cont.* 23: 1109-1122.

Verbruggen, A. (1997). Report on the Environment and Nature in Flanders 1996. Learning to change. Flemish Environment Agency (VMM).

Vestergren, R. & Cousins, I. T. (2013). Chapter 12: Human dietary exposure to per- and polyfluoroalkyl substances (PFASs). Pp. 279. Woodhead Publishing Series, Cambridge: UK.

Vico, G. & Brunsell, N. A. (2018). Tradeoffs between water requirements and yield stability in annual vs. perennial crops. *Adv. Wat. Res.* 112: 189-202.

Viegas, S., Faísca, V. M., Dias, H., Clérigo, A., Carolino, E., et al. (2013). Occupational exposure to poultry dust and effects on the respiratory system in workers. *Journ. Tox. Env. Health.* 76: 230-239.

Villanueva, P. (2005). MLE-Based Procedure for Left-censored Data Excel Spreadsheet. Office of Pesticide Programs. U.S., Environmental Protection Agency, Washington, DC.

VLAM. (2017). Evolutie van het verbruik van agrovoedingsproducten in België. Gfk Panel Services E-Benelux.

Vorst, K. L., Saab, N., Silva, P., Curtzwiler, G. & Steketee, A. (2021). Risk assessment of per- and polyfluoroalkyl substances (PFAS) in food: Symposium proceedings. *Trends Food Sci. Techn.* 116: 1203-1211.

Waegeneers, N., De Steur, H., De Temmerman, L., Van Steenwinkel, S., Gellynck, X., et al. (2009). Transfer of soil contaminants to home-produced eggs and preventive measures to reduce contamination. *Sci. Tot. Env.* 407: 4438-4446.

Wäldchen, J., Schöning, I., Mund, M., Schrumpf, M., Bock, S., et al. (2012). Estimation of clay content from easily measurable water content of air-dried soil. *Journ. Plant Nutr. Soil Sci.* 175: 367-376.

Walinga, I., van Vark, W., Houba, V. J. G. & van der Lee, J. J. (1989). Plant analysis procedures. *Soil and Plant Analysis, Part 7*, p. 13-16. Agricultural University, Wageningen: The Netherlands.

Wang, F., Zhao, C., Gao, Y., Fu, J., Gao, K., et al. (2019). Protein-specific distribution patterns of perfluoroalkyl acids in egg yolk and albumen samples around a fluorochemical facility. *Sci. Tot. Env.* 650: 2697-2704.

Wang, T. T., Ying, G. G., Shi, W. J., Zhao, J. L., Liu, Y. S., et al. (2020) Uptake and translocation of perfluorooctanoic acid (PFOA) and perfluorooctane sulfonic acid (PFOS) by wetland plants: tissue- and cell-level distribution visualization with desorption electrospray ionization mass spectrometry (DESI-MS) and transmission electron microscopy equipped with energy-dispersive spectroscopy (TEM-EDS). *Env. Sci. Techn.* 54: 6009-6020.

Wang, Y., Fu, J., Wang, T., Liang, Y., Pan, Y., et al. (2010). Distribution of perfluorooctane sulfonate and other perfluorochemicals in the ambient environment around a manufacturing facility in China. *Env. Sci. Techn.* 21: 8062-8067.

Wang, Y., Munir, U. & Huang, Q. (2023). Occurrence of per- and polyfluoroalkyl substances (PFAS) in soil: Sources, fate, and remediation. *Soil Env. Health.* 1: 100004-100018.

Wang, Z., Buser, A. M., Cousins, I. T., Demattio, S., Drost, W., et al. (2021). A New OECD Definition for Per- and Polyfluoroalkyl Substances. *Env. Sci. Techn.* 23: 15575-15578.

Wang, Z., Cousins, I. T., Scheringer, M. & Hungerbühler, K. (2015). Hazard assessment of fluorinated alternatives to long-chain perfluoroalkyl acids (PFAAs) and their precursors: Status quo, ongoing challenges and possible solutions. *Env. Int.* 75: 172-179.

Wang, Z. H., Zhao, H. & Li, J. (2022). Spatiotemporal distribution of perfluoroalkyl acid in Chinese eggs. *Food Add. Cont. B.* 15: 1-11.

Washington, J. W., Naile, J. E., Jenkins, T. M. & Lynch, D. G. (2014). Characterizing Fluorotelomer and Polyfluoroalkyl Substances in New and Aged Fluorotelomer-Based Polymers for Degradation Studies with GC/MS and LC/MS/MS. *Env. Sci. Techn.* 48: 5762-5769.

Weaver, J. E. & Bruner, W. E. (1927). *Root Development of Vegetable Crops*. McGraw-Hill Book Company, New York: USA.

Wellmitz, J., Bandow, N. & Koschorreck, J. (2023). Long-term trend data for PFAS in soils from German ecosystems, including TOP assay. *Sci. Tot. Env.* 893: 164586-164587.

Wen, B., Wu, Y., Zhang, H., Liu, Y., Hu, X., et al. (2016). The roles of protein and lipid in the accumulation and distribution of perfluorooctane sulfonate (PFOS) and perfluorooctanoate (PFOA) in plants grown in biosolids-amended soils. *Env. Poll.* 216: 682-688.

Wilson, T. B., Stevenson, G., Crough, R., de Araujo, J., Fernando, N., et al. (2020). Evaluation of Residues in Hen Eggs After Exposure of Laying Hens to Water Containing Per- and Polyfluoroalkyl Substances. *Env. Tox. Chem.* 40: 735-743.

Windal, I., Hanot, V., Marchi, J., Huysmans, G., Van Overmeire, I., et al. (2009). PCB and organochlorine pesticides in home-produced eggs in Belgium. *Sci. Tot. Env.* 407: 4430-4437.

Xiang, L., Chen, X., Yu, P., Li, X., Zhao, H., et al. (2020). Oxalic Acid in Root Exudates Enhances Accumulation of Perfluorooctanoic Acid in Lettuce. *Env. Sci. Techn.* 54: 13046-13055.

Xiang, L., Qiu, J., Chen, Q., Yu, P., Liu, B., et al. (2023). Development, Evaluation, and Application of Machine Learning Models for Accurate Prediction of Root Uptake of Per- and Polyfluoroalkyl Substances. *Env. Sci. Techn.* 57: 18317-18328.

Xiao, F., Simcik, M. F., Halbach, T. R. & Gulliver, J. S. (2015). Perfluorooctane sulfonate (PFOS) and perfluorooctanoate (PFOA) in soils and groundwater of a U.S. metropolitan area: Migration and implications for human exposure. *Wat. Res.* 72: 64-74.

Xing, Y., Zhou, Y., Zhang, X., Lin, X., Li, J., et al. (2023). The sources and bioaccumulation of per- and polyfluoroalkyl substances in animal-derived foods and the potential risk of dietary intake. *Sci. Tot. Env.* 905: 167313-167325.

Xu, B., Liu, S., Zhou, J. L., Zheng, C., Jin, W., et al. (2021a). PFAS and their substitutes in groundwater: Occurrence, transformation and remediation. *Journ. Haz. Mat.* 412: 125159-125171.

Xu, C., Song, X., Liu, Z., Ding, X., Chen, H., et al. (2021b). Occurrence, source apportionment, plant bioaccumulation and human exposure of legacy and emerging per- and polyfluoroalkyl substances in soil and plant leaves near a landfill in China. *Sci. Tot. Env.* 776: 145731-145741.

Xu, B., Qiu, W., Du, J., Wan, Z., Zhou, J. L., et al. (2022). Translocation, bioaccumulation, and distribution of perfluoroalkyl and polyfluoroalkyl substances (PFASs) in plants. *iScience.* 25: 104061-104076.

Yan, A., Wang, Y., Tan, S. N., Yusof, M. L. M., Ghosh, S., et al. (2020). Phytoremediation: A Promising Approach for Revegetation of Heavy Metal-Polluted Land. *Front. Plant Sci.* 11: 1-15.

Yang, J., Huang, Y., Zhao, G., Li, B., Qin, X., et al. (2022). Phytoremediation potential evaluation of three rhubarb species and comparative analysis of their rhizosphere characteristics in a Cd- and Pb-contaminated soil. *Chemosphere.* 296: 134045-134056.

Yannopoulos, P. C. (2011). Chapter 21: Quick and Economic Spatial Assessment of Urban Air Quality, *Adv. Air Poll. InTech.* pp. 391. London: UK.

You, C., Jia, C. & Pan, G. (2010). Effect of salinity and sediment characteristics on the sorption and desorption of perfluorooctane sulfonate at sediment-water interface. *Env. Poll.* 158: 1343-1347.

Zafeiraki, E., Costopoulou, D., Vassiliadou, I., Leondiadis, L., Dassenakis, E., et al. (2016). Perfluoroalkylated substances (PFASs) in home and commercially produced chicken eggs from the Netherlands and Greece. *Chemosphere.* 144: 2106-2112.

Zeilmaker, M. J., Janssen, P., Versteegh, A., Van Pul, A., De Vries, W., et al. (2016). Risicoschatting emissie PFOA voor omwonenden. Locatie: DuPont/Chemours, Dordrecht, Nederland. RIVM Rapport 2016-0049.

Zeng, Z., Song, B., Xiao, R., Zeng, G., Gong, J., et al. (2019). Assessing the human health risks of perfluorooctane sulfonate by in vivo and in vitro studies. *Env. Int.* 126: 598-610.

Zergui, A., Boudalia, S. & Joseph, M. L. (2023). Heavy metals in honey and poultry eggs as indicators of environmental pollution and potential risks to human health. *Journ. Food Comp. Anal.* 119: 105255-105266.

Zhang, L., Ren, X. & Guo, L. (2013). Structure-Based Investigation on the Interaction of Perfluorinated Compounds with Human Liver Fatty Acid Binding Protein. *Env. Sci. Techn.* 47: 11293-11301.

Zhang, L., Verweij, R. A. & Van Gestel, C. A. M. (2019). Effect of soil properties on Pb bioavailability and toxicity to the soil invertebrate *Enchytraeus crypticus*. *Chemosphere* 217: 9-17.

Zhang, M., Wang, P., Lu, Y., Shi, Y., Wang, C., et al. (2021a). Transport and environmental risks of perfluoroalkyl acids in a large irrigation and drainage system for agricultural production. *Env. Int.* 157: 106856-106866.

Zhang, W., Pang, S., Lin, Z., Mishra, S., Bhatt, P., et al. (2021b). Biotransformation of perfluoroalkyl acid precursors from various environmental systems: advances and perspectives. *Env. Poll.* 272: 115908-115923.

Zhao, S., Fang, S., Zhu, L., Liu, L., Liu, Z., et al. (2014). Mutual impacts of wheat (*Triticum aestivum* L.) and earthworms (*Eisenia fetida*) on the bioavailability of perfluoroalkyl substances (PFASs) in soil. *Env. Poll.* 184: 495-501.

Zhou, Y., Yao, Q. & Zhu, H. (2020). Soil Organic Carbon Attenuates the Influence of Plants on Root-Associated Bacterial Community. *Front. Microb.* 11: 594890-594901.

Zhu, Y., Li, Y., Liu, X., Yang, X., Song, X., et al. (2023). Bioaccessibility of per- and polyfluoroalkyl substances in food and dust: Implication for more accurate risk assessment. *Sci. Tot. Env.* 868: 161739-161747.

Zipperer, W. C. & Pickett, S. T. A. (2012). *Urban Ecology: Patterns of Population Growth and Ecological Effects*. John Wiley and Sons Ltd, pp. 1-8.

Supplementary information

Chapter 2

Section 2.1: Optimization extraction method

Prior to the extraction of the egg samples, three analytical methods were tested on a blank matrix sample (= commercial egg free of PFAS contamination) in order to select a relatively robust, accurate and sensitive extraction procedure (see supplementary information: optimization extraction method). To this end, two previously validated methods, Chromabond HR-WAX solid phase extraction based on weak anion-exchange principle and clean-up extraction using graphitized Envicarb carbon powder (hereafter referred to as WAX and Envicarb, respectively), were tested (adopted from Powley et al. (2005) and Groffen et al. (2019c)). Additionally, a combination of both methods was evaluated using sample clean-up with Envicarb prior to extraction with WAX. These methods were compared to each other in terms of extraction recovery.

Whole egg content of the blank matrix sample was homogenized by repeated high-speed vortexing and sonication. Then, the egg content was split up in 18 aliquots of 0.3 g (\pm 0.01 mg) each and these were spiked with 10 ng of a mixture of unlabeled:labeled internal standards (1:1). Nine aliquots were boiled at 99.9 °C for 10 minutes in polypropylene (PP) tubes. Both boiled and raw egg samples (each $N = 3$) were then extracted with each of the three candidate methods. Procedural blanks (= ISTD spiked ACN solution) were included for each analytical method and a non-extracted labelled standard solution diluted in 50:50 ACN:MilliQ water was also prepared for calculating extraction recoveries. In terms of extraction quality, the Envicarb method performed best resulting in higher extraction recoveries for the majority of PFAS compared to the other two procedures, both for raw and boiled eggs (Fig. S2.1). Therefore, this extraction method was chosen for the extraction of the collected egg samples.

Figures

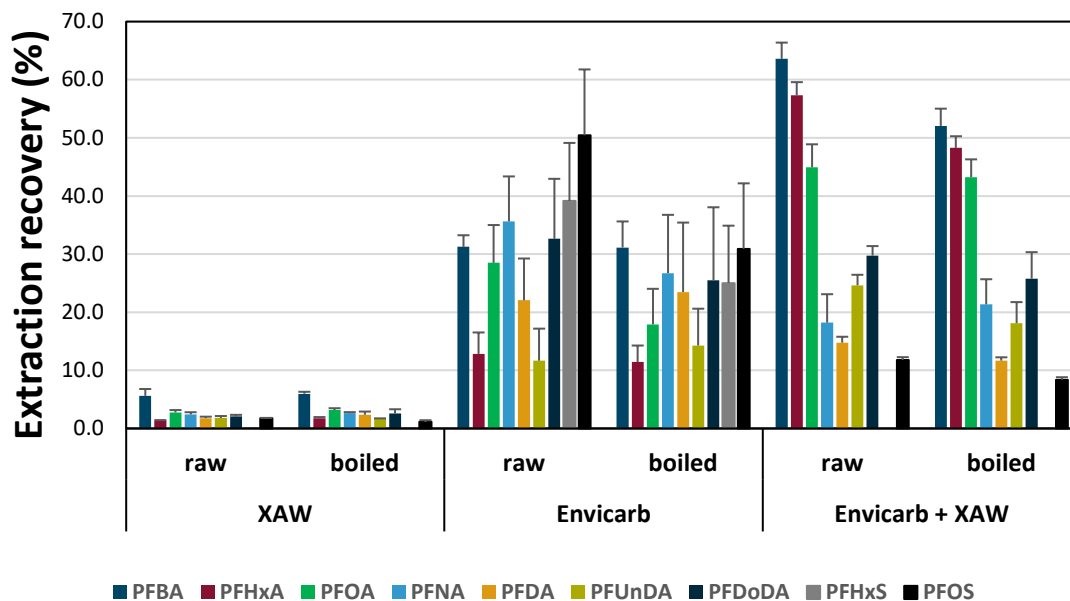


Fig. S2.1: Mean extraction recoveries (%) of the internal standard, spiked at 10 ng, of each PFAS compound using three different extraction procedures for raw and boiled eggs. The internal standard of PFHxS was <LOQ when using weak anion exchange solid-phase extraction (WAX) procedure and a combination of clean-up extraction with graphitized carbon powder and WAX (Envicarb + WAX). Error bars represent standard deviations. Sample mass: 0.3 g; $N = 3$.

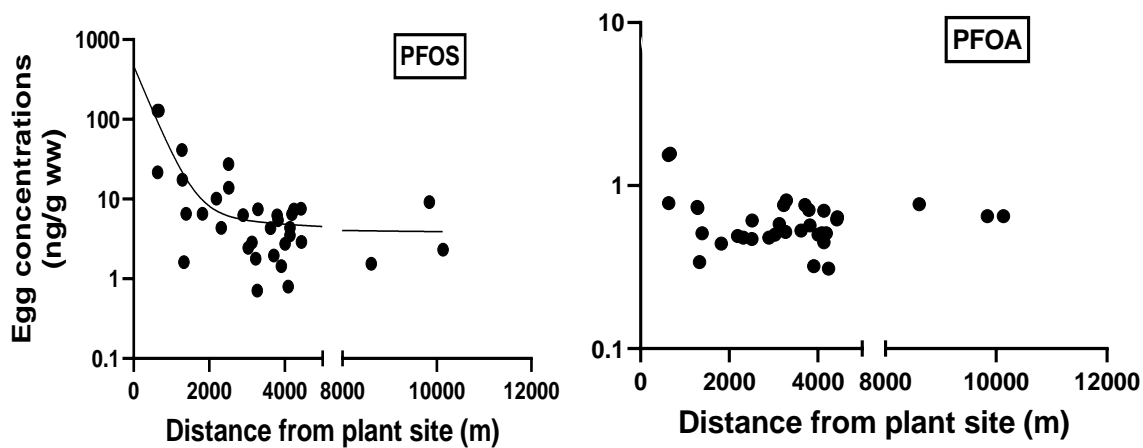


Fig. S2.2: Significant decrease ($P < 0.05$; $R^2 0.68$) of PFOS concentrations (ng/g ww) in home-produced eggs of free ranging laying hens from the fluorochemical plant site in Antwerp, Belgium. Exponential curve has been added. For PFOA, no significant relationship ($P > 0.05$) with distance from the fluorochemical plant site was found ($N = 35$).

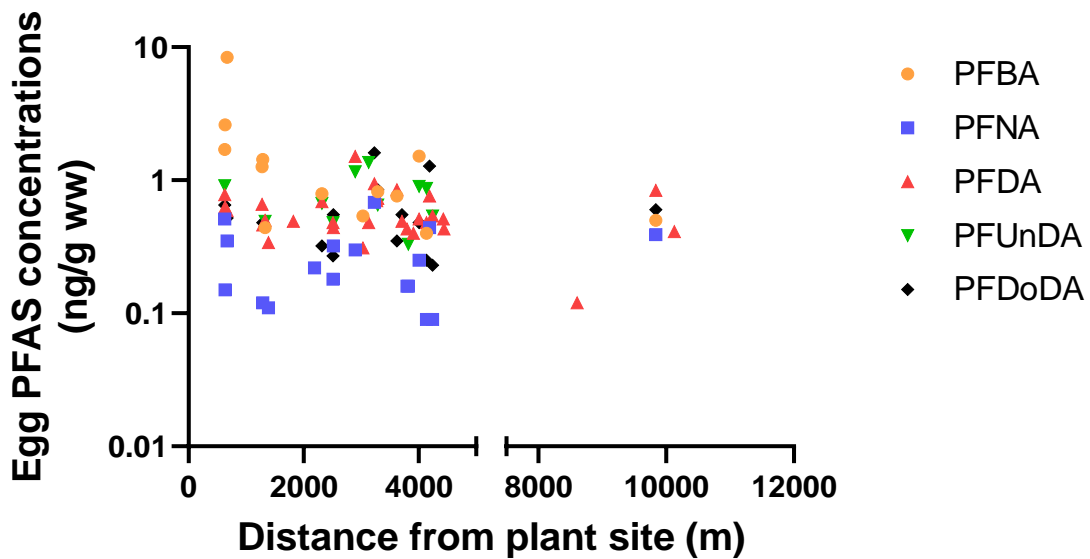


Fig. S2.3: PFAS concentrations (ng/g ww) in function of the distance from the fluorochemical plant site (m) in home-produced eggs of free ranging laying hens from the fluorochemical plant site in Antwerp, Belgium. No significant concentration changes in relation to the fluorochemical plant site were found for these PFAS, although PFBA marginally significantly decreased from the plant site onwards ($P = 0.06$; $R^2 = 0.43$; $N = 21$)

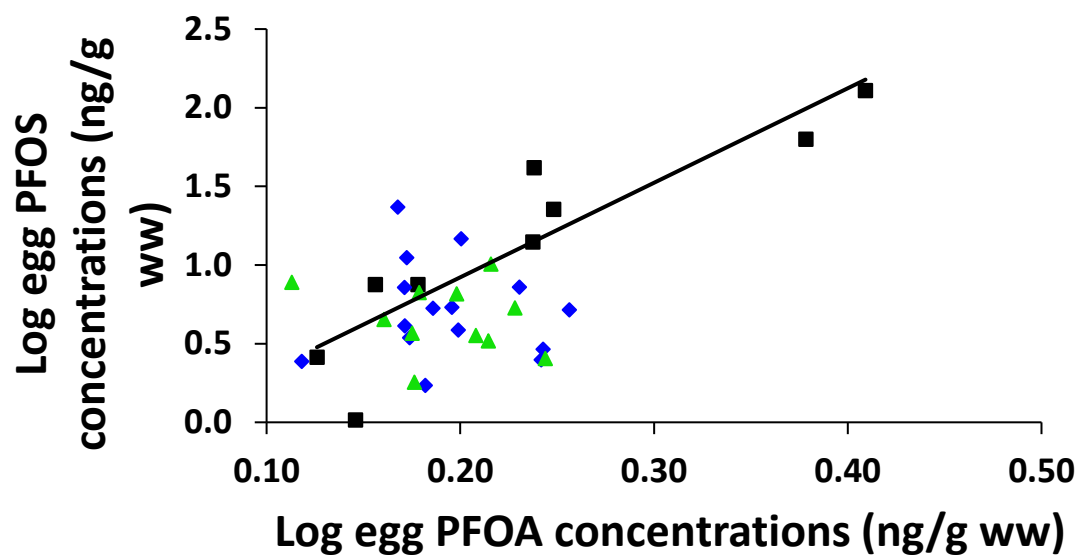


Fig. S2.4: Significant positive relationship ($P < 0.001$; $R^2 = 0.81$) between PFOS and PFOA concentrations (ng/g ww) in home-produced eggs of free ranging laying hens from buffer zone A (0-2 km, black squares) from the fluorochemical plant site in Antwerp, Belgium. No significant correlations were observed with respect to buffer zone B (2-4 km, blue circles) and zone C (4-10 km, green triangles).

Tables

Table S2.1: Self-reporting survey by which information on the flock size, main origin provided feed and age category of the laying hens from each volunteer was obtained.

Question	Answer
What is the flock size of the laying hens?	Number (N)
What is the main origin of feed provided to the laying hens?	Kitchen leftover (LF), commercial feed (CF) or a mix of both (M)
To which average age category do the laying hens belong?	Young layers (<1 year old)/older layers (1-2 years old)/old layers (>2 years old)

Table S2.2: PFAS concentrations, in ng/g wet weight, in commercial eggs (*N* = 3) that were used for the method optimization.

PFAS compound	Commercial egg concentration (ng/g wet weight)
PFBA	<LOQ
PFPeA	<LOQ
PFHxA	<LOQ
PFHpA	<LOQ
PFOA	<LOQ
PFNA	<LOQ
PFDA	<LOQ
PFUnDA	<LOQ
PFDoDA	<LOQ
PFTTrDA	<LOQ
PFTeDA	<LOQ
PFBS	<LOQ
PFHxS	<LOQ
PFOS	<LOQ
PFDS	<LOQ
HFPO-DA (GenX)	<LOQ
NaDONA	<LOQ

Table S2.3: MRM transitions, mass-labelled internal standards (ISTDs), cone voltages (V) and collision energy (eV) for the target per- and polyfluoroalkyl substances (PFAS) and their internal standard (Table was adopted from Groffen et al. (2021)).

Compound	Precursor ion (m/z)	Product ion (m/z)		Cone Voltage (V)	Collision energy (eV) for diagnostic transition1	Collision energy (eV) for diagnostic transition 2	Internal standard (ISTD) used for quantification
		Diagnostic product ion 1	Diagnostic product ion 2				
PFBA	213	169	169	19	19	50	¹³ C ₄ -PFBA
PFPeA	263	219	219	15	10	45	¹³ C ₄ -PFBA
PFHxA	313	269	119	19	21	65	[1,2- ¹³ C ₂]PFHxA
PFHpA	363	319	169	24	40	30	[1,2- ¹³ C ₂]PFHxA
PFOA	413	369	169	22	13	60	[1,2,3,4- ¹³ C ₄]PFOA
PFNA	463	419	169	28	17	20	[1,2,3,4,5- ¹³ C ₅]PFNA
PFDA	513	469	219	25	29	29	[1,2- ¹³ C ₂]PFDA
PFUnDA	563	519	169	18	30	35	[1,2- ¹³ C ₂]PFUnDA
PFDoDA	613	569	319	22	21	30	[1,2- ¹³ C ₂]PFDoDA
PFTTrDA	663	619	319	26	21	30	[1,2- ¹³ C ₂]PFDoDA
PFTeDA	713	669	169	28	21	21	[1,2- ¹³ C ₂]PFDoDA
PFBS	299	80	99	40	65	45	¹⁸ O ₂ -PFHxS
PFHxS	399	80	99	22	30	60	¹⁸ O ₂ -PFHxS
PFOS	499	80	99	60	58	58	[1,2,3,4- ¹³ C ₄]PFOS
PFDS	599	80	99	29	63	63	[1,2,3,4- ¹³ C ₄]PFOS
HFPO-DA (GenX)	285	169		30	20		[1,2,3,4- ¹³ C ₄]PFOA
NaDONA	376.8	250.7	84.8	23	35	32	[1,2,3,4- ¹³ C ₄]PFOA
¹³ C ₄ -PFBA	217	172	172	19	19	50	
[1,2- ¹³ C ₂]PFHxA	315	269	119	19	21	65	
[1,2,3,4- ¹³ C ₄]PFOA	417	372	172	22	13	60	
[1,2,3,4,5- ¹³ C ₅]PFNA	468	423	172	28	17	20	
[1,2- ¹³ C ₂]PFDA	515	470	220	25	29	29	
[1,2- ¹³ C ₂]PFUnDA	565	520	170	18	32	35	
[1,2- ¹³ C ₂]PFDoDA	615	570	320	22	21	30	
¹⁸ O ₂ -PFHxS	403	84	103	22	30	60	
[1,2,3,4- ¹³ C ₄]PFOS	503	80	99	60	58	58	

Table S2.4: Literature data of the mean body mass for various age interval groups of the general Belgian population, which were used to estimate the dietary intake of PFAS via consumption of home-produced eggs. Data were adopted from De Hoge gezondheidsraad (2003) and Van der Heyden et al. (2018).

Age group (years)	Sex	Mean body weight (kg)
3-5		18.0
6-9		24.3
10 - 13		37.5
14-17	Male	59.5
	Female	52.9
18-64	Male	76.2
	Female	63.1

Chapter 3

Section 3.1: Sample collection

The composite soil sample was collected with a stainless gauge auger from the top layer (0-5 cm) of the chicken enclosure in the private garden and consisted of three subsamples (each ± 50 g): these samples were gathered from the central feeding spot of the laying hens, in front of the entrance of the shelter house and from areas in which the laying hens frequently took sand baths. The rain water samples (50 ml in PP tube) were collected directly from open drinking water recipients in the chicken enclosure or indirectly from rainwater casks, depending on which source of water the volunteer provided as drinking water to the laying hens. Two individual eggs from free-ranging laying hens (age 1-3 years) were collected and their independency was assured by selecting only volunteers that housed minimally two active laying hens and by only collecting eggs that were laid on the same day. Pools of juvenile and adult earthworms (*Lumbricus terrestris*) were collected throughout the chicken enclosure with a stainless shovel and their life-stage was identified through the absence (= juvenile)/presence (= adult) of the clitellum. Pools of three individual samples from minimally two homegrown crop species were collected from the cultivation area, depending on their availability. To ensure good sampling coverage, pooled samples from the individual crop species were preferably collected both from the sides and the middle section of the vegetable garden.

Section 3.2: Soil physicochemical characteristics

The pH of freshly collected soil samples was measured using a multimeter electrode (WTW Multi 3430 SET F, probe SenTix 940, Weilheim, Germany), after thoroughly mixing 5 ± 0.1 g of soil with 25 mL of KCl (1M) solution and leaving to rest for 1 h. The soil electrical conductivity was measured following the International Standard Organization's protocol 11265:1994. To this end, 25 mL of deionized H₂O was added to 5 ± 0.1 g of fresh soil and leaving to rest for 30 min at room temperature to dissolve all electrolytes. After filtering the extract through a glass fiber filter, the conductivity was measured with a multimeter (WTW Multi 3430 SET F, TetraCon 92 probe, Weilheim, Germany). The soil clay content (particle size $<2 \mu\text{m}$) was analyzed based on the principle of laser diffraction

with the Malvern Mastersizer 2000 and Hydro 2000G (Malvern Instruments Ltd, Malvern, UK). Fresh soil aliquots of 1 ± 0.1 g were digested with 15 mL of 33% technical grade H_2O_2 and 10 mL of technical grade HCl at room temperature to degrade organic material and iron complexes in the soil. After 24 hours, the digestion reactions were catalyzed by adding another 25 mL of H_2O_2 to the samples and boiling them until the reaction faded. Prior to clay content analysis, the samples were sieved through a sieve with 2.0 mm mesh size. The soil organic matter content was measured based on the loss on ignition (LOI) method, following the procedure of Heiri et al (2001). Around 5 ± 0.1 g of soil, oven-dried at $60^\circ C$, was weighed into foiled aluminum bags which had been dried at $105^\circ C$ for two hours. Then, the soil was dried at $105^\circ C$ for 48 hours after which it was stored in a desiccator to cool down until room temperature. The samples were weighed and thereafter incinerated in a muffle furnace at $550^\circ C$ for six hours. Lastly, the samples were weighed again and the TOC was calculated using the following equation:

$$LOI_{550}(\%) = 100 * \frac{(DW_{105} - DW_{550})}{DW_{105}}$$

$$TOC(\%) = \frac{LOI_{550}}{1.742}$$

with DW defined as the dry weight of the soil sample after drying at $105^\circ C$ or $550^\circ C$ and 1.742 being the “Van Bemmelen” factor, assuming that 58% of the total organic matter is organic carbon (Nelson and Sommers, 1996).

Exchangeable base cations were analyzed according to Brown’s procedures. Briefly, the soil wet weight was volumetrically determined by drying at $105^\circ C$. Afterwards, 25 ml of NH_4Ac buffer solution (pH = 7) was added to 2.5 ± 0.1 g of oven-dried ($60^\circ C$) soil and the sample was three-dimensionally shaken for one hour. Then, the pH of the extracts was measured with a multimeter (WTW Multi 3430 SET F, probe SenTix 940, Weilheim, Germany) and they were filtered using a $0.45 \mu m$ polyester syringe filter. In duplo titration curves were set up by adding 0.1 mL of CH_3COOH (0.1 M) acid in steps to 50 mL of NH_4Ac buffer solution (pH = 7) until pH 6 was reached. Based on the calculated moisture content and H^+ concentration, the exchangeable basic cations (Ca^{2+} , Mg^{2+} , K^+

and Na^+) and exchangeable acidic cations (Al^{3+} , Fe^{3+} and Mn^{2+}) could be measured in the extracts using an iCAP6300 Duo ICP-OES (Thermo Fisher Scientific, Waltham, USA).

The analyses of total organic nitrogen (TON) and total organic phosphorous (TOP) as well as the inorganic PO_4^{3-} , NH_4^+ and NO_3^- fractions followed procedures as detailed by Walinga et al. (1989). For both TON and TOP determination, aliquots of soil (0.3 ± 0.01 g) were dried at 70°C for two hours. Then, 2.5 mL of destruction reagent ($\text{Se-H}_2\text{SO}_4\text{-C}_7\text{H}_6\text{O}_3$) was added to each weighed sample. After two hours of waiting time, the samples were placed in a HotBlock digestion system at 100°C for two hours. The samples were cooled until room temperature was reached and 0.5 mL of H_2O_2 was added. When the reaction faded, the samples were transferred back to the HotBlock system at 300°C for another two hours. After a cooldown period until room temperature, 75 mL of deionized H_2O was added to the final solution and the samples were homogenized by thorough hand-shaking. Hereafter, the final extracts were measured for total N and P on the Skalar Primacs analyzer.

The extractable inorganic P and N fractions were analyzed based on ammonium acetate-EDTA and KCl extraction procedures, respectively, as described by Houba et al. (1989). To this end, two aliquots of soil samples were weighed of 5 ± 0.1 g and 10 ± 0.1 g, for respectively P and N fractions. Then, 25 mL of ammonium acetate-EDTA and KCl was added to these samples, respectively. Samples were thoroughly shaken and were stored in the fridge for 1 hour to rest. Then, the final extracts were analyzed for total PO_4^{3-} , NH_4^+ and NO_3^- fractions on an iCAP6300 Duo ICP-OES (Thermo Fisher Scientific, Waltham, USA).

Section 3.3: PFAA chemical extraction

Prior to extraction, each sample was weighed and spiked with 80 μL of a 125 $\text{pg } \mu\text{L}^{-1}$ mass-labeled perfluoroalkyl carboxylic acid (PFCA) and perfluoroalkyl sulfonic acid (PFSA) mixture solution (ISTD, Wellington Laboratories, Guelph, Canada). Hereafter, 10 mL of acetonitrile (ACN) was added to the samples after which they were thoroughly vortex-mixed. The samples were sonicated three times for 10 min and vortex-mixed in between the periods. Then, samples were placed overnight on a shaking (135 rpm, room temperature, GFL3 020, VWR International, Leuven, Belgium). Afterwards, samples were centrifuged (4°C , 10 min, 2400 rpm, 1037 g, Eppendorf centrifuge 5804R, rotor A-4-44) and the resulting supernatant was transferred to a 15 ml PP tube. The homogenates of eggs

(0.30 ± 0.01 g), earthworms (0.15 ± 0.01 g) and vegetables (0.30 ± 0.01 g) were then extracted using a protocol described by Powley et al. (2005) with few adjustments. The supernatant was vacuum-dried to approximately 0.5 mL using a rotational vacuum concentrator (30 °C, type 5301, Hamburg, Germany). The extract was transferred to a PP Eppendorf tube which contained 0.05 g of graphitized carbon powder (Supelclean ENVI-Carb, Sigma-Aldrich, Overijse, Belgium) and 35 μ L of glacial acetic acid to remove chemical impurities. Subsequently, the 15 mL tube was rinsed twice with 250 μ L of ACN, which was transferred to the Eppendorf tube. The extracts were vortex-mixed and centrifuged (4 °C, 10 min, 10,000 rpm, 1037 g, Eppendorf centrifuge 5415R, rotor F 45-24-11), after which the supernatant was transferred to a new Eppendorf tube and vacuum-dried until nearly complete dryness using a rotational-vacuum-concentrator (Eppendorf concentrator 5301, 30 °C, type 5301, Hamburg, Germany). Finally, 100 μ L of a 2% ammonium hydroxide solution (dissolved in ACN) was added to the dried extract and filtered through a 13 mm Acrodisc Ion Chromatography Syringe Filter with 0.2 μ m Supor (PES) membrane (VWR International, Leuven, Belgium) into a PP injector vial prior to instrumental analysis.

The oven-dried soil (0.30 ± 0.01 g) and rain water (10 ± 0.1 mL) samples were extracted according to an extraction protocol described by Groffen et al. (2019c) based on solid-phase extraction (SPE). Chromabond HR-WAX SPE cartridges (Macherey–Nagel, Germany) were conditioned and equilibrated with 5 mL of ACN and 5 mL of Milli-Q (MQ; 18.2 m Ω , TOC: 2.0 ppb, Merck Millipore, Belgium), respectively. The samples were then loaded onto the cartridges and washed with 5 mL of a 25 mM ammonium acetate solution (dissolved in MQ; VWR International, Belgium) and 2 mL of ACN. Thereafter, cartridges were eluted with 2 \times 1 mL of a 2% ammonium hydroxide solution (dissolved in ACN). This eluent was vacuum-dried until nearly complete dryness using a rotational-vacuum-concentrator (Eppendorf concentrator 5301, 30 °C, type 5301, Hamburg, Germany). Then, 100 μ L of 2% ammonium hydroxide solution was added to the dried extract and it was thoroughly vortex-mixed. Finally, the extracts were filtered through an Ion Chromatography Acrodisc 13 mm syringe filter with a 0.2 μ m Supor polyethersulfone (PES) membrane (VWR International, Leuven, Belgium) into a PP injector vial.

Table S3.1: MRM transitions, mass-labeled internal standards (ISTDs), cone voltages (V) and collision energy (eV) for the target poly- and perfluoroalkyl substances and their internal standard (Table was adopted from Groffen et al. (2021)).

Compound	Precursor ion (m/z)	Product ion (m/z)		Cone Voltage (V)	Collision energy (eV) for diagnostic transition1	Collision energy (eV) for diagnostic transition 2	Internal standard (ISTD) used for quantification
		Diagnostic product ion 1	Diagnostic product ion 2				
PFBA	213	169	169	19	19	50	¹³ C ₄ -PFBA
PFPeA	263	219	219	15	10	45	¹³ C ₄ -PFBA
PFHxA	313	269	119	19	21	65	[1,2- ¹³ C ₂]PFHxA
PFHpA	363	319	169	24	40	30	[1,2- ¹³ C ₂]PFHxA
PFOA	413	369	169	22	13	60	[1,2,3,4- ¹³ C ₄]PFOA
PFNA	463	419	169	28	17	20	[1,2,3,4,5- ¹³ C ₅]PFNA
PFDA	513	469	219	25	29	29	[1,2- ¹³ C ₂]PFDA
PFUnDA	563	519	169	18	30	35	[1,2- ¹³ C ₂]PFUnDA
PFDoDA	613	569	319	22	21	30	[1,2- ¹³ C ₂]PFDoDA
PFTTrDA	663	619	319	26	21	30	[1,2- ¹³ C ₂]PFDoDA
PFTeDA	713	669	169	28	21	21	[1,2- ¹³ C ₂]PFDoDA
PFBS	299	80	99	40	65	45	¹⁸ O ₂ -PFHxS
PFHxS	399	80	99	22	30	60	¹⁸ O ₂ -PFHxS
PFOS	499	80	99	60	58	58	[1,2,3,4- ¹³ C ₄]PFOS
PFDS	599	80	99	29	63	63	[1,2,3,4- ¹³ C ₄]PFOS
HFPO-DA	285	169		30	20		[1,2- ¹³ C ₂]PFHxA
NaDONA	376.8	250.7	84.8	23	35	32	[1,2,3,4- ¹³ C ₄]PFOA
¹³ C ₄ -PFBA	217	172	172	19	19	50	
[1,2- ¹³ C ₂]PFHxA	315	269	119	19	21	65	
[1,2,3,4- ¹³ C ₄]PFOA	417	372	172	22	13	60	
[1,2,3,4,5- ¹³ C ₅]PFNA	468	423	172	28	17	20	
[1,2- ¹³ C ₂]PFDA	515	470	220	25	29	29	
[1,2- ¹³ C ₂]PFUnDA	565	520	170	18	32	35	
[1,2- ¹³ C ₂]PFDoDA	615	570	320	22	21	30	
¹⁸ O ₂ -PFHxS	403	84	103	22	30	60	
[1,2,3,4- ¹³ C ₄]PFOS	503	80	99	60	58	58	

Section 3.4: Data processing

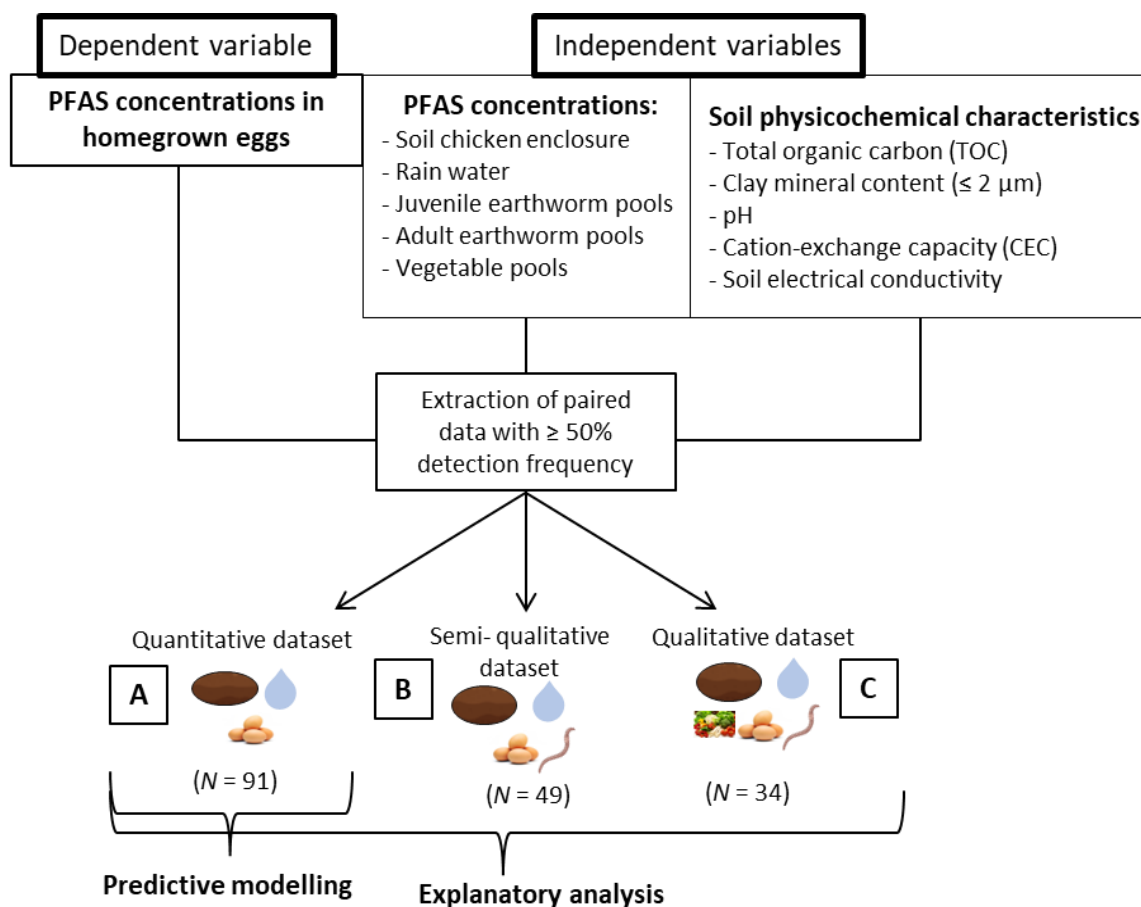


Fig. S3.2: Schematic overview of the raw dataset (dependent and independent variables) and data processing workflow from the present study which resulted into three sub datasets, of which the quantitative dataset (A) was used for the predictive modelling and the qualitative datasets (B and C) for the explanatory analysis of the multiple regression modelling: A) soil PFAS concentrations, rain water PFAA concentrations and soil physicochemical characteristics; B) soil PFAA concentrations, rain water PFAA concentrations, soil physicochemical characteristics, juvenile and adult earthworm PFAA concentrations; C) soil PFAA concentrations, rain water PFAA concentrations, soil physicochemical characteristics, juvenile earthworm PFAS concentrations and vegetable pool PFAA concentrations.

Section 3.5: Statistical analyses

Table S3.2: Data of the measured PFAA concentrations in chicken enclosure soil (in ng/g dry weight) and in homegrown eggs (in ng/g wet weight) along with the relevant soil physicochemical properties from the dataset of 2022, which was used as external validation dataset for the final predictive models.

Compound	Matrix	Location									
		ID1	ID2	ID3	ID4	ID5	ID6	ID7	ID8	ID9	ID10
PFOS	soil	1.98	0.960	5.99	2.13	4.58	1.63	4.04	0.118	1.05	2.08
	egg	27.2	1.26	233	17.5	117	3.51	35.7	9.39	10.3	112
PFBA	soil	0.454	0.125	1.59	0.085	0.494	0.085	0.152	0.175	0.085	0.324
	egg	0.351	0.806	2.32	0.367	3.11	0.459	1.12	0.458	0.563	0.618
PFOA	soil	0.700	0.219	1.04	0.558	0.557	0.269	0.593	0.404	0.395	0.423
	egg	0.683	0.577	2.40	0.484	1.05	0.250	0.407	0.430	0.690	0.459
PFNA	soil	0.187	0.154	0.452	0.132	0.196	0.080	0.214	0.076	0.233	0.290
	egg	0.395	0.101	0.553	0.131	0.355	0.122	0.185	0.155	0.343	0.462
PFDA	soil	0.841	0.665	0.871	0.503	0.775	0.420	0.727	0.271	0.495	0.609
	egg	1.22	0.604	1.38	0.660	1.05	0.580	0.530	0.582	1.20	1.87
PFUnDA	soil	0.274	0.119	0.196	0.116	0.278	0.320	0.265	0.331	0.196	0.110
	egg	0.406	0.070	0.871	0.239	0.596	0.320	0.407	0.312	0.960	1.08
PFDoDA	soil	0.926	0.095	0.313	0.425	0.698	0.774	0.518	0.290	0.372	0.712
	egg	4.35	0.877	8.86	1.80	7.17	1.24	2.44	1.70	3.17	14.1
PFTrDA	soil	0.137	0.293	0.237	0.259	0.205	0.260	0.307	0.174	0.270	0.185
	egg	2.98	0.239	13.2	2.03	6.40	1.57	2.71	1.70	3.92	14.9
PFTeDA	soil	0.240	0.347	0.579	0.828	0.444	0.191	0.709	0.441	0.391	0.503
	egg	7.25	0.301	21.1	4.57	11.2	3.59	6.66	4.12	6.70	28.7
TOC		3.85	6.45	4.61	4.25	4.52	5.17	11.60	4.35	2.65	5.72
Soil physicochemical property											
Clay content		2.39	1.23	3.80	3.02	2.55	1.99	2.38	2.52	2.22	2.57
pH _{kcl}		7.48	6.70	6.38	6.61	6.98	5.72	7.19	7.38	6.22	6.91
Ca ²⁺		12.1	21.5	22.4	14.4	20.31	8.66	24.3	14.9	10.3	15.7
Mg ²⁺		2.35	3.99	1.65	1.53	2.01	1.30	3.54	4.30	1.45	3.37
Mn ²⁺		0.074	0.060	0.178	0.094	0.162	0.083	0.197	0.163	0.086	0.179
Al ³⁺		0.035	0.050	0.023	0.026	0.029	0.067	0.070	0.025	0.037	0.017
Fe ³⁺		0.027	0.028	0.027	0.025	0.021	0.025	0.030	0.046	0.045	0.028

Table S3.3: Overview of the model quality metrics for the predictive models of egg PFAA concentrations with and without soil physicochemical characteristics as predictor variables.

Compound	Model type	Model significance level	Adjusted R^2	AIC value	RMSE	MAE
PFOS	without soil physicochemical characteristics	$P < 0.0001$ $F_{8,80} = 19.0$	41.2	3.95	0.99	0.76
	with soil physicochemical characteristics	$P < 0.0001$ $F_{1,87} = 62.6$	62.1	-28.5	0.77	0.58
PFBA	without soil physicochemical characteristics	$P < 0.0001$ $F_{1,87} = 18.2$	16.3	-229	0.27	0.2
	with soil physicochemical characteristics	$P < 0.0001$ $F_{6,82} = 7.21$	29.8	-240	0.23	0.18
PFOA	without soil physicochemical characteristics	$P < 0.0001$ $F_{1,87} = 45.8$	34.5	-86.8	0.6	0.48
	with soil physicochemical characteristics	$P < 0.0001$ $F_{5,83} = 36.1$	66.6	-145	0.41	0.28
PFNA	without soil physicochemical characteristics	$P < 0.0001$ $F_{1,87} = 110$	55.3	-380	0.12	0.09
	with soil physicochemical characteristics	$P < 0.0001$ $F_{7,81} = 21.5$	61.9	-389	0.1	0.07
PFDA	without soil physicochemical characteristics	$P = 0.11$ $F_{1,87} = 2.58$	1.79	-239	0.26	0.2
	with soil physicochemical characteristics	$P < 0.0001$ $F_{7,81} = 3.06$	25.8	-252	0.22	0.17
PFUnDA	without soil physicochemical characteristics	$P < 0.05$ $F_{1,87} = 3.49$	2.76	-239	0.26	0.19
	with soil physicochemical characteristics	$P < 0.0001$ $F_{8,80} = 7.46$	37.1	-273	0.19	0.14
PFDoDA	without soil physicochemical characteristics	$P = 0.20$ $F_{1,87} = 1.70$	0.798	-82	0.62	0.48
	with soil physicochemical characteristics	$P < 0.05$ $F_{3,85} = 3.90$	9.12	-87	0.58	0.45
PFTrDA	without soil physicochemical characteristics	$P = 0.55$ $F_{1,87} = 0.348$	0.286	-117	0.51	0.41
	with soil physicochemical characteristics	$P < 0.001$ $F_{6,82} = 5.22$	22.3	-136	0.43	0.34
PFTeDA	without soil physicochemical characteristics	$P = 0.07$ $F_{1,87} = 2.94$	2.15	-18.2	0.88	0.71
	with soil physicochemical characteristics	$P < 0.0001$ $F_{7,81} = 6.54$	30.6	-44.8	0.74	0.61

Table S3.4: Overview of the calculated variance inflation factors (VIFs) of each predictor variable in the predictive models of the egg PFAA concentrations.

Predictive modeling									
PFAAs	Soil concentration	TOC	Clay content	pH _{KCl}	Mn ²⁺	Fe ³⁺	Al ³⁺	Mg ²⁺	Ca ²⁺
PFOS	1.22	1.89	1.32	1.10	1.92	1.76	1.38	NA	NA
PFBA	1.13	NA	1.34	1.09	1.20	NA	NA	NA	1.18
PFOA	1.17	NA	NA	1.11	NA	1.32	1.18	1.24	NA
PFNA	1.32	1.95	1.40	1.04	1.76	1.75	NA	NA	NA
PFDA	1.52	1.98	1.35	1.13	1.69	1.67	NA	1.94	NA
PFUnDA	1.11	NA	1.32	1.14	1.78	1.37	1.42	1.30	NA
PFDoDA	1.15	1.39	1.20	1.13	1.63	NA	NA	NA	NA
PFTrDA	1.12	1.39	1.19	1.06	1.64	NA	NA	NA	NA
PFTeDA	1.20	NA	1.24	1.12	1.68	NA	1.47	1.27	Na

Table S3.5: Overview of the calculated variance inflation factors (VIFs) of each explanatory variable in the regression models of the explanatory analysis.

Explanatory analysis				
PFAAs	Soil concentration	juvenile worm concentration	adult worm concentration	vegetable pool concentration
PFOS	1.77	2.31	2.21	NA
PFBA	1.06	1.25	1.22	1.02
PFOA	1.00	1.03	1.04	1.01
PFNA	1.00	1.01	1.01	1.03
PFDA	1.07	1.09	1.02	1.01
PFUnDA	1.06	1.13	1.11	1.04
PFDoDA	1.07	1.34	1.35	1.09
PFTrDA	1.01	1.40	1.40	1.03
PFTeDA	1.04	1.36	1.37	1.04

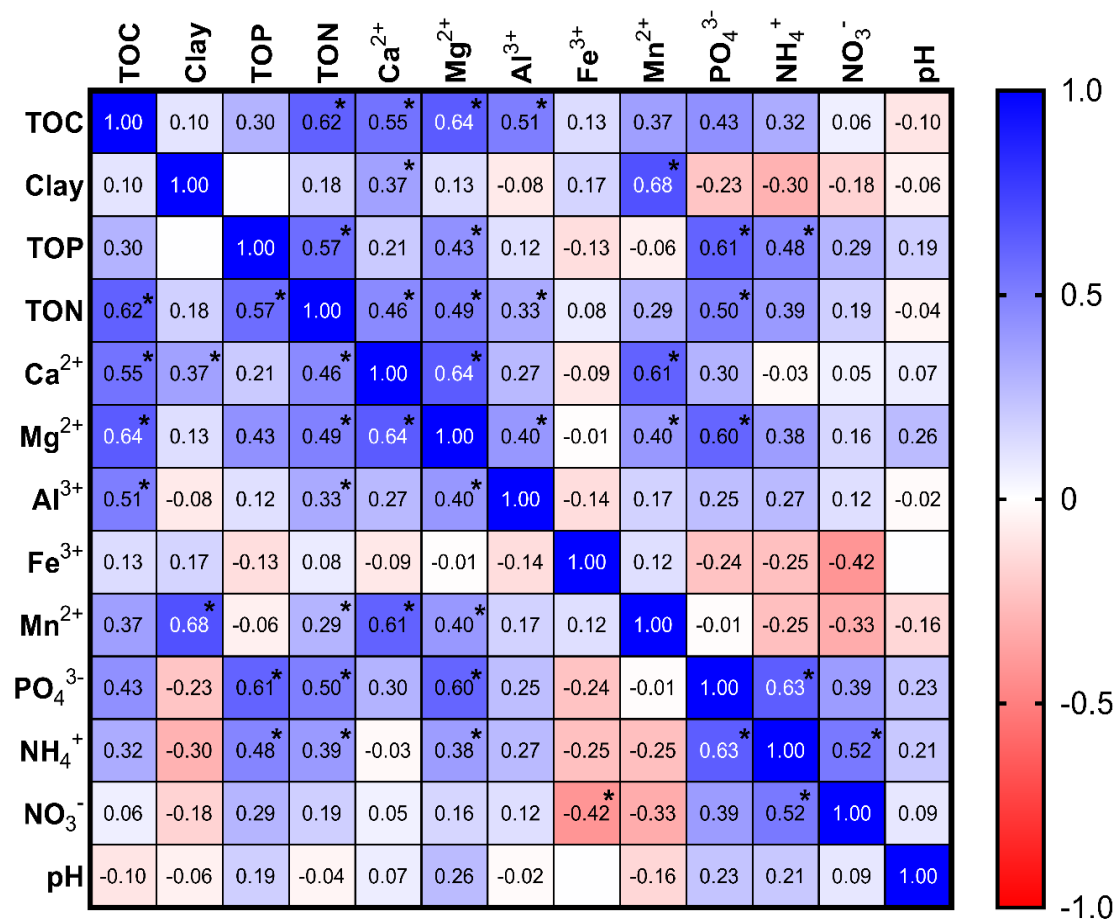


Fig. S3.2: Pearson correlation heatmap of soil physicochemical properties showing significant (*: $P \leq 0.05$) correlation coefficient values among the variables.

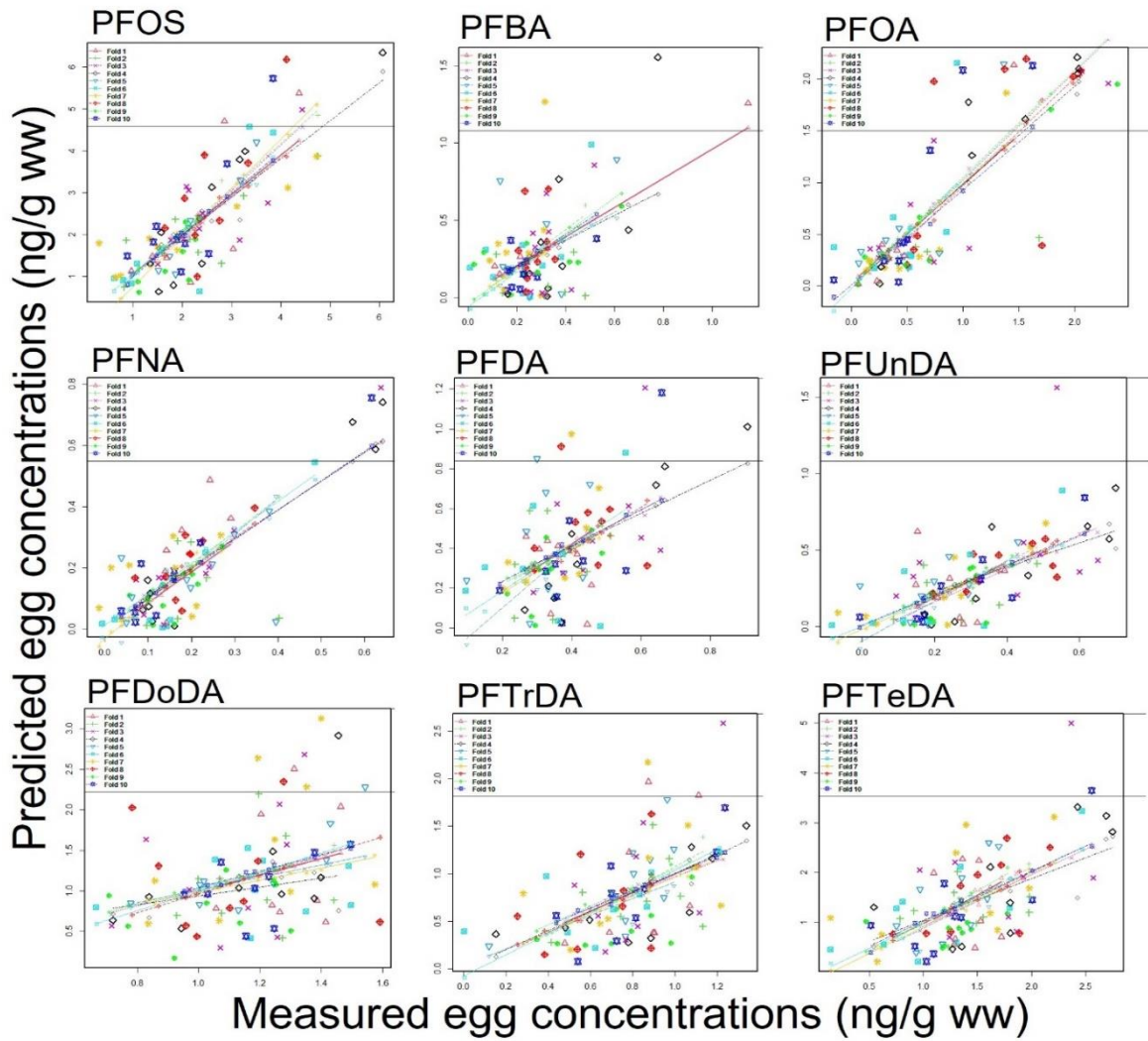


Fig. S3.3: Internal validation of the predictive models for nine PFAAs showing 10-fold cross-validation of the predicted egg concentrations from the final regression models and the cross-validated predicted egg concentrations.

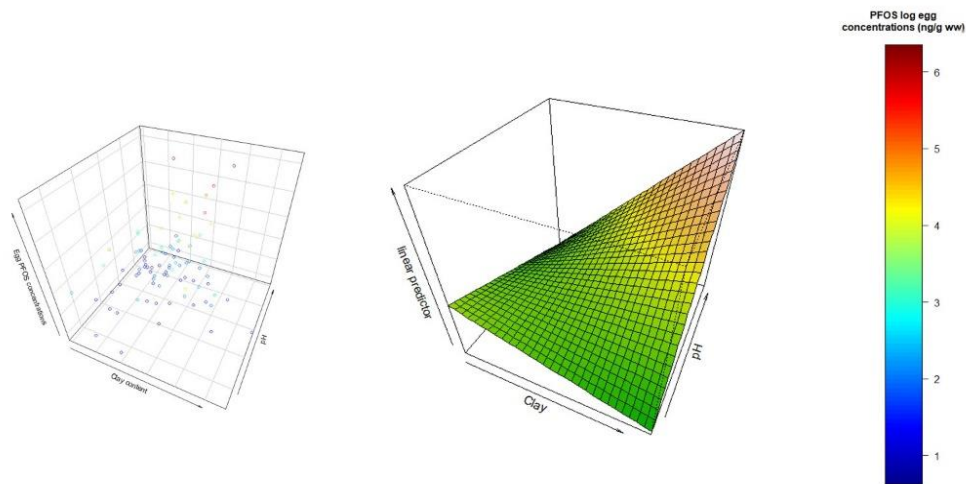


Fig. S3.4: 3D surface plot showing the synergistic interaction between pH and clay content and their relationship with egg PFAS concentrations. Example in figure: PFOS egg concentrations.

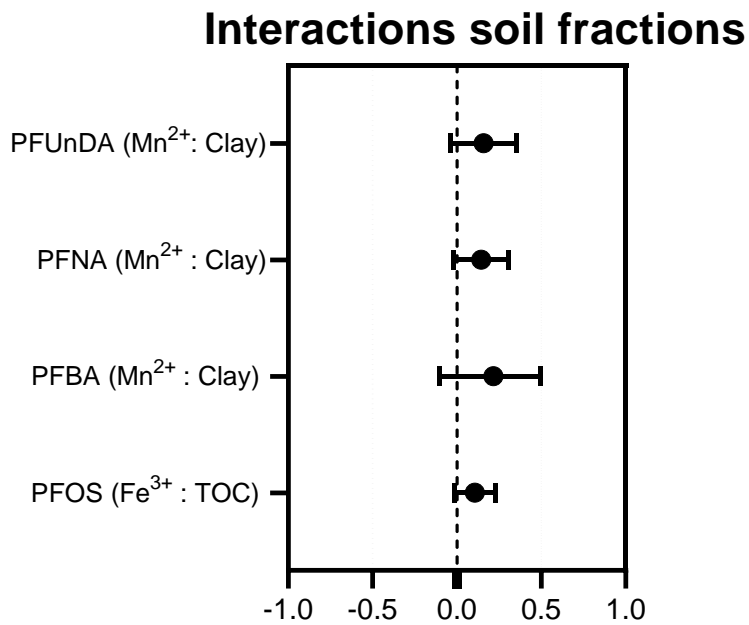


Fig. S3.5: Additional significant interactions between the exchangeable metal cations (Mn²⁺ and Fe³⁺) and the soil clay content/total organic carbon content.

Section 3.6: Estimations PFAA intake via dust inhalation

Based on literature data, rough and simple estimations of PFAA intake via dust inhalation were calculated and compared with the corresponding intake via soil consumption to assess the relative importance of both exposure sources to the free-ranging laying hens. The following assumptions were considered for the calculation of dust and soil PFAA intake:

- Chickens have an average respiration volume of 1.20 m³/day (Sedlmajer et al., 2009).
- Dust intake per hen per day: three dust intake scenarios of 0.100, 0.01 and 0.001 ng/m³ dust concentration were selected. These values are based on air measurements from the Flemish Environment Agency (VMM) nearby the fluorochemical plant in Antwerp and at a non-suspect background site (Peters et al., 2022).
- Soil consumption per hen per day: three soil intake scenarios were considered of 2, 5 and 10 grams of soil per hen per day (based on Stephens et al., 1995).

As an example, the intake calculations below were conducted for PFDoDA, one of the compounds for which no significant relationship was found with the soil concentrations (Fig. 3.3). An average soil concentration of 0.189 ng/g dw (Table 2) was considered.

PFDoDA intake via dust inhalation per hen per day:

Best-case scenario: 1.20 m³ /day * 0.001 ng/m³ = 0.0012 ng/day

Modal-case scenario: 1.20 m³/day * 0.01 mg/m³ = 0.012 ng/day

Worse-case scenario: 1.20 m³/day * 0.100 mg/m³ = 0.120 ng/day

PFDoDA intake via soil consumption per hen per day:

Best-case scenario: 2 g/day * 0.189 ng/g dw = 0.378 ng/day

Modal-case scenario: $5 \text{ g/day} * 0.189 \text{ ng/g dw} = 0.945 \text{ ng/day}$

Worse-case scenario: $10 \text{ g/day} * 0.189 \text{ ng/g dw} = 1.89 \text{ ng/day}$

Chapter 4

Section 4.1: Study area

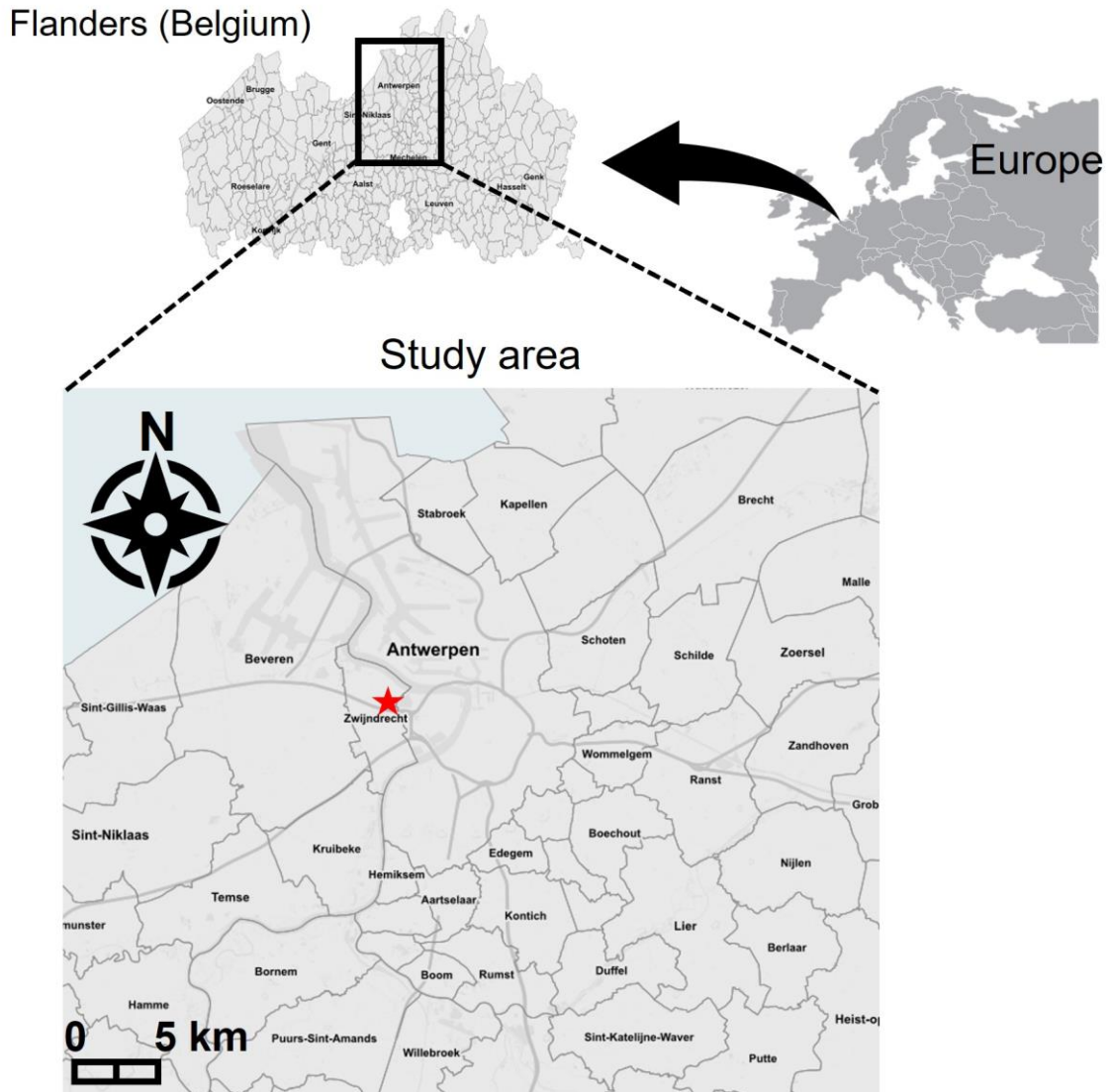


Fig. S4.1: Study area showing the region of Antwerp (Belgium, Europe) in which the soil, rain water and vegetable samples were collected from the private vegetable gardens ($N = 88$). The red star indicates the major fluorochemical plant site in Antwerp (Belgium).

Section 4.2: vegetable food categories and pretreatment

Table S4.1: Overview of the collected crop samples, classified according to their functional category, which were collected in private gardens along a distance gradient from a fluorochemical plant site in Antwerp (Belgium). The samples received different pretreatments, including washing with milli-Q water and/or removal of inedible parts. NA = no pretreatment applied.

Category	Type	Pretreatment
Walnuts (N = 19)	NA	removal of outer shell and fruit peel
Tree fruits (N = 36)	apple	washing, removal of stem and seeds
	pear	washing, removal of stem and seeds
	plum	washing
	fig	washing, removal of outer shell
Small fruits (N = 37)	grape	washing
	blackberry	washing
	blueberry	washing
	strawberry	removal of stem and washing
	redcurrant	washing
	kiwiberry	washing
	passion fruit	removal of outer shell
Root vegetables (N = 13)	carrot	washing and removal of peel
	beetroot	removal of stems and leaves, washing and peeling
Fruit vegetables (N = 29)	paprika	removal of stem and seeds, washing
	zucchini	removal of stem and washing
	cucumber	removal of stem and washing
	pumpkin	removal of peel
	tomato	removal of stem and washing
	pickle	removal of stem and washing
Shoot vegetables (N = 34)	rhubarb	removal of leaves and washing
	celery	removal of leaves and washing
	leak	removal of roots and outer leaves, washing
Leafy vegetables (N = 19)	lettuce	removal of outer leaves and washing
	spinach	removal of blooming stems and washing
	warmos	removal of outer leaves and washing
Legumes (N = 6)	bean	removal of stem and washing
	legume	removal of peel and washing
Herbs (N = 4)	plain parsley	washing

Section 4.3: PFAS targeted analytes and chemical analyses

Prior to extraction, each sample was weighed and spiked with 10 ng of mass-labeled perfluoroalkyl carboxylic acid (PFCA) and perfluoroalkyl sulfonic acid (PFSA) mixture solution (ISTD, Wellington Laboratories, Guelph, Canada). Hereafter, 10 mL of acetonitrile (ACN) was added to the samples after which they were thoroughly vortex-mixed. The samples were sonicated three times for 10 min and vortex-mixed in between the periods. Then, samples were placed overnight on a shaking (135 rpm, room temperature, GFL3 020, VWR International, Leuven, Belgium). Afterwards, samples were centrifuged (4 °C, 10 min, 2400 rpm, 1037 *g*, Eppendorf centrifuge 5804R, rotor A-4-44) and the resulting supernatant was transferred to a 15 ml PP tube.

The oven-dried soil (0.30 ± 0.01 g) and rainwater (10 ± 0.1 ml) samples were extracted according to an extraction protocol described by Groffen et al. (2019c) based on solid-phase extraction (SPE). Chromabond HR-WAX SPE cartridges (Macherey–Nagel, Germany) were conditioned and equilibrated with 5 mL of ACN and 5 mL of Milli-Q (MQ; 18.2 mΩ, TOC: 2.0 ppb, Merck Millipore, Belgium), respectively. The samples were then loaded onto the cartridges and washed with 5 mL of a 25 mM ammonium acetate solution (dissolved in MQ; VWR International, Belgium) and 2 mL of ACN. Thereafter, cartridges were eluted with 2×1 mL of a 2% ammonium hydroxide solution (dissolved in ACN). This eluent was vacuum-dried until nearly complete dryness using a rotational-vacuum-concentrator (Eppendorf concentrator 5301, 30 °C, type 5301, Hamburg, Germany). Then, 100 µL of a 2% ammonium hydroxide solution was added to the dried extract and it was thoroughly vortex-mixed. Finally, the extracts were filtered through an Ion Chromatography Acrodisc 13 mm syringe filter with a 0.2 µm Supor polyethersulfone (PES) membrane (VWR International, Leuven, Belgium) into a PP injector vial.

The homogenates of vegetables (0.30 ± 0.01 g) were extracted using a protocol described by Powley et al. (2005) with few adjustments. The supernatant was vacuum-dried to approximately 0.5 mL using a rotational vacuum concentrator (30°C, type 5301, Hamburg, Germany). The extract was transferred to a PP Eppendorf tube which contained 0.05 g of graphitized carbon powder (Supelclean ENVI-Carb, Sigma-Aldrich, Overijse, Belgium) and 35 µL of glacial acetic acid to remove chemical impurities. Subsequently, the 15 mL tube was rinsed twice with 250 µL of ACN, which was transferred to the Eppendorf tube. The extracts were vortex-mixed and centrifuged (4°C, 10 min, 10,000 rpm, 1037 *g*, Eppendorf centrifuge 5415R, rotor F 45-24-11), after which the supernatant was transferred to a new Eppendorf tube and vacuum-dried until nearly complete dryness using a

rotational-vacuum-concentrator (Eppendorf concentrator 5301, 30°C, type 5301, Hamburg, Germany). Finally, 100 µL of a 2% ammonium hydroxide solution (dissolved in ACN) was added to the dried extract and filtered through a 13 mm Acrodisc Ion Chromatography Syringe Filter with 0.2 µm Supor (PES) membrane (VWR International, Leuven, Belgium) into a PP injector vial prior to instrumental analysis.

The soil, rainwater and vegetable food samples were measured for 29 targeted PFAS analytes using ultrahigh performance liquid chromatography (ACQUITY, TQD, Waters, Milford, MA, USA) coupled to a tandem quadrupole (TQD) mass spectrometer (UPLC-MS/MS), operating in negative electrospray ionization (Table S4.2). The different target analytes were separated using an ACQUITY UPLC BEH C18 VanGuard Precolumn (2.1 × 50 mm; 1.7 µm, Waters, USA). The mobile phase solvents consisted of ACN- and HPLC-grade water, which were both dissolved in 0.1% HPLC-grade formic acid. The solvent gradient started at 65% of water to 0% of water in 3.4 min and back to 65% water at 4.7 min. The flow rate was set to 450 µL/min and the injection volume was 6 µL (partial loop). PFAS contamination that might originate from the LC-system was retained by insertion of an ACQUITY BEH C18 pre-column (2.1 × 30 mm; 1.7 µm, Waters, USA) between the solvent mixer and the injector. The target PFAS analytes were identified and quantified based on multiple reaction monitoring (MRM) of the diagnostic transitions that are displayed in Table S4.2.

Table S4.2: Overview of the multiple reaction monitoring (MRM) transitions for the precursor and product ion of all targeted per- and polyfluoroalkyl substances (PFAS) along with the mass-labelled internal standards (ISTDs) used for the quantification. The cone voltage (V) and collision energy (eV) used for the fragmentation and detection of the targeted PFAS and their internal standard are also given. Table was adopted from Groffen et al. (2021) with minor adjustments.

Compound	Precursor ion (m/z)	Product ion (m/z)		Cone Voltage (V)	Collision energy (eV) for diagnostic transition1	Collision energy (eV) for diagnostic transition 2	Internal standard (ISTD) used for quantification
		Diagnostic product ion 1	Diagnostic product ion 2				
PFBA	213	169	169	19	19	50	¹³ C ₄ -PFBA
PFPeA	263	219	219	15	10	45	¹³ C ₄ -PFBA
PFHxA	313	269	119	19	21	65	[1,2- ¹³ C ₂]PFHxA
PFHpA	363	319	169	24	40	30	[1,2- ¹³ C ₂]PFHxA
PFOA	413	369	169	22	13	60	[1,2,3,4- ¹³ C ₄]PFOA
PFNA	463	419	169	28	17	20	[1,2,3,4,5- ¹³ C ₅]PFNA
PFDA	513	469	219	25	29	29	[1,2- ¹³ C ₂]PFDA
PFUnDA	563	519	169	18	30	35	[1,2- ¹³ C ₂]PFUnDA
PFDoDA	613	569	319	22	21	30	[1,2- ¹³ C ₂]PFDoDA
PFTTrDA	663	619	319	26	21	30	[1,2- ¹³ C ₂]PFDoDA
PFTeDA	713	669	169	28	21	21	[1,2- ¹³ C ₂]PFDoDA
PFBS	299	80	99	40	65	45	¹⁸ O ₂ -PFHxS

PFPeS	349	80	99	40	40	40	[1,2,3,4- ¹³ C ₄]PFOS
PFHxS	399	80	99	22	30	60	¹⁸ O ₂ -PFHxS
PFHpS	449	80	98.5	40	47	45	[1,2,3,4- ¹³ C ₄]PFOA
PFOS	499	80	99	60	58	58	[1,2,3,4- ¹³ C ₄]PFOS
PFDS	599	80	99	29	63	63	[1,2,3,4- ¹³ C ₄]PFOS
FBSA	298	78	219	40	38	27	¹⁸ O ₂ -PFHxS
NaDONA	376.8	250.7	84.8	23	35	32	[1,2,3,4- ¹³ C ₄]PFOA
HFPO-DA	285	169		30	20		[1,2- ¹³ C ₂]PFHxA
PF4OPeA	228.8	85		20	20		[1,2,3,4- ¹³ C ₄]PFOA
PF5OHxA	279	85		20	20		[1,2- ¹³ C ₂]PFHxA
3,6-OPFHpA	201	85		30	25		[1,2- ¹³ C ₂]PFHxA
4:2 FTS	327	307	80	20	25	33	[1,2,3,4- ¹³ C ₄]PFOS
6:2 FTS	427	407	80	20	25	33	[1,2,3,4- ¹³ C ₄]PFOS
8:2 FTS	527	507	81	36	40	40	[1,2,3,4- ¹³ C ₄]PFOS
9CL-PF3ONS	531	350.5	83	46	32	37	[1,2,3,4,5- ¹³ C ₅]PFNA

11CL- PF3OUdS	631	451	83	50	40	35	[1,2- ¹³ C ₂]PFUnDA
PFEESA	315	135	69	30	20	55	[1,2- ¹³ C ₂]PFDA
¹³ C ₄ -PFBA	217	172	172	19	19	50	
[1,2- ¹³ C ₂]PFHxA	315	269	119	19	21	65	
[1,2,3,4- ¹³ C ₄]PFOA	417	372	172	22	13	60	
[1,2,3,4,5- ¹³ C ₅]PFNA	468	423	172	28	17	20	
[1,2- ¹³ C ₂]PFDA	515	470	220	25	29	29	
[1,2- ¹³ C ₂]PFUnDA	565	520	170	18	32	35	
[1,2- ¹³ C ₂]PFDoDA	615	570	320	22	21	30	
¹⁸ O ₂ -PFHxS	403	84	103	22	30	60	
[1,2,3,4- ¹³ C ₄]PFOS	503	80	99	60	58	58	

Section 4: PFAS quality control and assurance

During the homogenization of the biotic samples, solvent blanks (= 10 mL of ACN) were included every 10 samples to check for cross contamination between the samples. For the extraction, one procedural blank (= 10 mL ACN spiked with 10 ng of mass-labeled perfluoroalkyl carboxylic acid (PFCA) and perfluoroalkyl sulfonic acid (PFSA) mixture (Internal Standard, ISTD; MPFAC-MXA, Wellington Laboratories, Guelph, Canada) was included per 15 samples to verify any contamination during the extraction. In the case of batch contamination, the procedural blank values were subtracted from the subsequently measured samples. During the PFAS analysis, instrumental blanks (ACN) were regularly injected to rinse the columns and prevent cross contamination between injections. Calibration curves were prepared by adding a constant amount of the ISTD to varying concentrations of an unlabeled PFAS mixture. The serial dilution of this mixture was performed in ACN. A linear regression function with highly significant linear fit (all $R^2 > 0.98$; all $P < 0.001$) described the ratio between concentrations of unlabeled and labeled PFAS. Individual PFAS were quantified using their corresponding ISTD with exception of perfluoropentanoic acid (PFPeA), perfluoroheptanoic acid (PFHpA), perfluorotridecanoic acid (PFTrDA), perfluorotetradecanoic acid (PFTeDA), perfluorobutane sulfonic acid (PFBS), perfluorodecane sulfonic acid (PFDS) and the perfluoroalkylether acids. These analytes were all quantified using the ISTD of the compound closest in terms of functional group and size (Table S4.2), which was validated by Groffen et al. (2021).

Limits of quantification (LOQs) were calculated for each detected analyte, in matrix, as the concentration corresponding to a peak signal-to-noise ratio of 10 (Table S4.3). The matrix extraction recovery of the ISTD was calculated based on the peak-signal area of the ISTDs in the samples divided by the peak-signal area of a extracted procedural blank and ranged from 8.06 to 106% and averaged 44.0%, 81.4% and 89.3% for rainwater, soil and the crops.

Table S4.3: Limits of quantification (LOQ), assessed in matrix, for all the detected analytes in the examined matrices. Dw = dry weight; ww = wet weight.

Compound	Soil (ng/g dw)	Rainwater (ng/L)	Fruit (ng/g ww)	Vegetables (ng/g ww)	Walnuts (ng/g ww)
PFBA	0.366	0.424	0.026	0.028	0.065
PFPeA	0.058	0.467	0.021	0.020	0.028
PFHxA	0.120	0.677	0.013	0.026	0.039
PFHpA	0.097	1.12	0.051	0.045	0.110
PFOA	0.056	0.791	0.018	0.069	0.085
PFNA	0.065	0.738	0.020	0.013	0.008
PFDA	0.091	1.32	0.014	0.013	0.029
PFUnDA	0.055	1.28	0.015	0.012	0.042
PFDoDA	0.097	1.40	0.053	0.049	0.060
PFTTrDA	0.089	1.47	0.026	0.022	0.046
PFTeDA	0.142	1.51	0.108	0.075	0.094
PFBS	0.240	2.23	0.112	0.104	0.066
PFHxS	0.130	1.06	0.061	0.074	0.098
PFHpS	0.157	1.20	0.019	0.027	0.024
PFOS	0.038	0.301	0.021	0.025	0.016
PFDS	0.024	0.964	0.151	0.166	0.152
4:2 FTS	0.128	1.12	0.059	0.056	0.011
6:2 FTS	0.066	1.19	0.089	0.072	0.093
8:2 FTS	0.109	1.54	0.103	0.098	0.101
FBSA	0.093	0.489	0.069	0.072	0.094
PF5OHxA	0.126	0.841	0.121	0.102	0.099
11Cl-PF3OUdS	0.014	0.954	0.028	0.090	0.100
PFEESA	0.016	1.26	0.103	0.110	0.122

Section 4.5: Soil physicochemical characteristics

The pH of freshly collected soil samples was measured using a multimeter electrode (WTW Multi 3430 SET F, probe SenTix 940, Weilheim, Germany), after thoroughly mixing 5 ± 0.1 g of soil with 25 mL of KCl (1M) solution and leaving to rest for 1 h. The soil electrical conductivity was measured following the International Standard Organization's protocol 11265:1994. To this end, 25 mL of deionized H₂O was added to 5 ± 0.1 g of fresh soil and leaving to rest for 30 min at room temperature to dissolve all electrolytes. After filtering the extract through a glass fiber filter, the conductivity was measured with a multimeter (WTW Multi 3430 SET F, TetraCon 92 probe, Weilheim, Germany). The soil clay content (particle size $<2 \mu\text{m}$) was analyzed based on the principle of laser diffraction

with the Malvern Mastersizer 2000 and Hydro 2000G (Malvern Instruments Ltd, Malvern, UK). Fresh soil aliquots of 1 ± 0.1 g were digested with 15 mL of 33% technical grade H_2O_2 and 10 mL of technical grade HCl at room temperature to degrade organic material and iron complexes in the soil. After 24 hours, the digestion reactions were catalyzed by adding another 25 mL of H_2O_2 to the samples and boiling them until the reaction faded. Prior to clay content analysis, the samples were sieved through a sieve with 2.0 mm mesh size. The soil organic matter content was measured based on the loss on ignition (LOI) method, following the procedure of Heiri et al (2001). Around 5 ± 0.1 g of soil, oven-dried at $60^\circ C$, was weighed into foiled aluminum bags which had been dried at $105^\circ C$ for two hours. Then, the soil was dried at $105^\circ C$ for 48 hours after which it was stored in a desiccator to cool down until room temperature. The samples were weighed and thereafter incinerated in a muffle furnace at $550^\circ C$ for six hours. Lastly, the samples were weighed again and the TOC was calculated using the following equation:

$$LOI_{550}(\%) = 100 * \frac{(DW_{105} - DW_{550})}{DW_{105}}$$

$$TOC(\%) = \frac{LOI_{550}}{1.742}$$

with DW defined as the dry weight of the soil sample after drying at $105^\circ C$ or $550^\circ C$ and 1.742 being the “Van Bemmelen” factor, assuming that 58% of the total organic matter is organic carbon (Nelson and Sommers, 1996).

Exchangeable base cations were analyzed according to Brown’s procedures. Briefly, the soil wet weight was volumetrically determined by drying at $105^\circ C$. Afterwards, 25 ml of NH_4Ac buffer solution (pH = 7) was added to 2.5 ± 0.1 g of oven-dried ($60^\circ C$) soil and the sample was three-dimensionally shaken for one hour. Then, the pH of the extracts was measured with a multimeter (WTW Multi 3430 SET F, probe SenTix 940, Weilheim, Germany) and they were filtered using a $0.45 \mu m$ polyester syringe filter. Titration curves (*in duplo*) were set up by adding 0.1 mL of CH_3COOH (0.1 M) acid in steps to 50 mL of NH_4Ac buffer solution (pH = 7) until pH 6 was reached. Based on the calculated moisture content and H^+ concentration, the exchangeable basic cations (Ca^{2+} , Mg^{2+} , K^+ and Na^+) and exchangeable acidic cations (Al^{3+} , Fe^{3+} and Mn^{2+}) could be measured in the extracts using an iCAP6300 Duo ICP-OES (Thermo Fisher Scientific, Waltham, USA).

The analyses of total organic nitrogen (TON) and total organic phosphorous (TOP) as well as the inorganic PO_4^{3-} , NH_4^+ and NO_3^- fractions followed procedures as detailed by Walinga et al. (1989).

For both TON and TOP determination, aliquots of soil (0.3 ± 0.01 g) were dried at 70°C for two hours. Then, 2.5 mL of reagent ($\text{Se-H}_2\text{SO}_4\text{-C}_7\text{H}_6\text{O}_3$) was added to each weighed sample. After two hours, the samples were placed in a HotBlock digestion system at 100°C for two hours. The samples were cooled until room temperature was reached and 0.5 mL of H_2O_2 was added. When the reaction faded, the samples were transferred back to the HotBlock system at 300°C for another two hours. After a cooldown period until room temperature, 75 mL of deionized H_2O was added to the final solution and the samples were homogenized by thorough hand-shaking. Hereafter, the final extracts were measured for total N and P on the Skalar Primacs analyzer.

The extractable inorganic P and N fractions were analyzed based on ammonium acetate-EDTA and KCl extraction procedures, respectively, as described by Houba et al. (1989). To this end, two aliquots of soil samples were weighed of 5 ± 0.1 g and 10 ± 0.1 g, for respectively P and N fractions. Then, 25 mL of ammonium acetate-EDTA and KCl was added to these samples, respectively. Samples were thoroughly shaken and were stored in the fridge for 1 hour to rest. Then, the final extracts were analyzed for total PO_4^{3-} , NH_4^+ and NO_3^- fractions on an iCAP6300 Duo ICP-OES (Thermo Fisher Scientific, Waltham, USA).

Table S4.4: Correlation matrix between the individual soil physicochemical characteristics of the vegetable gardens. Correlation coefficients in bold represent significant ($P < 0.05$) relationships.

	PO ₄ ³⁻	NH ₄ ⁺	NO ₃ ⁻	TON	TOP	TOC	Clay	CON	Ca ²⁺	K ⁺	Mg ²⁺	Na ⁺	Al ³⁺	Fe ³⁺	Mn ²⁺	pH
PO ₄ ³⁻	1	0.12	0.54	0.21	0.17	0.28	-	-0.04	0.17	0.08	0.18	0.04	0.25	0.07	-0.10	0.29
NH ₄ ⁺		1.00	0.15	0.03	0.26	0.20	0.09	-0.07	0.06	0.06	-0.05	0.07	0.23	0.17	0.02	0.01
NO ₃ ⁻			1.00	0.27	0.26	0.13	0.14	0.00	0.08	0.05	-0.01	0.07	0.11	0.01	-0.17	0.12
TON				1.00	0.61	0.59	0.15	0.06	0.14	0.09	0.21	0.00	0.09	0.17	0.07	0.18
TOP					1.00	0.14	0.17	0.16	0.06	0.08	0.02	0.05	0.16	0.06	0.02	0.12
TOC						1.00	0.11	-0.13	0.36	0.16	0.30	0.01	0.08	0.13	0.15	0.30
Clay							1.00	-0.02	0.44	0.17	0.21	0.05	0.09	0.12	0.60	0.06
CON								1.00	0.14	0.56	0.42	0.63	0.08	0.05	0.19	0.04
Ca ²⁺									1.00	0.54	0.70	0.33	0.19	0.26	0.66	0.27
K ⁺										1.00	0.81	0.67	0.42	0.23	0.44	0.02
Mg ²⁺											1	0.47	0.34	0.29	0.57	0.12
Na ⁺												1	0.23	0.01	0.26	0.11
Al ³⁺													1	0.24	0.20	0.10
Fe ³⁺														1	-0.14	0.05
Mn ²⁺															1	0.12
pH																1

Section 4.6: soil and crop concentrations in function of major point source

The soil concentrations in every soil depth layer followed a strong distance gradient (Fig. S4.2) in function of the distance towards the fluorochemical plant in Antwerp (Belgium). The majority of variation in soil concentrations falls within 4 km distance from this plant site, exemplified by the slopes for every soil depth layer (Fig. S4.1). Therefore, the soil data were divided into two separate sub datasets (zone A = 0-4 km from the plant site, zone B = 4-30 km from the plant site) to enable representative comparisons of PFAS concentrations among the soil depth layers. On the other hand, Σ PFAS concentrations in the edible parts of the considered crop categories did not show any

significant distance gradient with respect to the fluorochemical plant (Fig.S2b), thus was not further split into sub datasets.

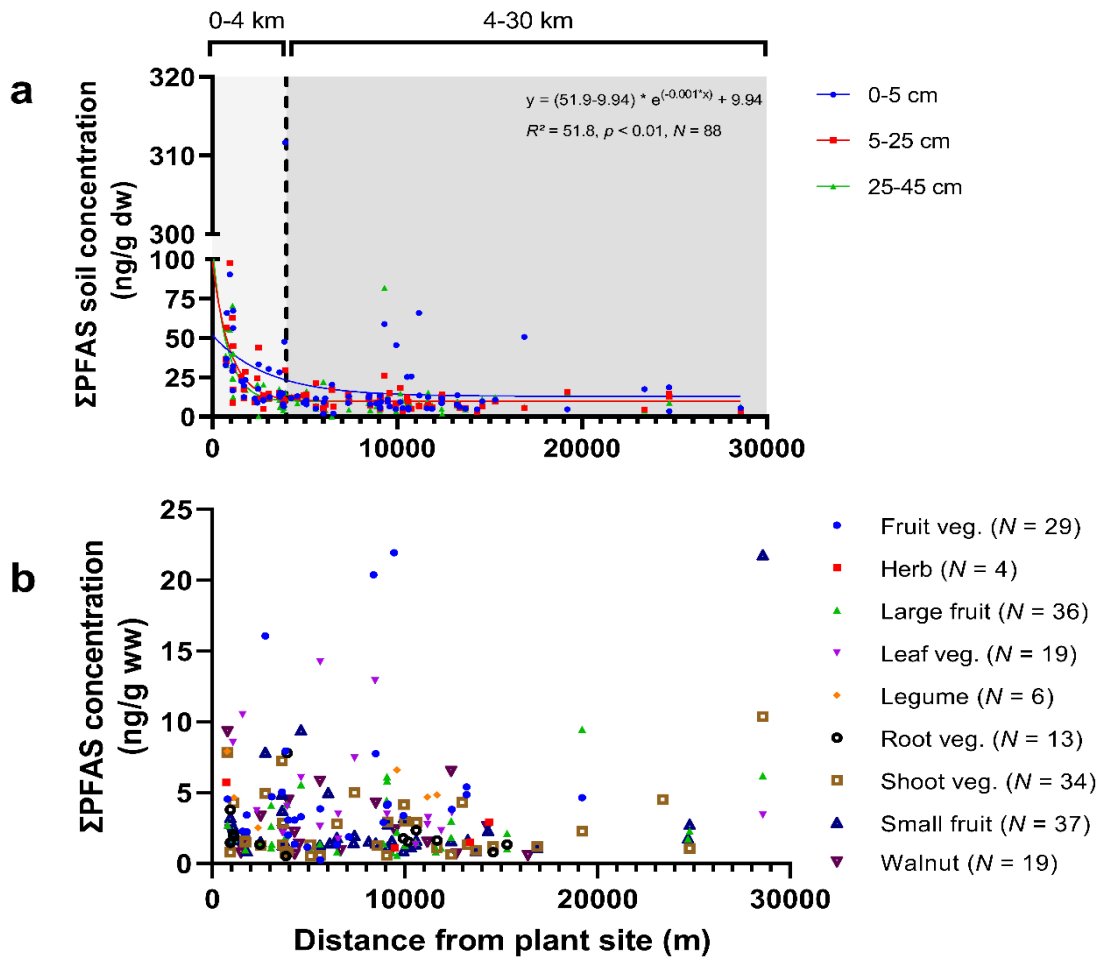


Fig. S4.2: a) Σ PFAS soil concentrations, in ng/g dry weight (dw), of the examined soil depth layers (blue: 0-5 cm, red: 5-25 cm, green: 25-45 cm) in the vegetable garden segment of private backyards, showing an exponential decrease with increasing distance from the major fluorochemical plant in Antwerp (Belgium). The exponential slope equation for the 5-25 cm depth layer is provided as an example for description of the exponential curves. b) Σ PFAS concentrations, in ng/g wet weight (ww), in the crop categories which showed no significant distance gradient with respect to the fluorochemical plant in Antwerp (Belgium).

Section 4.7: Crop species-specific root depth

In Table S4.5, the soil depth layer corresponding to the maximum root intensity zone for the considered crop species of the present study are given, which is henceforth referred to as the species-specific root zone. These data were adopted from studies conducted in field conditions.

Table S4.5: Overview of the selected species-specific soil depth layers as measure for the soil PFAS concentrations in the predictive models, based on the soil depth at which max. root intensity was commonly reported in literature for the respective vegetable food species of the present study.

Vegetable food category	Species		Soil depth max. root intensity (cm)	Species-specific soil depth layer (cm)	Literature reference
Fruit vegetable	Tomato (<i>Solanum lycopersicum</i>)	N = 6	30-45	25-45	Machado et al. (2003)
	Zucchini (<i>Cucurbita pepo</i>)	N = 8	30-60	25-45	Dragovic et al. (2012)
	Pumpkin (<i>Cucurbita sp.</i>)	N = 4	>60	25-45	Dragovic et al. (2012)
Leaf vegetable	Lettuce (<i>Lactuca sativa</i>)	N = 7	20	5-25	Thorup-Kristensen (2001)
Shoot vegetable	Leek (<i>Allium ampeloprasum</i> var. <i>porrum</i>)	N = 1	10-20	5-25	Smit et al. (1996)
	Celery (<i>Apium graveolens</i> var. <i>dulce</i>)	N = 1	25-50	25-45	Christiansen et al. (2006)
	Rhubarb (<i>Rheum rhabarbarum</i>)	N = 21	>200	25-45	Weaver and Bruner (1927)
Root vegetable	Carrot (<i>Daucus carota</i> subsp. <i>sativa</i>)	N = 5	35	25-45	Thorup-Kristensen (2001)
Legume	Garden pea (<i>Pisum sativum</i>)	N = 4	15	5-25	Fan et al. (2016)
Small fruit	Strawberry (<i>Fragaria sp.</i>)	N = 5	30-45	25-45	Weaver and Bruner (1927)
	Black- and raspberry (<i>Rubus sp.</i>)	N = 6	30-45	25-45	Ames (2006)

From a biological perspective, the soil concentration corresponding to these species-specific root zone depths may be a relevant measure of soil in the MLR models, as nutrient/water uptake and concurrent PFAS uptake may be largest in these specific soil depths for a given crop species. Nevertheless, plants can deviate from these biologically expected root growth distributions and adapt to opportunistic root-growth strategies due to different biological- and physicochemical soil conditions (Niu et al., 2013; Schenk and Jackson, 2002). For instance, plants can grow primarily shallow, lateral root systems in the subsurface soil layer (0-30 cm) due to frequent water irrigation and nutrient input (Fort et al., 2017; Sharma et al., 2017), which can be common practices in private gardens. Therefore, the soil concentration of every examined depth layer was also included as candidate measure for soil in the MLR models. Finally, crops may also acquire water and nutrients

from the top soil in their early-life stage while progressively more uptake from deeper soil layers may take place as their growth proceeds which would be representative of the mean soil concentration of the three depth layers. Therefore, five MLR models were constructed which were identical in terms of model structure but differed in their measure of the soil concentration variable. Three MLR models were built with the soil concentration from the 0-5 cm, 5-25 cm and 25-45 cm layer as variables, respectively. The fourth MLR model contained the species-specific soil concentration, corresponding to the depth layer at which the biologically maximum root intensity is observed for the given species (based on literature data). The final model contained the mean soil concentration based on the three soil depths. Then, the MLR model with the lowest AIC value was selected for further model refinement and predictions.

Section 4.8: evaluation and validation criteria of the predictive models

For the final best-fit predictive models of the vegetable food concentrations, diagnostic plots were run to evaluate model assumptions including linearity, normality and homoscedasticity of the residuals. Variance inflation factors (VIFs) were calculated for all the significant predictors to assess the degree of collinearity among them (Table S4.6). If VIF was ≥ 2.5 , the variable with the lowest partial R^2 was excluded from the model, following Johnston et al. (2018). Considerable degree of collinearity was observed between exchangeable Mg^{2+} and Ca^{2+} , after which the latter one was excluded from the regression models.

Table S4.6: Overview of the calculated variance inflation factors (VIFs) for each explanatory variable in the regression models. Considerable collinearity ($VIF > 2.80$) was observed between exchangeable Mg^{2+} and Ca^{2+} .

Variance inflation factors									
PFAS	Soil concentration	TOP	Clay content	Fe^{3+}	Al^{3+}	Mg^{2+}	Ca^{2+}	NH_4^+	NO_3^-
PFBA	1.38	1.49	1.57	1.71	1.47	2.84	3.50	1.29	1.24
PFPeA	1.22	1.34	1.63	1.68	1.45	2.82	3.49	1.34	1.25
PFHxA	1.11	1.34	1.58	1.57	1.46	2.81	3.53	1.25	1.27
PFOA	1.22	1.35	1.63	1.69	1.45	2.82	3.49	1.34	1.25
PFDA	1.05	1.34	1.58	1.59	1.45	2.81	3.49	1.25	1.24
PFUnDA	1.16	1.35	1.57	1.57	1.45	2.89	3.55	1.27	1.25
PFDoDA	1.18	1.40	1.57	1.67	1.45	2.81	3.49	1.29	1.24
PFTTrDA	1.30	1.51	1.58	1.58	1.47	3.00	3.68	1.27	1.24
PFTeDA	1.08	1.35	1.59	1.60	1.45	2.83	3.50	1.25	1.24

Section 4.9: Detailed overview PFAS concentrations in soil, rain water and vegetable food

Table S4.7: Overview of the mean PFAS concentrations (ng/g dry weight) in the three examined soil depth layers (0-5 cm, 5-25 cm and 25-45 cm) of the vegetable garden segment from private gardens, situated ≤ 4 km and > 4 km from a major fluorochemical plant in Antwerp (Belgium). The min. – max. concentration range is denoted between brackets. ϵ = concentration of one datapoint. LOQ = limit of quantification. ND = not detected.

PFAS	LOQ	0-5 cm		5-25 cm		25-45 cm	
		<4 km (N = 30)	>4 km (N = 58)	<4 km (N = 30)	>4 km (N = 58)	<4 km (N = 30)	>4 km (N = 58)
		2.60	1.45	2.49	1.34	2.33	1.17
PFBA	0.366	(<LOQ-42.9)	(<LOQ-49.5)	(<LOQ-59.5)	(<LOQ-4.55)	(<LOQ-15.0)	(<LOQ-35.4)
		0.112	0.180	0.140	0.208	0.268	0.335
PFPeA	0.058	(<LOQ-1.16)	(<LOQ-0.592)	(<LOQ-0.512)	(<LOQ-2.32)	(<LOQ-3.01)	(<LOQ-4.81)
		0.534	0.495	0.635	0.597	0.689	0.650
PFHxA	0.120	(<LOQ-1.95)	(<LOQ-1.95)	(<LOQ-1.46)	(<LOQ-4.28)	(<LOQ-2.26)	(<LOQ-5.06)
		0.173	0.203	0.311	0.340	0.284	0.313
PFHpA	0.097	(<LOQ-0.938)	(<LOQ-0.938)	(<LOQ-1.48)	(<LOQ-4.36)	(<LOQ-2.67)	(<LOQ-3.15)
		1.18	1.14	1.26	1.22	1.71	1.67
PFOA	0.056	(0.627-5.41)	(0.084-4.36)	(<LOQ-4.12)	(<LOQ-3.14)	(<LOQ-3.17)	(<LOQ-41.9)
		0.238	0.234	0.233	0.229	0.202	0.199
PFNA	0.065	(<LOQ-0.473)	(<LOQ-1.46)	(<LOQ-0.587)	(<LOQ-1.52)	(<LOQ-0.620)	(<LOQ-0.778)
		0.635	0.727	0.636	0.728	0.517	0.609
PFDA	0.091	(0.359-1.34)	(<LOQ-2.21)	(<LOQ-0.949)	(<LOQ-7.03)	(<LOQ-1.20)	(<LOQ-2.58)
		0.203	0.207	0.225	0.229	0.174	0.178
PFUnDA	0.055	(<LOQ-0.392)	(<LOQ-0.679)	(<LOQ-0.529)	(<LOQ-0.941)	(<LOQ-0.502)	(<LOQ-0.526)
		1.34	1.76	0.856	1.28	0.530	0.954
PFDoDA	0.097	(0.317-2.85)	(<LOQ-48.1)	(<LOQ-2.47)	(<LOQ-10.2)	(<LOQ-2.18)	(<LOQ-7.38)
		0.303	0.402	0.345	0.444	0.241	0.341
PFTTrDA	0.089	(<LOQ-0.722)	(<LOQ-3.63)	(<LOQ-0.882)	(<LOQ-4.40)	(<LOQ-1.19)	(<LOQ-3.02)
		0.653	0.668	0.569	0.584	0.410	0.426
PFTeDA	0.142	(<LOQ-1.77)	(<LOQ-5.86)	(<LOQ-1.81)	(<LOQ-4.55)	(<LOQ-1.38)	(<LOQ-2.67)
		4.66	6.79	0.273	2.40	0.795	1.16
PFBS	0.240	(<LOQ-19.2)	(<LOQ-302)	(<LOQ-11.4)	(<LOQ-80.8)	(<LOQ-5.47)	(<LOQ-2.51)
		<LOQ	0.216	0.153	0.352	<LOQ	0.600
PFHxS	0.130	(<LOQ-0.184)	(<LOQ-0.433)	(<LOQ-4.60)	(<LOQ-0.704)	(<LOQ-2.14)	(<LOQ-1.20)
		<LOQ	<LOQ	<LOQ	<LOQ	<LOQ	<LOQ
PFHpS	0.157	(<LOQ-0.600)	(<LOQ-0.150)	(<LOQ-0.804)	(<LOQ-0.949)	(<LOQ-1.83)	(<LOQ-0.305)
		10.1	3.45	8.70	2.07	8.37	1.74
PFOS	0.038	(0.818-34.1)	(<LOQ-20.0)	(<LOQ-28.7)	(<LOQ-7.77)	(<LOQ-30.3)	(<LOQ-16.7)
		<LOQ	<LOQ	<LOQ	<LOQ	<LOQ	<LOQ
PFDS	0.024	(<LOQ-0.056)	ND	ND	ND	(<LOQ-0.181)	(<LOQ-0.043)
		5.48	0.859	5.05	0.940	4.93	0.720
FBSA	0.093	(<LOQ-39.7)	(<LOQ-5.99)	(<LOQ-35.8)	(<LOQ-5.74)	(<LOQ-37.4)	(<LOQ-5.33)
		0.659	0.795	0.212	0.347	0.195	0.331
6:2 FTS	0.066	(<LOQ-2.44)	(<LOQ-44.1)	(<LOQ-1.12)	(<LOQ-6.09)	(<LOQ-3.42)	(<LOQ-2.43)
		<LOQ	0.229	<LOQ	0.163	<LOQ	0.230
8:2 FTS	0.109	ND	(<LOQ-0.458)	(<LOQ-1.87)	(<LOQ-0.327)	ND	(<LOQ-0.460)
9Cl-							
PF3ONS	0.041	0.303 ϵ	0.046 ϵ	ND	ND	ND	ND

Table S4.8: Overview of the mean and min.-max. PFAS concentrations (ng/L) in the rainwater samples from private gardens in Antwerp (Belgium). LOQ = limit of quantification.

Compound	Mean concentration (ng/L)	Min.-max range
PFBA	31.6	<LOQ-604
PFPeA	3.33	<LOQ-113
PFHxA	19.8	<LOQ-691
PFHpA	<LOQ	<LOQ-30.8
PFOA	29.8	<LOQ-286
PFNA	2.95	<LOQ-48.3
PFDA	10.4	<LOQ-101
PFUnDA	<LOQ	<LOQ-44.2
PFDoDA	<LOQ	<LOQ-19.1
PFTTrDA	<LOQ	<LOQ-17.5
PFTeDA	<LOQ	<LOQ-15.6
PFBS	2.97	<LOQ-71.9
PFHxS	2.04	<LOQ-68.3
PFOS	4.71	<LOQ-79.7
6:2 FTS	<LOQ	<LOQ-22.0
FBSA	14.3	<LOQ-708

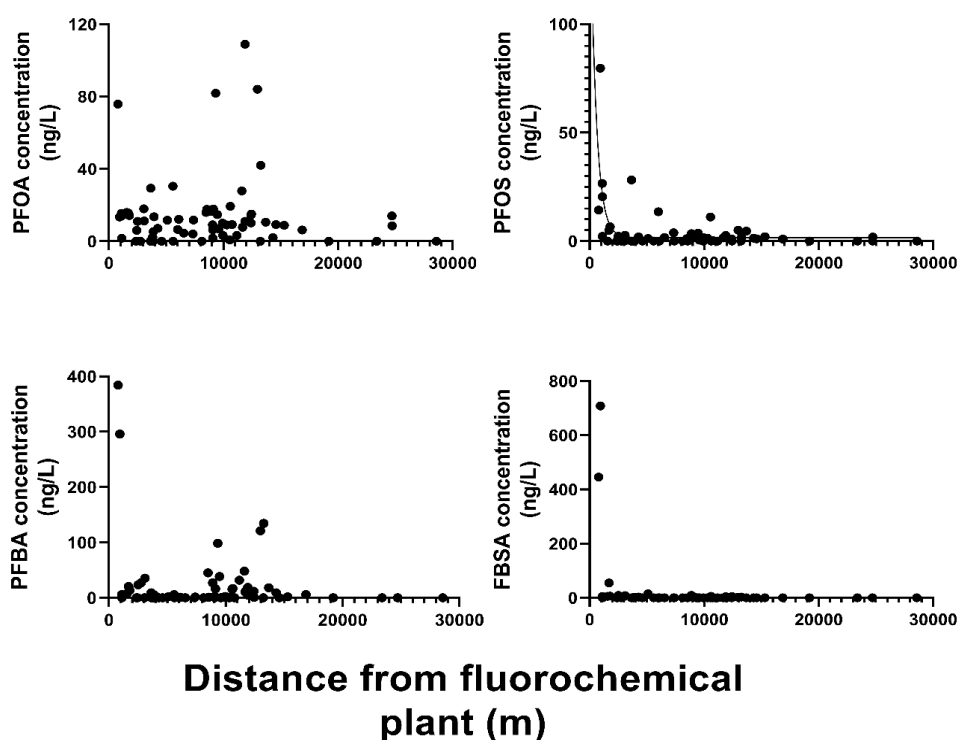


Fig. S4.3: PFAS concentrations (ng/L) in rainwater in function of the distance (m) from the plant site for compounds of which the soil concentrations were significantly inversely related with the distance from the fluorochemical plant site in Antwerp (Belgium). Rainwater concentrations for PFOS significantly decreased in an exponential way with increasing distance from the plant site ($P < 0.01$; $R^2 = 0.44$).

Table S4.9: Overview of the mean and min.-max. PFAS concentrations (ng/g wet weight) in the collected crop samples (vegetable subcategories, fruit subcategories and walnuts) of the vegetable garden segment from private gardens in Antwerp (Belgium). LOQ = limit of quantification. ND = not detected.

PFAS	Vegetable categories						Fruit categories		Walnut
	Fruit veg.	Herb	Leaf veg.	Legume	Root veg.	Shoot veg.	Small fruit	Large fruit	
PFBA	0.663	0.967	0.508	0.917	0.202	0.270	0.241	0.468	0.190
	<LOQ-7.22	<LOQ-3.26	<LOQ-4.15	<LOQ-4.59	<LOQ-0.530	<LOQ-1.76	<LOQ-1.83	<LOQ-4.41	<LOQ-1.64
PFPeA	0.073	0.057	0.099	0.111	0.028	0.163	0.257	0.393	0.214
	<LOQ-0.477	<LOQ-0.137	<LOQ-0.837	<LOQ-0.247	<LOQ-0.153	<LOQ-0.905	<LOQ-1.06	<LOQ-2.78	<LOQ-0.805
PFHxA	0.194	0.228	0.232	0.129	0.127	0.128	0.185	0.106	0.043
	<LOQ-0.864	<LOQ-0.396	<LOQ-1.11	<LOQ-0.601	<LOQ-0.739	<LOQ-0.718	<LOQ-1.28	<LOQ-0.590	<LOQ-0.178
PFHpA	0.056	<LOQ	<LOQ	0.086	<LOQ	0.006	<LOQ	<LOQ	<LOQ
	<LOQ-0.330	<LOQ	<LOQ-0.517	<LOQ-0.493	<LOQ	<LOQ-0.092	<LOQ-0.495	<LOQ-0.393	<LOQ
PFOA	0.336	0.719	0.398	0.220	0.225	0.327	0.256	0.188	0.145
	<LOQ-3.03	0.199-1.85	<LOQ-2.27	0.099-0.360	<LOQ-0.927	<LOQ-1.55	<LOQ-1.20	<LOQ-0.883	<LOQ-0.488
PFNA	0.023	<LOQ	0.020	<LOQ	<LOQ	<LOQ	0.027	<LOQ	<LOQ
	<LOQ-0.302	<LOQ	<LOQ-0.148	<LOQ	<LOQ-0.062	<LOQ-0.214	<LOQ-0.547	<LOQ-0.067	<LOQ-0.049
PFDA	0.182	0.232	0.217	0.121	0.145	0.150	0.138	0.104	0.045
	<LOQ-0.715	<LOQ-0.427	<LOQ-0.772	<LOQ-0.307	<LOQ-0.832	<LOQ-0.485	<LOQ-0.642	<LOQ-0.589	<LOQ-0.144
PFUnDA	0.109	0.162	0.118	0.124	0.090	0.096	0.054	0.029	0.539
	<LOQ-0.507	<LOQ-0.321	<LOQ-0.518	<LOQ-0.462	<LOQ-0.323	<LOQ-0.534	<LOQ-0.414	<LOQ-0.374	<LOQ-5.01
PFDoDA	0.365	0.376	0.515	0.494	0.346	0.348	0.363	0.282	0.291
	<LOQ-0.978	0.151-0.692	0.082-2.03	0.124-1.41	0.104-1.42	<LOQ-1.28	<LOQ-0.951	<LOQ-0.619	0.105-0.745
PFTrDA	0.190	<LOQ	0.080	0.037	0.059	0.107	0.129	0.063	0.049
	<LOQ-3.00	<LOQ	<LOQ-0.982	<LOQ-0.117	<LOQ-0.210	<LOQ-0.987	<LOQ-1.89	<LOQ-0.491	<LOQ-0.115
PFTeDA	0.236	<LOQ	0.124	0.136	0.183	0.157	0.204	0.163	<LOQ
	<LOQ-0.899	<LOQ	<LOQ-0.528	<LOQ-0.342	<LOQ-0.639	<LOQ-1.23	<LOQ-1.03	<LOQ-0.560	<LOQ-0.355
PFBS	0.038	<LOQ	0.655	0.184	0.074	0.284	0.177	0.151	0.013
	<LOQ-0.500	<LOQ	<LOQ-9.56	<LOQ-0.992	<LOQ-0.809	<LOQ-4.79	<LOQ-4.02	<LOQ-4.12	<LOQ-0.109
PFHxS	<LOQ	<LOQ	<LOQ	<LOQ	0.083	<LOQ	<LOQ	0.074	<LOQ
	<LOQ-0.128	<LOQ	<LOQ-0.484	<LOQ	<LOQ-0.712	<LOQ-0.746	<LOQ-0.845	<LOQ-0.694	<LOQ-0.292
PFHpS	<LOQ	<LOQ	<LOQ	<LOQ	<LOQ	<LOQ	<LOQ	<LOQ	0.032
	<LOQ-0.028	<LOQ	<LOQ	<LOQ	<LOQ	0.083	<LOQ	<LOQ	<LOQ-0.299
PFOS	<LOQ	0.053	0.033	0.010	0.017	0.061	0.016	<LOQ	0.013

	<LOQ- 0.067	<LOQ- 0.188	<LOQ- 0.286	<LOQ- <LOQ	<LOQ- 0.120	<LOQ- 0.832	<LOQ- 0.241	<LOQ- 0.023	<LOQ- 0.043
4:2 FTS	1.24	0.309	0.671	0.546	0.808	0.388	0.325	0.384	0.823
	<LOQ- 4.52	<LOQ- 1.24	<LOQ- 2.93	<LOQ- 2.20	<LOQ- 3.48	<LOQ- 6.11	<LOQ- 2.55	<LOQ- 4.64	<LOQ- 6.57
6:2 FTS	0.567	<LOQ	0.567	<LOQ	<LOQ	0.224	0.457	0.108	<LOQ
	<LOQ- 11.	<LOQ- <LOQ	<LOQ- 10.6	<LOQ- <LOQ	<LOQ- 0.132	<LOQ- 5.71	<LOQ- 13.5	<LOQ- 1.82	<LOQ- 0.147
8:2 FTS	<LOQ								
	<LOQ- 0.298	<LOQ- <LOQ	<LOQ- <LOQ	<LOQ- <LOQ	<LOQ- <LOQ	<LOQ- <LOQ	<LOQ- 0.189	<LOQ- 0.103	<LOQ- <LOQ
FBSA	0.846	<LOQ	0.079	<LOQ	0.268	0.083	0.142	0.210	0.129
	<LOQ- 17.9	<LOQ- <LOQ	<LOQ- 1.22	<LOQ- 0.220	<LOQ- 1.82	<LOQ- 1.14	<LOQ- 2.57	<LOQ- 1.82	<LOQ- 1.82
PF50HxA	ND	ND	ND	ND	ND	ND	0.004	ND	ND
							0.146- <LOQ		
11Cl- PF3OUdS	ND	ND	ND	ND	ND	ND	<LOQ	<LOQ	ND
							<LOQ- 0.150	<LOQ- 0.081	
PFEESA	ND	ND	ND	ND	ND	ND	<LOQ	<LOQ	ND
							<LOQ- 1.36	<LOQ- <LOQ	

Section 4.10: PFAS concentrations soil depth layer

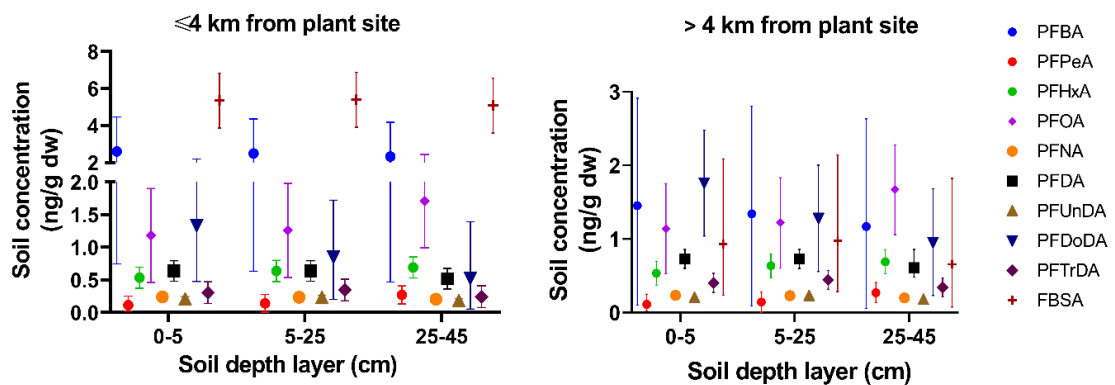


Fig. S4.4: Comparison of the mean PFAS concentrations (ng/g dry weight) among the three examined soil depth layers (0-5 cm, 5-25 cm and 25-45 cm) of the vegetable garden segment from private gardens, situated ≤ 4 km ($N = 30$) and >4 km ($N = 56$) from a major fluorochemical plant site in Antwerp (Belgium). No significant differences in soil concentrations were observed among the soil depth layers (all $P > 0.05$). The error bar represents the lower and upper 95% confidence interval.

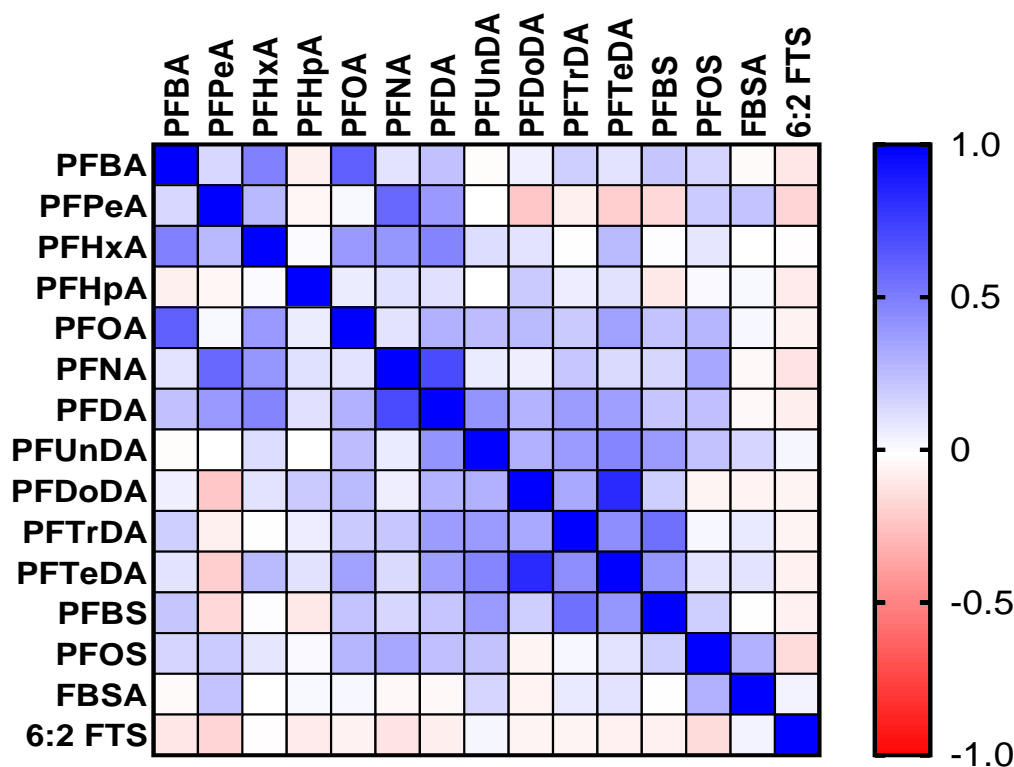
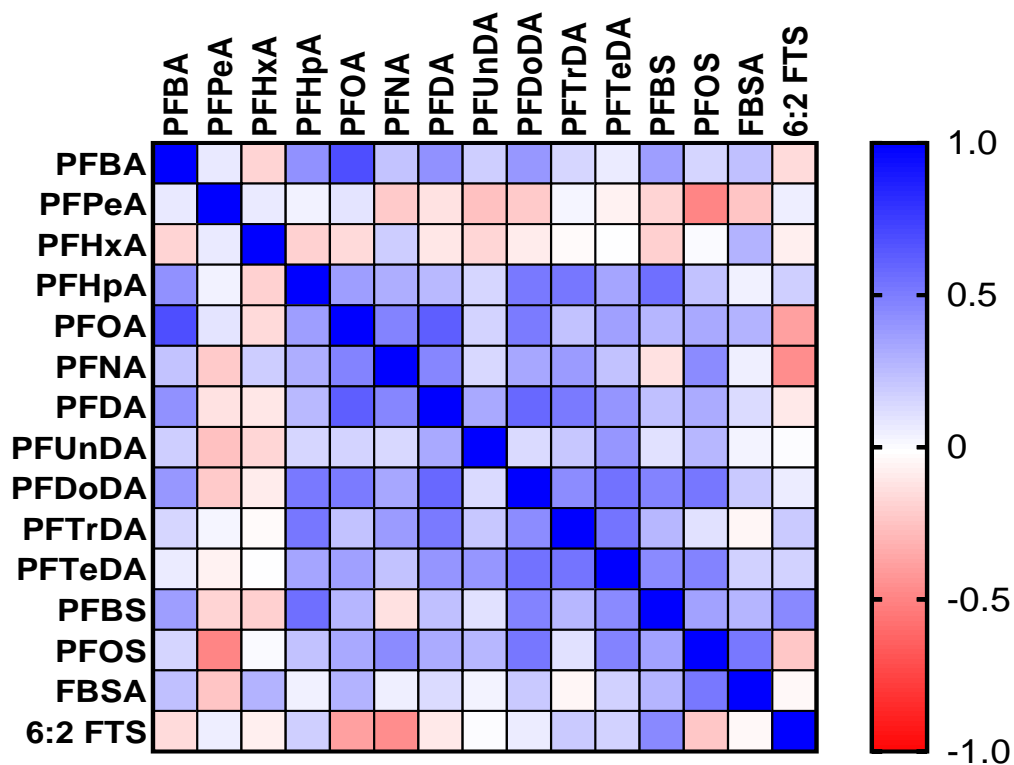


Fig. S4.5: Heatmaps showing the correlation structure among the topsoil (0-5 cm) samples of the private gardens close (0-4 km) to the plant site (upper heatmap) and remotely (>4 km) from the plant site (lower heatmap).

Chapter 5

Section 5.1: PFAS extraction soil and eggs

The soil samples were extracted using solid-phase extraction based on the principle of weak-anion exchange, according to the protocol described by Groffen et al. (2019b) with small adjustments. First, Chromabond HR-WAX extraction cartridges (Macherey-Nagel, Germany) were conditioned and equilibrated with 5 mL of ACN and Milli-Q water (MQ; 18.2 mΩ, TOC: 2.0 ppb, Merck Millipore, Belgium), respectively. Then, the cartridges were loaded with the sample extract and were washed with 5 mL of a 25 mM ammonium acetate buffer solution (dissolved in MQ) and 2 mL of ACN. Finally, the bound PFAS onto the sorbent of the cartridge were eluted using two times 1 mL of a 2% ammonium hydroxide solution (NH₄OH, dissolved in ACN). This eluent was vacuum-dried until nearly complete dryness using a rotational-vacuum-concentrator (Eppendorf concentrator 5301, 30 °C, type 5301, Hamburg, Germany). Then, 100 µL of 2% NH₄OH was added to the dried extract after which it was thoroughly vortex-mixed. Finally, the extracts were filtered through an Ion Chromatography Acrodisc 13 mm syringe filter with a 0.2 µm Supor polyethersulfone (PES) membrane (VWR International, Leuven, Belgium) into a PP injector vial.

The egg samples were extracted with a clean-up step extraction using graphitized carbon powder following the protocol described by Powley et al. (2005) with minor modifications. After the centrifugation step, the supernatant was vacuum-dried to ± 0.5 mL of extract with a rotational-vacuum-concentrator (Eppendorf concentrator 5301, 30 °C, type 5301, Hamburg, Germany). The dried extract was transferred to a PP Eppendorf tube which contained 0.05 g of graphitized carbon powder (Supelclean ENVI-Carb, Sigma-Aldrich, Overijse, Belgium) and 35 µL of glacial acetic acid (CH₃COOH) to remove chemical impurities. Subsequently, the 15 mL tube was rinsed twice with 250 µL of ACN, which was transferred to the same Eppendorf tube. The extracts were vortex-mixed and centrifuged (4 °C, 10 min, 10 000 rpm, 1037 g, Eppendorf centrifuge 5415R, rotor F 45-24-11), after which the supernatant was transferred to a new Eppendorf tube and vacuum-dried until nearly complete dryness using a rotational-vacuum-concentrator. Finally, 100 µL of a 2% NH₄OH solution was added to the dried extract and filtered through a 13 mm Acrodisc Ion Chromatography Syringe Filter with 0.2 µm Supor (PES) membrane (VWR International, Leuven, Belgium) into a PP injector vial prior to instrumental analysis.

Table S5.1: Overview of the multiple reaction monitoring (MRM) transitions for the precursor and product ion of all targeted per- and polyfluoroalkyl substances (PFAS) along with the mass-labelled internal standards (ISTDs) used for the quantification. The cone voltages (V) and collision energy (eV) used for the fragmentation and detection of the targeted PFAS and their internal standard are also given. Table was adopted from Lasters et al. (2022) with adjustments.

Compound	Precursor ion (m/z)	Product ion (m/z)		Cone Voltage (V)	Collision energy (eV) for diagnostic transition1	Collision energy (eV) for diagnostic transition 2	Internal standard (ISTD) used for quantification
		Diagnostic product ion 1	Diagnostic product ion 2				
PFBA	213	169	169	19	19	50	¹³ C ₄ -PFBA
PFPeA	263	219	219	15	10	45	¹³ C ₄ -PFBA
PFHxA	313	269	119	19	21	65	[1,2- ¹³ C ₂]PFHxA
PFHpA	363	319	169	24	40	30	[1,2- ¹³ C ₂]PFHxA
PFOA	413	369	169	22	13	60	[1,2,3,4- ¹³ C ₄]PFOA
PFNA	463	419	169	28	17	20	[1,2,3,4,5- ¹³ C ₅]PFNA
PFDA	513	469	219	25	29	29	[1,2- ¹³ C ₂]PFDA
PFUnDA	563	519	169	18	30	35	[1,2- ¹³ C ₂]PFUnDA
PFDoDA	613	569	319	22	21	30	[1,2- ¹³ C ₂]PFDoDA
PFTrDA	663	619	319	26	21	30	[1,2- ¹³ C ₂]PFDoDA
PFTeDA	713	669	169	28	21	21	[1,2- ¹³ C ₂]PFDoDA
PFBS	299	80	99	40	65	45	¹⁸ O ₂ -PFHxS
PFPeS	349	80	99	40	40	40	[1,2,3,4- ¹³ C ₄]PFOS

PFHxS	399	80	99	22	30	60	¹⁸ O ₂ -PFHxS
PFHpS	449	80	98.5	40	47	45	[1,2,3,4- ¹³ C ₄]PFOA
PFOS	499	80	99	60	58	58	[1,2,3,4- ¹³ C ₄]PFOS
PFDS	599	80	99	29	63	63	[1,2,3,4- ¹³ C ₄]PFOS
FBSA	298	78	219	40	38	27	
NaDONA	376.8	250.7	84.8	23	35	32	[1,2,3,4- ¹³ C ₄]PFOA
HFPO-DA	285	169		30	20		[1,2- ¹³ C ₂]PFHxA
PF4OPeA	228.8	85		20	20		[1,2,3,4- ¹³ C ₄]PFOA
PF5OHxA	279	85		20	20		[1,2- ¹³ C ₂]PFHxA
3,6-OPFHpA	201	85		30	25		[1,2- ¹³ C ₂]PFHxA
4:2 FTS	327	307	80	20	25	33	[1,2,3,4- ¹³ C ₄]PFOS
6:2 FTS	427	407	80	20	25	33	[1,2,3,4- ¹³ C ₄]PFOS
8:2 FTS	527	507	81	36	40	40	[1,2,3,4- ¹³ C ₄]PFOS
9Cl-PF3ONS	531	350.5	83	46	32	37	[1,2,3,4,5- ¹³ C ₅]PFNA
11Cl- PF3OUdS	631	451	83	50	40	35	[1,2- ¹³ C ₂]PFUnDA
PFEESA	315	135	69	30	20	55	[1,2- ¹³ C ₂]PFDA
¹³ C ₄ -PFBA	217	172	172	19	19	50	

[1,2- ¹³ C ₂]PFHxA	315	269	119	19	21	65
[1,2,3,4- ¹³ C ₄]PFOA	417	372	172	22	13	60
[1,2,3,4,5- ¹³ C ₅]PFNA	468	423	172	28	17	20
[1,2- ¹³ C ₂]PFDA	515	470	220	25	29	29
[1,2- ¹³ C ₂]PFUnDA	565	520	170	18	32	35
[1,2- ¹³ C ₂]PFDoDA	615	570	320	22	21	30
¹⁸ O ₂ -PFHxS	403	84	103	22	30	60
[1,2,3,4- ¹³ C ₄]PFOS	503	80	99	60	58	58

Table S5.2: Time series data showing the limit of quantification (LOQ), geometric mean, min. and max. PFAS concentrations (in ng/g dw) of all detected compounds in the top soil layer (0-5 cm) of chicken enclosures from private gardens across the Province of Antwerp (Belgium) from 2010 until 2022, within and outside the 4 km distance range from the major fluorochemical point source in Antwerp (Belgium). For 2010, only data for PFOS were available and were adopted from D'Hollander et al. (2011). ND = not detected; NA = data not available.

Compound	LOQ	2010		2019		2021		2022	
		<4 km (N = 3)	>4 km (N = 26)	<4 km (N = 11)	>4 km (N = 23)	<4 km (N = 13)	>4 km (N = 45)	<4 km (N = 6)	>4 km (N = 4)
PFBA	0.110	NA	NA	<LOQ (<LOQ-<LOQ)	<LOQ (<LOQ-0.474)	0.153 (<LOQ-3.61)	<LOQ (<LOQ-1.27)	0.217 (<LOQ-0.833)	<LOQ (<LOQ-0.176)
PFPeA	0.058	NA	NA	ND	<LOQ-0.432)	ND	<LOQ (<LOQ-1.04)	<LOQ (<LOQ-0.075)	<LOQ (<LOQ-0.144)
PFHxA	0.120	NA	NA	<LOQ (<LOQ-0.103)	<LOQ (<LOQ-0.642)	0.218 (<LOQ-0.901)	0.341 (<LOQ-1.23)	0.405 (0.245-0.642)	0.365 (0.277-0.456)
PFOA	0.056	NA	NA	0.617 (0.339-2.16)	1.82 (0.056-6.15)	1.02 (0.634-2.07)	0.884 (0.309-2.17)	0.530 (0.219-1.04)	0.393 (0.269-0.558)
PFNA	0.065	NA	NA	<LOQ (<LOQ-0.386)	<LOQ (<LOQ-0.172)	0.181 (<LOQ-0.815)	0.162 (<LOQ-0.790)	0.103 (0.079-0.158)	0.088 (<LOQ-0.193)
PFDA	0.091	NA	NA	0.110 (<LOQ-0.609)	0.104 (<LOQ-0.414)	0.377 (<LOQ-0.890)	0.575 (<LOQ-1.45)	0.693 (0.565-0.775)	0.410 (0.271-0.503)
PFUnDA	0.055	NA	NA	<LOQ (<LOQ-0.612)	0.095 (<LOQ-0.627)	0.133 (<LOQ-0.446)	0.207 (<LOQ-0.574)	0.143 (<LOQ-0.278)	0.141 (<LOQ-0.331)
PFDoDA	0.097	NA	NA	<LOQ (<LOQ-1.15)	0.102 (<LOQ-1.62)	0.473 (<LOQ-1.81)	0.598 (<LOQ-2.48)	0.417 (0.095-0.806)	0.478 (0.290-0.774)
PFTTrDA	0.089	NA	NA	ND	<LOQ (<LOQ-0.177)	0.204 (<LOQ-1.82)	0.191 (<LOQ-1.26)	0.219 (0.137-0.307)	0.237 (0.174-0.270)
PFTeDA	0.142	NA	NA	ND	<LOQ (<LOQ-0.414)	0.220 (<LOQ-0.802)	0.202 (<LOQ-1.07)	0.444 (0.240-0.709)	0.407 (0.191-0.828)
PFBS	0.240	NA	NA	<LOQ (<LOQ-1.69)	<LOQ (<LOQ-0.159)	0.433 (<LOQ-9.30)	<LOQ (<LOQ-1.16)	15.6 (6.79-44.5)	5.08 (2.97-8.15)
PFOS	0.038	25.8 (21.3-33.7)	0.909 (0.100-4.30)	5.36 (2.17-21.6)	0.899 (0.081-2.99)	6.26 (0.056-29.5)	1.30 (0.042-4.56)	2.86 (1.57-5.79)	1.04 (0.318-2.13)
FBSA	0.093	NA	NA	ND	ND	0.708 (<LOQ-30.4)	<LOQ (<LOQ-0.965)	2.48 (<LOQ-7.68)	0.151 (<LOQ-2.23)
4:2 FTS	0.081	NA	NA	ND	ND	ND	0.537 (0.377-0.763)	ND	ND
6:2 FTS	0.066	NA	NA	ND	ND	<LOQ (<LOQ-8.90)	0.136 (<LOQ-74.4)	0.254 (<LOQ-0.953)	0.125 (0.083-0.278)

Table S5.3: Time series data showing the limit of quantification (LOQ), geometric mean, min. and max. PFAS concentrations (in ng/g dw) of all detected compounds in the top soil layer (0-5 cm) of vegetable gardens from private gardens across the Province of Antwerp (Belgium) from 2019 until 2022, within and outside the 4 km distance range from the major fluorochemical point source in Antwerp (Belgium). ND = not detected; NA = data not available. Concentrations with an epsilon symbol (ε) represent the concentration of one datapoint and, therefore, no min.-max. range could be provided.

Compound	LOQ	2019		2021		2022	
		<4 km (N = 9)	>4 km (N = 11)	<4 km (N = 11)	>4 km (N = 34)	<4 km (N = 8)	>4 km (N = 5)
PFBA	0.366	0.622 (<LOQ-1.66)	0.265 (<LOQ-1.78)	0.611 (<LOQ-42.9)	0.484 (<LOQ-49.5)	0.921 (0.289-2.90)	0.329 (<LOQ-0.757)
		0.110 (<LOQ-0.284)	0.080 (<LOQ-0.311)	0.062 (<LOQ-0.253)	<LOQ (<LOQ-0.472)	0.075 (<LOQ-0.175)	<LOQ (<LOQ-0.101)
PFHxA	0.120	0.432 (0.138-0.816)	0.416 (<LOQ-1.09)	0.342 (<LOQ-1.38)	0.352 (<LOQ-1.95)	0.416 (<LOQ-1.50)	0.852 (0.430-1.50)
		<LOQ (<LOQ-0.160)	<LOQ (<LOQ-0.164)	0.268 (<LOQ-1.12)	0.105 (<LOQ-0.938)	0.074 (<LOQ-0.514)	0.107 (<LOQ-0.514)
PFOA	0.056	1.34 (0.653-2.18)	1.10 (0.426-3.12)	1.22 (0.650-5.41)	0.818 (0.084-4.36)	1.20 (0.606-3.72)	0.780 (0.458-1.74)
		0.192 (0.105-0.423)	0.141 (<LOQ-0.364)	0.208 (<LOQ-0.434)	0.170 (<LOQ-0.558)	0.245 (0.090-1.09)	0.225 (<LOQ-1.10)
PFDA	0.091	0.591 (0.362-1.30)	0.633 (0.327-1.45)	0.585 (0.359-1.34)	0.643 (<LOQ-1.54)	0.671 (0.545-0.978)	0.532 (0.292-0.720)
		0.173 (<LOQ-0.335)	0.203 (<LOQ-0.666)	0.189 (<LOQ-0.392)	0.154 (<LOQ-0.679)	0.245 (0.084-0.931)	0.156 (<LOQ-0.931)
PFDoDA	0.097	0.763 (0.317-1.68)	0.797 (0.282-2.32)	1.11 (0.590-2.85)	0.981 (<LOQ-3.45)	0.552 (<LOQ-1.29)	0.402 (<LOQ-0.997)
		0.213 (<LOQ-0.414)	0.235 (0.133-0.363)	0.257 (<LOQ-0.722)	0.310 (<LOQ-3.63)	0.870 (0.403-4.78)	0.676 (0.300-4.78)
PFTeDA	0.142	0.395 (0.185-1.63)	0.426 (<LOQ-1.96)	0.411 (<LOQ-1.26)	0.448 (<LOQ-2.34)	0.736 (0.377-1.29)	0.789 (0.567-1.29)
		0.323 (<LOQ-0.738)	<LOQ (<LOQ-0.619)	0.968 (<LOQ-19.2)	<LOQ (<LOQ-80.8)	<LOQ (<LOQ-1.29)	<LOQ (<LOQ-1.29)
PFHxS	0.130	ND	ND	0.513 (0.497-0.529)	1.03 (0.530-2.02)	<LOQ (<LOQ-0.463)	<LOQ (<LOQ-0.271)
PFHpS	0.157	ND	ND	2.99 ε	0.412 ε	ND	ND
PFOS	0.038	8.06 (2.19-31.5)	2.03 (0.860-7.08)	7.82 (1.19-25.7)	1.30 (<LOQ-6.39)	2.86 (0.698-10.5)	1.07 (0.372-2.65)
		0.044 (<LOQ-0.139)	0.040 (<LOQ-0.508)	0.034 ε	0.073 (0.044-0.120)	0.049 (<LOQ-0.069)	0.039 (<LOQ-0.053)
FBSA	0.093	6.68 (2.40-16.3)	0.578	2.44 (0.155-39.7)	0.194 (<LOQ-5.99)	0.983 (0.334-2.30)	1.78

			(<LOQ- 7.87)			(0.085- 7.17)	
		0.338 (0.129- 0.886)	0.232 (0.179- 0.274)	0.311 (<LOQ-2.44)	0.070 (<LOQ-44.1)	0.613 (<LOQ- 14.0)	1.16 (0.436-14.1)
6:2 FTS	0.066		0.171 (<LOQ- 1.87)	ND	0.224 (0.128- 0.394)	ND	ND
8:2 FTS	0.109	ND	ND	0.303 ϵ	0.046 ϵ	ND	ND
9CI-PF3ONS	0.041	ND	ND				

Table S5.4: Time series data showing the limit of quantification (LOQ), geometric mean, min. and max. PFAS concentrations (in ng/g ww) of all detected compounds in homegrown eggs of free-ranging laying hens from private gardens across the Province of Antwerp (Belgium) from 2010 until 2022, within and outside the 4 km distance range from the major fluorochemical point source in Antwerp (Belgium). ND = not detected; NA = data not available. Concentrations with an epsilon symbol (ε) represent the concentration of one datapoint and, therefore, no min.-max. range could be provided.

Compound	LOQ	2010		2018		2019		2021		2022	
		<4 km (N = 3)	>4 km (N = 26)	<4 km (N = 24)	>4 km (N = 11)	<4 km (N = 11)	>4 km (N = 23)	<4 km (N = 13)	>4 km (N = 45)	<4 km (N = 6)	>4 km (N = 4)
PFBA	0.080	NA	NA	0.167 (<LOQ-8.40)	<LOQ (<LOQ-1.52)	0.568 (0.134- 3.73)	0.283 (<LOQ-1.15)	0.331 (<LOQ-2.51)	0.095 (<LOQ- 0.966)	1.06 (0.351- 3.11)	0.457 (0.367- 0.563)
PFPeA	0.027	NA	NA	ND	ND	ND	0.027 ε	<LOQ (<LOQ- 0.132)	0.028 (<LOQ-1.30)	ND	0.117 ε
PFHxA	0.057	NA	NA	ND	ND	0.161 (<LOQ- 0.209)	0.128 (<LOQ- 0.240)	<LOQ (<LOQ- 0.114)	<LOQ (<LOQ- 0.152)	0.650 (0.304- 1.76)	0.316 (0.098- 0.956)
PFHpA	0.021	NA	NA	ND	ND	0.053 (0.034- 0.083)	0.044 (0.024- 0.126)	ND	ND	ND	ND
PFOA	0.076	2.47 (1.41-5.07)	0.275 (0.066-1.26)	0.601 (0.317- 2.40)	0.557 (0.309- 0.770)	0.992 (0.229- 7.03)	3.98 (0.259- 8.13)	0.246 (<LOQ- 0.559)	0.243 (<LOQ- 0.943)	0.755 (0.407- 2.40)	0.436 (0.250- 0.690)
PFNA	0.071	NA	NA	0.066 (<LOQ- 0.730)	0.093 (0.038- 0.441)	0.347 (0.095- 1.20)	0.200 (<LOQ- 0.968)	<LOQ (<LOQ- 0.435)	0.099 (<LOQ- 0.628)	0.296 (0.101- 0.553)	0.171 (0.122- 0.343)
PFDA	0.120	NA	NA	0.380 (<LOQ-1.60)	0.313 (<LOQ- 0.842)	0.784 (0.342- 2.34)	0.574 (0.161- 1.75)	<LOQ (<LOQ- 0.583)	0.302 (<LOQ-1.65)	1.01 (0.530- 1.87)	0.719 (0.580- 1.20)
PFUnDA	0.110	NA	NA	<LOQ (<LOQ-1.37)	<LOQ (<LOQ- 0.902)	0.728 (0.344- 3.78)	0.532 (0.202- 1.48)	<LOQ (<LOQ- 0.861)	<LOQ (<LOQ- 0.606)	0.432 (<LOQ-1.08)	0.389 (0.239- 0.960)
PFDoDA	0.171	NA	NA	<LOQ (<LOQ-1.60)	0.174 (<LOQ-1.28)	1.36 (0.187- 13.6)	1.75 (0.349- 17.5)	1.98 (0.707- 11.2)	2.24 (0.517- 21.9)	4.50 (0.877- 14.1)	1.86 (1.25-3.18)
PFTTrDA	0.079	NA	NA	ND	ND	1.32 (0.227- 12.3)	0.576 (<LOQ-2.60)	1.16 (0.336- 6.15)	1.08 (0.219- 7.78)	3.67 (0.239- 14.9)	2.15 (1.57-3.92)

PFTeDA	0.240	NA	NA	ND	ND	8.67 (1.15-147)	3.86 (0.444- 26.6)	1.43 (0.240- 8.38)	1.82 (0.240- 18.3)	6.80 (0.301- 28.7)	4.61 (3.59-6.70)
PFBS	0.073	NA	NA	ND	ND	0.250 (<LOQ-4.28)	<LOQ (0.366)	0.812 (0.173- 3.15)	0.108 (<LOQ- 0.166)	0.087 (<LOQ- 0.609)	<LOQ (0.088)
PFHxS	0.132	NA	NA	3.40 €	3.6 €	0.543 (<LOQ-6.44)	<LOQ (<LOQ-2.27)	0.596 (0.402- 0.725)	ND	0.208 (<LOQ-2.41)	<LOQ (<LOQ-1.73)
PFOS	0.032	528 (110-3473)	5.76 (0.400-52.8)	5.75 (<LOQ- 128.6)	3.55 (0.799- 9.15)	50.7 (3.94-571)	8.07 (1.70-95.6)	20.1 (2.02-215)	3.32 (0.856- 48.3)	39.4 (1.26-233)	8.78 (3.52-17.5)
PFDS	0.421	NA	NA	ND	ND	0.577 (0.520- 0.641)	ND	1.26 (0.950- 1.68)	ND	ND	ND
FBSA	0.483	NA	NA	NA	NA	ND	ND	<LOQ (<LOQ- 0.781)	ND	1.21 (1.09-1.35)	ND

Table S5.5: Time series data of all the examined matrices in the present study, showing the mean concentration ratios of three pairs of PFCA homologues for evaluating potential indications of PFAS originating from atmospheric oxidation of precursor fluorotelomer alcohols (FTOHs) to PFCAs. Ratios in bold fall in the expected 1/1 to 6/1 ratio range typical for atmospheric oxidation of FTOHs to PFCAs, while ratios of > 8/1 are indicative of direct PFCA emissions, as described by Prevedouros et al. (2006).

PFOA/PFNA ratio						
Matrix	Soil chicken enclosure		Soil vegetable garden		Homegrown eggs	
Distance zone	Zone A	Zone B	Zone A	Zone B	Zone A	Zone B
2018	NA	NA	NA	NA	17.4	8.46
2019	41.9	70.9	7.56	9.28	9.32	31.0
2021	28.1	25.0	7.88	5.92	15.0	4.21
2022	15.3	10.6	6.49	6.72	2.98	2.63

PFDA/PFUnDA ratio						
Distance zone	Zone A	Zone B	Zone A	Zone B	Zone A	Zone B
2018	NA	NA	NA	NA	18.37	4.59
2019	15.6	1.40	5.30	3.62	1.12	1.11
2021	4.20	4.20	4.05	5.43	2.70	4.12
2022	8.36	5.45	4.37	5.73	3.00	1.92

PFDODA/PFTrDA ratio						
Distance zone	Zone A	Zone B	Zone A	Zone B	Zone A	Zone B
2018	NA	NA	NA	NA	NA	NA
2019	19.5	3.56	3.99	4.07	1.20	3.49
2021	9.16	4.98	6.31	3.79	1.76	2.17
2022	2.66	2.11	1.33	1.46	1.46	0.87

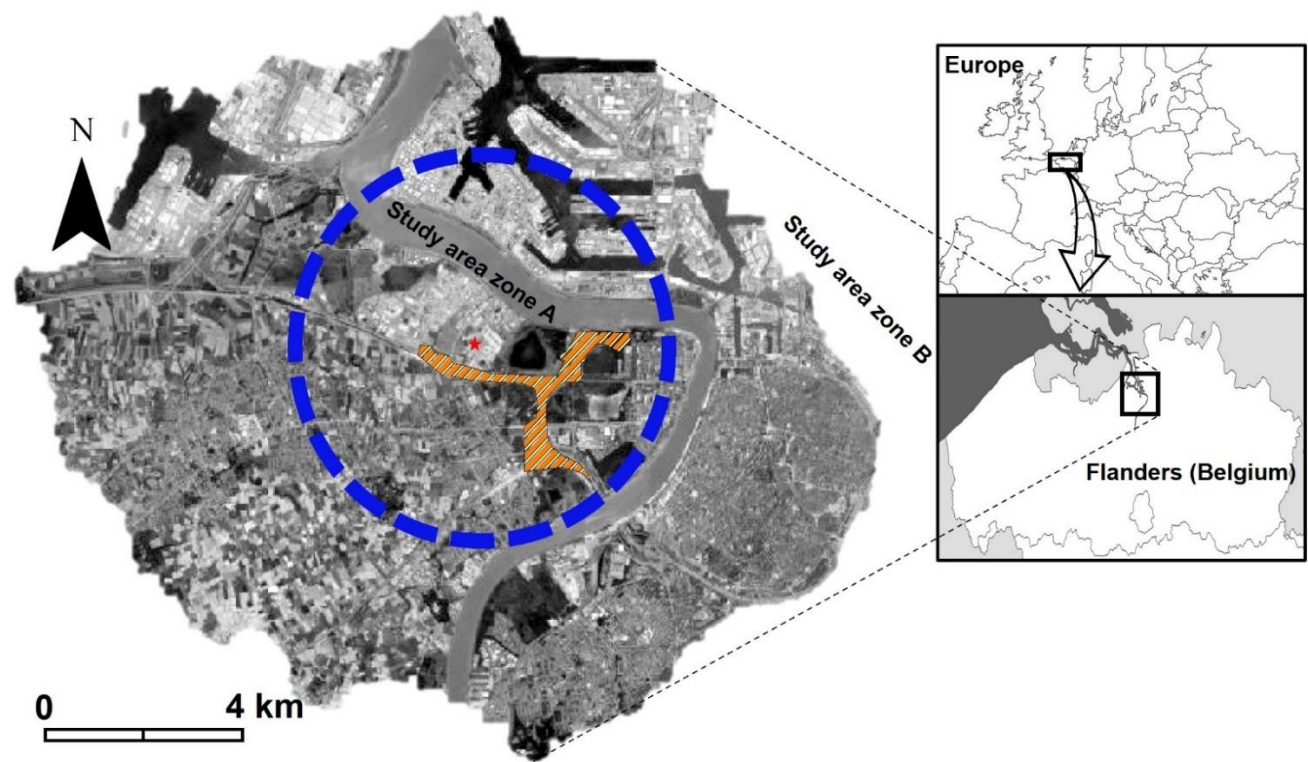


Fig. S5.1: Part of the study area in the Province of Antwerp (Belgium) which shows the region in which private gardens were sampled nearby (≤ 4 km: study area zone A, blue dashed circle) the fluorochemical plant (red star) in Antwerp and remotely (>4 km: study area zone B) from the major fluorochemical plant. The location of the Oosterweel Link (OW) road works site is displayed by the dashed orange polygon.

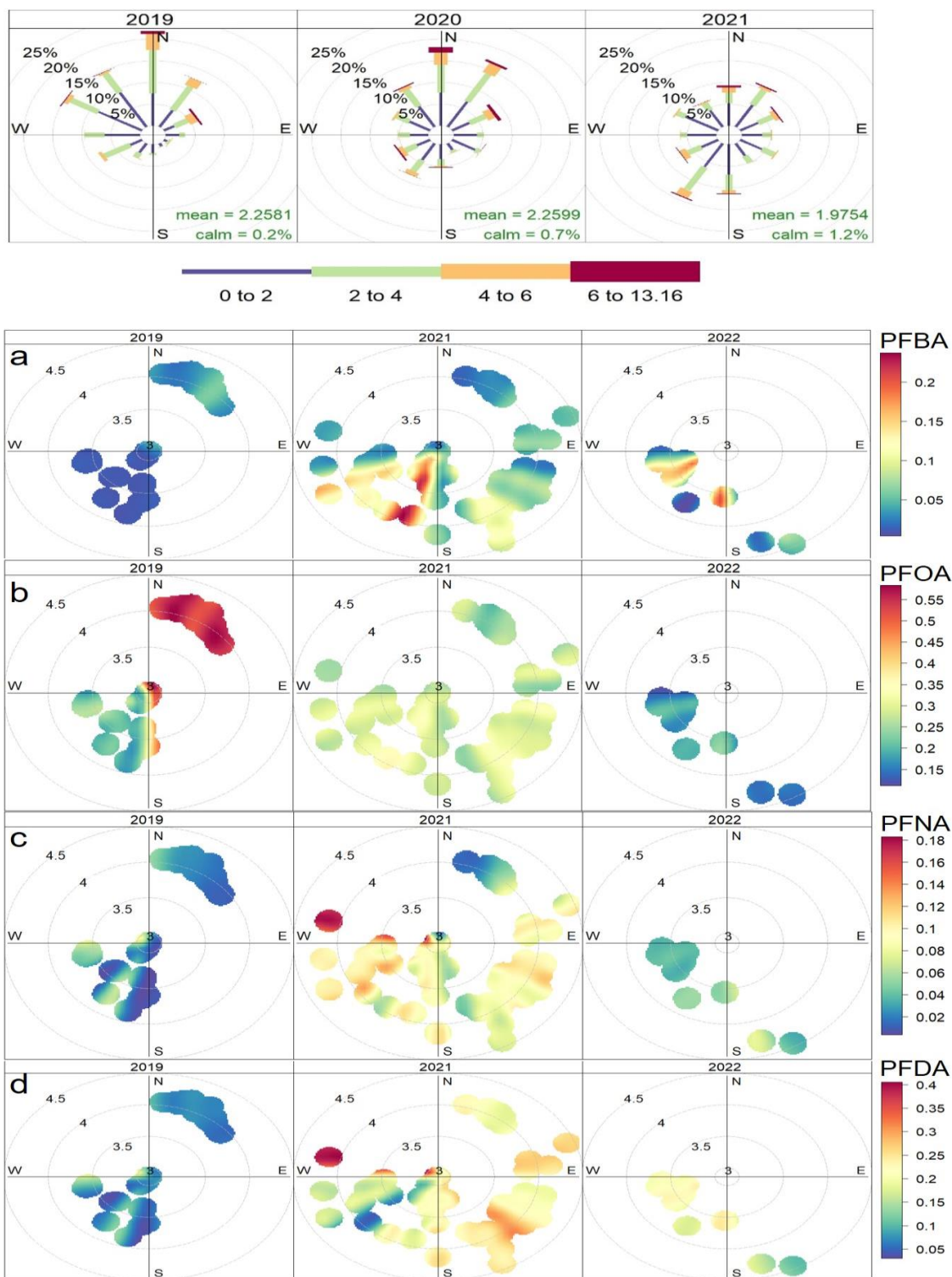


Fig. S5.2: Wind rose diagram showing the annual percentage distribution of wind directions and wind speed in nearby the fluorochemical plant site (top graph). Bivariate polar plots showing the soil concentration range (= colour scale; in log ng/g dry weight) of PFBA (a), PFOA (b), PFNA (c), PFDA (d), PFUnDA (e), PFDoDA (f), PFTTrDA (g), PFTeDA (h), PFBS (i) and PFOS (j) in top soil (0-5 cm) of chicken enclosures from private gardens in the Province of Antwerp (Belgium) throughout the sampling years. The centre of each polar plot represents the fluorochemical plant site in Antwerp (Belgium) and the concentric circles show the radially increasing distance (in log m) from this plant site.

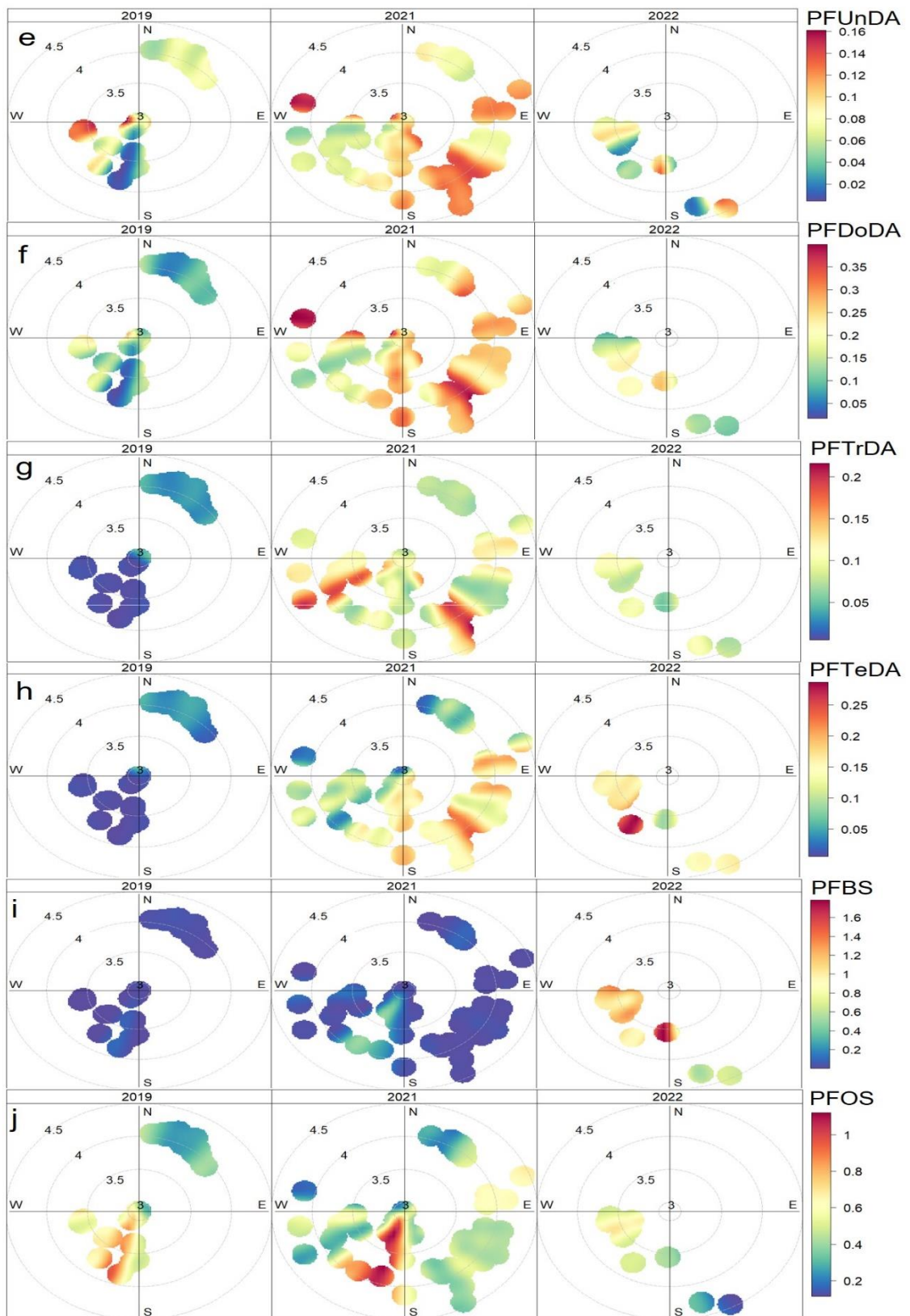


Fig. S5.2: (continued).

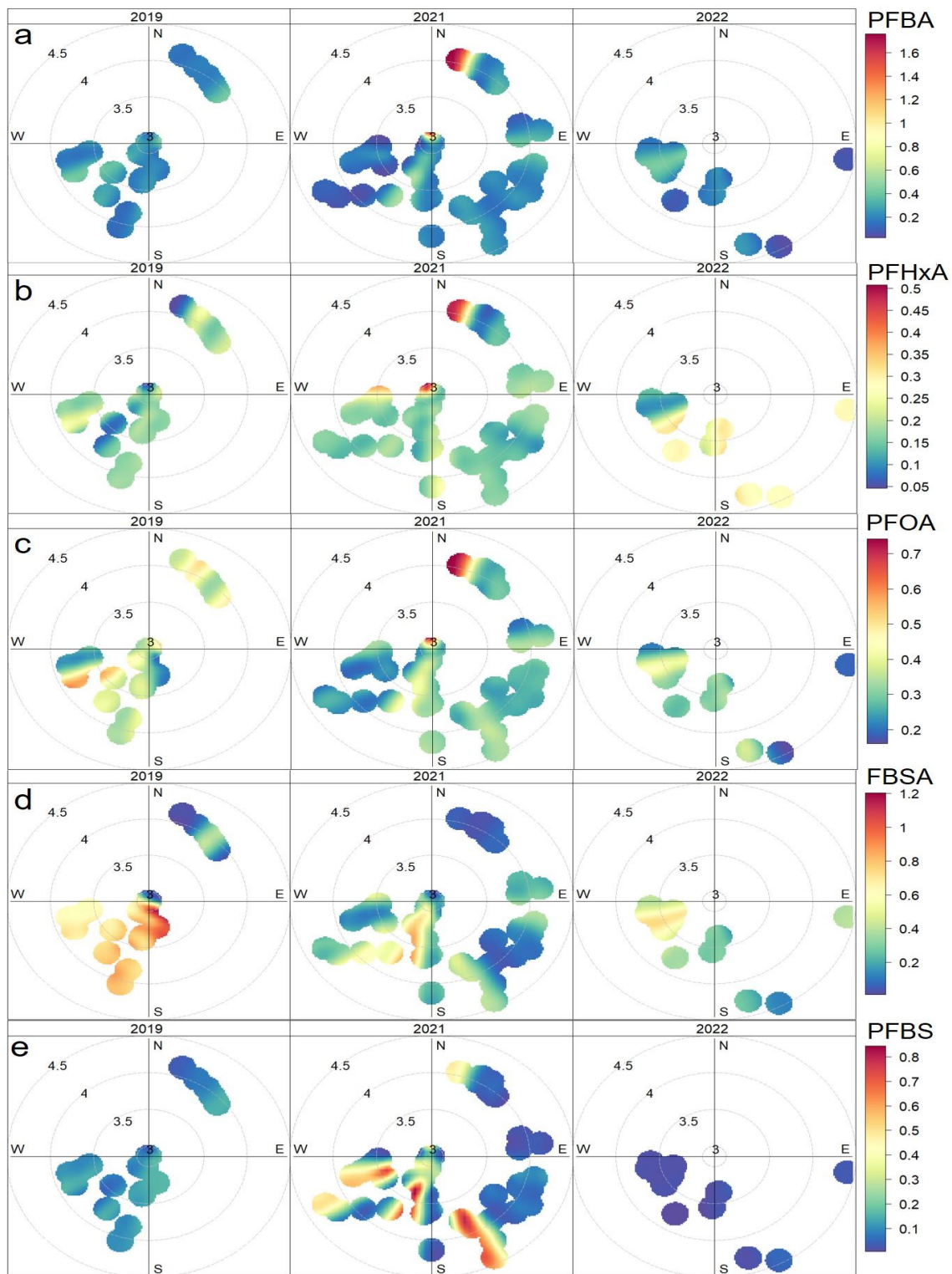


Fig. S5.3: Bivariate polar plots showing the soil concentration range (= colour scale; in log ng/g dry weight) of PFBA (a), PFHxA (b), PFOA (c), FBSA (d), PFBS (e) and PFOS (f) in the top soil layer (0-5 cm) of vegetable gardens from private gardens in the Province of Antwerp (Belgium) throughout the sampling years. The centre of each polar plot represents the fluorochemical plant site in Antwerp (Belgium) and the concentric circles show the radially increasing distance (in log m) from this plant site.

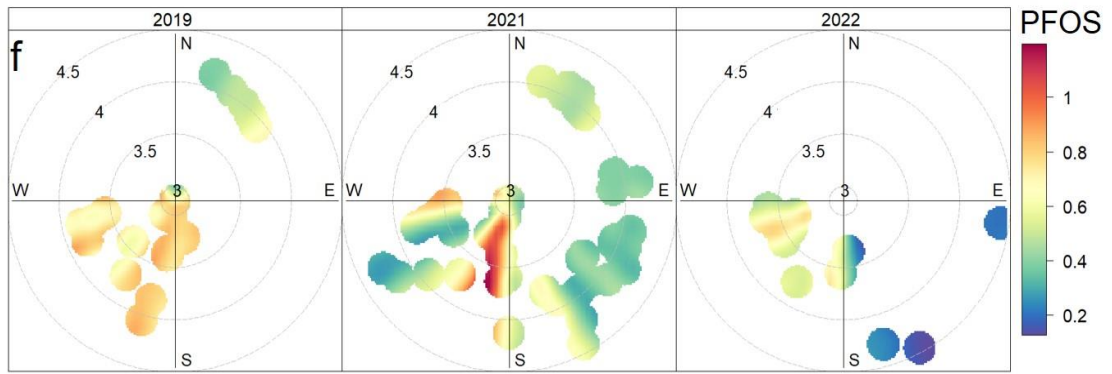


Fig. S5.3: (continued).

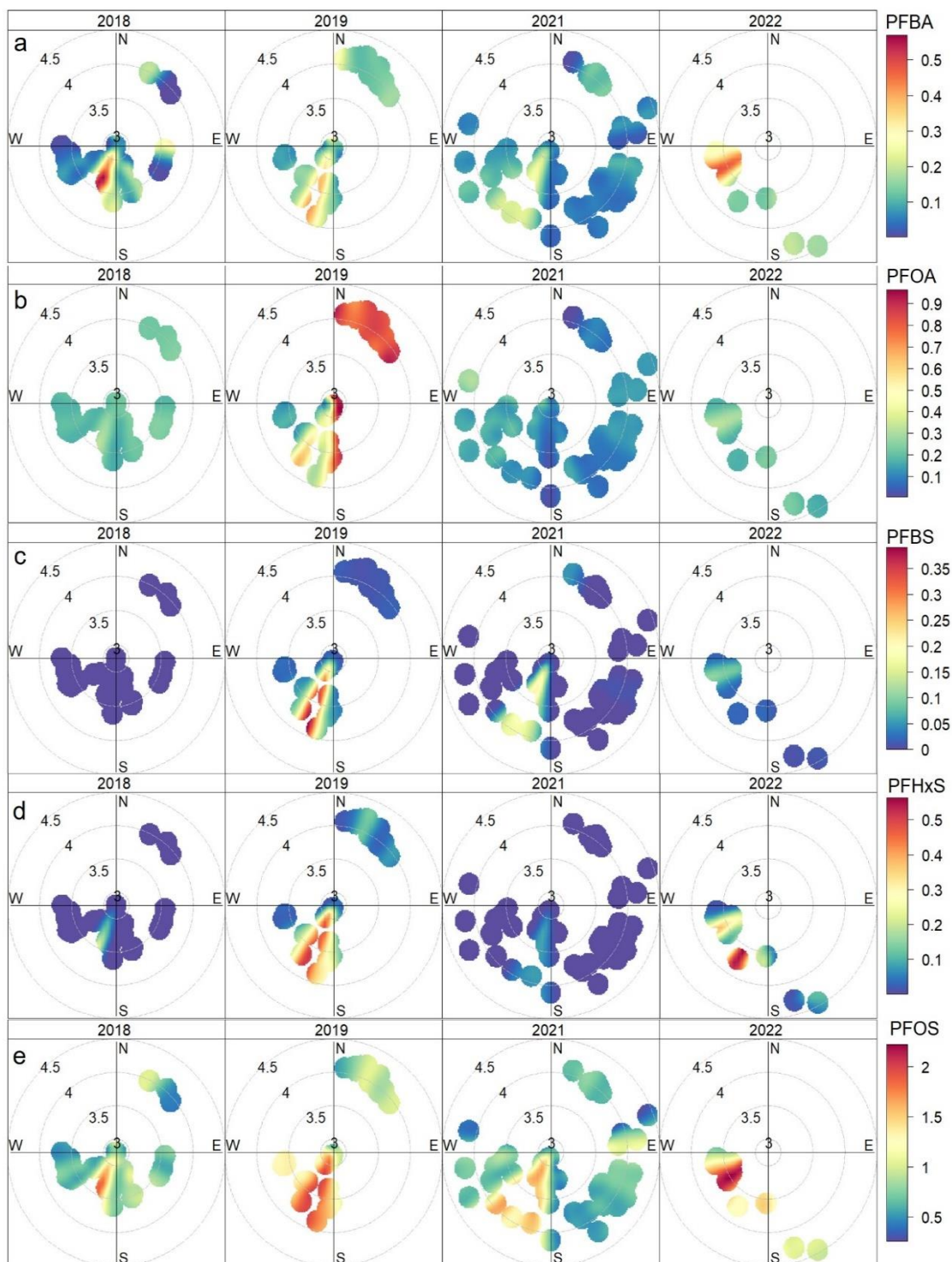


Fig. S5.4: Bivariate polar plots showing the concentration range (= colour scale; in log ng/g wet weight) of PFBA (a), PFHxA (b), PFOA (c), FBSA (d), PFBS (e) and PFOS (f) in homegrown eggs from private gardens in the Province of Antwerp (Belgium) throughout the sampling years. The centre of each polar plot represents the fluorochemical plant site in Antwerp (Belgium) and the concentric circles show the radially increasing distance (in log m) from this plant site.

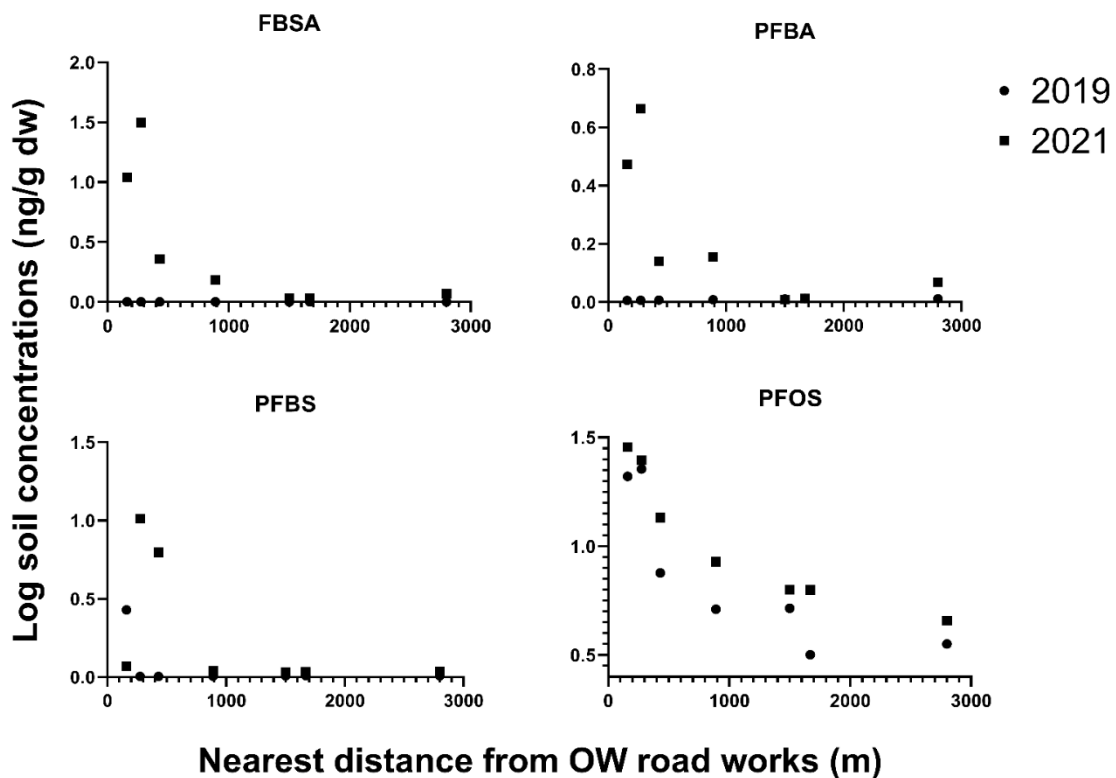


Fig. S5.5: Significant correlations between the nearest distance (in m) of the repeatedly sampled chicken enclosures from the Oosterweel road works (OW) in Antwerp (Belgium) and the chicken enclosure soil PFAS concentrations (in ng/g dw) for 2019 (before the OW, black dots) and 2021 (during the OW, black rectangles). Correlation plots are only shown for those compounds that showed significantly changed concentrations from 2019 to 2021 and correlations for vegetable garden soil are not shown as only limited concentration changes were observed for this matrix, compared to those in the chicken enclosure soil.

Curriculum Vitae

Personal information

Name: Robin Lasters

Date of Birth (d/m/y): 26-03-1993

Place of Birth: Bornem, Belgium

Mobile Phone: +32 4 98 37 88 62

E-mail: robinlasters@gmail.com

Education

- | | |
|--------------|---|
| 2012-2015 | Bachelor of Science, Biology
Thesis: Exploratiegedrag en respons tot nieuw voedsel bij wilde Zuid-Afrikaanse groene meerkatten (<i>Chlorocebus pygerythrus</i>) |
| 2015-2017 | Master of Science, Biology: Evolutionary and Behavioural Biology (Great Distinction)
Thesis: The accumulation and reproductive effects of perfluoroalkyl acids in wild great tits (<i>Parus major</i>) along a pollution gradient in Antwerp |
| 2017-2018 | Scientific assistant in the research groups Evolutionary Ecology (EVECO) and Systemic Physiological and Ecotoxicological Research (SPHERE) |
| 2018-present | PhD Researcher
Faculty of Science, Department of Biology
ECOSPHERE research group |

Thesis: Poly- and perfluoroalkyl substances (PFAS) in private gardens: factors affecting accumulation in homegrown food and characterization of human exposure risk

Publications

First author

Lasters, R., Groffen, T., Lopez-Antia, A., Bervoets, L. & Eens, M. (2019). Variation in PFAA concentrations and egg parameters throughout the egg-laying sequence in a free-living songbird (the great tit, *Parus major*): Implications for biomonitoring studies. *Environmental Pollution*. 246: 237-248.

Lasters, R., Groffen, T., Bervoets, L. & Eens, M. (2021). Perfluoroalkyl acid (PFAA) profile and concentrations in two co-occurring tit species: distinct differences indicate non-generalizable results across passerines. *Science of The Total Environment*. 761: 143301-143309.

Lasters, R., Groffen, T., Eens, M., Coertjens, D., Gebbink, W. A., Hofman, J. & Bervoets L. (2022). Home-produced eggs: An important human exposure pathway of perfluoroalkylated substances (PFAS). *Chemosphere*. 308: 136283-136293.

Lasters, R., Van Sundert, K., Groffen, T., Buytaert, J., Eens, M. & Bervoets, L. (2023). Prediction of perfluoroalkyl acids (PFAAs) in homegrown eggs: Insights into abiotic and biotic factors affecting bioavailability and derivation of potential remediation measures. *Environment International*. 181: 108300-108313.

Lasters, R., Groffen, T., Eens, M. & Bervoets, L. (2024). Dynamic spatiotemporal changes of per- and polyfluoroalkyl substances (PFAS) in private gardens at different distances from a fluorochemical plant. *Environmental Pollution*. 346: 123613-123624.

Lasters, R., Groffen, T., Eens, M. & Bervoets, L. (*in prep.*). Per- and perfluoroalkyl substances in homegrown crops: accumulation and human exposure risk.

Co-author

Groffen, T., Lasters, R., Lopez-Antia, A., Prinsen, E., Bervoets, L. & Eens, M. (2019). Limited reproductive impairment in a passerine bird species exposed along a perfluoroalkyl acid (PFAA) pollution gradient. *Science of The Total Environment*. 652: 718-728.

Lopez-Antia, A., Groffen, T., Lasters, R., AbdElgawad, H., Sun, J., Asard, H., Bervoets, L. & Eens, M. (2019). Perfluoroalkyl Acids (PFAAs) Concentrations and Oxidative Status in Two Generations of Great Tits Inhabiting a Contamination Hotspot. *Environmental Science & Technology*. 53: 1617-1626.

Groffen, T., Lasters, R., Lemière, F., Willems, T., Eens, M., Bervoets, L. & Prinsen, E. (2019). Development and validation of an extraction method for the analysis of perfluoroalkyl substances (PFASs) in environmental and biotic matrices. *Journal of Chromatography B*. 1116: 30-37.

Groffen, T., Lasters, R., Bervoets, L., Prinsen, E. & Eens, M. (2020). Are Feathers of a Songbird Model Species (The Great Tit, *Parus major*) Suitable for Monitoring Perfluoroalkyl Acids (PFAAs) in Blood Plasma? *Environmental Science & Technology*. 54: 9334-9344.

Byns, C., Teunen, L., Groffen, T., Lasters, R. & Bervoets, L. (2022). Bioaccumulation and trophic transfer of perfluorinated alkyl substances (PFAS) in marine biota from the Belgian North Sea: Distribution and human health risk implications. *Environmental Pollution*. 311: 119907-11918.

Groffen, T., Prinsen, E., Stoffels, O. D., Maas, L., Vincke, P., Lasters, R., Eens, M. & Bervoets, L. (2022). PFAS accumulation in several terrestrial plant and invertebrate species reveals species-specific differences. *Environmental Science & Pollution Research*. 30: 23820-23835.

Colles, A., Bierkens, J., Jacobs, G., Govarts, E., Van Holderbeke, M., Touchant, K., Cops, J., Willems, H., Franken, C., Den Hond, E., Groffen, T., Lasters, R. & Bervoets, L. (2022). Per- en polyfluoralkylstoffen in en rond de woning. Verantwoordelijke uitgever Departement Omgeving, Vlaams Planbureau voor Omgeving, versie november 2022, studie in opdracht van Departement Omgeving en OVAM.

important human exposure source to perfluoroalkyl acids (PFAAs)

03/05/2020-07/05/2020

Poster presentation SETAC Europe 30th annual meeting (virtual): *Exposure of lettuce to perfluoroalkylated acids (PFAS) in naturally contaminated soil: accumulation patterns and toxicokinetics*

03/05/2021-06/05/2021

Poster presentation SETAC Europe 31st annual meeting (virtual): *Distribution of perfluoroalkylated acids (PFAAs) in environmental matrices and self-cultivated food in Antwerp*

15/05/2022-19/05/2022

Poster presentation SETAC Europe 32nd annual meeting (Copenhagen, Denmark): *Distribution of per- and polyfluoroalkyl substances (PFAS) in home-produced food across Flanders*

07/12/2022

Poster presentation BelTox annual meeting (Antwerp, Belgium): *Predictability of perfluoroalkyl substances (PFAS) in homegrown eggs using local environmental and biotic variables*

30/04/2023-04/05/2023

Poster presentation SETAC 33rd annual meeting (Dublin, Ireland): *Predictability of perfluoroalkyl substances (PFAS) in homegrown eggs using local environmental and biotic variables*

10/09/2023-14/09/2023

Oral presentation DIOXIN 43rd annual meeting (Maastricht, The Netherlands): *Predictability of perfluoroalkylated substances (pfas) in homegrown eggs using local environmental and biotic variables*

Lectures and talks

19/04/2022

Oral lecture research group PLECO (virtual webinar, main speaker): *Forever chemicals forever a problem? Gardening with PFAS in the backyard*

31/03/2022	Oral lecture municipality of Zwijndrecht (virtual webinar, speaker): <i>PFAS onderzoek in voeding uit private tuinen</i>
19/09/2023	Oral lecture Department of Environment & Health from Flemish Government (virtual webinar, speaker): <i>Meten in mens en omgeving: Een blik op recente PFAS onderzoeksresultaten</i>
10/10/2023	Oral lecture Natuurpunt (Melsele, Antwerpen, main speaker): <i>PFAS in mijn tuin?</i>
23/04/2024	Oral lecture Public Waste Agency of Flanders (virtual webinar, main speaker): <i>PFAS in tuinen</i>

Public dissemination & media coverage

29/05/2021	Scientific contribution (newspaper) for <i>De Tijd</i> : https://www.tijd.be/politiek-economie/belgie/algemeen/de-donkere-gifwolk-boven-oosterweel/10309766.html
01/06/2021	Scientific contribution (newspaper) for <i>Het Nieuwsblad</i> : https://www.nieuwsblad.be/cnt/dmf20210531_98035445
30/06/2021	Scientific contribution (newspaper) for <i>Het Laatste nieuws</i> (HLN): https://www.hln.be/binnenland/onderzoek-uantwerpen-toont-aan-dat-pfas-vervuiling-rond-3m-voorbije-10-jaar-is-afgenomen~aadc1902/?cb=0d64ede41c24419e66f2cfdef5037a85&auth_rd=1
05/07/2021	Scientific opinion (newspaper) for <i>De Standaard</i> : https://www.standaard.be/cnt/dmf20210704_97453837
22/09/2021	Scientific contribution (PANO, television documentary) for <i>VRT</i>

23/05/2024

Scientific contribution (Ze zeggen dat, television program) for *VTM*

Grants and awards

10/10/2019

Doctoral fellowship fundamental research from the Research Foundation – Flanders (FWO)

07/12/2022

Best scientific poster presentation BelTox conference

General skills

Communicational

Writing and reviewing of scientific papers, projects and reports. Oral presentations of research outcome in Dutch and English to (inter)national scientific-, public- and laymen audiences. Dissemination of research via the media (articles and oral interviews for television programs).

Networking & Teamwork

Recruitment of study participants for scientific research. Organization of scientific conferences. Research collaboration with research institutes and governmental organizations. Maintenance of (inter)national research collaborations.

Leadership & Creativity

Supervision and guidance of bachelor and master students with thesis projects and practical courses. Development and invention of innovative research ideas, experiments, projects and strategies.

Problem solving

Analytical method development of PFAS in abiotic and biotic matrices. Tackling and adjust unforeseen delays and technical deviations. Critical evaluation and analysis of research results.

Time management & flexibility

Timely follow-up of research projects, conducting laborious and demanding fieldwork.

Technical knowledge & practical skills

Fieldwork sampling techniques of various samples, including manipulation of songbirds. Physicochemical analyses of water and soil properties. Chemical extraction and analyses of pollutants. Setting-up and conducting toxicological experiments. Experience with Microsoft programs, GIS software, statistical analyses in R and Graphpad.